

MANAGING FOR ECOSYSTEM RESILIENCE IN A NON-STATIONARY WORLD

by

Caleb Powell Roberts

A DISSERTATION

Presented to the Faculty of

The Graduate College at the University of Nebraska

In Partial Fulfillment of Requirements

For the Degree of Doctor of Philosophy

Major: Agronomy & Horticulture

(Applied Ecology)

Under the Supervision of Professors Dirac Twidwell and Craig R. Allen

Lincoln, Nebraska

May, 2019

MANAGING FOR ECOSYSTEM RESILIENCE IN A NON-STATIONARY WORLD

Caleb P. Roberts, Ph.D.

University of Nebraska, 2019

Advisors: Dirac Twidwell and Craig R. Allen

Globally, environmental change is on the rise, and ecological resilience of many ecosystems is eroding. This is leading to increases in regime shifts, where fundamental structures and functions of ecosystems change. Loss of resilience and regime shifts can strongly affect human well-being via alteration or loss of ecosystem services such as food production and biodiversity. The ability to quantify ecosystem resilience and detect early warnings of regime shifts would allow land managers, land owners, and policymakers to make informed decisions, appropriate conservation efforts, and take adaptive measures in the midst of ecological change and uncertainty. In this dissertation, I investigate methods for quantifying ecosystem resilience, novel tools for detecting early warnings of regime shifts, and review current natural resource management policies to determine their ability to foster and maintain ecosystem resilience. Overall results include development of a method for detecting spatiotemporal early warnings of regime shifts decades ahead of time, interpretable metrics for quantifying and comparing ecological resilience over time, and frameworks for prioritizing conservation efforts and land management in this era of non-stationarity. With the current global level of anthropogenic disturbance, these findings demonstrate that assuming constant, linear behavior in ecological systems and not taking preemptive, preventative, and adaptive measures in the face of change will lead to conservation failures and loss of ecosystem services. Instead, this dissertation

provides support for a land management paradigm that embraces ecological complexity, takes action at meaningful scales, and is proactive.

DEDICATION

For Sara first, then for anyone who finds it useful.

ACKNOWLEDGEMENTS

I would like to thank my advisors, Dr. Dirac Twidwell and Dr. Craig R. Allen for their wisdom, mentoring, and giving many, many hours to reading my drafts. I also thank my committee members Drs. David G. Angeler, Larkin A. Powell, and Brady W. Allred for their advice and contributions.

The support of my colleagues Victoria M. Donovan, Daniel R. Uden, Jessica L. Burnett, Christine H. Bielski, Carissa L. Wonkka, and Dillon T. Fogarty has been invaluable to completing this dissertation and my growth as a scientist. Thank you all; it has meant so much. I am proud to call you friends.

There are also many who made my dissertation possible through facilitating field work, providing data, and giving crucial insights. Among these, I extend particular thanks to Ritch Nelson, Chris Helzer, Shawn Stratton, and Amanda Hefner.

Most importantly, I thank my wife Sara Elizabeth Bailey Roberts. You are the best and kindest person I have ever known, and I would not have—could not have—done this without you. Thank you for your patience and grace and encouragement throughout this journey. I can't wait to start the next one with you.

And finally, thank God for fire and birds and prairies and woods.

GRANT ACKNOWLEDGEMENTS

This work was supported by Department of Defense Strategic Environmental Research Development Program W912HQ-15-C-0018, Nebraska Game & Parks Commission W-125-R-1, the USDA NIFA McIntire Stennis project 1008861, the Nebraska Cooperative Fish and Wildlife Research Unit, and the University of Nebraska-Lincoln's Institute of Agriculture and Natural Resources. The Nature Conservancy also provided partial support for this work through the Nebraska Chapter's J.E. Weaver Competitive Grants Program. The Nebraska Cooperative Fish and Wildlife Research Unit is jointly supported by a cooperative agreement between the U.S. Geological Survey, the Nebraska Game and Parks Commission, the University of Nebraska, Lincoln, Nebraska, the United States Fish and Wildlife Service and the Wildlife Management Institute.

TABLE OF CONTENTS

DEDICATION	iv
ACKNOWLEDGEMENTS	v
GRANT ACKNOWLEDGEMENTS	vi
TABLE OF CONTENTS.....	vii
LIST OF TABLES	xv
LIST OF FIGURES.....	xxii
CHAPTER 1: INTRODUCTION.....	1
LITERATURE CITED	7
CHAPTER 2: EARLY WARNINGS FOR STATE TRANSITIONS.....	10
ABSTRACT	10
INTRODUCTION.....	11
LITERATURE REVIEW AND METHODOLOGY	14
SYNTHESIS OF METRICS	16
Known driving state variables/Limited number of state variables	16
Known OR unknown driving state variables/Unlimited number of state variables ..	20
DISCUSSION	27
Management Implications	33
LITERATURE CITED	36
TABLES	51
FIGURES	57

CHAPTER 3: SHIFTING SPATIAL REGIMES IN A CHANGING CLIMATE	62
ABSTRACT	62
MAIN TEXT	63
METHODS.....	76
Experimental Design	76
Statistical Analysis	78
TABLES.....	83
LITERATURE CITED	86
CHAPTER 4: SPATIAL REGIMES: MONITORING FOR EMERGENCE	94
ABSTRACT	94
INTRODUCTION.....	96
METHODS.....	99
Study site	99
Data collection	100
Spatial boundary identification.....	102
Capturing emergence of new spatial regimes over time.....	104
RESULTS.....	106
Spatial boundary identification.....	106
Detecting emergence of spatial regimes	107
DISCUSSION	109
LITERATURE CITED	114

TABLES.....	120
FIGURES	121
CHAPTER 5: PREDICTING REGIMES SHIFTS IN OPEN, COMPLEX SYSTEMS	126
ABSTRACT	126
INTRODUCTION.....	127
Study site	131
Data.....	132
Testing wombling	135
RESULTS.....	137
Wombling identifies boundaries between ecological regimes	137
Wombling predicts changes in spatial regime boundaries	139
DISCUSSION	141
LITERATURE CITED	144
TABLES.....	152
FIGURES	153
CHAPTER 6: CONSERVATION IN THE ERA OF NON-STATIONARITY: RARE	
SPECIES DIVERSITY TRACKS CONTINENTAL REGIME MOVEMENT	160
ABSTRACT	160
INTRODUCTION.....	161
METHODS.....	163
Data Collection	163

Statistical Analysis	164
RESULTS.....	168
DISCUSSION	169
LITERATURE CITED	172
TABLES.....	180
FIGURES	186
CHAPTER 7: CROSS-SCALE RESILIENCE AND COMMUNITY ECOLOGY.....	189
ABSTRACT	189
INTRODUCTION.....	190
METHODS.....	192
Background on the cross-scale resilience model.....	192
Identifying biotic communities.....	193
Calculating cross-scale resilience metrics	194
Test I: Relationship between cross-scale resilience and richness.....	195
Test 2: Relationship between cross-scale resilience and turnover	195
Test 3: Relationship between cross-scale resilience and community similarity and abrupt shifts	196
RESULTS.....	198
Relationship between cross-scale resilience and richness	198
Relationship between cross-scale resilience and turnover	199

Relationship between cross-scale resilience and community similarity and abrupt shifts.....	199
DISCUSSION	200
LITERATURE CITED	205
TABLES.....	212
FIGURES	217
CHAPTER 8: A TEST OF THE SPATIAL PREDICTION OF THE CROSS-SCALE RESILIENCE MODEL	225
ABSTRACT	225
INTRODUCTION.....	226
METHODS.....	229
Study area	229
Data collection.....	230
Statistical analysis.....	232
RESULTS.....	235
Scale domain responses to disturbance	235
Changes in cross-scale functional redundancy, diversity	236
DISCUSSION	237
LITERATURE CITED	241
TABLES.....	247
FIGURES	254

CHAPTER 9: DOUBLETHINK AND SCALE MISMATCH POLARIZE POLICIES

FOR AN INVASIVE TREE	256
ABSTRACT	256
INTRODUCTION.....	257
METHODS.....	260
Focal species.....	260
Study site	263
Data collection.....	265
Evaluating policy-ecology agreement	270
RESULTS.....	271
Ecoregion-level abundance.....	271
Individual land parcels (20-ha).....	271
Policy assessment	272
DISCUSSION	274
Policy implications	278
LITERATURE CITED	280
TABLES.....	293
FIGURES	297
CHAPTER 10: FIRE LEGACIES IN EASTERN PONDEROSA PINE FORESTS	304
ABSTRACT	304
INTRODUCTION.....	306

METHODS.....	309
Study Site.....	309
Site Selection	311
Tree density and Coarse Woody Debris	312
Understory Woody Plant Community Composition	312
Bird Community Composition	313
Analyses.....	313
RESULTS.....	315
Tree Density	315
Coarse Woody Debris.....	315
Understory Woody Plant Community Composition	316
Bird Community Composition	317
DISCUSSION	319
ACKNOWLEDGEMENTS	323
LITERATURE CITED	324
TABLES.....	335
FIGURES	342
APPENDIX A: TO HOLD A BEAUTIFUL, BURNING SNAKE.....	348
I.....	348
II.....	355

III.	361
-----------	-----

LIST OF TABLES

Chapter 2

Table 2. 1: Glossary of terms.....	51
Table 2. 2: Literature review [†] of the total number of papers and the percentage using a quantitative metric [‡] for early warning and regime shift detection in Rangeland Ecology & Management and other journals in the discipline.	53
Table 2. 3: Questions and situational examples for determining when using regime shift/early warning indicator metrics (EWI metrics) could be appropriate. For each question/situation, the “Why” and “Why not” columns provide positive and negative support, respectively, for the use of EWI metrics.....	54

Chapter 3

Table 3. 1: For each year of analysis, number of North American Breeding Bird Survey routes falling within the belt transect, number of routes used in analysis (where ≥ 40 bird species were recorded in a given year), and number of routes removed from analysis (where < 40 bird species were recorded in a given year).	83
Table 3. 2: Power table for use with the “discontinuity detector” method from Barichievy et al. (2018). Columns indicate the species richness at which “d-values” produced by the discontinuity detector indicate a significant gap between log-ranked body masses.....	85

Chapter 4

Table 4. 1: Assembly rules for smooth sumac (<i>Rhus glabra</i>) stand expansion in grasslands and resultant vegetative community composition and structure. Assembly rules are derived from known sumac ecology and are in turn used as rules for simulating the emergence of a smooth sumac spatial regime from observed vegetative community data along a transect at the Niobrara Valley Preserve, Nebraska, USA.	120
--	-----

Chapter 5

Table 5. 1: Model selection using AICc for two questions: 1) assessing relationships between vegetation (tree/grass) and bird community boundaries and 2) determining how bird boundaries responded to distance to vegetation boundaries. Columns indicate the question, the model covariates/smooth terms, the total number of covariates, the estimated AICc value, the delta AICc, and model weight.	152
--	-----

Chapter 6

Table 6. 1: Results from spatial modeling of North American breeding bird communities across a south-north belt transect from 1970 - 2015 using Redundancy Analysis (RDA) and distance-based Moran's eigenvector mapping (dbMEM). From left to right, columns indicate year, number of dbMEM axes detected per year, number of significant dbMEM axes per year, number of significant RDA axes per year, and adjusted R^2 of the minimum (final) RDA model.	180
--	-----

Table 6. 2: Model selection results for analyzing the relationship between richness/diversity of rare bird species (i.e., species with spatially stochastic abundance patterns) to the distance to spatial regime boundaries from 1970 - 2015 North American Breeding Bird Survey. From left to right, columns indicate the response variable, the model, the Akaikie Information Criterion adjusted for small sample sizes (AICc), the delta AICc, and the AICc weight.	183
Table 6. 3: Coefficients from top models resulting from model selection analyzing the relationship between richness/diversity of rare bird species (i.e., species with spatially stochastic abundance patterns) to the distance to spatial regime boundaries from 1970 - 2015 North American Breeding Bird Survey. From left to right, columns indicate the response variable, the predictor variables, the coefficient estimate, the coefficients' standard errors, and the coefficients' test statistics (z-value for richness models, t-value for diversity models).	185

Chapter 7

Table 7. 1: Results from linear mixed models testing the relationship between mean annual species turnover and mean resilience metrics (Response = Mean) and the standard deviation (Response = SD) of annual species turnover and mean resilience metrics at multiple hierarchical scales. Species turnover and resilience metrics were calculated from avian community data recorded at North American Breeding Bird Survey routes from 1966 - 2014 aggregated by US Environmental Protection Agency ecoregions. Columns
--

indicate ecoregion level, response type, variable name, coefficient estimate, standard error of coefficient estimate, and t-value estimate for coefficient. 212

Table 7. 2: Results from linear mixed models testing the relationship between community compositional change over time (slope of Jaccard index over time) and initial and mean resilience metrics at multiple hierarchical scales. Jaccard index and resilience metrics were calculated from avian community data recorded at North American Breeding Bird Survey routes from 1966 - 2014 aggregated by US Environmental Protection Agency ecoregions. Columns indicate ecoregion level, variable name, coefficient estimate, standard error of coefficient estimate, and t-value estimate for coefficient. 214

Table 7. 3: Results from binomial generalized linear mixed models testing synchrony between regime shifts (significant changes in detrended correspondence analysis axis-1 [DCA1]) and resilience metrics at multiple hierarchical scales. DCA1 and resilience metrics were calculated from avian community data recorded at North American Breeding Bird Survey routes from 1966 - 2014 aggregated by US Environmental Protection Agency ecoregions. Columns indicate ecoregion level, variable name, coefficient estimate, standard error of coefficient estimate, z-value estimate for coefficient, and P-value estimate for coefficient. 216

Chapter 8

Table 8. 1: Smooth term coefficient output for the generalized additive mixed model comparing response of breeding bird abundances across scale domains to oil and gas development at different spatial extents. From left to right, columns indicate the

smoothed predictor term (numbers indicate meters), estimated degrees of freedom of smooth term, the pseudo F statistic, and the estimated p-value..... 247

Table 8. 2: Species recorded across rangeland-dominated ecoregions in central North America, their functional groups, their mean log-transformed and untransformed body masses in grams. 247

Chapter 9

Table 9. 1: Percent land cover estimates for three ecoregions in Nebraska, USA. Columns indicate ecoregion name, the total land area within each ecoregion, the subset of land within ecoregions susceptible to eastern redcedar (ERC) invasion, the total land area classified as eastern redcedar, and the percent of susceptible land (i.e., cropland, riverine systems, wetland, and open water classes were not susceptible and were therefore removed from the analysis) covered by eastern redcedar. Land cover was estimated in 2010 and is derived from the Rainwater Basin Joint Venture 30 m remotely-sensed land cover dataset..... 293

Table 9. 2: Examples of agency policies and programs used to manage eastern redcedar and how they align with the scientific basis for invasive species management based on the density-impact invasion curve. Asterisks denote agency programs with scientific support..... 294

Chapter 10

Table 10. 1: Multiple comparisons of mean tree density and mean coarse woody debris at Fort Robinson State Park, Nebraska, 2016 by burn severity using linear models and Tukey post hoc tests. The first column indicates which burn severities are being compared. The following columns contain the t-values and adjusted p-values for live and snag densities. The burn severity classes represent high-severity (H), moderate-severity (M), low-severity (L), and unburnt (U).	335
Table 10. 2: Understory wood plant species observed across a burn severity gradient at Fort Robinson State Park, Nebraska, 2016. The species column indicates the scientific name of each species. The burn severity classes represent (from left to right): high-severity (H), moderate-severity (M), low-severity (L), and unburnt (U). Burn severity column values show the number of sampling locations for a given burn severity class in which species were detected. The number of asterisks indicate if a species was only observed in a single severity class (*) or a single site within a single severity class (**).	336
Table 10. 3: Multiple comparisons of understory woody plant and bird community compositions at Fort Robinson State Park, Nebraska, 2016 by burn severity using PERMANOVAs. The first column indicates which burn severities are being compared via PERMANOVA, the second column contains the initial F-values (from which unadjusted p-values derived), and the third column contains resultant p-values using false discovery rates to adjust for multiple comparisons. The burn severity classes represent high-severity (H), moderate-severity (M), low-severity (L), and unburnt (U).	338

Table 10. 4: Avian species observed across a burn severity gradient at Fort Robinson State Park, Nebraska, 2016. The burn severity classes represent (from left to right): high-severity (H), moderate-severity (M), low-severity (L), and unburnt (U). Burn severity column values show the number of sampling locations for a given burn severity class in which species were detected. The number of asterisks indicate if a species was only observed in a single severity class (*) or a single site within a single severity class (**).

..... 339

LIST OF FIGURES

Chapter 2

Figure 2. 1: A flowchart for determining which multivariate metrics for regime shift/early warning detection are appropriate for a given set of state variables. “Limited” state variables indicates those metrics are suitable for relatively small number of input variables, and “known drivers” means that the input state variables represent known fundamental influences on system state. The lowest tier lists appropriate metrics for a given data type. Metrics in bold have been tested as early warning indicators of regime shifts. Metrics not in bold have been proposed as early warning metrics but only tested as regime shift indicators..... 57

Figure 2. 2: The emergence of new states, and the potential to avoid collapses in existing states, has been a preeminent focus of rangeland ecology and management. Roberts et al. (in review) incorporate spatially-explicit application of a discontinuity analysis into field monitoring data collected along a 4 km transect at the Niobrara Valley Preserve, Nebraska, USA. This study identifies (A) the existing number and types of spatial regimes at the site, (B) the potential for using an early warning indicator in conjunction with the spatial regime concept to identify, via simulation of future field monitoring, the location and spatial scale at which a shrubland regime emerged, (C) and the expansion of the shrubland regime, at the cost to the previously dominant grassland regime, over time. 59

Figure 2. 3: Integrative metrics that accommodate multivariate data are being explored to assess their potential utility to detect early warning and regime change in complex

adaptive systems. Spanbaeur et al. (2014) compare various multivariate and univariate indicators using paleo-diatom data. Several populations of species experienced increased variability in this study, but conflicting patterns make it difficult to operationalize univariate statistics to characterize the behavior of this complex, multivariate system. Similar trends and observations might be expected in rangelands, but research has been limited, to date, to test these concepts and to assess their practical utility to rangeland managers. 60

Figure 2. 4: Future availability of remote sensing products with high spatiotemporal resolution has great potential to be incorporated into multivariate metrics used to detect early warning signals and regime shifts. Shown here are trends in annual percent cover of annual forbs/grasses, perennial forbs/grasses, shrubs, and bare ground from 1984-2017 within an area experiencing cheatgrass invasion. Bars denote the area of the Dun Glenn fire and subsequent smaller scale fires that burned within the original fire perimeter. 61

Chapter 3

Figure 3. 1: Shifts in spatial regime boundaries demonstrated by breeding bird body mass discontinuities from 1970 - 2015 in the North American Great Plains biome. The top panel depicts latitudinal spatial regime boundaries (y-axis) determined by log-ranked avian body mass discontinuities (x-axis). Black dots represent body mass aggregations identified via discontinuity analysis in each breeding bird survey route within the transect. Gray-scale boxes represent spatial regimes, and the northernmost and southernmost spatial regime boundaries are highlighted by blue and red lines,

respectively. The bottom panel depicts spatial regime boundaries (blue triangles = northernmost, red triangles = southernmost) detected each year, and lines represent modeled northernmost and southernmost spatial regime boundary movement over time with 90% confidence (grey ribbon). When northernmost and southernmost boundaries were the same (i.e., when only one spatial regime boundary was detected in a year), blue and red triangles overlap. 66

Figure 3. 2: Visualization and tracking of predicted decadal spatial regimes and their boundaries in the North American Great Plains biome. Black polygons represent the historic Great Plains biome extent. Colored bars represent average number and predicted extents of spatial regimes within the study area over five decades. 68

Figure 3. 3: Global changes influencing ecological regimes in central North America. Global changes such as agricultural land conversion, anthropogenic climate change, urbanization, woody plant encroachment, increasing frequency/intensities of fire, and energy development are all driving ecological change within the North American Great Plains in a putatively south-to-north trajectory. Predictable, directional (poleward) movement of spatial regime boundaries within the Great Plains corresponds to the trajectories of global change drivers. 69

Figure 3. 4: Spatial regime boundary movement between 37 - 42 degrees latitude across a network of protected areas covering in central North America. Black lines indicate level III US Environmental Protection Agency ecoregion boundaries, and green polygons indicate protected areas. The ecoregion labeled No. 1 is the Flint Hills ecoregion, and the ecoregion labeled No. 2 is the Western Corn Belt Plains ecoregion. Predicted spatial

regime boundaries (colored horizontal lines) correspond with linear prediction for the years 1970, 1985, 2000, and 2015 ($\square = 0.032 \pm 0.026$ degrees latitude per year; 90% confidence; $F = 4.093$; $P = 0.052$). 71

Chapter 4

Figure 4. 1: Spatial regimes in vegetative structure and composition identified along a 4 km north-south transect at the Niobrara Valley Preserve, Nebraska, USA. (A) Against a black-white Google Earth aerial image, spatial regimes are colorized by significant breaks in self-similarity identified by constrained hierarchical clustering (dendrogram) and the broken stick model. (B) Using significant regimes, distance-based redundancy analysis shows vegetative variables significantly associated with each regime (regime centroids depicted as colored dots corresponding to colors of dendrogram/transect). Location of text (vegetative variables) indicates the strength of association of “species” scores of the vegetative structural and compositional variables with the first two ordination axes. 121

Figure 4. 2: Spatial regimes identified in observed and simulated vegetative structure and composition along a 4 km north-south transect at the Niobrara Valley Preserve, Nebraska, USA. In the left panel, using the observed data as the initial time step ($t = 0$), a smooth sumac (*Rhus glabra*) shrub “island” was then simulated in the southernmost (green) spatial regime, and the shrub island expanded spatially in three consecutive time steps. Spatial regimes are colorized by significant breaks in self-similarity identified by the broken stick model. Numbers in top-left corners of each panel indicates the time step of

the simulation (i.e., 0 = initial time step [observed data], 1 = first simulated time step, etc.). In the right panel, biplots of distance-based redundancy analyses from three consecutive simulations of significant ($P \leq 0.05$) vegetative structure and composition along the southernmost “Sandhills” portion of the 4 km north-south transect at the Niobrara Valley Preserve, Nebraska, USA. Constrained hierarchical clustering outputs from simulations were used as constraints. Colored dots indicate the centroids of the site scores of each spatial regime (constraint), and text indicates the strength of association of “species” scores of the vegetative structural and compositional variables with the first two ordination axes. See Table S1 for text interpretation..... 122

Figure 4. 3: Spatial regimes identified in observed and simulated vegetative structure and composition along the southernmost “Sandhills” portion of the 4 km transect at the Niobrara Valley Preserve, Nebraska, USA. In the left panel, the initial time step ($t = 0$) used only observed data. A smooth sumac (*Rhus glabra*) shrub “island” was then simulated (red) and expanded spatially in three consecutive time steps. Spatial regimes are colorized by significant breaks in self-similarity identified by the broken stick model. Numbers in top-left corners of each panel indicates the time step of the simulation (i.e., $t = 0$ is the initial time step [observed data], $t = 1$ is the first simulated time step, etc.). In the right panel, biplots of distance-based redundancy analyses from three consecutive simulations of significant ($P \leq 0.05$) vegetative structure and composition along the southernmost “Sandhills” portion of the 4 km north-south transect at the Niobrara Valley Preserve, Nebraska, USA. Constrained hierarchical clustering outputs from simulations were used as constraints. Colored dots indicate the centroids of the site scores of each

spatial regime (constraint), and text indicates the strength of association of “species” scores of the vegetative structural and compositional variables with the first two ordination axes. See Table S1 for text interpretation..... 124

Chapter 5

Figure 5. 1: Generalized additive mixed models demonstrate the relationship between spatial regime boundaries derived from a “wombling” method applied to bird community data with known vegetative tree-grassland spatial regime boundaries derived from remotely-sensed spatial covariance. The y-axis depicts the smoothed, predicted relationship between wombling values (R^2) and spatial covariance values (i.e., not the predicted wombling values). The x-axis shows a scaled range of spatial covariance values. Higher wombling values indicate greater likelihood and strength of a boundary. Spatial covariance values at or near zero indicate no tree-grass boundary, and negative spatial covariance values indicate increasingly stark tree-grass regime boundaries. 153

Figure 5. 2: Generalized additive mixed models demonstrate the relationship between spatial regime boundaries derived from a “wombling” method applied to bird community data with distance to known vegetative tree-grassland spatial regime boundaries derived from remotely-sensed spatial covariance. The y-axis depicts the smoothed, predicted relationship between wombling values (R^2) and distance (log-transformed meters) to the nearest spatial regime boundary. Higher wombling values indicate greater likelihood and strength of a boundary. 154

Figure 5. 3: A selected portion of the study area that was likely to exhibit early warnings of changing spatial regime boundaries (regime shifts) due to encroaching tree regimes into grassland regimes. This portion was less disturbed and is near a ravine in which a few trees could have escaped fire and from which tree regimes could expand without fire disturbance. Panels correspond with 4 years in which tree regime boundaries (red shading) rapidly expanded and displaced grassland regimes. Dots indicate bird community sampling locations. Dot size corresponds with wombling (R^2) values, with larger dots indicating greater likelihood of a spatial regime boundary and smaller dots indicating greater similarity lower likelihood of a boundary..... 155

Figure 5. 4: A selected portion of the study area that was likely to have maintained stable tree-grass spatial regime boundaries due to receiving consistent application of fire and being near the center of a grassland regime. This portion was consistently and heavily disturbed by random and prescribed fires and military training. Panels correspond with 4 years of the 27-year-long study period. Dots indicate bird community sampling locations. Dot size corresponds with wombling (R^2) values, with larger dots indicating greater likelihood of a spatial regime boundary and smaller dots indicating greater similarity lower likelihood of a boundary. 156

Figure 5. 5: A selected portion of the study area that initially contained a boundary between tree-grass regimes and became centers of tree regimes as tree regimes displaced grasslands. This portion was near a major river that would have historically hosted a tree regime and would have provided a source for tree encroachment of grasslands. Panels correspond with 4 years of the 27-year-long study period. Dots indicate bird community

sampling locations. Dot size corresponds with wombling (R^2) values, with larger dots indicating greater likelihood of a spatial regime boundary and smaller dots indicating greater similarity lower likelihood of a boundary..... 157

Figure 5. 6: A selected portion of the study area increasingly fragmented by tree-grass regimes. Panels correspond with 4 years of the 27-year-long study period. Dots indicate bird community sampling locations. Dot size corresponds with wombling (R^2) values, with larger dots indicating greater likelihood of a spatial regime boundary and smaller dots indicating greater similarity lower likelihood of a boundary. 158

Figure 5. 7: Animation depicting changes in spatial regime boundaries from 1991 - 2017 across the entire study area of Fort Riley Army Base, KS, USA. Dots represent wombling R^2 values at sampling locations indicating boundaries (large dots) and areas of self-similarity (small dots) and annual shifts. Background coloration indicates spatial covariance of tree-grass regimes, where deeper reds indicate tree-grass boundaries, white indicates no boundary, and blues indicate positive spatial covariance. 158

Chapter 6

Figure 6. 1: Subcontinental predicted richness (A) and diversity (B) of rare bird species (species with spatially stochastic abundance patterns) over a 46-year period along a south-to-north latitudinal gradient in central North America. The x-axis indicates degrees latitude. Black lines are predicted richness and diversity values, gray-shaded ribbons are 80% bootstrapped confidence limits, and vertical red lines indicate spatial regime boundaries for each year. 186

Chapter 7

Figure 7. 1: Mean cross-correlation estimates and 85% confidence limits between species richness and cross-scale resilience metrics at multiple hierarchical scales. Y-axis indicates degree of correlation (r), and x-axis indicates lags ranging from -5 to 5, where lag 0 indicates annual correlation. Richness and resilience metrics were calculated from avian community data recorded at North American Breeding Bird Survey routes from 1966 - 2014 aggregated by US Environmental Protection Agency ecoregions. Ecoregions range from broad (Level II) to fine (Level IV). *Note: Cross Div = cross-scale diversity; Cross Red = cross-scale redundancy; Num Aggs = number of body mass aggregations; Within Red = within-scale redundancy*..... 217

Figure 7. 2: Coefficient estimates and 85% confidence limits from linear mixed models testing the relationship between mean annual species turnover and mean resilience metrics (red dots) and the standard deviation (SD) of annual species turnover and mean resilience metrics (blue dots) at multiple hierarchical scales. Species turnover and resilience metrics were calculated from avian community data recorded at North American Breeding Bird Survey routes from 1966 - 2014 aggregated by US Environmental Protection Agency ecoregions. Ecoregions range from broad (Level II) to fine (Level IV). *Note: Cross Div = cross-scale diversity; Cross Red = cross-scale redundancy; Num Aggs = number of body mass aggregations; Within Red = within-scale redundancy*..... 219

Figure 7. 3: Coefficient estimates and 85% confidence limits from binomial generalized linear mixed models testing synchrony between abrupt community shifts and resilience metrics at multiple hierarchical scales. Synchrony is defined as simultaneous occurrence of regime shifts (i.e., significant change in first axis of Detrended Correspondence Analysis) and significant shifts in resilience metrics. Abrupt community shifts and resilience metrics were derived from avian community data recorded at North American Breeding Bird Survey routes from 1966 - 2014 aggregated by US Environmental Protection Agency ecoregions. Ecoregions range from broad (Level II) to fine (Level IV). *Note: DCA = first axis of detrended correspondence analysis; Cross Div = cross-scale diversity; Cross Red = cross-scale redundancy; Num Aggs = number of body mass aggregations; Within Red = within-scale redundancy.* 221

Figure 7. 4: Comparison of synchrony between periods of significant avian abrupt community shifts (red blocks) and periods of significant changes in cross-scale resilience metrics across a sample of Level III Environmental Protection Agency ecoregions from 1966 - 2014. Black lines indicate predicted values from GAMs, grey shading indicates pointwise 85% confidence limits around predictions, and colored sections indicate regions of significant change in time series (where simulated confidence limits of derivatives from GAMs did not encompass zero). *Note: Cross Div = cross-scale diversity; Cross Red = cross-scale redundancy.* 223

Chapter 8

Figure 8. 1: Outputs from generalized additive mixed models testing the spatial prediction of the cross-scale resilience model, namely that response to loss of resource aggregations across scales will cause non-random declines in biota according to their scale domains. Y-axes indicate modeled responses of scale domains to oil and gas development (resource loss), and x-axes indicate the range of scale domains (median log-transformed body masses) detected in breeding bird communities in rangeland ecoregions in central North America. Panels reflect scales of resource loss (buffer size around bird survey transects)..... 254

Figure 8. 2: Changes in cross-scale resilience of breeding birds resulting from oil and gas development. Y-axis indicates number of species in scale domains determined to be affected by oil and gas development, colored by functional group. X-axis indicates the range of scale domains (median body masses) detected in breeding bird communities across rangeland ecoregions in central North America. The x-axis is on a natural log scale..... 255

Chapter 9

Figure 9. 1: Type II density-impact invasion curve adapted from Yokomizo et al. (2009). Depicts the sigmoidal relationship between an invasive species' density or area covered and the cost or impact to socio-ecological systems. The colored bar above the curve shows preferable management strategies for the four stages of invasion based on feasibility, likelihood of success, and cost-effectiveness..... 297

Figure 9. 2: Study site. Locations of three ecoregions that are a priority for grassland conservation, according to the Nebraska Legacy Project, and which form the basis for assessing the degree of concordance between policy and science in the management of the native invader eastern redcedar (<i>Juniperus virginiana</i>) in Nebraska, USA.	298
Figure 9. 3: Outline of the hierarchical invasive species management policy creation process for USA natural resources agencies. Arrows indicate the direction of hierarchical control, with federal legal mandates being the highest level. Columns represent the policy creation process (first column), examples of groups that create, enforce, and implement the policies (second column), and the policy-directed duties of the groups at each level (third column).	299
Figure 9. 4: Land cover classifications for the three ecoregions used in our assessment. A: Cherry County Wetlands, B: Central Loess Hills, C: Loess Canyons. Dataset used with permission from the Rainwater Basin Joint Venture.	300
Figure 9. 5: The relative impact costs of eastern redcedar on individual land parcels in each ecoregion. Shown here is the range of impacts related to abundance (not the relative distribution of land with eastern redcedar cover within each ecoregion). Sigmoidal line lengths depict the range of eastern redcedar density/cover located in at least one 50 acre (20.2 ha; 450 m x 450 meter) cell in each ecoregion in 2010, relative to eastern redcedar's known sigmoidal density-impact relationship.	301
Figure 9. 6: Mismatch between the science and policy of managing eastern redcedar invasions in Nebraska, USA. Aerial photographs show examples of each eastern redcedar invasion stage found in 20.2 ha parcels of land from each ecoregion. Photographs are	

arranged under the “theory-based management strategy” that would maximize the returns based on the density-impact model as well as under the “current management strategy” implemented in natural resources agency policies. As shown here, control of eastern redcedar only occurs during periods of exponential growth. Policies promote spread during incipient invasions and ignore opportunities for restoration following a regime shift. 302

Figure 9. 7: Agency policy prioritization for managing eastern redcedar invasions.

Current natural resources agency prioritization (shown as downward-pointing triangle, where greater width indicates greater prioritization) is based on eastern redcedar density and spatial pattern of abundance, but this directly counters theoretical foundations that guide non-native species invasions (shown as upward-pointing triangle, where greater width indicates greater prioritization). The aerial image is from Google Earth. 303

Chapter 10

Figure 10. 1: Images of a typical study site sampled in the summer of 2016 for unburned forest and low, moderate and high severity burned forests from the 1989 Fort Robinson wildfire. 342

Figure 10. 2: a. The northeastern distribution of ponderosa pine in the United States provided by the US Forest Service indicated in green b. The Pine Ridge region of Nebraska, with the 1989 Fort Robinson wildfire in red and ponderosa pine distribution in green c. The distribution of sampling sites of different fire severity classes, indicated by colored points, within the Fort Robinson (42.6693° N, 103.4689° W) wildfire perimeter

(black), ponderosa distribution in green and public land boundaries for Fort Robinson State Park and Peterson Wildlife Management Area (grey). 343

Figure 10. 3: Forest stand structure across a 27-year-old burn severity gradient at Ft.

Robinson State Park, Nebraska, 2016. The top panel shows boxplots of tree density per hectare for each burn severity class. The bottom panel shows boxplots of percent cover per 30 m transect of coarse woody debris for each burn severity class. The burn severity classes represent high-severity (High), moderate-severity (Moderate), low-severity (Low), and unburned (Unburned). 344

Figure 10. 4: Mean understory woody plant (panel A) and bird (panel B) species richness by burn severity in Fort Robinson State Park, Nebraska, 2016. Bars indicate 95%

confidence limits. The burn severity classes represent high-severity (High), moderate-severity (Moderate), and low-severity (Low), and unburned (Unburned). 345

Figure 10. 5: Mean constrained site scores and species scores for the first two axes of a canonical correspondence analysis for understory woody plant (panel A) and bird (panel

B) community composition data across a burn severity gradient in Fort Robinson State Park, Nebraska. Bars indicate 95% confidence limits of the mean site scores. The burn

severity classes represent high-severity (H), moderate-severity (M), low-severity (L), and unburned (U). Plant species scores are represented by the first two letters of genus and

the first two letters of species, and bird species scores correspond to American

Ornithological Union species abbreviations. See Tables S2, S4 for plant and bird species, respectively. 346

CHAPTER 1: INTRODUCTION

We live in a non-stationary world: waves of trees turn grasslands into forests, trees burn and forests fall into savannas or grasslands, humans plant new species that sprout and spread like wildfire, and whole biomes expand and contract like lungs, or even collapse and reemerge as completely novel ecologies (Archer et al., 2017; Hobbs et al., 2006; Staver, Archibald, & Levin, 2011). These are not new phenomena—they have been occurring for millennia (Baker, 2018; Keeley & Rundel, 2005; Mayewski et al., 2004). What is new is the rate at which they are occurring, our understanding of humanity's role in causing them, and our ability to measure them (Hampton et al., 2013; Rockström et al., 2009).

What is left, then, is how to act upon this knowledge. How can we grapple with global changes like climate change, afforestation of grasslands, loss of rangeland productivity to oil and gas development, and invasive species? And when these changes build into critical transitions—such that the fundamental ecological structures and processes that make ecosystems are altered and the goods and services humans derive from ecosystems are threatened—how do we respond? Do we continue with business as usual and hope for the best, or do we take proactive steps to predict changes and reverse the problems?

Although it cannot answer the “should we’s?” and “why’s?” implicit in these questions, the discipline of ecology is uniquely suited to answer the “how’s” explicit in

them. For instance, central pursuits in ecology include estimating the diversity and distribution of species (Hutchinson, 1959), understanding how systems absorb disturbance while maintaining their essential structures and functions (Holling, 1973), and transcending description to reach prediction (Peters, 1991). In response to these pursuits, ecological resilience theory and the allied complexity theory arose to attempt to describe and predict changes and behaviors of so-called complex adaptive systems—which ecosystems are counted as (Holling, 1973; Levin, 1998). These theories provided frameworks to account for and predict uncertainty, complexity, and non-stationarity in ecological systems. Broadly, resilience theory acknowledges that ecosystems are not static, that multiple alternative ecosystem states exist, and that the resilience of a system is an emergent attribute that determines how much disturbance the system can absorb before shifting into an alternate state (i.e., a regime shift) (Holling, 1973). Similarly, complexity theory assumes that the properties of a system are greater than the simple sum of its parts (meaning systems have emergent properties), that complex adaptive systems self-organize and exhibit self-similarity (hallmarks of ecosystems), perfect knowledge of system behavior cannot be attained, and uncertainty must therefore be embraced (Levin, 1998). Together, resilience and complexity theory provide a foundation for grappling with non-stationarity and for securing the goods and services ecosystems provide humanity.

Spawned from resilience and complexity theories, ecology has now begun pursuing tools capable of predicting ecosystem vulnerability to regime shifts, metrics for quantifying ecological resilience, and assessing how our current natural resource

management policies foster or erode resilience (Angeler & Allen, 2016; Scheffer et al., 2009; Twidwell, Allred, & Fuhlendorf, 2013). For example, the search for early warnings of regime shifts has exploded in the past two decades (Clements & Ozgul, 2018; Dakos, Carpenter, Nes, & Scheffer, 2015). Early warning indicators seek to detect signals of impending regime shifts in ecosystems and thereby provide managers and policymakers time to take action and “turn back from the brink” (Biggs, Carpenter, & Brock, 2009). Additionally, quantifying resilience has progressed from using subjective “resilience surrogates” to estimate resilience to metrics that more directly represent the cross-scale structure and function of ecosystems (Allen, Gunderson, & Johnson, 2005; Bennett, Cumming, & Peterson, 2005). These metrics are meant to enable tracking of resilience over time and space and determine how disturbances and management affect system resilience (Sundstrom et al., 2018). And finally, models of complex system behaviors such as models of invasive species impacts and models of ecological vulnerability have been developed to promote efficient, scientifically-based strategies for managing non-stationary natural resources (Yokomizo, Possingham, Thomas, & Buckley, 2009).

In this dissertation, I synthesize these theories and tools I have discussed to develop novel methodologies and strategies for managing ecosystems in a non-stationary world. The structure of this dissertation begins with a review of the current state of resilience and complexity-based tools in natural resources management (e.g., rangelands) and a synthesis of promising new concepts and methods. It then moves to several studies operationalizing and investigating individual tools and methods. I then end with two examples of applying resilience and complexity theory to current local (Nebraskan)

management issues (although I hope their implications extend well beyond Nebraska).

Below are more detailed previews of the following chapters.

In Chapter 2, I review the science of early warnings of regime shifts and propose new concepts and methods for detecting and acting upon non-stationarity (Roberts et al., 2018). Due to its historic contributions to understanding change and alternative states in ecology, the subdiscipline of rangeland ecology serves as the platform for this review. I review multivariate signals of early warning and then discuss the potential for the “spatial regimes” concept to push monitoring for early warnings in rangelands forward.

In Chapter 3, I operationalize the spatial regimes concept and test its ability to detect early warnings across continental spatial extents using 46 years of avian community data. I find that tracking spatial regimes can provide early warnings of regime shifts decades ahead of time. I then discuss implications of the mobilization of regimes across continents and how land management can leverage multi-decadal planning horizons.

In Chapters 4 and 5, I test the spatial regimes concept at smaller scales to determine if emergence of novel regimes can be detected and if spatial regime detection can assess spatial vulnerability in time and space. For Chapter 4, I use vegetation data from a 4 km spatial transect to identify spatial regime boundaries and show via simulation that monitoring frameworks using spatial regimes can detect emergence of novel regimes. For Chapter 5, I use remotely-sensed vegetation and avian survey data over 27 years to test a new method (dubbed “wombling” after its creator) to track

spatiotemporal vulnerability to regime shifts and determine if animal and plant regime boundaries covary in time and space.

In Chapter 6, I extend upon the spatial regimes tracking in Chapter 3: I identify scaling patterns in biotic communities and demonstrate non-stationary, yet predictable, patterns in rare and at-risk species distributions. These findings indicate that successful conservation efforts will account for moving targets (literally). Because species do not respond idiosyncratically to global change, management can be strategized, and explicit spatiotemporal prioritization can be achieved.

In Chapters 7 and 8, I turn to testing core predictions of resilience theory and the interpretability of resilience metrics. To do this, I use the cross-scale resilience model, which predicts the resilience of systems is determined by cross-scale patterns of functional diversity and redundancy. For Chapter 7, I find that resilience metrics do support core resilience predictions. These are: resilient systems can be unstable; resilience does not correlate with a particular species assemblage; but resilience does correlate and predict significant community change. Then in Chapter 8, I apply these cross-scale resilience metrics to assess the effects of a major anthropogenic disturbance, energy development in the Great Plains, on cross-scale structure and resilience of biotic communities.

And finally, in Chapters 9 and 10, I use models derived from resilience and complexity theory to assess current Nebraskan natural resource management policies. For Chapter 9, I review publicly-available Nebraskan natural resource management policies for the invasive tree *Juniperus virginiana*, which is contributing to an ongoing biome-

level regime shift from grassland to forest in the North American Great Plains (Roberts, Uden, Allen, & Twidwell, 2018). I find that current policies do not align with current science for managing invasive species; instead, policies evidence “doublethink” by fostering spread of these trees while simultaneously providing financial incentives to remove these same trees. In Chapter 10, I investigate the legacy of a mixed-severity fire that burnt 27 years ago in eastern ponderosa pine—the Pine Ridge region of Nebraska (Roberts et al., 2019). Although mixed-severity fire has been labeled “catastrophic” to ponderosa pine forests in the Nebraska State Wildlife Action Plan, I find that complexities generated from mixed-severity fire continued bolstering species and habitat diversity 27 years post-fire.

LITERATURE CITED

- Allen, C. R., Gunderson, L., & Johnson, A. (2005). The use of discontinuities and functional groups to assess relative resilience in complex systems. *Ecosystems*, 8(8), 958.
- Angeler, D. G., & Allen, C. R. (2016). Quantifying resilience. *Journal of Applied Ecology*, 53(3), 617–624.
- Archer, S. R., Andersen, E. M., Predick, K. I., Schwinning, S., Steidl, R. J., & Woods, S. R. (2017). Woody plant encroachment: Causes and consequences. In *Rangeland systems* (pp. 25–84). Springer.
- Baker, W. L. (2018). Transitioning western us dry forests to limited committed warming with bet-hedging and natural disturbances. *Ecosphere*, 9(6), e02288.
- Bennett, E., Cumming, G., & Peterson, G. (2005). A systems model approach to determining resilience surrogates for case studies. *Ecosystems*, 8(8), 945–957.
- Biggs, R., Carpenter, S. R., & Brock, W. A. (2009). Turning back from the brink: Detecting an impending regime shift in time to avert it. *Proceedings of the National Academy of Sciences*, 106(3), 826–831.
- Clements, C. F., & Ozgul, A. (2018). Indicators of transitions in biological systems. *Ecology Letters*, 21(6), 905–919.
- Dakos, V., Carpenter, S. R., Nes, E. H. van, & Scheffer, M. (2015). Resilience indicators: Prospects and limitations for early warnings of regime shifts. *Philosophical Transactions of the Royal Society B: Biological Sciences*, 370(1659), 20130263.

- Hampton, S. E., Strasser, C. A., Tewksbury, J. J., Gram, W. K., Budden, A. E., Batcheller, A. L., ... Porter, J. H. (2013). Big data and the future of ecology. *Frontiers in Ecology and the Environment*, 11(3), 156–162.
- Hobbs, R. J., Arico, S., Aronson, J., Baron, J. S., Bridgewater, P., Cramer, V. A., ... others. (2006). Novel ecosystems: Theoretical and management aspects of the new ecological world order. *Global Ecology and Biogeography*, 15(1), 1–7.
- Holling, C. S. (1973). Resilience and stability of ecological systems. *Annual Review of Ecology and Systematics*, 4(1), 1–23.
- Hutchinson, G. E. (1959). Homage to santa rosalia or why are there so many kinds of animals? *The American Naturalist*, 93(870), 145–159.
- Keeley, J. E., & Rundel, P. W. (2005). Fire and the miocene expansion of c4 grasslands. *Ecology Letters*, 8(7), 683–690.
- Levin, S. A. (1998). Ecosystems and the biosphere as complex adaptive systems. *Ecosystems*, 1(5), 431–436.
- Mayewski, P. A., Rohling, E. E., Stager, J. C., Karlén, W., Maasch, K. A., Meeker, L. D., ... others. (2004). Holocene climate variability. *Quaternary Research*, 62(3), 243–255.
- Peters, R. H. (1991). *A critique for ecology*. Cambridge University Press.
- Roberts, C. P., Donovan, V. M., Wonkka, C. L., Powell, L. A., Allen, C. R., Angeler, D. G., ... Twidwell, D. (2019). Fire legacies in eastern ponderosa pine forests. *Ecology and Evolution*, 10.1002/ece3.4879.

- Roberts, C. P., Twidwell, D., Burnett, J. L., Donovan, V. M., Wonkka, C. L., Bielski, C. L., ... others. (2018). Early warnings for state transitions. *Rangeland Ecology & Management*, 71, 659–670.
- Roberts, C. P., Uden, D. R., Allen, C. R., & Twidwell, D. (2018). Doublethink and scale mismatch polarize policies for an invasive tree. *PloS One*, 13(3), e0189733.
- Rockström, J., Steffen, W., Noone, K., Persson, Å., Chapin III, F. S., Lambin, E., ... others. (2009). Planetary boundaries: Exploring the safe operating space for humanity. *Ecology and Society*, 14(2).
- Scheffer, M., Bascompte, J., Brock, W. A., Brovkin, V., Carpenter, S. R., Dakos, V., ... Sugihara, G. (2009). Early-warning signals for critical transitions. *Nature*, 461(7260), 53.
- Staver, A. C., Archibald, S., & Levin, S. A. (2011). The global extent and determinants of savanna and forest as alternative biome states. *Science*, 334(6053), 230–232.
- Sundstrom, S. M., Angeler, D. G., Barichievy, C., Eason, T., Garmestani, A., Gunderson, L., ... others. (2018). The distribution and role of functional abundance in cross-scale resilience. *Ecology*, 99(11), 2421–2432.
- Twidwell, D., Allred, B. W., & Fuhlendorf, S. D. (2013). National-scale assessment of ecological content in the world's largest land management framework. *Ecosphere*, 4(8), 1–27.
- Yokomizo, H., Possingham, H. P., Thomas, M. B., & Buckley, Y. M. (2009). Managing the impact of invasive species: The value of knowing the density–impact curve. *Ecological Applications*, 19(2), 376–386.

CHAPTER 2: EARLY WARNINGS FOR STATE TRANSITIONS¹

ABSTRACT

New concepts have emerged in theoretical ecology with the intent to quantify complexities in ecological change that are unaccounted for in state-and-transition models and to provide applied ecologists with statistical early warning metrics able to predict and prevent state transitions. With its rich history of furthering ecological theory and its robust and broad-scale monitoring frameworks, the rangeland discipline is poised to empirically assess these newly proposed ideas while also serving as early adopters of novel statistical metrics that provide advanced warning of a pending shift to an alternative ecological regime. We review multivariate early warning and regime shift detection metrics, identify situations where various metrics will be most useful for rangeland science, and then highlight known shortcomings. Our review of a suite of multivariate-based regime shift/early warning indicators provides a broad range of metrics applicable to a wide variety of data types or contexts, from situations where a great deal is known about the key system drivers and a regime shift is hypothesized a

¹ Roberts, C. P., Twidwell, D., Burnett, J. L., Donovan, V. M., Wonkka, C. H., Bielski, C. L., ... & Jones, M. O. (2018). Early Warnings for State Transitions. *Rangeland Ecology & Management*. 71(6), 659-670.

CPR contributed to conceptualization, formal analysis, data curation, all writing aspects, visualization, and project administration. DT, JLB, VMD, CHB, CLW, CRA, DGA, ASG, TE, SMS, MOJ, BWA, and DEN contributed to conceptualization and writing selected sections.

priori, to situations where the key drivers and the possibility of a regime shift are both unknown. These metrics can be used to answer ecological state-and-transition questions, inform policymakers, and provide quantitative decision-making tools for managers.

INTRODUCTION

Rangeland evaluation and monitoring have been intertwined with advances in ecological theory since the early 20th century (Clements, 1916; Sampson, 1917, 1919). Early successional theory (Clements, 1916) motivated evaluations that linked rangeland degradation to shifts in vegetation following an orderly successional trajectory (Sampson, 1917, 1919; West, 2003). Models of successional retrogression, introduced shortly after coordinated federal monitoring efforts, attempted to provide solutions to the deleterious grazing practices and unrestricted livestock use contributing to widespread soil erosion and increasing dominance of species with lower forage value (Dyksterhuis, 1949). The successional retrogression model dominated rangeland management for 50 years, until advances in alternative state theory and the inability of the succession-retrogression model to explain many changes in rangelands prompted a shift to the state-and-transition modeling framework introduced by Westoby, Walker, & Noy-Meir (1989). State-and-transition models are one of the most commonly-used management frameworks in the world (i.e. USDA Ecological Site Descriptions State-and-Transition Models), but capture only a small component of the complex, adaptive behaviors that ultimately determine why ecosystems persist or, alternatively, change form (Twidwell, Allred, & Fuhlendorf, 2013). New concepts have emerged in theoretical ecology with the intent to not only quantify complexities in ecological change inherently unaccounted for in state-and-

transition models but to also help applied ecologists “turn back from the brink” prior to reaching regime shifts (i.e. state transitions; definitions provided in Table 2.2.1) in ecological systems (Biggs, Carpenter, & Brock, 2009). These concepts center around the theory that ecological systems can exist in multiple, dynamic basins of attraction (i.e. regimes), fundamentally similar to “states” of the state-and-transition models (Briske, Bestelmeyer, Stringham, & Shaver, 2008; Scheffer & Carpenter, 2003).

Overwhelming disturbance(s) can push a regime past a threshold and into an alternate regime (D. D. Briske, Fuhlendorf, & Smeins, 2005; Folke et al., 2004; Scheffer & Carpenter, 2003). Systems that have undergone shifts to regimes with lower ecosystem service potential (e.g., desertification or woody encroachment of rangelands) may exhibit hysteretic behavior; that is, restoration to the previous regime would require more effort than if it had been initiated prior to the regime shift, or the restoration would be practically infeasible (Angeler & Allen, 2016; Folke et al., 2004; Scheffer, Carpenter, Foley, Folke, & Walker, 2001). Using metrics that signal early warning indicators (EWIs) and avoid regime shifts that are undesirable have therefore become a central pursuit in ecology (Andersen, Carstensen, Hernandez-Garcia, & Duarte, 2009; Brock & Carpenter, 2006, 2012; Dakos et al., 2012), especially for known regime changes that exhibit strong hysteretic behavior. Theoretical ecologists have explored the behavior of state variables in systems on the cusp of regime shifts or where regime shifts were known a priori (Carpenter et al., 2011; Mantua, 2004). Much work has been done to assess early warning signals of regime shifts with univariate data and simple model systems (Burthe et al., 2015); however, univariate indicators may not capture the true complexity of ecosystem

change possible with multivariate methods (Allen & Holling, 2008; Eason et al., 2016; Rodionov, 2004; Spanbauer et al., 2014).

The rangeland discipline, given its emphasis on long-term multivariate experimentation and monitoring programs that occur across multiple spatial and temporal scales, is poised to uniquely contribute to the science of early warnings and regime shifts in ecology. Theoretical ecology will benefit from the myriad of multivariate monitoring data available in rangelands to continue the tradition in rangelands of empirically testing new ideas associated with ecological assembly (Briske et al., 2005). The rangeland discipline will also benefit from merging convergent theoretical ecology concepts and techniques aimed at quantifying state transitions and providing a quantitative basis for making decisions in rangeland management (Allen et al., 2016; Angeler & Allen, 2016). But despite the applicability of early warning and regime shift theory to rangeland science, evidence suggests that rangeland science is lagging in the assessment of theoretical indicators used for regime shift prediction (Table 2.2). To date, most rangeland research has focused on qualitative assessments of state transitions, as opposed to quantitative and predictive metrics (Bestelmeyer et al., 2009; Twidwell et al., 2013; but see Bashari et al. 2008; Table 2.2).

In this paper, we review and discuss multivariate metrics used to detect early warnings and regime shifts along with their utility in rangeland evaluation and monitoring. We focus on multivariate metrics with potential utility for detecting rangelands in transition, as opposed to univariate indicators, because the rangeland discipline has a long history of multivariate data inventory and monitoring, and

comprehensive reviews of univariate metrics already exist that can guide rangeland specialists (Dakos et al., 2012). For each metric, we review the conceptual foundation leading to its proposed use as an early warning indicator of system-level change, highlight known shortcomings, and identify specific situations where each metric will be most useful for rangeland science, monitoring, and management. A suite of multivariate-based early warning and regime shift indicators were reviewed in this paper and provide a broad range of potential metrics applicable to a wide variety of data types and contexts - from situations where a great deal is known about the key system drivers and a regime shift is a priori hypothesized, to situations where the key drivers and the possibility of a regime shift are both unknown. We then provide three examples that showcase the potential utility of these metrics to future pursuits in rangeland science and management.

LITERATURE REVIEW AND METHODOLOGY

We conducted a formal review using Web of Science to compile different multivariate metrics used for early warning and regime shift detection (“Web of science,” 2016); accessed on January 2016 - June 2016). Accordingly, we used the following search terms: “Regime Shift AND Multivariate AND Each Metric Type”.

We found 70 articles that used multivariate early warning and regime shift metrics in ecological studies. In these articles, we found ten unique metrics, with the number of articles using each metric varying from 1 - 14 (Average Standard Deviates = 4, Conditional Probability Analysis = 1, Detrended Correspondence/Detrended Canonical Correspondence Analysis = 11, Discontinuity Analysis = 4, Fisher Information = 14, Generalized Modeling = 2, Intervention Analysis/Autoregressive Moving Averages = 5,

Redundancy Analysis-distance-based Moran's Eigenvector Map/Asymmetric Eigenvector Map = 11, Sequential T-test Analysis of Regime Shifts = 14, Vector Autoregressive Model = 4). Three metrics had been tested as EWI metrics (Conditional Probability Analysis, Discontinuity Analysis, Fisher Information), and the rest were regime shift detection metrics that have the potential to be or have been proposed as EWI metrics. Thus, we hereafter distinguish between "tested" and "proposed" EWI metrics. The earliest application of multivariate EWI metrics was in the early 1990's (Ebbesmeyer et al., 1991), and their use sharply increased beginning in the early 2000's ("Web of science," 2016). Most studies we found used EWI metrics for time-series and aquatic system applications (Kirkman et al., 2015; Mantua, 2004), with only two studies using EWI metrics to detect regime shifts in space or terrestrial systems (Sundstrom et al., 2017; Zurlini, Jones, Riitters, Li, & Petrosillo, 2014).

To assist in the appropriate selection and application of multivariate EWI metrics in rangeland applications, we categorized metrics hierarchically according to their assumptions and data type requirements (Figure 2.2.1) and organized the review accordingly. The primary division lies in whether driving state variables are known or unknown for the system in question (Table 2.3) and whether a relatively small (i.e., limited), or a relatively large (i.e., unlimited) number of state variables have been measured (Figure 2.2.1). The second division separates metrics by whether they require the spatial or temporal "location" of a regime shift to be hypothesized a priori (Figure 2.2.1). The tertiary division splits metrics by specific data type requirements (Figure 2.2.1).

SYNTHESIS OF METRICS

Known driving state variables/Limited number of state variables

Metrics in this division (known/limited) share two assumptions: driving state variables are known, and driving state variables interact with each other (Figure 2.2.1).

Known/limited metrics all use regression-like methods, estimate coefficients, and have implicit significance tests (Lade & Gross, 2012; Solow & Beet, 2005), making them similar to non-linear threshold modeling techniques (Sasaki, Okayasu, Jamsran, & Takeuchi, 2008). For these metrics, the regime is defined by modeling the interactions and variability amongst the chosen state variables, and a regime shift is detected when the behavior of state variables deviate significantly from a “typical” range at given level of confidence (Gal & Anderson, 2010; Lade, Tavoni, Levin, & Schlüter, 2013). Two of the known/limited metrics require a priori hypotheses of regime shift locations (Average Standard Deviates, Intervention Analysis/Autoregressive Moving Averages), and two known/limited metrics do not require a priori regime shift hypotheses (Vector Autoregression, Generalized Modeling). Known/limited metrics that do not require a regime shift to be hypothesized a priori can potentially provide early warnings if trends in state variable behavior approach the given confidence limit (Ives & Dakos, 2012).

These metrics can provide detailed quantitative and statistically rigorous results, but they require substantial system-specific a priori knowledge (Gal & Anderson, 2010; Rudnick & Davis, 2003). Major benefits of known/limited metrics include: (1) their ability to assess the validity of regime shifts and early warnings via null hypothesis tests and information theoretic approaches and (2) their ability to estimate the directionality

and relative importance of the chosen driving state variables via coefficient estimation (Gal & Anderson, 2010; Lade & Gross, 2012). Because known/limited metrics assume driving state variables are known, correctly selecting state variables is essential (Solow & Beet, 2005). Not including major driving variables or analyzing irrelevant variables could produce biased estimates or fail to detect regime shifts (S. R. Hare & Mantua, 2000). Additionally, overly conservative confidence requirements or biased estimates of “typical” ranges of state variable behavior may cause regime shift detection to lag (Ives & Dakos, 2012).

Regime shift hypothesized a priori

Average Standard Deviates

Average Standard Deviates (ASD), developed by Ebbesmeyer et al. (1991), is a proposed EWI metric that focuses on identifying significant regime shifts using the magnitude of change in multiple time series records between pre- and post- a priori identified regime shift dates. S. R. Hare & Mantua (2000), Rudnick & Davis (2003), and Mantua (2004) summarize the methods in detail. Regime shifts are considered significant if the sign of standard deviates in all years is the same within each “half record” (designated by the location of the a priori identified step change) but opposite between half records, and no value is within a standard error of zero. This method has been strongly contested by Rudnick & Davis (2003), who remark on how it is designed to specifically create a step change and is highly sensitive to false positives when there is noise in the data. Mantua (2004) suggests an alternative method to mitigate this weakness, but to our knowledge,

this has not been assessed within ecological regime shift literature. As of this review, ASD has been used solely in marine environments Mantua (2004).

Intervention Analysis/Autoregressive Moving Averages

Intervention analysis (IA; Wei, 1994) combined with autoregressive moving averages (ARMA) is a paired method for detecting significant changes in the mean of state variables in a time series while accounting for temporal autocorrelation (Andersen et al., 2009; Mantua, 2004). Together, intervention analysis and autoregressive moving average models (IA/ARMA) have been used to estimate the significance and magnitude of regime shifts in time series data (Gedalof, Smith, & others, 2001). IA/ARMA requires either a priori knowledge of the regime shift (intervention) or an estimate of the temporal location of the shift, which can be identified by visual inspection of the time series data (Mantua, 2004). Intervention analysis is a method for confirming the presence of a regime shift on time series data, and ARMA is used in combination with IA when temporal autocorrelation is present or suspected in the data. Although IA accounts for stochastic noise, it may provide more useful knowledge about a system when using detrended data (Mantua, 2004).

No regime shift hypothesized a priori

Vector Autoregressive Model

Vector Autoregressive Modeling (VAR) models interactions between state variables and estimates coefficients much like a least squares regression (Mantua, 2004) and identifies regime shifts as switches from locally steady states in fitted values (Gal & Anderson, 2010). A parametric bootstrapping technique can determine statistical significance of

changes in fitted values, and Markov-switching techniques can be added (Gal and Anderson, 2010). VAR has been applied to time-series data in aquatic systems and simulated data (Gal & Anderson, 2010; Ives & Dakos, 2012; Mantua, 2004; Solow & Beet, 2005). VAR can detect unknown (not hypothesized a priori) regime shifts and accounts for autocorrelation between variables and observations (Ives & Dakos, 2012). VAR cannot detect a regime shift in the first or last observation of a time-series, potentially causing lagged early warnings of regime shifts (Gal & Anderson, 2010). However, fitted values approaching the limit of the typical range of variability in a system could still provide an early warning signal (Ives & Dakos, 2012).

Generalized Modeling

Introduced by Lade & Gross (2012), generalized modeling (GM) as a proposed EWI metric creates dynamical functions to describe each variable and their interactions with other variables. Across a macroscopic time-scale, certain variables are assumed to change rapidly and stochastically around a locally stable state (“fast” variables), whereas others change gradually (“slow variables”). GM detects early warnings or regime shifts when eigenvalues in the “fast” variables shift away from their locally-stable state (Lade & Gross, 2012). The GM metric is advantageous in that it requires relatively few time-series data points to robustly detect early warnings or regime shifts (Lade & Gross, 2012; Lade et al., 2013), and it can account for stochastic fluctuations in fast variables (Lade and Gross, 2012). However, high levels of noise in fast variables are known to decrease the accuracy of regime shift detection (Lade & Gross, 2012). Although GM has received

little rigorous statistical testing in ecology, it shares many potential applications with the VAR metric (Lade & Gross, 2012).

Known OR unknown driving state variables/Unlimited number of state variables

Overall, metrics in this division (unknown/unlimited) have fewer assumptions than the previous division (Angeler & Johnson, 2012; Spanbauer et al., 2016; Figure 2.2.1). They do not require a priori knowledge about which state variables drive system form and function (although known driving state variables can be used), can readily accept an unlimited number of state variable inputs, and do not require a priori hypotheses of the spatial or temporal locations of regime shifts (Carstensen, Telford, & Birks, 2013; Eason et al., 2016; Rodionov, 2004; Sundstrom et al., 2017; Zurlini et al., 2014). However, a few unknown/unlimited metrics have specific data type requirements, which produce tertiary divisions (Figure 2.2.1). Metrics that accept any type or combination of state variables (Sequential T-test Analysis of Regime Shifts, Detrended Correspondence Analysis, Detrended Canonical Correspondence Analysis, Redundancy Analysis/distance-based Moran Eigenvector Maps or Asymmetric Eigenvector Maps, Fisher Information) define regimes by condensing state variables into a single value as a series of data points (e.g. a time-series, a spatial transect). These values fall within a stable range of variability, and regime shifts occur when values exceed a pre-determined range of variability (e.g., Karunanithi, Garmestani, Eason, & Cabezas (2011); Baho, Drakare, Johnson, Allen, & Angeler (2014)). Discontinuity analysis, identifies gaps, or scale-breaks, in continuous, rank-ordered data of a single type (Allen & Holling, 2008). Finally, Conditional Probability Analysis requires explicitly spatial data to detect shifts in

cross-scale spatial state variable connectivity (Zurlini et al., 2014). Major advantages of unknown/unlimited metrics include their flexibility and the fact that three have been tested for EWI applications (Fisher Information, Discontinuity Analysis, Conditional Probability Analysis; Figure 2.2.1). Additionally, these metrics can consider an unlimited number of state variables and combinations of data types (except for Discontinuity Analysis and Conditional Probability Analysis-see below; Figure 2.2.1), and they require little to no a priori system knowledge (Mayer, Pawlowski, Fath, & Cabezas, 2007; Tian, Kidokoro, Watanabe, & Iguchi, 2008). Some of these metrics are also capable of significance tests or information theoretic model selection (e.g., Detrended Correspondence Analysis, Detrended Canonical Correspondence Analysis, Sequential T-test Analysis of Regime Shifts, Redundancy Analysis-distance-based Moran's Eigenvector Maps/Asymmetric Eigenvector Maps; Rodionov & Overland 2005), but unlike known/limited metrics, they do not estimate coefficients, meaning significance tests for unknown/unlimited metrics may produce less specific conclusions than other approaches (Baho et al., 2014; Rodionov, 2004). However, the ability to include unlimited state variables may lead to including extraneous variables that could in turn lead to spurious regime shift detections (Sundstrom, Allen, & Barichev, 2012). Also, because these metrics do not require input state variables to be drivers or to interact, they provide little information on the directionality or relative importance of state variables regarding regime shifts (Vance, Eason, & Cabezas, 2015).

Any variable type

Fisher Information

Fisher Information (FI) is a tested EWI metric, and previous applications demonstrate its utility for early warning detection, regime shift detection, and land management decisions (Eason et al., 2016; González-Mejía, Vance, Eason, & Cabezas, 2015; Sundstrom et al., 2017). FI is a measure of the amount of information surrounding an unknown parameter that is obtainable by observation (Fisher, 1922). It is rooted in statistical estimation theory and has been applied in variety of disciplines ranging from quantum mechanics to ecosystem dynamics (Fath & Cabezas, 2004; Frieden & Gatenby, 2010; Mayer et al., 2007; C. W. Pawlowski, Fath, Mayer, & Cabezas, 2005). FI was recently adapted to assess changes in system behavior and detect regime shifts in complex ecological and social ecological systems (Eason & Cabezas, 2012; Fath, Cabezas, & Pawlowski, 2003; González-Mejía, Eason, Cabezas, & Suidan, 2014; Karunanithi et al., 2011; Sundstrom et al., 2017; Vance et al., 2015). As a measure of overall system order, FI defines regimes as steady or increasing order and regime shifts as sudden losses of order (Eason, Garmestani, & Cabezas, 2014; Mayer et al., 2007). Losses of order occur when state variables exceed their typical range of variability (Eason et al., 2016; Spanbauer et al., 2014). In addition to advantages shared with other unknown/unlimited metrics, FI can detect regime shifts and early warnings regardless of resolution or length of the data set (Eason et al., 2016; Spanbauer et al., 2014). For example, Spanbauer et al. (2014) applied FI to a time series dataset on over 100 species of freshwater diatoms across > 7,000 year period and found evidence of long term instability preceding a regime shift in community structure. Although FI has primarily been used to assess temporal dynamics, Sundstrom et al. (2017) also used this method to detect regime shifts in space (i.e., spatial regime

boundaries) in terrestrial and aquatic community data. Researchers have used FI with other approaches including the variance index (Carpenter & Brock, 2006; Sundstrom et al., 2017) and discontinuity analysis (Spanbauer et al., 2016).

Sequential T-Test Analysis of Regime Shifts

Sequential T-Test Analysis of Regime Shifts (STARS) was initially proposed by Rodionov (2004) as a method for testing for the occurrence of climatic regime shifts. STARS can provide early warning indicators of a regime shift via formal statistical significance tests by using a sequential data processing technique that allows for exploratory analysis that is not dependent on a priori hypothesis for locating regime shifts (Rodionov, 2004). STARS has been applied to a range of time series data beyond climate, including invertebrate and vertebrate community composition data (Chiba, Sugisaki, Nonaka, & Saino, 2009; Kirkman et al., 2015; Tian et al., 2008; Wood & Austin, 2009), snowpack characteristics (Irannezhad, Ronkanen, & Kløve, 2015), streamflow (Johnston & Shmagin, 2008), sea surface temperature (Friedland & Hare, 2007) and thermohaline characteristics (Matić, Grbec, & Morović, 2011). This method works well in collaboration with variable reduction techniques such as Principal Components Analysis, allowing for the inclusion of a large range of climatic, environmental and ecological data categories (McQuatters-Gollop & Vermaat, 2011).

Detrended Correspondence Analysis & Detrended Canonical

Correspondence Analysis

Detrended correspondence analysis (DCA) and detrended canonical correspondence analysis (DCCA) are two multivariate ordination methods typically used on sparse

ecological data (Ter Braak, 1986), often where ecological community assemblage data on species with normal distributions with respect to environmental gradients need to be detrended (remove arch effects; Hill & Gauch Jr (1980). DCA and DCCA have been used as regime shift detection methods by searching for flickering, skewness, and autocorrelation of variance over time in community or assemblage diversity and structure (Carstensen et al., 2013). For instance, by using a single ordinated axis, DCA identified a livestock grazing threshold gradient and possible regime shift on rangeland plant communities (Sasaki et al., 2008), and DCCA has been used to estimate historic diatom Beta diversity (Hobbs et al., 2010; Liu, Wu, & Zhao, 2013). DCCA and DCA may be less reliable in detecting changes in systems if the response variable does not follow a Gaussian distribution (Ter Braak, 1986).

Redundancy Analysis - distance-based Moran's Eigenvector

Maps/Asymmetric Eigenvector Maps

Redundancy Analysis (RDA)-distance-based Moran's Eigenvector Maps/Asymmetric Eigenvector Maps (dbMEM/AEM) is a proposed EWI metric that detects regime shifts and changes in ecological structure by identifying ecological patterns at different spatial or temporal scales; that is, it disentangles decadal, interannual, seasonal and intraseasonal patterns in time series or continental, regional and local patterns in data (Angeler, Viedma, & Moreno, 2009; Borcard & Legendre, 2002; Borcard, Legendre, Avois-Jacquet, & Tuomisto, 2004). A refinement of the principal coordinate of neighbor matrix approach, this metric instead uses RDA and models space or time with a dbMEM or dbAEM approach (Angeler et al., 2009; Dray, Legendre, & Peres-Neto, 2006). Rather

than using spatial coordinates or a linear time vector directly, dbMEM and AEM carry out a fourier transformation to spectrally decompose the spatial/temporal relationships among data points into orthogonal eigenfunctions. The resulting functions look like sine waves (or distorted sine waves if the sampling is irregular) of distinct frequencies that are then used as predictor variables in the RDA (Angeler, Trigel, Drakare, Johnson, & Goedkoop, 2010). The number and structure of predictor variables obtained for analysis depends on the length/spatial extent and resolution/grain of the underlying data set. dbMEM differs from AEM in that the latter includes a linear vector in addition to the sine waves, which allows modeling unidirectional processes in time and space (e.g., hydrological flow in streams; Baho et al., 2014; Göthe, Sandin, Allen, & Angeler, 2014). The RDA-dbMEM/AEM methods uses rigorous permutation testing, allowing for the determination of robust patterns and numerical assessment of the relative importance of patterns detected at each scale using the amount of adjusted variance explained. This metric has been used in both spatial and temporal contexts with data from lakes and streams (Angeler et al., 2014), marine systems (Angeler et al., 2014), ancient aquatic systems (Spanbauer et al., 2014), and terrestrial ecosystems (Widenfalk, Malmström, Berg, & Bengtsson, 2016). These analyses often focus on assessing the organization of the complex behavior and resilience of these systems and their application in management (Angeler & Allen, 2016).

Continuous variables of the same Type

Discontinuity Analysis

Discontinuity analysis (DA) is a method developed to objectively identify discontinuities, or scale breaks, in rank-ordered data, and it has been tested as an EWI metric (Allen & Holling, 2008; Nash et al., 2014; Spanbauer et al., 2016; Sundstrom et al., 2012). DA arises from ecological theory that posits ecosystems are multi-scaled and hierarchical as a result of structuring processes operating over discrete ranges of spatial and temporal scales (Allen & Starr, 1982; C. S. Holling, 1992). Both ecological structure and the species that interact with that structure are scaled in the sense that they function within a limited and particular range of spatial and temporal scales (Allen & Holling, 2008). Animal body masses, which are highly allometric with life-history traits, fall into size classes detectable by DA and can be used as a proxy for the complex spatial and temporal scales of ecological structure and structuring processes (Nash et al., 2014). Changes in body mass size classes in a system over time or space can therefore suggest changes in ecological regimes when regime shifts represent shifts in basic ecological structuring processes (Peterson, Allen, & Holling, 1998). For example, used in conjunction with constrained hierarchical clustering, DA detected early warnings of regime shifts in paleodiatom data in freshwater lakes by identifying shifts in the number and location of diatom body mass discontinuities (Spanbauer et al., 2016). DA also detected simplified fish size classes in degraded coral reefs compared to healthier reefs (Nash, Graham, Wilson, & Bellwood, 2013).

Explicitly spatial variables

Conditional Probability Analysis

Conditional Probability Analysis (CPA) uses explicitly spatial data to detect regime shifts by assessing changes in spatial cross-scale land use-land cover connectivity (Zurlini et al., 2014). Using multiple spatial data layers, it calculates proportional land use-land cover (P_c) and connectivity (i.e. adjacency; P_{cc}) within moving spatial windows of various sizes. As P_c of a given land use-land cover type increases, P_{cc} increases steadily until a threshold point is breached. At this threshold, a regime shift occurs: as a new land use-land cover regime spreads, P_c abruptly increases exponentially and P_{cc} increases much more slowly. In the single study we found using CPA, the authors detected an early warning of a regime shift toward desertification as a result of increased agricultural land connectivity in an urban-rural region of southern Italy (Zurlini et al., 2014).

DISCUSSION

The rangeland discipline has one of the longest histories of using large-scale rangeland inventories and analyses to influence major land management decisions and avoid alternative ecological regimes with less ecosystem service potential (West, 2003). In North America, the first well-coordinated national inventory of terrestrial resources occurred in the US in 1934 to address concerns over ecological transformations due to soil erosion (National Erosion Reconnaissance Survey). In the decades following, US land management agencies have launched multiple inventory frameworks aimed at maintaining favorable conditions and preventing deleterious regime shifts such as monitoring range quality, estimating degree of rangeland degradation, maintaining so-called climax communities, and tracking the degree of invasion by exotic species (West, 2003). But although monitoring efforts have been successful at identifying ecosystem

changes after their occurrence, they often rely on subjective expert opinion or system-specific knowledge applied after the fact, thereby removing the ability to predict surprises inevitable in ecological systems (Twidwell et al., 2013).

The early warning and regime shift detection metrics we review are meant to avoid problems associated with subjectivity and system-specific knowledge requirements. These metrics are often specifically designed to predict surprise, and can be applied to presently available rangeland monitoring inventories to directly answer rangeland management and state-transition concerns in a spatially-explicit manner. While spatial regime metrics have not undergone robust experimental evaluation in ecology and even less in the rangeland discipline (Table 2.2), many robust multivariate rangeland datasets have potential for testing and applying the early warning indicators that can be applied to multivariate data (e.g., the Natural Resources Conservation Service’s “Natural Resources Inventory”, the US Forest Service’s “Forest Inventory and Analysis Program”, the US Department of Agriculture’s Animal and Plant Health Inspection Service’s “Mormon Cricket/Grasshopper Assessment Program”; USDA NRCS, 2015; USDA Forest Service, 2018; USDA APHIS, 2018). For instance, the generalizability of unknown/unlimited metrics such as Fisher Information or Sequential T-test Analysis of Regime Shifts makes them amenable for use in surveillance monitoring frameworks that collect broad swathes of data of various types and any state variable could be of interest (Hutto & Belote, 2013). Additionally, some unknown/unlimited metrics like RDA-dbMEM/AEM and Discontinuity Analysis have the potential identify regime shifts and early warning while also estimating the complexity and resilience of rangelands-thereby

providing more detailed information on the state of the system and potentially how close or far it is from a regime shift. Conversely, sites with long-term monitoring (e.g., Long-Term Ecological Research (LTER) sites, Department of Defense lands, or individual properties) or where long-term data might be available in the future, and where the drivers are known (e.g. percent cover of woody plants at Konza Prairie LTER, bare ground at Jornada Basin LTER; Jornada Basin LTER, 2018; Konza Prairie LTER, 2018), known/limited metrics have high potential for early warning applications, depending on how data were collected: for instance, fitted values for percent bare ground at Jornada Basin flickering outside “typical” range of variability or consistently moving toward the boundaries of the typical range of variability could represent early warnings of a state transition [Dakos et al. (2012); Ives & Dakos (2012); Solow & Beet (2005). Similarly, EWI metrics requiring hypothesized regime shift locations (e.g., Average Standard Deviates, Intervention Analysis/Autoregressive Moving Averages) can be used in a post-hoc manner with long-term data, and they could also potentially be turned to produce early warnings by sequentially hypothesizing regime shifts in time series data. EWI metrics can also be used to detect regime shifts in spatial rangeland datasets (i.e., as has been assessed with Fisher Information for breeding bird data; Sundstrom et al., 2017).

The new concept of spatial regimes brings together early warning, regime shift, and state-transition theories by identifying where ecological regime shifts/state-transitions are taking place in space and time. Derived from regime shift and alternative state theory, spatial regimes are defined as spatially explicit ecological systems maintained by feedback mechanisms that exhibit self-similarity in structure and

composition within their boundaries (Allen et al., 2016; @ Sundstrom et al., 2017). The abundance of spatial data for rangelands (e.g., remotely-sensed vegetation indices, fire history data, land use-land cover data), the geographic breadth of monitoring sites (e.g., the NRCS Natural Resources Inventory's sites distributed throughout private agricultural lands across the United States), and the geographic site-descriptive goals of many rangeland initiatives (e.g., Ecological Site Descriptions) suggest high potential for applying the spatial regime concept in conjunction with EWI metrics in rangelands. For instance, we report only a single article using an EWI metric in a spatial regime context (Sundstrom et al., 2017) and none in rangelands (Table 2.2), but other EWI metrics with similar approaches to Fisher Information (e.g., Sequential T-test Analysis of Regime Shifts, Discontinuity Analysis) could also be used for spatial regime detection on large-scale (e.g., the US Geological Survey's "North American Breeding Bird Survey") or local-scale (e.g., georeferenced Long-Term Ecological Research site) datasets. Likewise, Conditional Probability Analysis, as a tested EWI metric that requires explicitly spatial data, could potentially be used to detect spatial regimes via cross-scale connectivity in remotely-sensed rangeland data, searching for early warnings in loss of rangeland heterogeneity, for signs of fragmentation, or for signs of over-connectedness and rigidity traps (Fuhlendorf & Engle, 2001; Hobbs et al., 2008; Peters, Havstad, Archer, & Sala, 2015; Zurlini et al., 2014).

Ignoring the interaction between space and time when searching for patterns indicating early warnings and regime shifts can lead to ecological misinterpretations of underlying structure of state variables (Allen, Angeler, Garmestani, Gunderson, &

Holling, 2014; Baho, Futter, Johnson, & Angeler, 2015; Nash et al., 2014). For instance, temporal early warnings of regime shifts in yeast populations were found to be suppressed in systems with high levels of connectivity, suggesting that EWI performance is jeopardized by ignoring integrated spatial-temporal components (Dai, 2013). To incorporate interactions between scale-specific spatial and temporal processes into early warning and regime shift modeling, approaches such as spatial/temporal eigenfunction analyses (e.g. the RDA-dbMEM/AEM metric reviewed above; Blanchet, Legendre, & Borcard, 2008) have arisen to identify characteristic spatial and temporal scales at which processes act to structure the distribution of species in a community (Dray et al., 2006, 2012; Peres-Neto & Legendre, 2010; T. W. Smith & Lundholm, 2010). Often spatial/temporal eigenvectors are combined with canonical ordination techniques or other multivariate community models to account for spatial-temporal patterns in community data, thereby offering increased performance for detecting regime shifts in systems where there is strong coupling of spatial and temporal variation at multiple scales (Legendre & Gauthier, 2014). Although many EWI metrics do not, spatial/temporal eigenfunction analyses often require large-scale and/or long-term data relative to the community of interest, making the intensive monitoring data collected by rangeland scientists and managers imperative for using these EWI metrics and disentangling spatiotemporal scaling issues.

To identify situations when EWI metrics would be useful and appropriate, primary considerations relate to system characteristics, research questions, data availability and social or policy concerns (Table 2.3; Figure 2.2.1). Although EWI

metrics often require little a priori knowledge of systems, some system-specific information can help decide which or if EWI metrics are appropriate (Lade et al., 2013; Mantua, 2004). For instance, the presence of hysteresis or thresholds may increase the cost of restoration, making detecting early warnings of regime shifts the more palatable option. Choosing when to use a metric will also depend on the research goal (e.g. active experimentation on regime shifts or passive monitoring), and data availability (sample sizes, is it spatial?, is it temporal?; Figure 2.2.1). In addition to ecological and statistical considerations, social or policy concerns can influence when or if to use EWI metrics. EWI metrics can provide evidence, and even estimates of confidence, to support the presence or absence of thresholds and regime shifts (Ives & Dakos, 2012; Rodionov, 2004). This can be used to inform policymakers and provide decision-making tools for managers. For example, an early warning signal could represent a policy “trigger point” for initiating management or restoration (Eason et al., 2016; Lindenmayer, Piggott, & Wintle, 2013). Data constraints (e.g., time-series and spatial data with sufficient resolution to cover relevant ecological scales are usually absent), the lack of detailed knowledge for many traits, organisms and processes represent a general limitation to the application of regime shift detection in rangelands. However, several extant national or regional monitoring programs may provide data for testing the regime shift indicators reviewed in this paper. Several experimental monitoring initiatives (Nutrient Network, 2018; Borer et al., 2014) are underway to overcome this limitation.

Management Implications

Early warning metrics and regime shift detection provide practical tools to assess rangeland vulnerability and resilience in the face of rapid environmental change. Here, we draw upon three examples where the scientific exploration of these metrics can benefit core pursuits in the rangeland discipline. We encourage readers to read the full articles to obtain more information.

Example 1: Earlier detection of rangelands in transition: Decades of field monitoring data have been collected in rangelands with the hope of providing earlier signals of rangeland transitions. Roberts et al. (in review) identify spatial regimes in actual grassland monitoring data (Figure 2.2a) and then demonstrate the potential to use an EWI to detect, via simulation of future field monitoring, (i) the spatial scale at which a new shrubland regime emerged and expanded over time (Figure 2.2b) and (ii) the potential to detect earlier warning of transitions via flickering (Figure 2.2c), an established early warning signal (Dakos et al., 2012). The study drew from actual field monitoring data collected across a 4 km transect at the Niobrara Valley Preserve, Nebraska, USA. Sampling of community composition and structure identified the presence of smooth sumac (*Rhus glabra*) within an expansive Sandhills grassland prairie, but constrained hierarchical clustering did not identify the patch with sumac as one of the current spatial regimes present at the site. A simulation was conducted over time, using known assembly rules derived from previous research, to test the potential for future field monitoring to be paired with the clustering method in order to detect the emergence of a sumac-dominant regime over time. A major implication from this study is that early

warning indicators can be used to identify the location and scale of shifting spatial regime boundaries, which could serve as “trigger points” for enacting management actions or changing policies in an adaptive monitoring/management framework (Lindenmayer et al., 2013).

Example 2: Preparing management for system-level change: A fundamental problem in the development of leading indicators is that the performance of univariate indicators have been inconsistent, with high uncertainty surrounding their potential to predict future regime change (Brock & Carpenter, 2012). Traditional (univariate) leading indicators also typically require the critical variables driving transitions to be known a priori, which is unrealistic in a future characterized by novelty and uncertainty.

Spanbauer et al. (2014) and Sundstrom et al. (2017) assess some of the multivariate indicators featured in this review and compare their utility to univariate indicators (Figure 2.3). These papers reveal a general problem all-too familiar to rangeland scientists and managers; that is, monitoring and management focused on a particular species or state variable of interest effectively masks community-level analyses from detecting system-level change. Both papers show that acting based on traditional univariate indicators becomes infeasible given the inconsistent signals and lack of spatial boundary detection needed to differentiate patterns among multiple populations of interest. In contrast, the authors conclude that more integrated measures that accommodate multivariate data have the potential to better reflect the reality of complex and adaptive ecological systems, like rangelands, and how to operationalize spatially-explicit signals of regime change.

Example 3: Advances in rangeland monitoring and application: Investments in technological innovation and computer processing is leading to rapid growth in strategic targeting tools that makes huge amounts of information and data readily accessible for rangeland science and planning. For example, utilizing robust ground level measurements, machine learning, and high performance cloud based computing, Jones et al. (2018) produce annual maps with historical (1984-2018), continuous cover data (0 to 100%) of plant functional groups for US rangelands (Figure 2.4). The data product removes the barrier of single class, arbitrarily-delineated categorical data (e.g., where a pixel, landscape, or region is classified solely as grassland, shrubland, or tree), which removes information necessary to explore the potential utility of the early warning and regime shift metrics featured in this review. In addition, by utilizing frameworks that do not require or utilize a priori knowledge of states but instead focuses on transitions that are detectable and measurable, it is possible to identify spatial risks or vulnerabilities to transitions and then concentrate management activities where it is most needed and will be most effective. The coupling of these data and frameworks will prompt a shift from the static inventory and state mapping paradigm (Steele, Bestelmeyer, Burkett, Smith, & Yanoff, 2012) within rangeland ecology to one of variability and transitions (Fuhlendorf & Engle, 2001; Twidwell et al., 2013).

Overall, the EWI metrics we review and, more broadly, the early warning/spatial regime paradigm represent quantitative, more objective decision-making tools for rangeland management in the face of ecological uncertainty (Allen et al., 2017; Allen, Fontaine, Pope, & Garmestani, 2011; Lindenmayer et al., 2013). Traditional inventory

and monitoring efforts are not designed with the spatial specificity needed to provide indicators of sudden change in many rangeland systems; however, statistical theory is advancing to be able to better incorporate broad-scale monitoring and inventory data for purposes of early warning and regime shift detection. Rangeland science is in a solid position to experimentally assess and integrate these metrics into monitoring and management, given the discipline's long-term focus on broad-scale monitoring and inventory data. Moving forward, the quantitative metrics reviewed herein could fit within joint efforts to couple adaptive management and monitoring as part of a co-learning process - where the utility of the metrics are tested and the monitoring necessary for their application is critiqued while also using an iterative decision-making process to guide their adoption.

LITERATURE CITED

- Allen, C. R., & Holling, C. (2008). *Discontinuities in ecosystems and other complex systems*. Columbia University Press.
- Allen, C. R., Angeler, D. G., Cumming, G. S., Folke, C., Twidwell, D., & Uden, D. R. (2016). Quantifying spatial resilience. *Journal of Applied Ecology*, 53(3), 625–635.
- Allen, C. R., Angeler, D. G., Fontaine, J. J., Garmestani, A. S., Hart, N. M., Pope, K. L., & Twidwell, D. (2017). Adaptive management of rangeland systems. In *Rangeland systems* (pp. 373–394). Springer.
- Allen, C. R., Angeler, D. G., Garmestani, A. S., Gunderson, L. H., & Holling, C. S. (2014). Panarchy: Theory and application. *Ecosystems*, 17(4), 578–589.

- Allen, C. R., Fontaine, J. J., Pope, K. L., & Garmestani, A. S. (2011). Adaptive management for a turbulent future. *Journal of Environmental Management*, 92(5), 1339–1345.
- Allen, T. F., & Starr, T. B. (1982). Hierarchy perspectives for ecological complexity.
- Andersen, T., Carstensen, J., Hernandez-Garcia, E., & Duarte, C. M. (2009). Ecological thresholds and regime shifts: Approaches to identification. *Trends in Ecology & Evolution*, 24(1), 49–57.
- Angeler, D. G., & Allen, C. R. (2016). Editorial: Quantifying resilience. *Journal of Applied Ecology*, 53(3), 617–624.
- Angeler, D. G., & Johnson, R. K. (2012). Temporal scales and patterns of invertebrate biodiversity dynamics in boreal lakes recovering from acidification. *Ecological Applications*, 22(4), 1172–1186.
- Angeler, D. G., Allen, C. R., Birgé, H. E., Drakare, S., McKie, B. G., & Johnson, R. K. (2014). Assessing and managing freshwater ecosystems vulnerable to environmental change. *Ambio*, 43(1), 113–125.
- Angeler, D. G., Trigtal, C., Drakare, S., Johnson, R. K., & Goedkoop, W. (2010). Identifying resilience mechanisms to recurrent ecosystem perturbations. *Oecologia*, 164(1), 231–241.
- Angeler, D. G., Viedma, O., & Moreno, J. (2009). Statistical performance and information content of time lag analysis and redundancy analysis in time series modeling. *Ecology*, 90(11), 3245–3257.

- Baho, D. L., Drakare, S., Johnson, R. K., Allen, C. R., & Angeler, D. G. (2014). Similar resilience attributes in lakes with different management practices. *PloS One*, 9(3), e91881.
- Baho, D. L., Futter, M. N., Johnson, R. K., & Angeler, D. G. (2015). Assessing temporal scales and patterns in time series: Comparing methods based on redundancy analysis. *Ecological Complexity*, 22, 162–168.
- Bestelmeyer, B. T., Tugel, A. J., Peacock Jr, G. L., Robinett, D. G., Shaver, P. L., Brown, J. R., ... Havstad, K. M. (2009). State-and-transition models for heterogeneous landscapes: A strategy for development and application. *Rangeland Ecology & Management*, 62(1), 1–15.
- Biggs, R., Carpenter, S. R., & Brock, W. A. (2009). Turning back from the brink: Detecting an impending regime shift in time to avert it. *Proceedings of the National Academy of Sciences*, 106(3), 826–831.
- Blanchet, F. G., Legendre, P., & Borcard, D. (2008). Forward selection of explanatory variables. *Ecology*, 89(9), 2623–2632.
- Borcard, D., & Legendre, P. (2002). All-scale spatial analysis of ecological data by means of principal coordinates of neighbour matrices. *Ecological Modelling*, 153(1), 51–68.
- Borcard, D., Legendre, P., Avois-Jacquet, C., & Tuomisto, H. (2004). Dissecting the spatial structure of ecological data at multiple scales. *Ecology*, 85(7), 1826–1832.

- Borer, E. T., Seabloom, E. W., Gruner, D. S., Harpole, W. S., Hillebrand, H., Lind, E. M., ... others. (2014). Herbivores and nutrients control grassland plant diversity via light limitation. *Nature*, 508(7497), 517.
- Briske, D. D., Fuhlendorf, S. D., & Smeins, F. (2005). State-and-transition models, thresholds, and rangeland health: A synthesis of ecological concepts and perspectives. *Rangeland Ecology & Management*, 58(1), 1–10.
- Briske, D., Bestelmeyer, B., Stringham, T., & Shaver, P. (2008). Recommendations for development of resilience-based state-and-transition models. *Rangeland Ecology & Management*, 61(4), 359–367.
- Brock, W. A., & Carpenter, S. R. (2006). Variance as a leading indicator of regime shift in ecosystem services. *Ecology and Society*, 11(2), 9.
- Brock, W. A., & Carpenter, S. R. (2012). Early warnings of regime shift when the ecosystem structure is unknown. *PLoS One*, 7(9), e45586.
- Burthe, S. J., Henrys, P. A., Mackay, E. B., Spears, B. M., Campbell, R., Carvalho, L., ... others. (2015). Do early warning indicators consistently predict nonlinear change in long-term ecological data? *Journal of Applied Ecology*.
- Carpenter, S. R., Cole, J. J., Pace, M. L., Batt, R., Brock, W., Cline, T., ... others. (2011). Early warnings of regime shifts: A whole-ecosystem experiment. *Science*, 332(6033), 1079–1082.
- Carpenter, S., & Brock, W. (2006). Rising variance: A leading indicator of ecological transition. *Ecology Letters*, 9(3), 311–318.

- Carstensen, J., Telford, R. J., & Birks, H. J. B. (2013). Diatom flickering prior to regime shift. *Nature*, 498(7455), E11–E12.
- Chiba, S., Sugisaki, H., Nonaka, M., & Saino, T. (2009). Geographical shift of zooplankton communities and decadal dynamics of the kuroshio–Oyashio currents in the western north pacific. *Global Change Biology*, 15(7), 1846–1858.
- Clements, F. E. (1916). *Plant succession: An analysis of the development of vegetation*. Carnegie Institution of Washington.
- Dai, A. (2013). Increasing drought under global warming in observations and models. *Nature Climate Change*, 3(1), 52–58.
- Dakos, V., Carpenter, S. R., Brock, W. A., Ellison, A. M., Guttal, V., Ives, A. R., ... others. (2012). Methods for detecting early warnings of critical transitions in time series illustrated using simulated ecological data. *PloS One*, 7(7), e41010.
- Dray, S., Legendre, P., & Peres-Neto, P. R. (2006). Spatial modelling: A comprehensive framework for principal coordinate analysis of neighbour matrices (pcnm). *Ecological Modelling*, 196(3), 483–493.
- Dray, S., Péliissier, R., Couteron, P., Fortin, M.-J., Legendre, P., Peres-Neto, P., ... others. (2012). Community ecology in the age of multivariate multiscale spatial analysis. *Ecological Monographs*, 82(3), 257–275.
- Dyksterhuis, E. (1949). Condition and management of range land based on quantitative ecology. *Journal of Range Management*, 2(3), 104–115.

- Eason, T., & Cabezas, H. (2012). Evaluating the sustainability of a regional system using fisher information in the san luis basin, colorado. *Journal of Environmental Management*, 94(1), 41–49.
- Eason, T., Garmestani, A. S., & Cabezas, H. (2014). Managing for resilience: Early detection of regime shifts in complex systems. *Clean Technologies and Environmental Policy*, 16(4), 773–783.
- Eason, T., Garmestani, A. S., Stow, C. A., Rojo, C., Alvarez-Cobelas, M., & Cabezas, H. (2016). Managing for resilience: An information theory-based approach to assessing ecosystems. *Journal of Applied Ecology*.
- Ebbesmeyer, C. C., Cayan, D. R., McLain, D. R., Nichols, F. H., Peterson, D. H., & Redmond, K. T. (1991). 1976 step in the pacific climate: Forty environmental changes between 1968-1975 and 1977-1984.
- Fath, B. D., & Cabezas, H. (2004). Exergy and fisher information as ecological indices. *Ecological Modelling*, 174(1), 25–35.
- Fath, B. D., Cabezas, H., & Pawlowski, C. W. (2003). Regime changes in ecological systems: An information theory approach. *Journal of Theoretical Biology*, 222(4), 517–530.
- Fisher, R. A. (1922). On the mathematical foundations of theoretical statistics. *Philosophical Transactions of the Royal Society of London. Series A, Containing Papers of a Mathematical or Physical Character*, 222, 309–368.

- Folke, C., Carpenter, S., Walker, B., Scheffer, M., Elmqvist, T., Gunderson, L., & Holling, C. S. (2004). Regime shifts, resilience, and biodiversity in ecosystem management. *Annu. Rev. Ecol. Evol. Syst.*, 35, 557–581.
- Frieden, R., & Gatenby, R. A. (2010). *Exploratory data analysis using fisher information*. Springer Science & Business Media.
- Friedland, K. D., & Hare, J. A. (2007). Long-term trends and regime shifts in sea surface temperature on the continental shelf of the northeast united states. *Continental Shelf Research*, 27(18), 2313–2328.
- Fuhlendorf, S. D., & Engle, D. M. (2001). Restoring heterogeneity on rangelands: Ecosystem management based on evolutionary grazing patterns: We propose a paradigm that enhances heterogeneity instead of homogeneity to promote biological diversity and wildlife habitat on rangelands grazed by livestock. *BioScience*, 51(8), 625–632.
- Gal, G., & Anderson, W. (2010). A novel approach to detecting a regime shift in a lake ecosystem. *Methods in Ecology and Evolution*, 1(1), 45–52.
- Gedalof, Z., Smith, D. J., & others. (2001). Interdecadal climate variability and regime-scale shifts in pacific north america. *Geophysical Research Letters*, 28(8), 1515–1518.
- González-Mejía, A. M., Eason, T. N., Cabezas, H., & Suidan, M. T. (2014). Social and economic sustainability of urban systems: Comparative analysis of metropolitan statistical areas in ohio, usa. *Sustainability Science*, 9(2), 217–228.

- González-Mejía, A. M., Vance, L., Eason, T. N., & Cabezas, H. (2015). *Assessing and measuring environmental impact and sustainability*. J. J. Klemes.
- Göthe, E., Sandin, L., Allen, C. R., & Angeler, D. G. (2014). Quantifying spatial scaling patterns and their local and regional correlates in headwater streams: Implications for resilience. *Ecology and Society*, 19(3), 15.
- Hare, S. R., & Mantua, N. J. (2000). Empirical evidence for north pacific regime shifts in 1977 and 1989. *Progress in Oceanography*, 47(2), 103–145.
- Hill, M. O., & Gauch Jr, H. G. (1980). Detrended correspondence analysis: An improved ordination technique. *Vegetatio*, 42(1-3), 47–58.
- Hobbs, N. T., Galvin, K. A., Stokes, C. J., Lockett, J. M., Ash, A. J., Boone, R. B., ... Thornton, P. K. (2008). Fragmentation of rangelands: Implications for humans, animals, and landscapes. *Global Environmental Change*, 18(4), 776–785.
- Hobbs, W. O., Telford, R. J., Birks, H. J. B., Saros, J. E., Hazewinkel, R. R., Perren, B. B., ... Wolfe, A. P. (2010). Quantifying recent ecological changes in remote lakes of north america and greenland using sediment diatom assemblages. *PloS One*, 5(4), e10026.
- Holling, C. S. (1992). Cross-scale morphology, geometry, and dynamics of ecosystems. *Ecological Monographs*, 62(4), 447–502.
- Hutto, R. L., & Belote, R. (2013). Distinguishing four types of monitoring based on the questions they address. *Forest Ecology and Management*, 289, 183–189.

- Irannezhad, M., Ronkanen, A.-K., & Kløve, B. (2015). Effects of climate variability and change on snowpack hydrological processes in finland. *Cold Regions Science and Technology*, 118, 14–29.
- Ives, A. R., & Dakos, V. (2012). Detecting dynamical changes in nonlinear time series using locally linear state-space models. *Ecosphere*, 3(6), 1–15.
- Johnston, C. A., & Shmagin, B. A. (2008). Regionalization, seasonality, and trends of streamflow in the us great lakes basin. *Journal of Hydrology*, 362(1), 69–88.
- Jones, M. O., Allred, B. W., Naugle, D. E., Maestas, J. D., Donnelly, P., Metz, L. J., ... others. (2018). Innovation in rangeland monitoring: Annual, 30 m, plant functional type percent cover maps for us rangelands, 1984–2017. *Ecosphere*, 9(9), e02430.
- [dataset] Jornada Basin Long-Term Ecological Research (LTER). 2018.
<https://jornada.nmsu.edu/lter/data/all>
- Karunanithi, A. T., Garmestani, A. S., Eason, T., & Cabezas, H. (2011). The characterization of socio-political instability, development and sustainability with fisher information. *Global Environmental Change*, 21(1), 77–84.
- Kirkman, S. P., Yemane, D., Atkinson, L. J., Kathena, J., Nsiangango, S. E., Singh, L., ... Samaai, T. (2015). Regime shifts in demersal assemblages of the benguela current large marine ecosystem: A comparative assessment. *Fisheries Oceanography*, 24(S1), 15–30.
- [dataset] Konza Prairie Long-Term Ecological Research (LTER). 2018.
<http://lter.konza.ksu.edu/data>

- Lade, S. J., & Gross, T. (2012). Early warning signals for critical transitions: A generalized modeling approach. *PLoS Comput Biol*, 8(2), e1002360.
- Lade, S. J., Tavoni, A., Levin, S. A., & Schlüter, M. (2013). Regime shifts in a social-ecological system. *Theoretical Ecology*, 6(3), 359–372.
- Legendre, P., & Gauthier, O. (2014). Statistical methods for temporal and space–time analysis of community composition data. *Proceedings of the Royal Society of London B: Biological Sciences*, 281(1778), 20132728.
- Lindenmayer, D. B., Piggott, M. P., & Wintle, B. A. (2013). Counting the books while the library burns: Why conservation monitoring programs need a plan for action. *Frontiers in Ecology and the Environment*, 11(10), 549–555.
- Liu, Y., Wu, G., & Zhao, X. (2013). Recent declines in china’s largest freshwater lake: Trend or regime shift? *Environmental Research Letters*, 8(1), 014010.
- Mantua, N. (2004). Methods for detecting regime shifts in large marine ecosystems: A review with approaches applied to north pacific data. *Progress in Oceanography*, 60(2), 165–182.
- Matić, F., Grbec, B., & Morović, M. (2011). Indications of climate regime shifts in the middle adriatic sea. *Acta Adriatica*, 52(2).
- Mayer, A. L., Pawlowski, C., Fath, B. D., & Cabezas, H. (2007). Applications of fisher information to the management of sustainable environmental systems. In *Exploratory data analysis using fisher information* (pp. 217–244). Springer.

- McQuatters-Gollop, A., & Vermaat, J. E. (2011). Covariance among north sea ecosystem state indicators during the past 50 years—Contrasts between coastal and open waters. *Journal of Sea Research*, 65(2), 284–292.
- Nash, K. L., Allen, C. R., Angeler, D. G., Barichievy, C., Eason, T., Garmestani, A. S., ... others. (2014). Discontinuities, cross-scale patterns, and the organization of ecosystems. *Ecology*, 95(3), 654–667.
- Nash, K. L., Graham, N. A., Wilson, S. K., & Bellwood, D. R. (2013). Cross-scale habitat structure drives fish body size distributions on coral reefs. *Ecosystems*, 16(3), 478–490.
- [dataset] Nutrient Network. 2018. <http://www.nutnet.umn.edu/>
- Pawlowski, C. W., Fath, B. D., Mayer, A. L., & Cabezas, H. (2005). Towards a sustainability index using information theory. *Energy*, 30(8), 1221–1231.
- Peres-Neto, P. R., & Legendre, P. (2010). Estimating and controlling for spatial structure in the study of ecological communities. *Global Ecology and Biogeography*, 19(2), 174–184.
- Peters, D. P., Havstad, K. M., Archer, S. R., & Sala, O. E. (2015). Beyond desertification: New paradigms for dryland landscapes. *Frontiers in Ecology and the Environment*, 13(1), 4–12.
- Peterson, G., Allen, C. R., & Holling, C. S. (1998). Ecological resilience, biodiversity, and scale. *Ecosystems*, 1(1), 6–18.
- Rodionov, S. N. (2004). A sequential algorithm for testing climate regime shifts. *Geophysical Research Letters*, 31(9).

- Rodionov, S., & Overland, J. E. (2005). Application of a sequential regime shift detection method to the bering sea ecosystem. *ICES Journal of Marine Science: Journal Du Conseil*, 62(3), 328–332.
- Rudnick, D. L., & Davis, R. E. (2003). Red noise and regime shifts. *Deep Sea Research Part I: Oceanographic Research Papers*, 50(6), 691–699.
- Sampson, A. W. (1917). *Important range plants: Their life history and forage value*. US Department of Agriculture.
- Sampson, A. W. (1919). *Plant succession in relation to range management*. US Department of Agriculture.
- Sasaki, T., Okayasu, T., Jamsran, U., & Takeuchi, K. (2008). Threshold changes in vegetation along a grazing gradient in mongolian rangelands. *Journal of Ecology*, 96(1), 145–154.
- Scheffer, M., & Carpenter, S. R. (2003). Catastrophic regime shifts in ecosystems: Linking theory to observation. *Trends in Ecology & Evolution*, 18(12), 648–656.
- Scheffer, M., Carpenter, S., Foley, J. A., Folke, C., & Walker, B. (2001). Catastrophic shifts in ecosystems. *Nature*, 413(6856), 591–596.
- Smith, T. W., & Lundholm, J. T. (2010). Variation partitioning as a tool to distinguish between niche and neutral processes. *Ecography*, 33(4), 648–655.
- Solow, A. R., & Beet, A. R. (2005). A test for a regime shift. *Fisheries Oceanography*, 14(3), 236–240.

- Spanbauer, T. L., Allen, C. R., Angeler, D. G., Eason, T., Fritz, S. C., Garmestani, A. S., ... Stone, J. R. (2014). Prolonged instability prior to a regime shift. *PloS One*, 9(10), e108936.
- Spanbauer, T. L., Allen, C. R., Angeler, D. G., Eason, T., Fritz, S. C., Garmestani, A. S., ... Sundstrom, S. M. (2016). Body size distributions signal a regime shift in a lake ecosystem. In *Proc. r. soc. b* (Vol. 283, p. 20160249). The Royal Society.
- Steele, C. M., Bestelmeyer, B. T., Burkett, L. M., Smith, P. L., & Yanoff, S. (2012). Spatially explicit representation of state-and-transition models. *Rangeland Ecology & Management*, 65(3), 213–222.
- Sundstrom, S. M., Allen, C. R., & Barichievy, C. (2012). Species, functional groups, and thresholds in ecological resilience. *Conservation Biology*, 26(2), 305–314.
- Sundstrom, S. M., Eason, T., Nelson, R. J., Angeler, D. G., Barichievy, C., Garmestani, A. S., ... others. (2017). Detecting spatial regimes in ecosystems. *Ecology Letters*, 20(1), 19–32.
- Ter Braak, C. J. (1986). Canonical correspondence analysis: A new eigenvector technique for multivariate direct gradient analysis. *Ecology*, 67(5), 1167–1179.
- Tian, Y., Kidokoro, H., Watanabe, T., & Iguchi, N. (2008). The late 1980s regime shift in the ecosystem of tsushima warm current in the japan/east sea: Evidence from historical data and possible mechanisms. *Progress in Oceanography*, 77(2), 127–145.

- Twidwell, D., Allred, B. W., & Fuhlendorf, S. D. (2013). National-scale assessment of ecological content in the world's largest land management framework. *Ecosphere*, 4(8), 1–27.
- [dataset] USDA Animal and Plant Health Inspection Service (APHIS). 2018. Grasshopper-Mormon Cricket. https://www.aphis.usda.gov/aphis/ourfocus/planthealth/plant-pest-and-disease-programs/pests-and-diseases/grasshopper-mormon-cricket/CT_Grasshopper_Mormon_Cricket
- [dataset] USDA Forest Service. 2018. Forest Inventory and Analysis National Program. <http://www.fia.fs.fed.us/>.
- [dataset] USDA Natural Resources Conservation Service, 1997 National Resources Inventory, Revised September 2015.
- Vance, L., Eason, T., & Cabezas, H. (2015). An information theory-based approach to assessing the sustainability and stability of an island system. *International Journal of Sustainable Development & World Ecology*, 22(1), 64–75.
- Web of science. (2016).
- Wei, W. W.-S. (1994). *Time series analysis*. Addison-Wesley publ Reading.
- West, N. E. (2003). History of rangeland monitoring in the usa. *Arid Land Research and Management*, 17(4), 495–545.
- Westoby, M., Walker, B., & Noy-Meir, I. (1989). Opportunistic management for rangelands not at equilibrium. *Journal of Range Management*, 266–274.

- Widenfalk, L. A., Malmström, A., Berg, M. P., & Bengtsson, J. (2016). Small-scale collembola community composition in a pine forest soil—Overdispersion in functional traits indicates the importance of species interactions. *Soil Biology and Biochemistry*, *103*, 52–62.
- Wood, R. J., & Austin, H. M. (2009). Synchronous multidecadal fish recruitment patterns in chesapeake bay, usa. *Canadian Journal of Fisheries and Aquatic Sciences*, *66*(3), 496–508.
- Zurlini, G., Jones, K. B., Riitters, K. H., Li, B.-L., & Petrosillo, I. (2014). Early warning signals of regime shifts from cross-scale connectivity of land-cover patterns. *Ecological Indicators*, *45*, 549–560.

TABLES

Table 2. 1: Glossary of terms.

Term	Definition
Early Warning Indicator	"hypothesized to signal the loss of system resilience and have been shown to precede critical transitions in theoretical models, paleoclimate times series, and in laboratory as well as whole lake experiments" (Gsell et al. 2016)
Hysteresis	<p>"in which the forward and backward switches occur at different critical conditions" (Scheffer et al. 2001)</p> <p>"the path out is not the same as the path in" (Angeler and Allen 2016)</p>
Regime	"configuration in terms of abundance and composition, function and process, of a system...The terms state and regime are often used interchangeably. However, regime specifically refers to the processes and feedbacks that confer dynamic structure to a given state of a system" (Angeler and Allen 2016)
Regime Shift	<p>"conspicuous jumps from one rather stable [regime] to another" (Scheffer et al. 2001)</p> <p>"Sudden shifts in ecosystems, whereby a threshold is passed and the core functions, structure, and processes of the new regime are fundamentally different from the previous regime and hysteresis is present." (Scheffer and Carpenter 2003)</p>
Regime Shift Metric	"statistical metrics of system resilience [that] have been hypothesized to provide advance warning of sudden shifts in ecosystems" (Gsell et al. 2016)
State	"The 'state' of a system at a particular instant in time is the collection of values of the 'state' variables at that time...the term 'state' is loosely used to describe a characteristic of the system, rather than its state. For example, the lake is in a eutrophic 'state', or the rangeland is in a shrub-dominated 'state'." (Walker et al. 2002)
State-and-Transition Models	"..a framework to accommodate a broader spectrum of vegetation dynamics on the basis of managerial, rather than ecological, criteria... initially designed for application on rangelands characterized by discontinuous and nonreversible

vegetation dynamics.” Based on “1) potential alternative vegetation states [at] a site, 2) potential transitions between vegetation states, and 3) recognition of opportunities to achieve favorable transitions and hazards to avoid unfavorable transitions between vegetation states” (Briske et al. 2005)

State Variable

Biotic and abiotic system features that define and contrast system states. State variables can be “driving state variables” of system states (i.e., sufficient changes in driving state variables are known to alter system states) or simply indicative of system state.

Threshold

“Thresholds are equivalent to tipping points and may be detected as discontinuities or bifurcation points in complex systems” (Angeler and Allen 2016)

Table 2. 2: Literature review[†] of the total number of papers and the percentage using a quantitative metric[‡] for early warning and regime shift detection in Rangeland Ecology & Management and other journals in the discipline.

Search term	In the journal of Rangeland Ecology & Management	In other journals in the discipline with the additional search term:	
		Rangeland	Ecology
State and Transition	147 (21%)	2,250 (30%)	3,450 (27%)
Alternative States	36 (31%)	953 (32%)	5,690 (30%)
State Transition	24 (17%)	580 (35%)	8,470 (30%)
Early Warning	18 (17%)	5,340 (26%)	17,500 (71%)
Regime Shift	7 (29%)	672 (42%)	110,000 (46%)
Early Warning Indicator	2 (0%)	87 (61%)	1,000 (42%)
Spatial Regime	0 (0%)	9 (33%)	310 (68%)

[†]Search returns were based on a formal review in Google Scholar. Values given in the table represent the sum of all search returns. Values in parentheses represent the percentage (%) of search returns including a quantitative metric.

[‡]Quantitative metrics considered in our search include: autocorrelation, autoregressive model, autoregressive moving averages, average standard deviates, BDS test, coefficient of variation, conditional heteroscedasticity, conditional probability analysis, detrended canonical correspondence analysis, detrended correspondence analysis, detrended fluctuation analysis indicator, discontinuity analysis, fisher information, generalized modeling, intervention analysis, kurtosis, return rate, sequential T-test analysis of regime shifts, skewness, spectral density, spectral exponent, spectral ratio, standard deviation, vector autoregressive modeling.

Table 2. 3: Questions and situational examples for determining when using regime shift/early warning indicator metrics (EWI metrics) could be appropriate. For each question/situation, the “Why” and “Why not” columns provide positive and negative support, respectively, for the use of EWI metrics.

Should I use Regime Shift or Early Warning Indicator metrics...	Why?	Why not?
<i>System Considerations</i>		
If hysteresis <i>is</i> present or likely?	<ul style="list-style-type: none"> • EWI metrics can allow management to prevent known or unknown imminent regime shifts. • Restoration of desirable states will be very costly or infeasible. 	<ul style="list-style-type: none"> • There is extensive knowledge of system drivers and hysteresis. Thus, applying finances, time, and effort to preventative management is more beneficial.
If hysteresis <i>is not</i> present or likely?	<ul style="list-style-type: none"> • Restoration of desirable states, although possible or simple, will still be very costly. 	<ul style="list-style-type: none"> • Same as above. • The cost to restore the desirable state is low.
<i>Research Question Considerations</i>		
While actively experimenting with thresholds or regime shifts?	<ul style="list-style-type: none"> • EWI metrics can quantitatively identify when/where thresholds or regime shifts occur. • Some EWI metrics can identify and rank relative influences of driving state variables (see Figure 1). 	<ul style="list-style-type: none"> • Experimentation on thresholds could cause catastrophic or expensive consequences, so EWI metrics are not useful or advisable. • Early warning may not be necessary; simply identifying regime shifts (e.g., with proposed EWI or regime shift detection metrics) may be sufficient.
While passively monitoring state variables?	<ul style="list-style-type: none"> • EWI metrics can provide early warnings for unknown or unforeseen regime shifts. • EWI metrics can provide an estimate of the typical range of variability in a state. 	<ul style="list-style-type: none"> • There are other statistical metrics or procedures in place.
To identify historic thresholds or regime shifts?	<ul style="list-style-type: none"> • Many EWI metrics have been used extensively to identify historic thresholds and regime shifts. • EWI metrics can provide 	<ul style="list-style-type: none"> • Early warning may not be necessary; simply identifying regime shifts (e.g., with proposed EWI or regime shift detection metrics) may be sufficient. • Some EWI metrics produce

	<p>quantitative and qualitative evidence of the present/absence of thresholds and regime shifts.</p> <ul style="list-style-type: none"> Some EWI metrics have explicit significance tests and can provide levels of confidence (see Figure 1). 	<p>conflicting results when identifying historic regime shifts, so choosing the most appropriate metric can be challenging.</p>
To detect spatial regimes?	<ul style="list-style-type: none"> Some EWI metrics are amenable to detecting spatial regimes. There is sufficient spatial data of the appropriate type to run EWI metrics amenable to detecting spatial regimes (see Figure 1). 	<ul style="list-style-type: none"> Data type requirements are not met for EWI metrics suitable for detecting spatial regimes.
At any spatiotemporal scale?	<ul style="list-style-type: none"> Some EWI metrics are amenable to detecting spatial and temporal regimes. There is sufficient spatial and temporal data of the appropriate type to run EWI metrics. 	<ul style="list-style-type: none"> Data type requirements are not met for EWI metrics suitable for detecting spatio-temporal regimes.
<i>Data Availability Considerations</i>		
If long-term temporal monitoring data is available?	<ul style="list-style-type: none"> Many EWI metrics were designed and have been well-studied in temporal contexts. Long-term temporal data can provide more accurate portrayals of the typical range of variability in a state. This in turn can increase the accuracy of EWI metrics. Historic thresholds and regime shifts can be identified, providing insight into potential regime shift hazards in the future. 	<ul style="list-style-type: none"> There is extensive knowledge of system drivers and hysteresis. Thus, applying finances, time, and effort to preventative management is more beneficial.
If only spatial data is available?	<ul style="list-style-type: none"> Some EWI metrics can use explicitly spatial data to detect early warnings of regime shifts (see Figure 1). Some EWI metrics can use spatial data to identify spatial ecological regimes. 	<ul style="list-style-type: none"> Patterns may not be detectable with only one point in time.
If driving state variables are known?	<ul style="list-style-type: none"> Some EWI metrics are designed for detecting thresholds or regime shifts with known driving state variables (see Figure 1). Knowing driving state variables may increase the performance of 	<ul style="list-style-type: none"> Monitoring known driving state variables may suffice for detecting imminent regime shifts and prioritizing management.

	EWI metrics and allow more accurate and earlier regime shift detection.	
<i>Social or Policy Considerations</i>		
If social, policy, or legal concerns require confirmation of thresholds or regime shifts?	<ul style="list-style-type: none"> • EWI metrics can provide quantitative and qualitative evidence of the presence/absence of thresholds and regime shifts. • Policy or law mandates use of particular conceptual frameworks (e.g., state-transition models, ecological site descriptions) that would benefit from inclusion of quantitative metrics. • Some EWI metrics have explicit significance tests and can provide levels of confidence (see Figure 1). 	<ul style="list-style-type: none"> • Available data are insufficient or not appropriate to detect early warning and regime shifts at the scale necessary to guide policy or to avoid misinterpretation and misuse. • There is extensive knowledge of system drivers and hysteresis, so applying finances, time, and effort for preventative management is less of a priority than focusing on sociopolitical constraints.

FIGURES

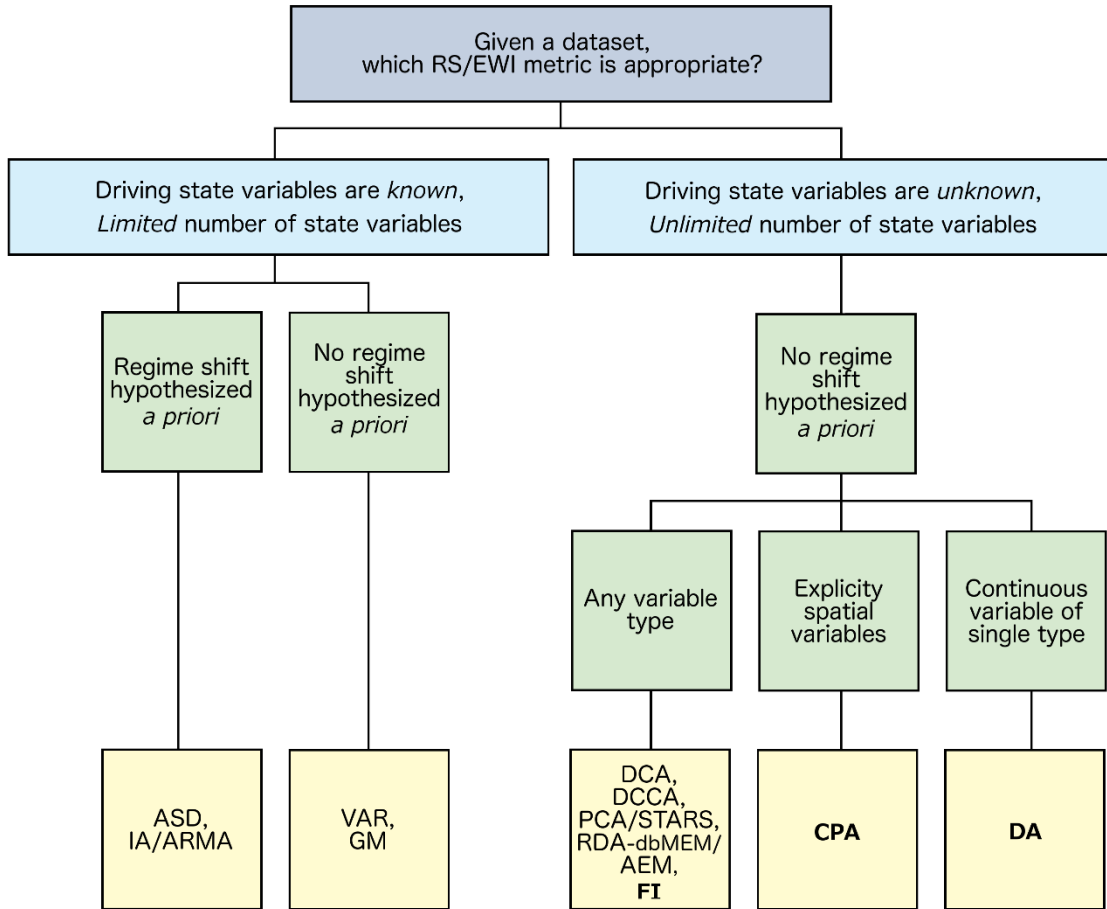


Figure 2. 1: A flowchart for determining which multivariate metrics for regime shift/early warning detection are appropriate for a given set of state variables. “Limited” state variables indicates those metrics are suitable for relatively small number of input variables, and “known drivers” means that the input state variables represent known fundamental influences on system state. The lowest tier lists appropriate metrics for a given data type. Metrics in bold have been tested as early warning indicators of regime shifts. Metrics not in bold have been proposed as early warning metrics but only tested as regime shift indicators.

Note: RS = proposed early warning indicator, EWI = tested early warning indicator, ASD = Average Standard Deviates, IA/ARMA = Intervention Analysis/Autoregressive Moving Averages, VAR = Vector Autoregression, GM = Generalized Modeling, DCA = Detrended Correspondence Analysis, DCCA = Detrended Canonical Correspondence Analysis, PCA/STARS = Principal Components Analysis/Sequential T-Test Analysis of Regime Shifts, RDA-dbMEM/AEM = Redundancy Analysis- , FI = Fisher Information, CPA = Conditional Probability Analysis, DA = Discontinuity Analysis

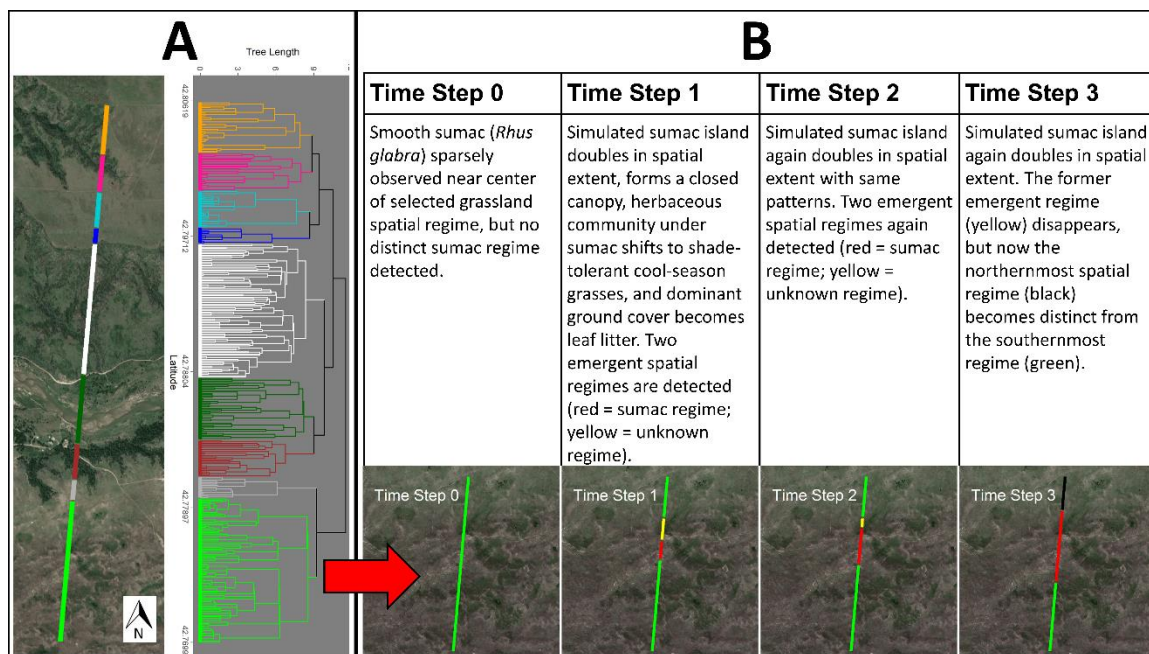


Figure 2. 2: The emergence of new states, and the potential to avoid collapses in existing states, has been a preeminent focus of rangeland ecology and management. Roberts et al. (in review) incorporate spatially-explicit application of a discontinuity analysis into field monitoring data collected along a 4 km transect at the Niobrara Valley Preserve, Nebraska, USA. This study identifies (A) the existing number and types of spatial regimes at the site, (B) the potential for using an early warning indicator in conjunction with the spatial regime concept to identify, via simulation of future field monitoring, the location and spatial scale at which a shrubland regime emerged, (C) and the expansion of the shrubland regime, at the cost to the previously dominant grassland regime, over time.

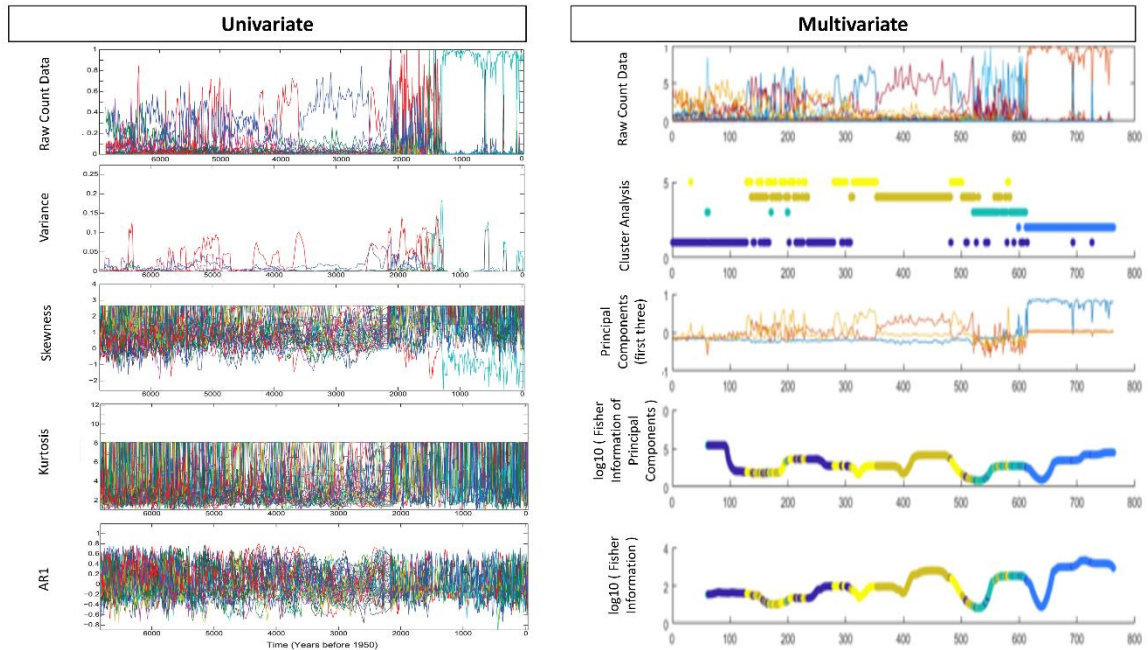


Figure 2. 3: Integrative metrics that accommodate multivariate data are being explored to assess their potential utility to detect early warning and regime change in complex adaptive systems. Spanbaeur et al. (2014) compare various multivariate and univariate indicators using paleo-diatom data. Several populations of species experienced increased variability in this study, but conflicting patterns make it difficult to operationalize univariate statistics to characterize the behavior of this complex, multivariate system. Similar trends and observations might be expected in rangelands, but research has been limited, to date, to test these concepts and to assess their practical utility to rangeland managers.

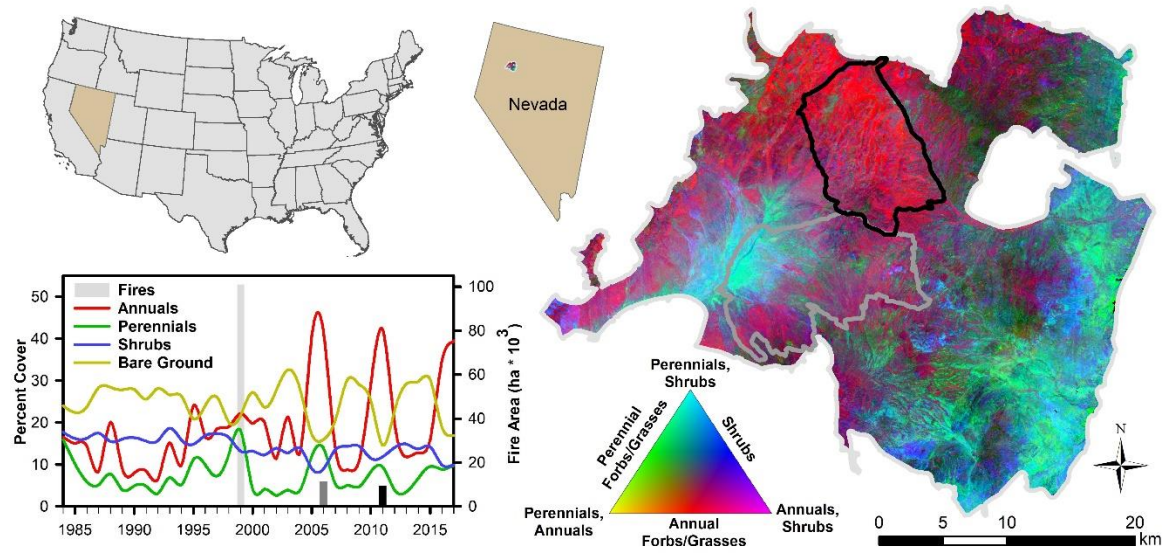


Figure 2. 4: Future availability of remote sensing products with high spatiotemporal resolution has great potential to be incorporated into multivariate metrics used to detect early warning signals and regime shifts. Shown here are trends in annual percent cover of annual forbs/grasses, perennial forbs/grasses, shrubs, and bare ground from 1984-2017 within an area experiencing cheatgrass invasion. Bars denote the area of the Dun Glenn fire and subsequent smaller scale fires that burned within the original fire perimeter.

CHAPTER 3: SHIFTING SPATIAL REGIMES IN A CHANGING CLIMATE²

ABSTRACT

In the present era of rapid global change, development of early warnings of ecological regime shifts is a major focus in ecology. Identifying and tracking shifts in spatial regimes is a new approach with potential to enhance understanding of ecological responses to global change. Here, we identify spatial regimes in avian community data and track regime movements over 46 years in the North American Great Plains. We found evidence of strong, directional non-stationarity. The northernmost spatial regime boundary moved >590 km northward, and the southernmost boundary moved >260 km northward. Tracking spatial regimes affords decadal planning horizons and moves beyond predominately temporal early warnings of the past by providing spatiotemporally explicit early warnings of regime shifts in systems without fixed boundaries.

² CPR contributed to conceptualization, programming, data validation, formal analysis, data curation, all writing aspects, visualization, and project administration. DT, CRA, and DGA contributed to conceptualization and all writing aspects.

MAIN TEXT

Ecological systems are complex and hierarchically organized in space and time (Allen, Angeler, Garmestani, Gunderson, & Holling, 2014), yet early efforts to quantify ecological resilience and predict regime shifts have focused on a single temporal dimension (Burthe et al., 2016; Dakos, Carpenter, Nes, & Scheffer, 2015). This approach has worked well when the spatial boundaries of ecosystems are readily evident. For example, theoretical inference of early warning and pending regime change has advanced in studies of shallow lake ecosystems, which have hard boundaries that make it possible for scientists to ignore external spatial dimensions of these complex systems prior to regime shifts (Carpenter et al., 2011; Dakos et al., 2012). Advancements have been made by extending early warning indicators such as autocorrelation into spatial contexts (Butitta, Carpenter, Loken, Pace, & Stanley, 2017; T. J. Cline et al., 2014; Kefi et al., 2014). However, the theory and methods still assume fixed spatial boundaries of regimes despite being situated in open, complex and dynamic systems (Clements & Ozgul, 2018).

The concept of spatial regimes represents a new frontier in resilience science that unifies both spatial and temporal dimensions into the study of regime persistence and change across ecosystems without fixed boundaries (Roberts et al., 2018; Sundstrom et al., 2017). Spatial regimes are defined as sudden spatial transitions separating ecological regimes, which are characterized by differences in core functions, structure, and processes whereby one regime is fundamentally different from the neighboring regime (Roberts et al., 2018; Scheffer, Carpenter, Foley, Folke, & Walker, 2001). The study of spatial regimes extends years of research in resilience science and regime shift theory,

which studied systems with well-known boundary limits and where critical transitions have been observed over time (Dakos et al., 2015; Scheffer et al., 2001). Two important features underpin spatial regime theory. First, spatial regimes exhibit self-similarity in structure and composition maintained by feedback mechanisms within discrete spatial boundaries at a given scale (Allen et al., 2016). The theory recognizes that all spatial regimes have geographic limits, but those limits may not be fixed or known (Allen et al., 2016). The limits separating neighboring regimes represent critical spatial transitions, meaning that where one spatial regime ends, another begins (Sundstrom et al., 2017). Spatial regimes move as a result of localized critical transitions over time (Allen et al., 2016; Roberts et al., 2018). To this end, there is no single appropriate scale to define critical transitions in space and how those spatial transitions move over time, so this body of theory has only recently advanced as more powerful metrics have emerged in recent years (Allen et al., 2016; Clements & Ozgul, 2018).

Here, we build on decades of ecological research on body mass size distributions (Angeler et al., 2016; Holling, 1992; Spanbauer et al., 2016) to disentangle alternative scientific predictions regarding the behavior of large-scale spatial regimes in an era of global environmental change. One prediction, based on an extension of resilience theory to date, is that external environmental forcing will cause idiosyncratic behavior in spatial regimes undergoing collapse, similar to the responses of individual species prior to extinction (Doncaster et al., 2016; Drake & Griffen, 2010). An alternative prediction is that spatial regimes are non-stationary and will be conserved because of strong self-organization (positive feedbacks), meaning that spatial regime boundaries will move in a

directional, orderly trajectory (Roberts et al., 2018; Sundstrom et al., 2017).

Disentangling the predictable and orderly from the unpredictable and idiosyncratic provides the foundation for advancing the history of science in early warnings of critical transitions in nature (Clements & Ozgul, 2018).

We analyzed 46-years of avian community data from the Great Plains of North America, revealing regional, poleward shifts in both the southernmost and northernmost spatial regime boundaries (Figure 3.1). The northernmost regime boundary has moved at a greater rate, moving > 590 km from 1970 baselines (0.121 ± 0.080 degrees latitude per year [13 km per year] at 90% confidence) compared to approximately 260 km for the southernmost boundary (0.053 ± 0.051 degrees latitude per year [6 km per year] at 90% confidence). These differential rates of spatial regime movement (northern vs. southern boundaries; Figure 3.1) match expectations associated with arctic amplification and accelerated change in northern versus southern latitudes of temperate North America (Cohen et al., 2014). Consistent with existing theoretical foundations (La Sorte, Hochachka, Farnsworth, Dhondt, & Sheldon, 2016), the regime moving more quickly also carries with it greater interannual volatility in its location (Figure 3.1).

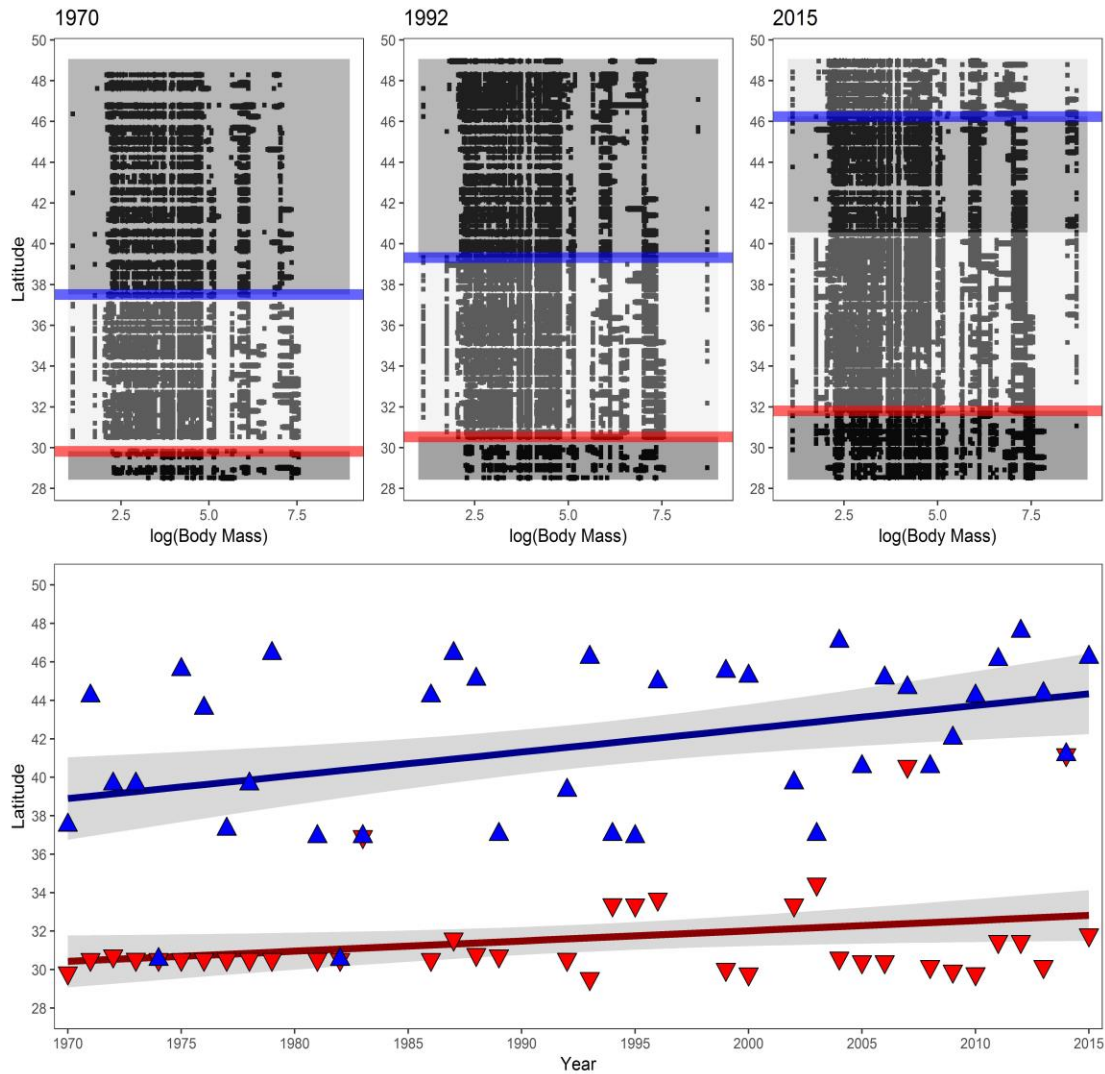


Figure 3. 1: Shifts in spatial regime boundaries demonstrated by breeding bird body mass discontinuities from 1970 - 2015 in the North American Great Plains biome. The top panel depicts latitudinal spatial regime boundaries (y-axis) determined by log-ranked avian body mass discontinuities (x-axis). Black dots represent body mass aggregations identified via discontinuity analysis in each breeding bird survey route within the transect. Gray-scale boxes represent spatial regimes, and the northernmost and southernmost spatial regime boundaries are highlighted by blue and red lines,

respectively. The bottom panel depicts spatial regime boundaries (blue triangles = northernmost, red triangles = southernmost) detected each year, and lines represent modeled northernmost and southernmost spatial regime boundary movement over time with 90% confidence (grey ribbon). When northernmost and southernmost boundaries were the same (i.e., when only one spatial regime boundary was detected in a year), blue and red triangles overlap.

Directional (northward) change in spatial regime boundaries occurred with relative stability in the number of spatial regimes identified over the past half-century (2.91 ± 0.39 , 90% confidence; Figure 3.2). The number of spatial regimes detected ranged from 0 - 5, with transitory regimes occurring periodically and a fourth, novel spatial regime emerging more consistently in the 2010's decade (i.e., 2010 - 2015; Figure 3.2). In the early decades of our study, spatial regime boundaries showed some congruence with the Great Plains biome's historic extent (Figure 3.2). But in subsequent decades, spatial regimes expanded (southernmost regime), moved northward (middle regime), and contracted (northern regimes), providing strong evidence that spatial regimes are rapidly reorganizing and diverging from historic biome extents by the 2010's (Figure 3.2).

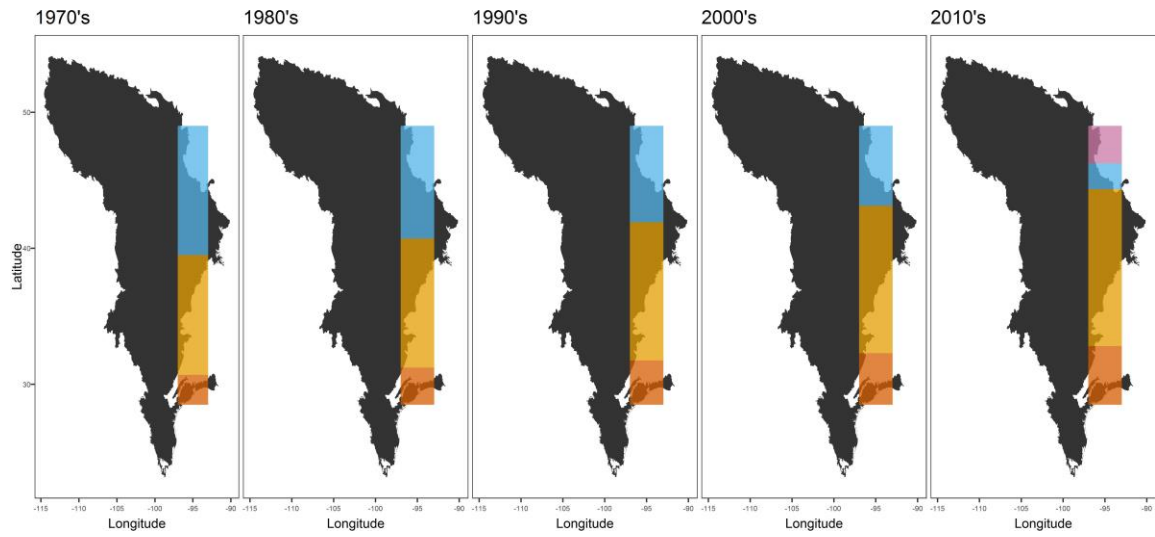


Figure 3. 2: Visualization and tracking of predicted decadal spatial regimes and their boundaries in the North American Great Plains biome. Black polygons represent the historic Great Plains biome extent. Colored bars represent average number and predicted extents of spatial regimes within the study area over five decades.

The cause of northern movement is unknown but is congruent with biogeographical patterns of change for multiple global change drivers in central North America. Climate change, anthropogenic pressures, wildfire trends, and woody plant invasions have all operated along a putatively south-to-north trajectory over the past several decades, particularly within the Great Plains (Allred et al., 2015; Boettiger, Ross, & Hastings, 2013; Brown, Johnson, Loveland, & Theobald, 2005; Chen, Hill, Ohlemüller, Roy, & Thomas, 2011; Donovan, Wonkka, & Twidwell, 2017; Engle, Coppedge, & Fuhlendorf, 2008; Johnston, 2014) (Figure 3.3). Irrespective of mechanism,

this finding suggests that spatial regimes, and the animal body mass distributions we use to identify regimes, are indeed conservative, as originally predicted.

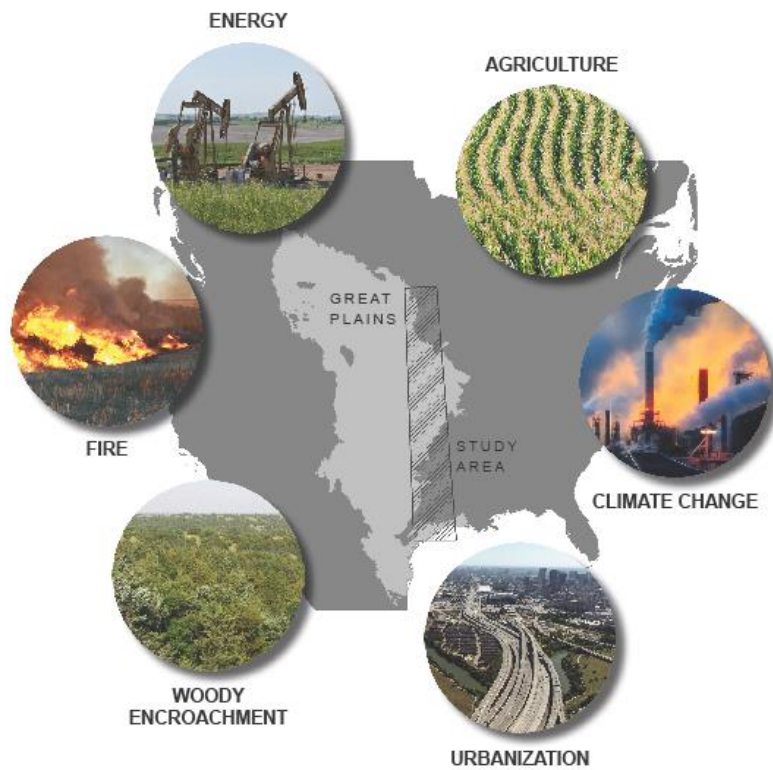


Figure 3. 3: Global changes influencing ecological regimes in central North America. Global changes such as agricultural land conversion, anthropogenic climate change, urbanization, woody plant encroachment, increasing frequency/intensities of fire, and energy development are all driving ecological change within the North American Great

Plains in a putatively south-to-north trajectory. Predictable, directional (poleward) movement of spatial regime boundaries within the Great Plains corresponds to the trajectories of global change drivers.

Our analysis also reveals that identifying spatial regimes and their boundaries are strong candidates for generic signals for early warning of regime change. We use the movement of spatial regime boundaries within the interior of central North America as an illustration (Figure 3.4). For a network of protected lands in this region, relevant early warnings would come from tracking spatial regime boundaries within a surrounding window (Figure 3.4). Knowing the “baseline” boundary in 1970 and its average northward movement pattern, protected lands in the Flint Hills ecoregion had decades of early warning that the entire ecoregion would soon experience an imminent transition, and protected lands in the Western Corn Belt Plains ecoregion had > 40 years of early warning (Figure 3.4).

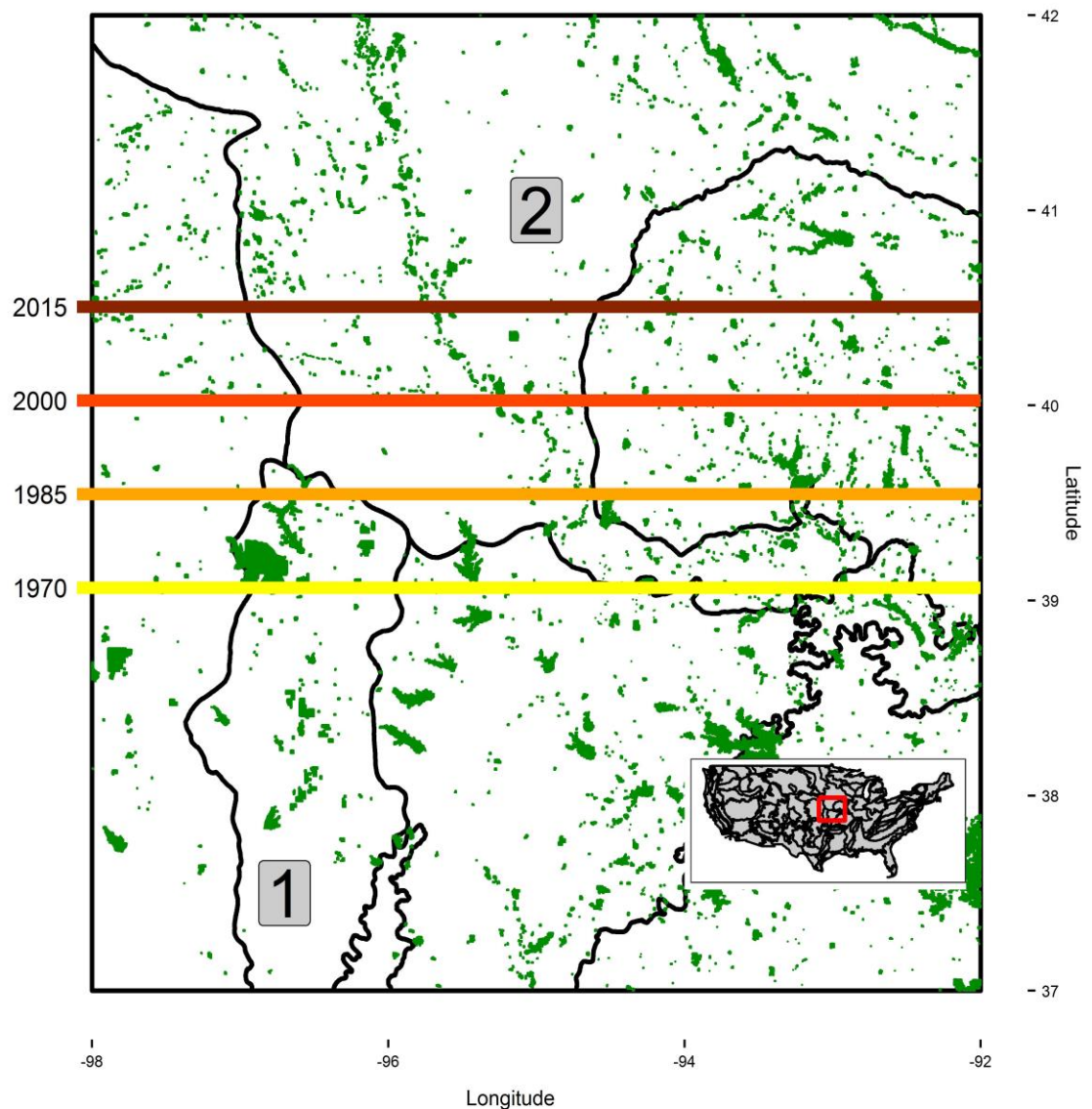


Figure 3. 4: Spatial regime boundary movement between 37 - 42 degrees latitude across a network of protected areas covering in central North America. Black lines indicate level III US Environmental Protection Agency ecoregion boundaries, and green polygons indicate protected areas. The ecoregion labeled No. 1 is the Flint Hills ecoregion, and the ecoregion labeled No. 2 is the Western Corn Belt Plains ecoregion. Predicted spatial

regime boundaries (colored horizontal lines) correspond with linear prediction for the years 1970, 1985, 2000, and 2015 ($\beta = 0.032 \pm 0.026$ degrees latitude per year; 90% confidence; $F = 4.093$; $P = 0.052$).

The addition of a spatial dimension without fixed boundaries to resilience quantification and regime shift detection allows for increased planning horizons in the face of global environmental change. Early warning detection using time series data without spatial context, or with spatial context but within fixed boundaries, has largely been done in hindsight (Burthe et al., 2016; Butitta et al., 2017; T. J. Cline et al., 2014; Dakos et al., 2015). Northward, predictable movement of spatial regimes provides an early warning for the entire northern Great Plains and signals increasing vulnerability to biome persistence of the Great Plains.

A spatial regime boundary moving closer to a given location is an early warning of an impending abrupt change-but a change that is relatively predictable as one regime replaces another. Theoretically, this should precede traditional generic signals of early warning of a pending regime shift (Hastings & Wysham, 2010). Traditional early warning signals such as critical slowing down, rising variance, and flickering rely on ecological data departing and returning to a baseline, which essentially requires a temporal lag before detecting even a single iteration of a signal (Hastings & Wysham, 2010; Kefi et al., 2014). Because they are also calculated from an aggregated array of samples at a given location, traditional signals also do not account for the spatial context within or outside of the location, meaning they must wait for signals to be of sufficient

magnitude to register as an early warning across the entire location (Burthe et al., 2016; Kefi et al., 2014; Scheffer et al., 2009).

It is noteworthy that the identification of most early warning signals for regime change have utilized spatially static systems, such as lakes or terrestrial systems within a fixed boundary (Boettiger et al., 2013; Carpenter et al., 2011; Clements & Ozgul, 2018; Butitta et al., 2017; Clements, Drake, Griffiths, & Ozgul, 2015). The bounds of most ecological systems are more open and not readily apparent. Because many systems have porous boundaries (e.g., grasslands, oceans), many taxa are highly mobile (e.g., birds, pelagic fish), and system boundaries can shift rhythmically or in response to change drivers (e.g., climatic, anthropogenic), using data derived from static or subjective spatial boundaries could drown out or misidentify early warning signals (Clements et al., 2015). Tracking spatial regimes opens a new frontier for the science of early warning detection that accounts for self-organized system boundaries and not just those most perceptible to human observers.

The science of early warning has been pursued with the intent to foster earlier adaptation in environmental management (Biggs, Carpenter, & Brock, 2009). Our analysis suggests this is possible at sub-continental scales. As a moving ecological regime approaches a given location, it becomes increasingly likely that the existing ecological regime will collapse and locations managed to reflect earlier regimes will become a “ghost of regimes past”. Acknowledging this reality has been difficult for ecosystem managers at a given location to accept, and laws such as the Endangered Species Act in the United States currently lack the flexibility necessary to solve this

general problem of managing for ghosts of past regimes because single species are often the prime conservation targets. For example, in the central portion of our study area (Figure 3.3), land managers are mandated to maintain populations of at-risk species such as Henslow's Sparrow and Bobolink at historic levels in spite of the fact that their individual distributions or associated regimes may have shifted decades previous (Craig, 2010). This means adaptation is unlikely within these protected areas despite advanced warning of regime change.

Policies that mandate management for ghosts of regimes past, regardless of the current surrounding regime, may be setting themselves up for failure in an era of global change and uncertainty (Craig, 2010; Twidwell, Allred, & Fuhlendorf, 2013). To illustrate, in our example of spatial regime boundaries shifting northward past a conservation land in central North America (Figure 3.4), land managers tasked with preserving historical plant-animal associations will continue to burn and mechanically remove woody plants to maintain remnants of the historic tallgrass prairie regime while simultaneously losing ground to encroaching woody regimes due to positive feedbacks (e.g., propagule pressure, avian seed dispersal) (Engle et al., 2008; Twidwell et al., 2013). Once these coercive management efforts wane, positive feedbacks will quickly shift to the current basin of attraction of the surrounding spatial regime (Allen et al., 2016; Baho, Drakare, Johnson, Allen, & Angeler, 2014). An alternative approach for land managers is to embrace northward-moving spatial regimes and align conservation efforts in northern protected areas congruent with the needs of species from a formerly southern area, and to ensure viable, dynamic, corridors where and when needed.

Spatial regimes may not follow global change trajectories when strong local drivers, such as immobile environmental filters (e.g., sandy soil substrates, alkaline soils) or anthropogenic barriers, exist. In these cases, theory predicts spatial regimes will contract and not “move through” these barriers (Ficetola, Mazel, & Thuiller, 2017; Glor & Warren, 2011). Over time, if global drivers outweigh local drivers, spatial regime boundaries may exhibit high variance as the local system collapses and reorganizes in the same location. For example, in our study, the southernmost spatial regime boundary (Figure 3.2) corresponds broadly with the coastal prairie, which is associated with unique sandy soil types and has experienced major landscape fragmentation and conversion via urbanization and energy development (Allred et al., 2015; Boettiger et al., 2013; Brown et al., 2005; Chen et al., 2011; Donovan et al., 2017; Engle et al., 2008; Johnston, 2014) (Figure 3.2). Indeed, the southernmost spatial regime boundary exhibited fidelity to the geographic boundary of the coastal prairie from 1970 - 1993 (Figure 3.1). But in the mid-1990’s, the southernmost boundary began to vary more widely in latitude between its original location to nearly the latitude of the historic northernmost boundary (Figure 3.1, 2.2).

Management of spatial regimes, given their conservative nature and tools to identify their boundaries, should encourage more adaptive measures that both 1) consider the current and potential future scale of change associated with underlying driving processes and 2) embrace ecological non-stationarity as part of short-term and long-term planning horizons. Specializations within ecology have struggled to fully move away from the legacy of equilibrium management, despite numerous resilience-based

management frameworks (Briske, Bestelmeyer, Stringham, & Shaver, 2008; Jantz et al., 2015; Twidwell et al., 2013). We see the addition of spatial dimensionality without fixed boundaries to resilience quantification and early warning detection, particularly how spatial regimes behave over time, as a necessary ingredient capable of launching environmental management forward in the Anthropocene. Spatial monitoring of regime change over time could further efforts to create collaborative networks among land stewards and more strategically develop protected areas acknowledging the strong non-stationarity that currently exists (Allen et al., 2016; Birgé, Allen, Craig, & Twidwell, 2018; Sundstrom et al., 2017). Instead of focusing on historic species assemblages and their idealized distribution envelopes, a successful network would focus on system-level maintenance of resilient, desirable regimes in the face of change.

METHODS

Experimental Design

BBS data manipulation

We collected 46 years (1970 - 2015) of the U.S. Geological Survey's North American Breeding Bird Survey data (BBS), which is a freely available dataset of avian community composition collected by trained observers along permanent, georeferenced roadside routes across the North American continent (Sauer et al., n.d.). Because routes were still being established in the initial years of the BBS, especially in the Great Plains and western portions of North America, to avoid biased estimates of presence/absence we consider route data starting in 1970, when approximately 50% of currently active routes had been established (Table 3.1). Along each approximately 39.5 km route, observers

make 50 stops (once every 0.8 km) and conduct point-count surveys at each stop. During a point-count survey, observers stand at the stop and record the abundance of any bird species they detect visually or aurally within a 0.402 km radius for three minutes. Surveys begin thirty minutes prior to local sunrise and last until the whole route is completed. To increase uniformity in bird detection probability, observers conduct surveys only on days with low wind speeds, high visibility, and little or no rain. Routes are distributed relatively evenly throughout the United States. Due to latitudinal differences in breeding season timing, routes may begin as early as May or as late as July.

Because of known negative observation biases for waterfowl and allied families and because water-dwelling avian families follow different body mass patterns than terrestrial avian families, we removed all species from the Anseriformes, Gaviiformes, Gruiformes, Pelecaniformes, Phaethontiformes, Phoenicopteriformes, Podicipediformes, Procellariiformes, and Suliformes families from the analysis (Holling, 1992; Sauer et al., n.d.). We also removed hybrids and unknowns, and we condensed subspecies to their respective species.

Belt transect

Multiple global change drivers are exerting influence in a south-to-north pattern within the Great Plains. For instance, in the Great Plains, climate change is shifting native and agricultural plant phenologies (Richardson et al., 2013) and geographic centers of species distributions (Hovick et al., 2016). Woody plant encroachment is causing regime shifts from historically grassland regimes to woodland or shrubland regimes (Engle et al., 2008); whole ecoregions in the southern Great Plains have shifted to woodlands in the

past century, and northern ecoregions are increasingly on the brink of wholesale regime shifts (Twidwell et al., 2013). Interacting with climate change and woody plant encroachment, fire frequency and size have also increased by >400% in the Great Plains, especially in the southern portions that have transitioned to woodlands (Donovan et al., 2017). Energy development such as oil and gas extraction reduced net primary productivity by approximately 4.5 Tg between 2000-2015, with much of the development focused on the southern Great Plains (Allred et al., 2015). Although the rate of agricultural land conversion had greatly slowed by the 1950s (Brown et al., 2005), the northern plains lost much of its remaining grassland after commodity prices surged at the beginning of the 21st century (Drummond et al., 2012). Urbanization and population growth in the Great Plains has continually increased in and around already populated areas (Brown et al., 2005), with the greatest growth occurring in the southern portions of the Great Plains.

In light of this, we selected a belt transect on the ecotone of the Great Plains and Eastern Temperate Forests extending from the Gulf of Mexico to the edge of the boreal forest in Canada. Specifically, the belt transect extended south-north from 28 - 49 degrees latitude (approximately 2300 km) and east-west from 93 - 97 degrees longitude (approximately 350 km).

Statistical Analysis

Identifying discontinuities

For each route falling within the belt transect, we identified discontinuities in avian community body masses by rank-ordering the log-transformed body masses of each

species observed at each route for each year. We obtained mean body mass estimates for all species in the analysis from the CRC Handbook of Avian Body Masses (Dunning Jr, 2007). We then used the “discontinuity detector” method (Barichievy et al., 2018) on the log-ranked body masses, which is based on the Gap Rarity Index for detecting discontinuities in continuous data (C. Stow, Allen, & Garmestani, 2007). For taxa with determinant growth, mean body mass has been shown to reliably differentiate size aggregations and is strongly allometric to the scales at which functions are carried out by organisms (Nash et al., 2014; Sundstrom & Allen, 2014). Because the discontinuity detector method is known to overestimate discontinuities in observations with low species richness, we removed any routes with < 40 species observed within a given year (Table 3.1). We used a power table (Lipsey, 1990) to account for sample size (the number of species observed at each BBS route in a given year) and average variance in body masses (Dunning Jr, 2007) to adjust the critical d-value (the value based on Monte Carlo simulations that identifies significant discontinuities) where N varied (Allen, Forsy, & Holling, 1999) (Table 3.2).

Spatial regime detection

To detect spatial regimes in each year, we ordered routes in ascending latitude and transformed the discontinuities into a data matrix for analysis. Specifically, in order from the lowest ranked body mass aggregation to the highest, we calculated the sizes of body mass aggregations (the log-ranked length of each aggregation), the sizes of gaps between aggregations (the log-ranked length of each gap), and the locations of aggregations (the log-transformed body mass of the species with the lowest body mass in each aggregation)

for each route (Spanbauer et al., 2016). We cast these into a matrix using the “dcast” function in the “reshape2” and “data.table” packages in R, where every row represented a route within a given year and every column an aggregation size, gap size, or aggregation location. We calculated separate Bray-Curtis dissimilarity matrices from each year’s data.

To identify spatial regimes, we ran constrained hierarchical clustering on each year’s distance matrix starting at the southernmost (lowest latitude) BBS route and proceeding by order of latitude to the northernmost BBS route (highest latitude). Constrained hierarchical clustering directionally separates multivariate data series into homogeneous, non-overlapping segments; that is, it constrains clusters so that only adjacent, contiguous samples (i.e., a contiguous segment of BBS routes along a spatial transect) are allowed to cluster (Galzin & Legendre, 1987; Spanbauer et al., 2016). This method is commonly used to delineate temporally-ordered regimes in paleo community data (Leys, Finsinger, & Carcaillet, 2014; Vermaire, Greffard, Saulnier-Talbot, & Gregory-Eaves, 2013) and to detect significant community transitions along spatial transects (Galzin & Legendre, 1987; Vormisto, Phillips, Ruokolainen, Tuomisto, & Vásquez, 2000). To perform constrained hierarchical clustering, we used the “chclust” function with the “CONISS” method from the “rioja” package in R.

We used the broken stick model (“bstick.chclust” from the “rioja” package in R) to determine the number of significant clusters (Bennett, 1996; Spanbauer et al., 2016). The broken stick method, commonly used in conjunction with constrained hierarchical clustering, tests the distribution of clusters from constrained hierarchical clustering against multiple null random distributions of clusters to ascertain the number of

significant clusters (Bennett, 1996; Leys et al., 2014; Spanbauer et al., 2016; Vermaire et al., 2013). Because constrained hierarchical clustering identifies homogeneous, non-overlapping areas of self-similarity, significant clusters can be interpreted as regimes, and boundaries between significant clusters can be interpreted as regime boundaries.

Therefore, we considered the latitudes of significant cluster boundaries from each year to be the location of spatial regime boundaries from that year (Spanbauer et al., 2016).

Tracking movement in spatial regimes

We tested for non-random movement in spatial regime boundaries over time by fitting generalized additive models (GAMs; “mgcv” package in R) to the northernmost and southernmost spatial regime boundaries. Because GAMs not detect nonlinearity in either the northernmost (edf = 1.00, $F = 6.56$, $P = 0.02$) and southernmost (edf = 1.00, $F = 3.21$, $P = 0.08$) spatial regime boundaries, we estimated the mean rate of movement in spatial regime boundaries via linear regression (Figure 3.1). We classified the northernmost boundary each year as the spatial regime boundary with the greatest latitude, and we classified the southernmost boundary each year as the spatial regime boundary with the lowest latitude. We excluded years from the linear regression analysis in which we detected no spatial regimes from the analysis (1980, 1984, 1985, 1990, 1991, 1997, 1998, 2001). For years in which only one spatial regime boundary was detected (i.e., years with only two spatial regimes), the single boundary was counted as both the northernmost and southernmost boundary.

We also assessed spatial regime boundary movement at the scale of a regional protected areas network. Specifically, we tracked spatial regime boundary movement

from 1970 - 2015 between 37 - 42 degrees latitude to assess the utility of spatial regime tracking for early warnings for land management and the length of planning horizons spatial regimes provided (Figure 3.3). As above, we quantified spatial regime boundary latitudinal movement over time via linear regression.

TABLES

Table 3. 1: For each year of analysis, number of North American Breeding Bird Survey routes falling within the belt transect, number of routes used in analysis (where ≥ 40 bird species were recorded in a given year), and number of routes removed from analysis (where < 40 bird species were recorded in a given year).

Year	N Routes in Transect	Used	Removed
1970	124	112	12
1971	122	122	0
1972	110	97	13
1973	128	120	8
1974	123	116	7
1975	128	121	7
1976	126	115	11
1977	133	122	11
1978	146	146	0
1979	148	148	0
1980	145	139	6
1981	139	139	0
1982	133	133	0
1983	134	134	0
1984	142	132	10
1985	135	135	0
1986	142	142	0
1987	146	146	0
1988	141	135	6
1989	135	131	4
1990	136	130	6
1991	143	135	8
1992	160	157	3
1993	165	159	6
1994	172	166	6
1995	191	183	8
1996	175	167	8
1997	174	150	24
1998	172	166	6
1999	176	164	12

2000	180	174	6
2001	178	169	9
2002	168	158	10
2003	202	191	11
2004	211	199	12
2005	207	193	14
2006	200	188	12
2007	204	204	0
2008	200	186	14
2009	205	197	8
2010	207	197	10
2011	209	199	10
2012	215	202	13
2013	210	210	0
2014	213	213	0
2015	195	195	0

Table 3. 2: Power table for use with the “discontinuity detector” method from Barichievsky et al. (2018). Columns indicate the species richness at which “d-values” produced by the discontinuity detector indicate a significant gap between log-ranked body masses.

Richness	d-value
40	0.48
50	0.53
60	0.58
70	0.65
80	0.71
90	0.75
100	0.78
110	0.8

LITERATURE CITED

- Allen, C. R., Angeler, D. G., Cumming, G. S., Folke, C., Twidwell, D., & Uden, D. R. (2016). Quantifying spatial resilience. *Journal of Applied Ecology*, 53(3), 625–635.
- Allen, C. R., Angeler, D. G., Garmestani, A. S., Gunderson, L. H., & Holling, C. S. (2014). Panarchy: Theory and application. *Ecosystems*, 17(4), 578–589.
- Allen, C. R., Forys, E. A., & Holling, C. (1999). Body mass patterns predict invasions and extinctions in transforming landscapes. *Ecosystems*, 2(2), 114–121.
- Allred, B. W., Smith, W. K., Twidwell, D., Haggerty, J. H., Running, S. W., Naugle, D. E., & Fuhlendorf, S. D. (2015). Ecosystem services lost to oil and gas in north america. *Science*, 348(6233), 401–402.
- Angeler, D. G., Allen, C. R., Barichievy, C., Eason, T., Garmestani, A. S., Graham, N. A., ... others. (2016). Management applications of discontinuity theory. *Journal of Applied Ecology*, 53(3), 688–698.
- Baho, D. L., Drakare, S., Johnson, R. K., Allen, C. R., & Angeler, D. G. (2014). Similar resilience attributes in lakes with different management practices. *PLoS One*, 9(3), e91881.
- Barichievy, C., Angeler, D. G., Eason, T., Garmestani, A. S., Nash, K. L., Stow, C. A., ... Allen, C. R. (2018). A method to detect discontinuities in census data. *Ecology and Evolution*, 8(19), 9614–9623.
- Bennett, K. D. (1996). Determination of the number of zones in a biostratigraphical sequence. *New Phytologist*, 132(1), 155–170.

- Biggs, R., Carpenter, S. R., & Brock, W. A. (2009). Turning back from the brink: Detecting an impending regime shift in time to avert it. *Proceedings of the National Academy of Sciences*, 106(3), 826–831.
- Birgé, H. E., Allen, C. R., Craig, R. K., & Twidwell, D. (2018). Resilience and Law in the Platte River Basin Social-Ecological System: Past, Present, and Future. In *Practical panarchy for adaptive water governance* (pp. 115–130). Springer.
- Boettiger, C., Ross, N., & Hastings, A. (2013). Early warning signals: The charted and uncharted territories. *Theoretical Ecology*, 6(3), 255–264.
- Briske, D., Bestelmeyer, B., Stringham, T., & Shaver, P. (2008). Recommendations for development of resilience-based state-and-transition models. *Rangeland Ecology & Management*, 61(4), 359–367.
- Brown, D. G., Johnson, K. M., Loveland, T. R., & Theobald, D. M. (2005). Rural land-use trends in the conterminous United States, 1950–2000. *Ecological Applications*, 15(6), 1851–1863.
- Burthe, S. J., Henrys, P. A., Mackay, E. B., Spears, B. M., Campbell, R., Carvalho, L., ... others. (2016). Do early warning indicators consistently predict nonlinear change in long-term ecological data? *Journal of Applied Ecology*, 53(3), 666–676.
- Butitta, V. L., Carpenter, S. R., Loken, L. C., Pace, M. L., & Stanley, E. H. (2017). Spatial early warning signals in a lake manipulation. *Ecosphere*, 8(10).
- Carpenter, S. R., Cole, J. J., Pace, M. L., Batt, R., Brock, W., Cline, T., ... others. (2011). Early warnings of regime shifts: A whole-ecosystem experiment. *Science*, 332(6033), 1079–1082.

- Chen, I.-C., Hill, J. K., Ohlemüller, R., Roy, D. B., & Thomas, C. D. (2011). Rapid range shifts of species associated with high levels of climate warming. *Science*, 333(6045), 1024–1026.
- Clements, C. F., & Ozgul, A. (2018). Indicators of transitions in biological systems. *Ecology Letters*, 21(6), 905–919.
- Clements, C. F., Drake, J. M., Griffiths, J. I., & Ozgul, A. (2015). Factors influencing the detectability of early warning signals of population collapse. *The American Naturalist*, 186(1), 50–58.
- Cline, T. J., Seekell, D. A., Carpenter, S. R., Pace, M. L., Hodgson, J. R., Kitchell, J. F., & Weidel, B. C. (2014). Early warnings of regime shifts: Evaluation of spatial indicators from a whole-ecosystem experiment. *Ecosphere*, 5(8), 1–13.
- Cohen, J., Screen, J. A., Furtado, J. C., Barlow, M., Whittleston, D., Coumou, D., ... others. (2014). Recent Arctic amplification and extreme mid-latitude weather. *Nature Geoscience*, 7(9), 627.
- Craig, R. K. (2010). Stationarity is dead-long live transformation: Five principles for climate change adaptation law. *Harv. Envtl. L. Rev.*, 34, 9.
- Dakos, V., Carpenter, S. R., Brock, W. A., Ellison, A. M., Guttal, V., Ives, A. R., ... others. (2012). Methods for detecting early warnings of critical transitions in time series illustrated using simulated ecological data. *PloS One*, 7(7), e41010.
- Dakos, V., Carpenter, S. R., Nes, E. H. van, & Scheffer, M. (2015). Resilience indicators: Prospects and limitations for early warnings of regime shifts. *Philosophical*

- Transactions of the Royal Society of London B: Biological Sciences*, 370(1659), 20130263.
- Doncaster, C. P., Alonso Chávez, V., Viguier, C., Wang, R., Zhang, E., Dong, X., ...
 Dyke, J. G. (2016). Early warning of critical transitions in biodiversity from compositional disorder. *Ecology*, 97(11), 3079–3090.
- Donovan, V. M., Wonkka, C. L., & Twidwell, D. (2017). Surging wildfire activity in a grassland biome. *Geophysical Research Letters*, 44(12), 5986–5993.
- Drake, J. M., & Griffen, B. D. (2010). Early warning signals of extinction in deteriorating environments. *Nature*, 467(7314), 456.
- Drummond, M. A., Auch, R. F., Karstensen, K. A., Sayler, K. L., Taylor, J. L., & Loveland, T. R. (2012). Land change variability and human–environment dynamics in the United States Great Plains. *Land Use Policy*, 29(3), 710–723.
- Dunning Jr, J. B. (2007). *CRC handbook of avian body masses*. CRC press.
- Engle, D. M., Coppedge, B. R., & Fuhlendorf, S. D. (2008). From the dust bowl to the green glacier: human activity and environmental change in Great Plains grasslands. In *Western north american juniperus communities* (pp. 253–271). Springer.
- Ficetola, G. F., Mazel, F., & Thuiller, W. (2017). Global determinants of zoogeographical boundaries. *Nature Ecology & Evolution*, 1(4), 0089.
- Galzin, R., & Legendre, P. (1987). The fish communities of a coral reef transect.
- Glor, R. E., & Warren, D. (2011). Testing ecological explanations for biogeographic boundaries. *Evolution*, 65(3), 673–683.

- Hastings, A., & Wysham, D. B. (2010). Regime shifts in ecological systems can occur with no warning. *Ecology Letters*, 13(4), 464–472.
- Holling, C. S. (1992). Cross-scale morphology, geometry, and dynamics of ecosystems. *Ecological Monographs*, 62(4), 447–502.
- Hovick, T. J., Allred, B. W., McGranahan, D. A., Palmer, M. W., Elmore, R. D., & Fuhlendorf, S. D. (2016). Informing conservation by identifying range shift patterns across breeding habitats and migration strategies. *Biodiversity and Conservation*, 25(2), 345–356.
- Jantz, S. M., Barker, B., Brooks, T. M., Chini, L. P., Huang, Q., Moore, R. M., ... Hurtt, G. C. (2015). Future habitat loss and extinctions driven by land-use change in biodiversity hotspots under four scenarios of climate-change mitigation. *Conservation Biology*, 29(4), 1122–1131.
- Johnston, C. A. (2014). Agricultural expansion: land use shell game in the US Northern Plains. *Landscape Ecology*, 29(1), 81–95.
- Kefi, S., Guttal, V., Brock, W. A., Carpenter, S. R., Ellison, A. M., Livina, V. N., ... Dakos, V. (2014). Early warning signals of ecological transitions: Methods for spatial patterns. *PloS One*, 9(3), e92097.
- La Sorte, F. A., Hochachka, W. M., Farnsworth, A., Dhondt, A. A., & Sheldon, D. (2016). The implications of mid-latitude climate extremes for North American migratory bird populations. *Ecosphere*, 7(3).

- Leys, B., Finsinger, W., & Carcaillet, C. (2014). Historical range of fire frequency is not the achilles' heel of the corsican black pine ecosystem. *Journal of Ecology*, 102(2), 381–395.
- Lipsey, M. W. (1990). *Design sensitivity: Statistical power for experimental research* (Vol. 19). Sage.
- Nash, K. L., Allen, C. R., Angeler, D. G., Barichievy, C., Eason, T., Garmestani, A. S., ... others. (2014). Discontinuities, cross-scale patterns, and the organization of ecosystems. *Ecology*, 95(3), 654–667.
- Richardson, A. D., Keenan, T. F., Migliavacca, M., Ryu, Y., Sonnentag, O., & Toomey, M. (2013). Climate change, phenology, and phenological control of vegetation feedbacks to the climate system. *Agricultural and Forest Meteorology*, 169, 156–173.
- Roberts, C. P., Twidwell, D., Burnett, J. L., Donovan, V. M., Wonkka, C. L., Bielski, C. L., ... others. (2018). Early warnings for state transitions. *Rangeland Ecology & Management*.
- Sauer, J. R., Niven, D. K., Hines, J. E., Ziolkowski, D. J., Pardieck, K. L., Fallon, J. E., & Link, W. A. (n.d.). "The North American Breeding Bird Survey, Results and Analysis 1966 - 2015" (Version 2.07.2017 USGS Patuxent Wildlife Research Center, Laurel, MD, 2017. Retrieved from {<https://www.pwrc.usgs.gov/bbs/>}
- Scheffer, M., Bascompte, J., Brock, W. A., Brovkin, V., Carpenter, S. R., Dakos, V., ... Sugihara, G. (2009). Early-warning signals for critical transitions. *Nature*, 461(7260), 53.

- Scheffer, M., Carpenter, S., Foley, J. A., Folke, C., & Walker, B. (2001). Catastrophic shifts in ecosystems. *Nature*, 413(6856), 591.
- Spanbauer, T. L., Allen, C. R., Angeler, D. G., Eason, T., Fritz, S. C., Garmestani, A. S., ... Sundstrom, S. M. (2016). Body size distributions signal a regime shift in a lake ecosystem. *Proc. R. Soc. B*, 283(1833), 20160249.
- Stow, C., Allen, C. R., & Garmestani, A. S. (2007). Evaluating discontinuities in complex systems: Toward quantitative measures of resilience. *Ecology and Society*, 12(1).
- Sundstrom, S. M., & Allen, C. R. (2014). Complexity versus certainty in understanding species' declines. *Diversity and Distributions*, 20(3), 344–355.
- Sundstrom, S. M., Eason, T., Nelson, R. J., Angeler, D. G., Barichievy, C., Garmestani, A. S., ... Knutson, M. (2017). Detecting spatial regimes in ecosystems. *Ecology Letters*, 20(1), 19–32.
- Twidwell, D., Allred, B. W., & Fuhlendorf, S. D. (2013). National-scale assessment of ecological content in the world's largest land management framework. *Ecosphere*, 4(8), 1–27.
- Vermaire, J. C., Greffard, M.-H., Saulnier-Talbot, É., & Gregory-Eaves, I. (2013). Changes in submerged macrophyte abundance altered diatom and chironomid assemblages in a shallow lake. *Journal of Paleolimnology*, 50(4), 447–456.
- Vormisto, J., Phillips, O., Ruokolainen, K., Tuomisto, H., & Vásquez, R. (2000). A comparison of fine-scale distribution patterns of four plant groups in an amazonian rainforest. *Ecography*, 23(3), 349–359.

CHAPTER 4: SPATIAL REGIMES: MONITORING FOR EMERGENCE³

ABSTRACT

1. The spatial regimes concept (where spatial regimes are defined as areas exhibiting self-similarity in structure and composition maintained by feedbacks within spatially explicit boundaries) is a promising candidate for detecting change and emergence of novel regimes in ecological monitoring. We seek to operationalize the spatial regimes concept by determining the potential for monitoring data to be used to 1) quantify the number of and track changes in spatial boundaries (i.e., potential spatial regimes) and 2) capture the emergence of new spatial regimes at multiple scales.
2. We collected vegetation data along a 4 km transect spanning a complex macrosystem of grassland, a river valley, and recently-burned forests in the Niobrara Valley Preserve, USA. We used constrained hierarchical clustering to identify spatially explicit, non-overlapping boundaries based on vegetative structural and compositional differences along the transect. We then tracked changes in boundaries resulting from the simulated emergence of a shrub regime

³ CPR contributed to conceptualization, programming, data validation, formal analysis, data curation, all writing aspects, visualization, and project administration. DT, JLB, VMD, CRA, DGA, and DAW contributed to conceptualization and writing selected sections.

in the grassland over three consecutive time steps at a local scale (where the simulated regime emerged) and at the macrosystem scale (the 4 km transect).

3. We detected 8 spatial boundaries in the macrosystem, distinguishing not only visually obvious boundaries in vegetative systems (e.g., the boundary between grassland and burnt woodland) but also less apparent boundaries (e.g., separations between mixed-grass and exotic prairies). Via tracking spatial boundaries, we detected emergence of the simulated shrub regime at the local and macrosystem scales. Tracking spatial boundaries also revealed an early warning signal at the macrosystem scale.
4. This operationalization of the spatial regimes concept successfully detected spatially explicit ecological change and emergence with no *a priori* knowledge. Spatial regimes merit application in adaptive monitoring frameworks to detect unexpected change and monitor management actions in protected areas.

INTRODUCTION

With ecological uncertainty propagating across global and local scales, there is increasing need for monitoring frameworks capable of detecting both known drivers of change as well as the emergence of abrupt, surprising changes, such as regime shifts across protected areas (e.g., shifts from grasslands to shrublands, from coral-dominated to algae dominated reefs; Scheffer, Carpenter, Foley, Folke, & Walker 2001; Nichols & Williams 2006). To meet this need, monitoring frameworks must explicitly incorporate and acknowledge ecological uncertainty; that is, have the ability to detect novel, emergent ecological change and early warnings of regime shifts in an adaptive monitoring framework (Lindenmayer & Likens, 2009; Lindenmayer, Piggott, & Wintle, 2013). However, current monitoring frameworks in protected areas are often designed to optimally detect known potential changes. For instance, monitoring plots may be stratified across communities or systems of conservation priority to maximize the ability to detect changes from one known system of conservation priority to a less desirable system (Hutto & Belote, 2013). Conversely, passive surveillance monitoring may be randomly distributed across a broad geographic region to attempt to temporal capture changes in a range of state variables known to drive system condition and functioning (Hutto & Belote, 2013; Roberts et al., 2018). By attempting to optimize either the specificity or breadth of monitoring, these frameworks become limited by assumptions of stationarity, lag behind temporal changes, or failing to detect emergence or early warnings of novel regimes (Lindenmayer & Likens, 2010; Magurran et al., 2010).

The spatial regimes concept is a promising candidate for incorporating spatially explicit ecological change and emergence of novelty into monitoring frameworks (Allen et al., 2016). Embedded within resilience theory, spatial regimes are defined as areas exhibiting self-similarity in structure and composition maintained by feedback mechanisms within spatially explicit boundaries (Roberts et al., 2018). The spatial regime concept brings together elements of both the equilibrium and non-equilibrium paradigms of species associations (Clements, 1916; Gleason, 1926; Allen et al., 2016). It distinguishes itself from historic community delineation in ecology by directly considering the spatial order of ecological regimes, the delineation of the boundaries separating regimes in space, and by enabling monitoring of changes in spatial regime boundaries over time (Roberts et al., 2018). By adding a spatial dimension and explicit spatial boundaries to regimes, spatial regimes extend upon traditional concepts of regime shifts and alternate states: spatial regimes can manifest as localized regime shifts (i.e., shifts in structure and composition) that do not necessarily cause a regime shift in the entire macrosystem (Roberts et al., 2018). For instance, in lake systems, localized early warning signals of regime shifts toward an algal-dominated eutrophic lake were detected by spatial early warning indicators, but this did not lead to a system-wide regime shift (Donangelo, Fort, Dakos, Scheffer & Van Nes, 2010; Cline et al., 2014). But localized shifts in spatial regimes have the potential to propagate across scales, leading to system-wide regime shifts (Allen et al., 2016). For example, localized spatial changes in terrestrial vegetation patterns can forecast system-wide regime shifts (Kefi et al., 2007;

Kefi et al., 2014), and cross-scale connectivity of land cover types (i.e., spatial regimes) can presage regional regime shifts (Zurlini et al., 2014).

However, like other approaches related to boundary detection, spatial regimes face the criticism of being unable to detect emergence or early warnings of novel regimes in monitoring data (Fagan, Fortin, & Soykan, 2003; Strayer, Power, Fagan, Pickett, & Belnap, 2003). Boundary detection has historically suffered from arbitrarily-defined “significance” of boundaries and, consequently, statistically significant boundaries that do not correspond to ecologically meaningful boundaries (Strayer et al., 2003). Likewise, arbitrary choices of monitoring scale (i.e., extent and resolution of sampling) can bias the number and locations of boundaries (Fagan et al., 2003). This problem is clearest when selecting an extent and resolution for systems without clear boundaries—such as open terrestrial systems where multiple stable states can exist within spatially-explicit boundaries and at multiple, hierarchical scales (Allen et al., 2016; Sundstrom et al., 2017). For example, in a terrestrial macrosystem in which grasslands are dominant but patches of shrub islands represent localized regime shifts with distinct feedbacks (i.e., spatial regimes; Ratajczak, Nippert, Hartman, & Ocheltree, 2011), choosing whether to consider the larger grassland macrosystem as the extent or individual patches may determine the detectability of early warnings of regime shifts (Kefi et al., 2014). Together, these issues can force boundary detection approaches to rely on *a priori* knowledge of system identities and scaling to establish significance of boundaries and scale breaks, thereby precluding detection of emergence of non-analogous regimes (Chave, 2013).

Spatial regimes have the potential to overcome these criticisms by virtue of 1) their acknowledgement of potential multiple ecological regimes (i.e., alternative states) to occur at a given spatial location and at localized, hierarchical spatial extents within a macrosystem and 2) not assuming fixed system identity, associations, or boundaries (Allen et al., 2016). To date, spatial regimes have been operationalized by identifying discontinuous spatial boundaries in biotic community compositions (Sundstrom et al., 2017). Extending this to detection of change and emergence in monitoring frameworks, spatial regimes could be operationalized by quantifying spatially-explicit boundaries in a system based on structure and composition and tracking changes in size and location of boundaries over time (Roberts et al., 2018). This may allow spatial regimes to detect emergence of novel regimes in monitoring data at multiple scales without requiring *a priori* knowledge of system structures, species, or feedbacks (Sundstrom et al., 2017). With this operationalization in a monitoring framework, we test the potential of the spatial regimes concept to 1) quantify the number and distribution of in spatial boundaries (i.e., potential spatial regimes) in a protected area comprised of a complex macrosystem and 2) capture the emergence of new spatial regimes at multiple scales by tracking changes in spatial boundaries.

METHODS

Study site

The study was located at The Nature Conservancy's Niobrara Valley Preserve in north central Nebraska, USA (42° 46' N, 100° 00' W). The Niobrara Valley Preserve is the flagship protected area for the Nature Conservancy in the North American Great Plains,

characterized by a complex and macrosystem of plant communities. North of the river, both mixed-grass and lowland tallgrass prairies occur, as well as post-fire ponderosa pine (*Pinus ponderosa*)-eastern redcedar (*Juniperus virginiana*) - bur oak (*Quercus macrocarpa*) woodlands that were burnt in stand-replacing wildfires in 2012 (Steinauer & Bragg, 1987). South of the river, deciduous forest of bur oak and American basswood (*Tilia americana*) line north-facing slopes, and cool groundwater springs provide habitat for isolated patches of paper birch (Steuter, Jasch, Ihnen, & Tieszen, 1990). The Sandhills prairie south of the valley edge consists of vegetated sand dunes, where grasses such as prairie sandreed (*Calamovilfa longifolia*), sand bluestem (*Andropogon hallii*), and little bluestem (*Schizachyrium scoparium*) are joined by forbs such as stiff sunflower (*Helianthus pauciflorus*) and silky prairie clover (*Dalea villosa*), and shrubs such as smooth sumac (*Rhus glabra*) and wild plum (*Prunus americana*). Climate is classified as continental, with mean daily temperatures ranging from -5.7 deg C in January to 24.0 deg C in July. Average annual precipitation is 559 mm, with 78% received during the April through September growing period.

Data collection

To identify spatial boundaries in vegetative communities, we collected vegetative structure and composition data along a 4 km transect. We oriented the transect along an approximately north-south axis (northern terminus = 42.80619 N, -100.0221 W; southern terminus = 42.76999 N, -100.0264 W; approximate bearing = 182 degrees) to capture a variety of vegetative communities within the NVP including northern grasslands, north

bank post-fire ponderosa pine-eastern redcedar-bur oak forest, riparian areas, south-bank woodlands, and Sandhills grasslands.

Along the transect, we collected data every 10 m for a total of 400 data points. At each point, we recorded herbaceous species composition, ground cover, understory canopy height, tree density, tree species composition, tree diameter at breast height, decay classes of snags, coarse woody debris cover, and coarse woody debris decay classes (Table S1). Specifically, we used the “point-intercept” method to measure ground cover, species composition (presence of any species touching the point), and height the tallest plant < 1.4 m tall (i.e., less than diameter at breast height) touching the point (Godínez-Alvarez, Herrick, Mattocks, Toledo, & Van Zee, 2009). Ground cover fell into water, bare soil, rock, moss, leaf litter, dead grass, fine woody debris (any not free-standing woody debris that was < 10 cm in diameter where crossing the transect), or coarse woody debris (any not free-standing woody debris that was > 10 cm in diameter where crossing the transect) categories. We used the “point-centered quarter” method to record tree species identity, diameter at breast height, decay class (if dead), and density of trees and/or snags (Cottam & Curtis, 1956). We estimated tree density at each point by averaging the distance of the closest four trees/snags in four quadrants divided by the cardinal directions from a “center” point on the transect (i.e., the data point); because of great distances between the transect and the closest trees where distances from the center exceeded 100 m (e.g., in pastures/grasslands), we recorded 101 m to indicate > 100 m distances. Finally, we used standard coarse woody debris assessment methods to measure total cover between points (length of transect intersected by coarse woody debris between

points 1 and 2, 2 and 3, etc.), number of coarse woody debris pieces in each decay class, and mean volume (Woldendorp, Keenan, Barry, & Spencer, 2004).

Spatial boundary identification

We combined all data into a single data matrix. To correct for rare species, we separately transformed herbaceous species composition (presence-absence) and tree species composition (number of each species at each point-center quarter recording) via the Hellinger transformation method of the “decostand” function in R package “vegan” (Legendre & Gallagher, 2001; J. Oksanen et al., 2007). Because we recorded structural and compositional data of multiple types (e.g., nominal ground cover type, ordinal decay classes, and continuous tree densities; Table S1), we calculated a distance matrix from the data matrix using “Gower” distance which allows for mixed data types (Laliberté & Legendre, 2010).

To identify spatially-explicit, non-overlapping spatial boundaries, we conducted constrained hierarchical clustering on the distance matrix. Constrained hierarchical clustering is useful for identifying spatial boundaries because it directionally (i.e., “chronologically” from start to end of a transect) separates multivariate data series into homogeneous segments; that is, it constrains clusters so that only adjacent samples or segments (i.e., along a spatial transect) are permitted to cluster (Galzin & Legendre, 1987; Spanbauer et al., 2016). This method is commonly used to chronologically identify regimes in paleo community data (e.g., Vermaire, Greffard, Saulnier-Talbot, & Gregory-Eaves, 2013; Leys, Finsinger & Carcaillet, 2014; Spanbauer et al., 2016), and, as in our study, has been used to detect significant community transitions along spatial transects

(Galzin & Legendre, 1987; Vormisto, Phillips, Ruokolainen, Tuomisto, & Vasquez, 2000).

We determined the number and location of significant clusters via the broken stick method (Bennett, 1996). Commonly used to determine significance of temporal breaks in chronological (e.g., paleo) data, the broken stick method tests the distribution of clusters from constrained hierarchical clustering against multiple null random distributions of clusters to ascertain the number of significant clusters (Bennett, 1996; Vermaire et al., 2013; Leys et al., 2014; Spanbauer et al., 2016). Then we associated every point along the spatial transect with its significant cluster (spatial boundary) identified by the broken stick model.

We assessed the ecological meaning of the identified spatial boundaries by investigating the structural and compositional variables associated with each significant cluster via a constrained ordination. Specifically, we used distance-based redundancy analysis (db-RDA), which allows for dissimilarity matrices using non-Euclidean distances (i.e., Gower distance; Laliberté & Legendre 2010). We set the multivariate Gower distance matrix as the response matrix, and we used the significant clusters (i.e., spatial areas between boundaries) identified by the broken stick method as constraints (predictors) for the db-RDA. We used the “capscale” function in the R package “vegan” to perform the db-RDA (Oksanen et al., 2007). We used the “envfit” function in the “vegan” package to determine the strength of variables’ associations with the first two ordination axes.

Capturing emergence of new spatial regimes over time

After identifying spatial boundaries along the entire transect, we tested the ability to use monitoring data to detect spatially explicit change and emergence of novelty in vegetative communities (i.e., spatial regimes) at multiple scales. We did this in a two-step process. First, we simulated an emerging regime shift via spatiotemporal changes in vegetative structure and community composition in the Sandhills portion of the study site (near the southern transect terminus). Second, we identified spatial boundaries for each simulated time step at two spatial scales—the scale of the macrosystem and the scale at which the regime shift was occurring (the Sandhills portion of the transect).

Simulation of emerging spatial regime

In Sandhills grasslands, smooth sumac is a clonal shrub known to cause locally discrete regime shifts from grassland to closed-canopy “shrub islands” (Hajny, Hartnett, & Wilson, 2011; Weaver & Kramer, 1932). These shrub islands produce positive feedbacks that inhibit fire spread by decreasing herbaceous plant biomass (fine fuel loads) within and immediately outside the island and depositing leaf litter which is not conducive to fire (Ratajczak, Nippert, & Collins, 2012; Ratajczak, Nippert, Hartman, & Ocheltree, 2011). Conversely, regime shifts toward smooth sumac shrub islands are inhibited in grassland regimes due to negative feedbacks related to fire; that is, unshaded grassland regimes (e.g., Sandhills grasslands) produce sufficient fuel loads to kill smooth sumac and prevent localized regime shifts to smooth sumac shrub islands if fire occurs with sufficient frequency (Ortmann, Miles, Stubbendieck, & Schacht, 1997). Thus, smooth sumac shrub islands and Sandhills grasslands are alternate stable states that can coexist in

the same macrosystem but cannot coexist in localized, discrete spatial areas (Hanjy et al., 2011).

Because monitoring within the Sandhills grassland spatial regime identified smooth sumac individuals, we chose to simulate the emergence and spread of a smooth sumac shrub island in the Sandhills grassland spatial regime. Additionally, because smooth sumac clonal rhizomes can emerge up to 10 m from the stand, our study design's grain size (10 m between sampling points) was suitable for detecting sumac stand expansion (Ortmann et al., 1997; Weaver & Kramer, 1932). Thus, we used the real locations of the smooth sumac patch we observed on the transect as a basis for simulating the growth of a smooth sumac "shrub island" within the known Sandhills grassland community.

To determine how the emergence and spread of a smooth sumac shrub island regime would affect vegetative structure and community composition, we used established "assembly rules" from the literature (Table 1). These assembly rules reflect localized changes imposed by the positive feedbacks of an emerging and spatially expanding smooth sumac shrub island regime in a grassland regime (Table 1). To do this, we developed a simple algorithm, the outline of which is as follows: 1) we used the data we recorded in the field as initial conditions (i.e., time step "0"); 2) in the Sandhills spatial regime, we imposed smooth sumac regime shift assembly rules (Table 1) over a 110 m area (i.e., 11 sampling points along the transect) where monitoring data had identified smooth sumac individuals while keeping all other points identical to initial conditions; 3) we simulated a subsequent time step (time step "2") in which we roughly doubled the spatial extent of the smooth sumac island to 210 m (i.e., 21 sampling points);

and 4) we simulated a final time step (time step “3”) in which we again roughly doubled the spatial extent of the smooth sumac island to 410 m (i.e., 41 sampling points).

Importantly, these simulations assume that negative feedbacks driven by fire are absent, meaning fire is actively suppressed or does not occur frequently enough to kill smooth sumac clones before they can begin enforcing positive feedbacks to favor a shrub island regime (e.g., reducing fuel loads by shading grasses and changing fuel structure).

Identifying emergent spatial regimes

With the simulated outcomes, we determined if tracking spatial boundaries can detect the imposed emergent sumac regime by repeating the “spatial regime identification” steps above on each simulated time step at the spatial extent of the macrosystem (the entire length of the transect) and at the localized extent of the regime shift (the southernmost, Sandhills grassland, regime). We also conducted db-RDA on the resultant spatial boundaries (clusters) in each time step to assess their ecological meaning.

RESULTS

Spatial boundary identification

We detected 8 spatial boundaries (i.e., 9 potential spatial regimes) in vegetative communities along the 4 km transect (Figure 4.1). For simplicity, hereafter we refer to the areas between significant spatial boundaries as “spatial regimes.” From north to south, spatial regimes manifested as 1) a grass-dominated regime characterized by exotic cool-season grasses (e.g., Kentucky bluegrass [*Poa pratensis*]) bordered by early decay stage Ponderosa pine snags, 2) a burnt (2012 wildfire), early successional regime within a

draw characterized by shrubs (e.g., raspberry [*Rubus* sp.], snowberry [*Symphoricarpos alba*]), grape (*Vitis* sp.) vines, and high densities of deciduous tree snags, 3) a grass dominated regime characterized by native bunchgrasses (e.g., little bluestem, Junegrass [*Koeleria macrantha*]) and forbs (e.g., pussytoes [*Antennaria* sp.]), 4) another grass dominated regime characterized by exotic cool-season grasses (e.g., smooth brome [*Bromis inermis*]), 5) a burnt (2012 wildfire) regime of coarse woody debris, high densities of small diameter, mid-decay stage eastern redcedar snags, bur oak snags and resprouts, and annual invasive grasses (e.g., cheatgrass [*Bromus tectorum*], Japanese brome [*Bromus japonicus*]), 6) a flatland near the river with closed-canopy smooth sumac patches, bunchgrass, and resprouting bur oak, 7) a mature tree-dominated regime of mature bur oak, more decayed coarse woody debris, and litter ground cover, 8) a small regime with native bunchgrasses, native cool-season grasses (e.g., Scribner's panic grass [*Panicum oligosanthos*]), and sedges (*Carex* sp.), and finally 9) a regime uniquely characterized by sand bluestem and prairie sandreed, as well as richness of herbaceous species, several forbs, and patches of hackberry trees (*Celtis occidentalis*) and wild plum shrubs (Figure 4.1).

Detecting emergence of spatial regimes

Macrosystem scale

At the extent of the macrosystem, the number of spatial boundaries decreased from the 8 observed in the initial conditions to 3 boundaries in the first simulated time step as the simulated smooth sumac island regime emerged in the Sandhills area. This resulted from the disappearance (i.e., not movement) of all boundaries between the northern grass-

dominated communities and the burnt early successional community (regimes 1 - 4 in the initial, observed data) and the disappearance of all boundaries between the burnt former ponderosa pine forest community and the flatland community (regimes 5 -6 in the initial, observed data). However, boundary movement and disappearance occurred in the southern portion of the transect: the boundary separating the tree-dominated community and the shrubby community adjacent to the Sandhills (regimes 7 - 8 in the initial, observed data) disappeared, while the Sandhills spatial regime boundary (regime 9 in the initial, observed data) shifted northward slightly. However, no smooth sumac spatial regime manifested within the Sandhills (Figure 4.2).

In the second time step, the number of spatial boundaries decreased to 3. This was a result of the boundary separating the burnt ponderosa pine forest and the river valley (regimes 2 – 3 of the second time step) disappearing. The southernmost Sandhills spatial regime remained the same as in the second time step data, and again a smooth sumac island regime did not manifest (Figure 4.2).

In the final time step, the number of spatial boundaries increased to 11 (Figure 4.2). Spatial boundaries returned to a configuration resembling the boundaries in the observed data. However, 2 boundaries appeared within the Sandhills area. Specifically, the Sandhills area, from north-to-south, split into a regime associated with bunchgrasses, a smooth sumac regime, and a regime associated with prairie sandreed (Figure 4.2).

Local scale

At the extent of the Sandhills' spatial boundaries, the appearance and expansion of our simulated smooth sumac island over time showed that 3 boundaries emerged within the

initially single Sandhills regime in the first time step (Figure 4.3). A spatial regime representing the simulated shrub island that was dominated by uniformly closed-canopy smooth sumac, Kentucky bluegrass, and high woody plant species richness emerged where expected—near the center of the original spatial regime. The former Sandhills grassland regime persisted north and south of the smooth sumac island regime (Figure 4.3). However, we also detected a novel spatial regime immediately north of the simulated smooth sumac island regime—one dominated by patches of tree hackberry and wild plum as well as sand bluestem.

In the second time step, these 3 boundaries persisted as the sumac island expanded (Figure 4.2).

In the final time step, the spatial boundaries fell to 2 as the sumac island expanded further (Figure 4.3). This resulted from two major changes: the novel spatial regime that appeared directly north of the sumac island in the first time step disappeared after being subsumed by the smooth sumac island regime, and the former Sandhills grassland regimes diverged strongly, with the northern regime being distinguished by sand bluestem, Scribner's panic grass, and western ragweed (*Ambrosia artemisiifolia*) and the southern regime becoming more associated with prairie sandreed (Figure 4.3). Notably, this boundary configuration is similar to the Sandhills boundaries identified in the final time step at the macrosystem scale (see above; Figure 4.3).

DISCUSSION

We show that operationalizing the spatial regimes concept for monitoring successfully captured the emergence of spatial regimes with no *a priori* knowledge. Quantifying the

number and distribution of spatial boundaries distinguished not only visually obvious boundaries in vegetative systems (e.g., the boundary between grassland and burnt woodland) but also less apparent boundaries (e.g., separations between mixed-grass and exotic prairies). Further, at the macrosystem scale (spatial extent), the disappearance and reappearance of spatial boundaries provided an early warning of the emergence of a shrub island spatial regime in the Sandhills grassland. This early warning behavior resembles the established “flickering” early warning identified in time series of closed systems (e.g., lakes) nearing a regime shift. In complex, noisy systems, flickering is an established early warning signal of regime shifts characterized by abrupt switches back and forth between basins of attraction prior to a complete regime shift (Dakos, Nes, & Scheffer, 2013; Kefi et al., 2014). In our study, flickering in the macrosystem manifested as loss of order in spatial boundary distribution and number followed by an abrupt near-return to the initial order of spatial regimes in the final time step. That spatial boundaries exhibited flickering at the larger scale (the macrosystem) contrasts with ecological scaling theory that posits the conservation of pattern at larger scales despite smaller-scale fluctuations (Chave, 2013). However, the fact that the simulated shrub island emerged in a large, structurally homogeneous, but compositionally noisy spatial regime (the Sandhills grassland) may also play a role in the flickering signal in the macrosystem. Future research should assess the relationship between flickering signals and the size, scale, and level of heterogeneity within macrosystems.

The ability to detect emergence and early warnings of shifts supports the application of our operationalization of the spatial regimes concept in adaptive

monitoring frameworks in protected areas. Our results show that monitoring that utilizes the spatial regimes concept could detect imminent change, possibly granting the opportunity to enact restorative or mitigation efforts to “turn back from the brink” (Biggs, Carpenter, & Brock, 2009). Our results demonstrate the capability of tracking spatial boundaries to be used in a “surveillance” monitoring framework—where the goal is simply to measure the status of the system and detect undesirable, emergent changes (i.e., a regime shift from grassland to shrubland; a shift to a non-analogous regime; Hutto & Belote 2013). From a surveillance perspective, tracking spatial boundaries can also provide “trigger points” that instigate management actions when early warning signals (e.g., flickering) or undesirable regimes emerge (Kefi et al., 2014; Lindenmayer et al., 2013). Similar to the use of regime shift indicators in the discipline of restoration ecology, the ability of spatial boundaries to detect the emergence of new regimes could be used to monitor the effectiveness, implementation, and ecological effects of management and restoration actions in protected areas, as well as the effects of ecological disturbances (Hutto & Belote, 2013; Lindenmayer, Likens, Haywood, & Miezis, 2011). For instance, if the management goal were to remove a smooth sumac island regime and restore a grassland regime, a monitoring framework using the spatial regimes concept could estimate the effectiveness of restoration by simply recording changes in grassland and sumac spatial boundaries in response to restoration actions (Suding & Hobbs, 2009). Examples of specific, quantitative restoration goals would then be an increase in grassland spatial regime extent or complete disappearance of the sumac spatial regime (Nichols & Williams, 2006).

By analyzing spatial regimes both at the extent of the emergent regimes and at the extent of the macrosystem, monitoring data can be used to detect near real-time emergence and early warnings of regime shifts. Like the resilience, alternative state, and regime shift theory it is based on, the spatial regimes concept assumes regimes exhibit distinct structure and function and are maintained by feedbacks at discontinuous, but interacting, hierarchical scale domains (Allen et al., 2016; Sundstrom et al., 2017). Changes or emergence in regimes nested within the macrosystem (i.e., at smaller scales) can “revolt” and cascade up to the larger scale macrosystem (Allen, Angeler, Garmestani, Gunderson, & Holling, 2014). In our study, we chose a geographic location and extent that would encompass a macrosystem with multiple nested spatial regimes such as forests, grasslands, and riparian areas, and we chose a sufficiently fine grain size to detect the appearance and expansion of a known driver of regime shifts in grasslands-shrub islands. Thus, our results indicate that quantifying spatial regimes in the macrosystems over time can provide an early warning of a regime shift somewhere in the macrosystem, and this larger-scale signal can then be used to prompt a finer-scale investigation of each regime within the macrosystem to pinpoint the emergent shrub island regime. Still, the scale of monitoring must be carefully chosen in order to detect emergence or early warnings of regime shifts (Fagan et al., 2003; Kefi et al., 2014). For instance, sampling at a finer grain size could have increased the probability of detecting an incipient smooth sumac spatial regime, but it would also likely have increased the total number of spatial regimes detected (e.g., xeric ridge and mesic swale regimes in the Sandhills grassland portion) and thus increased noise in monitoring data. Although quantifying meaningful

scale domains of spatial regimes remains an active line of research, our results provide a path forward for selecting ecologically-relevant scales when monitoring for spatial regimes.

LITERATURE CITED

- Allen, C. R., Angeler, D. G., Cumming, G. S., Folke, C., Twidwell, D., & Uden, D. R. (2016). Quantifying spatial resilience. *Journal of Applied Ecology*, 53(3), 625–635.
- Allen, C. R., Angeler, D. G., Garmestani, A. S., Gunderson, L. H., & Holling, C. S. (2014). Panarchy: Theory and application. *Ecosystems*, 17(4), 578–589.
- Bennett, K.D. (1996) Determination of the number of zones in a biostratigraphical sequence. *New Phytologist*, 132, 155–170.
- Biggs, R., Carpenter, S. R., & Brock, W. A. (2009). Turning back from the brink: Detecting an impending regime shift in time to avert it. *Proceedings of the National Academy of Sciences*, 106(3), 826–831.
- Chave, J. (2013). The problem of pattern and scale in ecology: What have we learned in 20 years? *Ecology Letters*, 16(s1), 4–16.
- Clements, F. E. (1916). *Plant succession: An analysis of the development of vegetation*. Carnegie Institution of Washington.
- Cline, T. J., Seekell, D. A., Carpenter, S. R., Pace, M. L., Hodgson, J. R., Kitchell, J. F., & Weidel, B. C. (2014). Early warnings of regime shifts: evaluation of spatial indicators from a whole- ecosystem experiment. *Ecosphere*, 5(8), 1-13.
- Cottam, G., & Curtis, J. T. (1956). The use of distance measures in phytosociological sampling. *Ecology*, 37(3), 451–460.
- Dakos, V., Nes, E. H. van, & Scheffer, M. (2013). Flickering as an early warning signal. *Theoretical Ecology*, 6(3), 309–317.

- Donangelo, R., Fort, H., Dakos, V., Scheffer, M., & Van Nes, E. H. (2010). Early warnings for catastrophic shifts in ecosystems: comparison between spatial and temporal indicators. *International Journal of Bifurcation and Chaos*, 20(02), 315–321.
- Fagan, W. F., Fortin, M.-J., & Soykan, C. (2003). Integrating edge detection and dynamic modeling in quantitative analyses of ecological boundaries. *AIBS Bulletin*, 53(8), 730–738.
- Galzin, R. & Legendre, P. (1987). The fish communities of a coral reef transect. *Pacific Science*, 41, 158–165.
- Gleason, H. A. (1926). The individualistic concept of the plant association. *Bulletin of the Torrey Botanical Club*, 7–26.
- Godínez-Alvarez, H., Herrick, J., Mattocks, M., Toledo, D., & Van Zee, J. (2009). Comparison of three vegetation monitoring methods: Their relative utility for ecological assessment and monitoring. *Ecological Indicators*, 9(5), 1001–1008.
- Hajny, K. M., Hartnett, D. C., & Wilson, G. W. (2011). *Rhus glabra* response to season and intensity of fire in tallgrass prairie. *International Journal of Wildland Fire*, 20(5), 709–720.
- Hutto, R. L., & Belote, R. (2013). Distinguishing four types of monitoring based on the questions they address. *Forest Ecology and Management*, 289, 183–189.
- Kéfi, S., Rietkerk, M., Alados, C. L., Pueyo, Y., Papanastasis, V. P., ElAich, A., & De Ruiter, P. C. (2007). Spatial vegetation patterns and imminent desertification in Mediterranean arid ecosystems. *Nature*, 449(7159), 213.

- Kefi, S., Guttal, V., Brock, W. A., Carpenter, S. R., Ellison, A. M., Livina, V. N., ...
Dakos, V. (2014). Early warning signals of ecological transitions: Methods for
spatial patterns. *PloS One*, 9(3), e92097.
- Laliberté, E., & Legendre, P. (2010). A distance-based framework for measuring
functional diversity from multiple traits. *Ecology*, 91(1), 299–305.
- Legendre, P., & Gallagher, E. D. (2001). Ecologically meaningful transformations for
ordination of species data. *Oecologia*, 129(2), 271–280.
- Leys, B., Finsinger, W., & Carcaillet, C. (2014). Historical range of fire frequency is not
the Achilles' heel of the Corsican black pine ecosystem. *Journal of ecology*,
102(2), 381-395.
- Lindenmayer, D. B., & Likens, G. E. (2009). Adaptive monitoring: A new paradigm for
long-term research and monitoring. *Trends in Ecology & Evolution*, 24(9), 482–
486.
- Lindenmayer, D. B., & Likens, G. E. (2010). The science and application of ecological
monitoring. *Biological Conservation*, 143(6), 1317–1328.
- Lindenmayer, D. B., Likens, G. E., Haywood, A., & Miezi, L. (2011). Adaptive
monitoring in the real world: Proof of concept. *Trends in Ecology & Evolution*,
26(12), 641–646.
- Lindenmayer, D. B., Piggott, M. P., & Wintle, B. A. (2013). Counting the books while
the library burns: Why conservation monitoring programs need a plan for action.
Frontiers in Ecology and the Environment, 11(10), 549–555.

- Magurran, A. E., Baillie, S. R., Buckland, S. T., Dick, J. M., Elston, D. A., Scott, E. M., ... Watt, A. D. (2010). Long-term datasets in biodiversity research and monitoring: Assessing change in ecological communities through time. *Trends in Ecology & Evolution*, 25(10), 574–582.
- Nichols, J. D., & Williams, B. K. (2006). Monitoring for conservation. *Trends in Ecology & Evolution*, 21(12), 668–673.
- Oksanen, J., Kindt, R., Legendre, P., O'Hara, B., Stevens, M. H. H., Oksanen, M. J., & Suggests, M. (2007). The vegan package. *Community Ecology Package*, 10, 631–637.
- Ortmann, J., Miles, K. L., Stubbendieck, J. L., & Schacht, W. H. (1997). Management of smooth sumac on grasslands. *University of Nebraska-Lincoln Extension*, G97–1319.
- Ratajczak, Z., Nippert, J. B., & Collins, S. L. (2012). Woody encroachment decreases diversity across north american grasslands and savannas. *Ecology*, 93(4), 697–703.
- Ratajczak, Z., Nippert, J. B., Hartman, J. C., & Ocheltree, T. W. (2011). Positive feedbacks amplify rates of woody encroachment in mesic tallgrass prairie. *Ecosphere*, 2(11), 1–14.
- Roberts, C. P., Twidwell, D., Burnett, J. L., Donovan, V. M., Wonkka, C. L., Bielski, C. L., ... Allen, C. R. (2018). Early warnings for state-transitions. *Rangeland Ecology & Management*, in press.

- Scheffer, M., Carpenter, S., Foley, J. A., Folke, C., & Walker, B. (2001). Catastrophic shifts in ecosystems. *Nature*, 413(6856), 591.
- Spanbauer, T. L., Allen, C. R., Angeler, D. G., Eason, T., Fritz, S. C., Garmestani, A. S., ... Sundstrom, S. M. (2016). Body size distributions signal a regime shift in a lake ecosystem. *Proc. R. Soc. B*, 283(1833), 20160249.
- Steinauer, E. M., & Bragg, T. B. (1987). Ponderosa pine (*Pinus ponderosa*) invasion of Nebraska sandhills prairie. *American Midland Naturalist*, 118(2), 358-365.
- Steuter, A. A., Jasch, B., Ihnen, J., & Tieszen, L. L. (1990). Woodland/Grassland Boundary Changes in the Middle Niobrara Valley of Nebraska Identified by $\delta^{13}\text{C}$ Values of Soil Organic Matter. *American Midland Naturalist*, 124(2), 301-308.
- Strayer, D. L., Power, M. E., Fagan, W. F., Pickett, S. T., & Belnap, J. (2003). A classification of ecological boundaries. *BioScience*, 53(8), 723–729.
- Suding, K. N., & Hobbs, R. J. (2009). Threshold models in restoration and conservation: A developing framework. *Trends in Ecology & Evolution*, 24(5), 271–279.
- Sundstrom, S. M., Eason, T., Nelson, R. J., Angeler, D. G., Barichievy, C., Garmestani, A. S., ... others. (2017). Detecting spatial regimes in ecosystems. *Ecology Letters*, 20(1), 19–32.
- Vermaire, J. C., Greffard, M. H., Saulnier-Talbot, É., & Gregory-Eaves, I. (2013). Changes in submerged macrophyte abundance altered diatom and chironomid assemblages in a shallow lake. *Journal of paleolimnology*, 50(4), 447-456.

- Vormisto, J., Phillips, O. L., Ruokolainen, K., Tuomisto, H., & Vásquez, R. (2000). A comparison of fine- scale distribution patterns of four plant groups in an Amazonian rainforest. *Ecography*, 23(3), 349-359.
- Weaver, J. E., & Kramer, J. (1932). Root system of *Quercus macrocarpa* in relation to the invasion of prairie. *Botanical Gazette*, 94(1), 51–85.
- Woldendorp, G., Keenan, R., Barry, S., & Spencer, R. (2004). Analysis of sampling methods for coarse woody debris. *Forest Ecology and Management*, 198(1-3), 133–148.
- Zurlini, G., Jones, K. B., Riitters, K. H., Li, B. L., & Petrosillo, I. (2014). Early warning signals of regime shifts from cross-scale connectivity of land-cover patterns. *Ecological indicators*, 45, 549-560.

TABLES

Table 4. 1: Assembly rules for smooth sumac (*Rhus glabra*) stand expansion in grasslands and resultant vegetative community composition and structure. Assembly rules are derived from known sumac ecology and are in turn used as rules for simulating the emergence of a smooth sumac spatial regime from observed vegetative community data along a transect at the Niobrara Valley Preserve, Nebraska, USA.

Sumac Ecology	Assembly/Simulation Rules	Citations
Sumac stands can double in stem number in its first years.	Allow sumac stand to double in spatial extent per time step.	Ortmann et al. 1997
Sumac ramets grow rapidly in their first years of growth.	Set sumac canopy height to vary randomly between 130 - 140 cm within the sumac stand.	Hanjy et al. 2011
Herbaceous species richness and biomass decline sharply under closed-canopy sumac stands, but invasive cool-season grasses (e.g., <i>Poa pratensis</i>) can establish.	Remove all herbaceous species under sumac stands and add <i>Poa pratensis</i> .	Ortmann et al. 1997; Ratajczak et al. 2011; Ratajczak et al. 2012
Sumac leaf litter accumulates under closed-canopy stands and inhibits herbaceous plant growth.	Set ground cover under sumac stands to “litter.”	Weaver & Kramer 1932
Trees can establish in sumac thickets.	Allow any observed trees to persist if the sumac stand surrounds them.	Ortmann et al. 1997

FIGURES

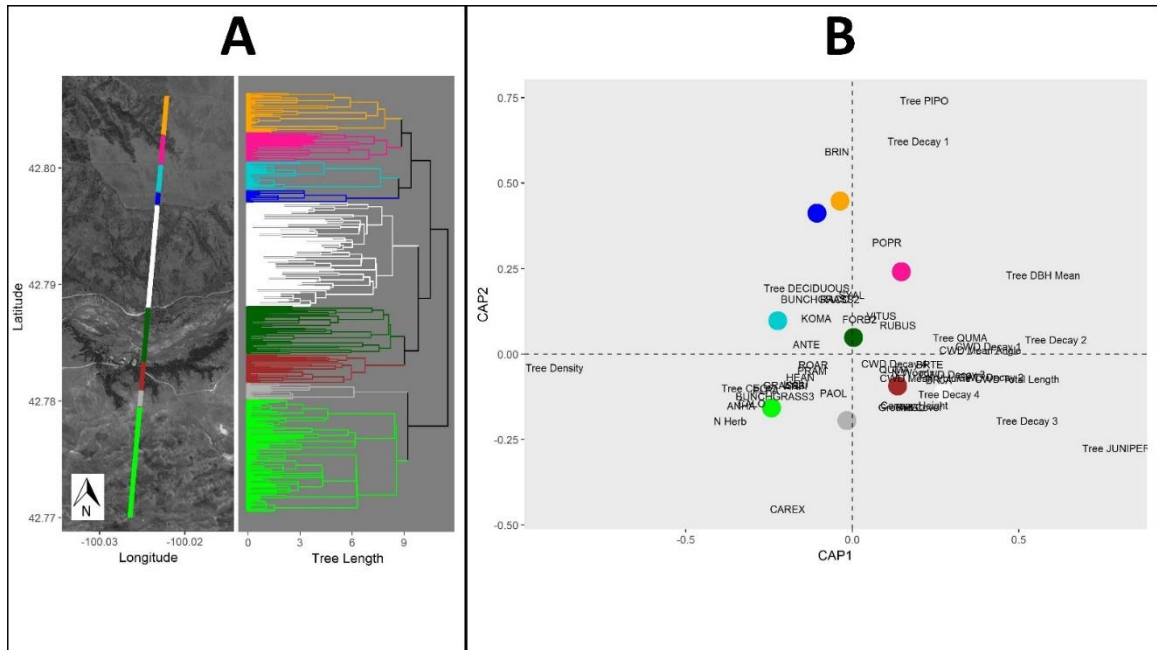


Figure 4. 1: Spatial regimes in vegetative structure and composition identified along a 4 km north-south transect at the Niobrara Valley Preserve, Nebraska, USA. (A) Against a black-white Google Earth aerial image, spatial regimes are colorized by significant breaks in self-similarity identified by constrained hierarchical clustering (dendrogram) and the broken stick model. (B) Using significant regimes, distance-based redundancy analysis shows vegetative variables significantly associated with each regime (regime centroids depicted as colored dots corresponding to colors of dendrogram/transect). Location of text (vegetative variables) indicates the strength of association of “species” scores of the vegetative structural and compositional variables with the first two ordination axes.

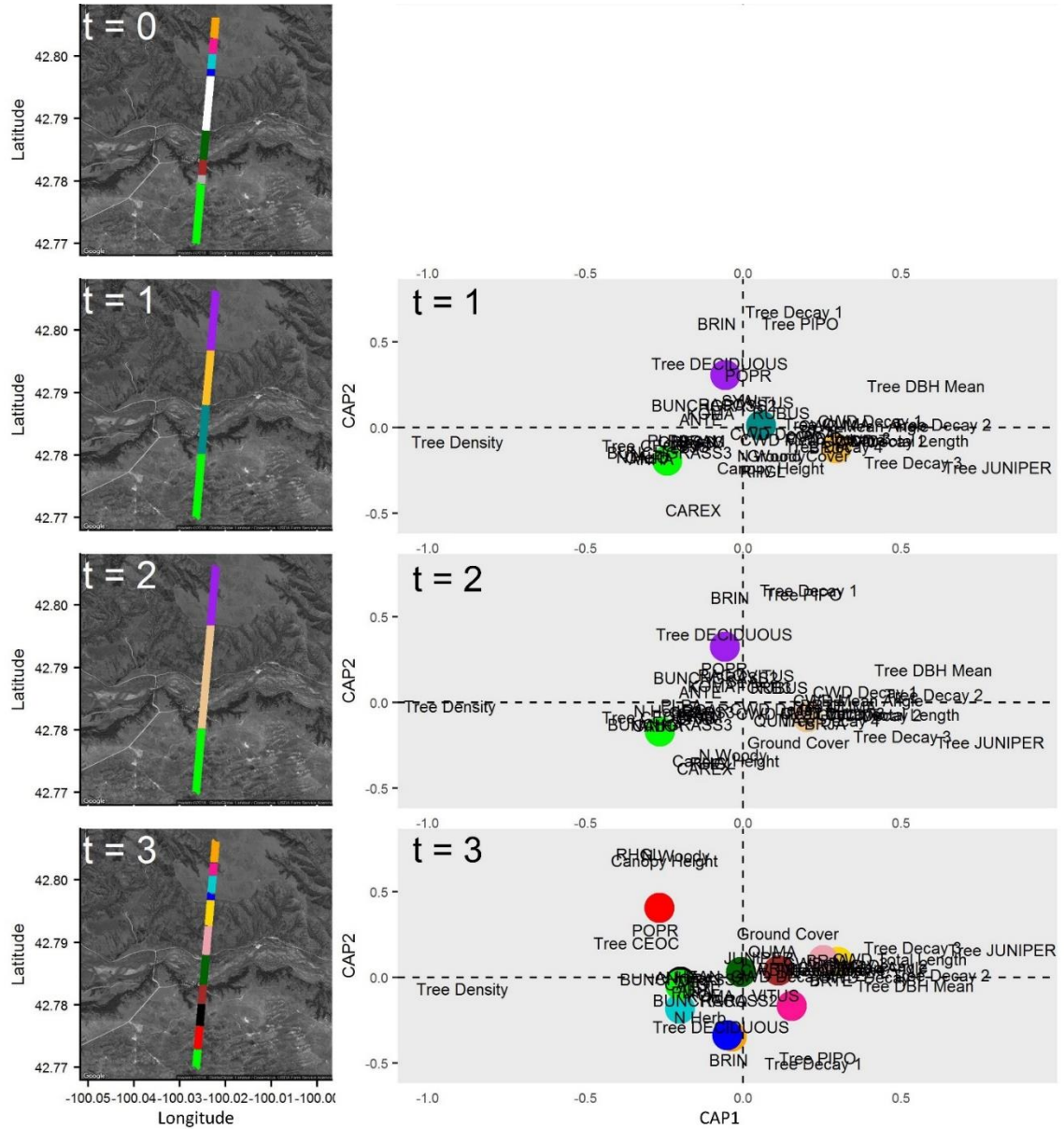


Figure 4. 2: Spatial regimes identified in observed and simulated vegetative structure and composition along a 4 km north-south transect at the Niobrara Valley Preserve, Nebraska, USA. In the left panel, using the observed data as the initial time step ($t = 0$), a smooth sumac (*Rhus glabra*) shrub “island” was then simulated in the southernmost (green) spatial regime, and the shrub island expanded spatially in three consecutive time steps.

Spatial regimes are colorized by significant breaks in self-similarity identified by the broken stick model. Numbers in top-left corners of each panel indicates the time step of the simulation (i.e., 0 = initial time step [observed data], 1 = first simulated time step, etc.). In the right panel, biplots of distance-based redundancy analyses from three consecutive simulations of significant ($P \leq 0.05$) vegetative structure and composition along the southernmost “Sandhills” portion of the 4 km north-south transect at the Niobrara Valley Preserve, Nebraska, USA. Constrained hierarchical clustering outputs from simulations were used as constraints. Colored dots indicate the centroids of the site scores of each spatial regime (constraint), and text indicates the strength of association of “species” scores of the vegetative structural and compositional variables with the first two ordination axes. See Table S1 for text interpretation.

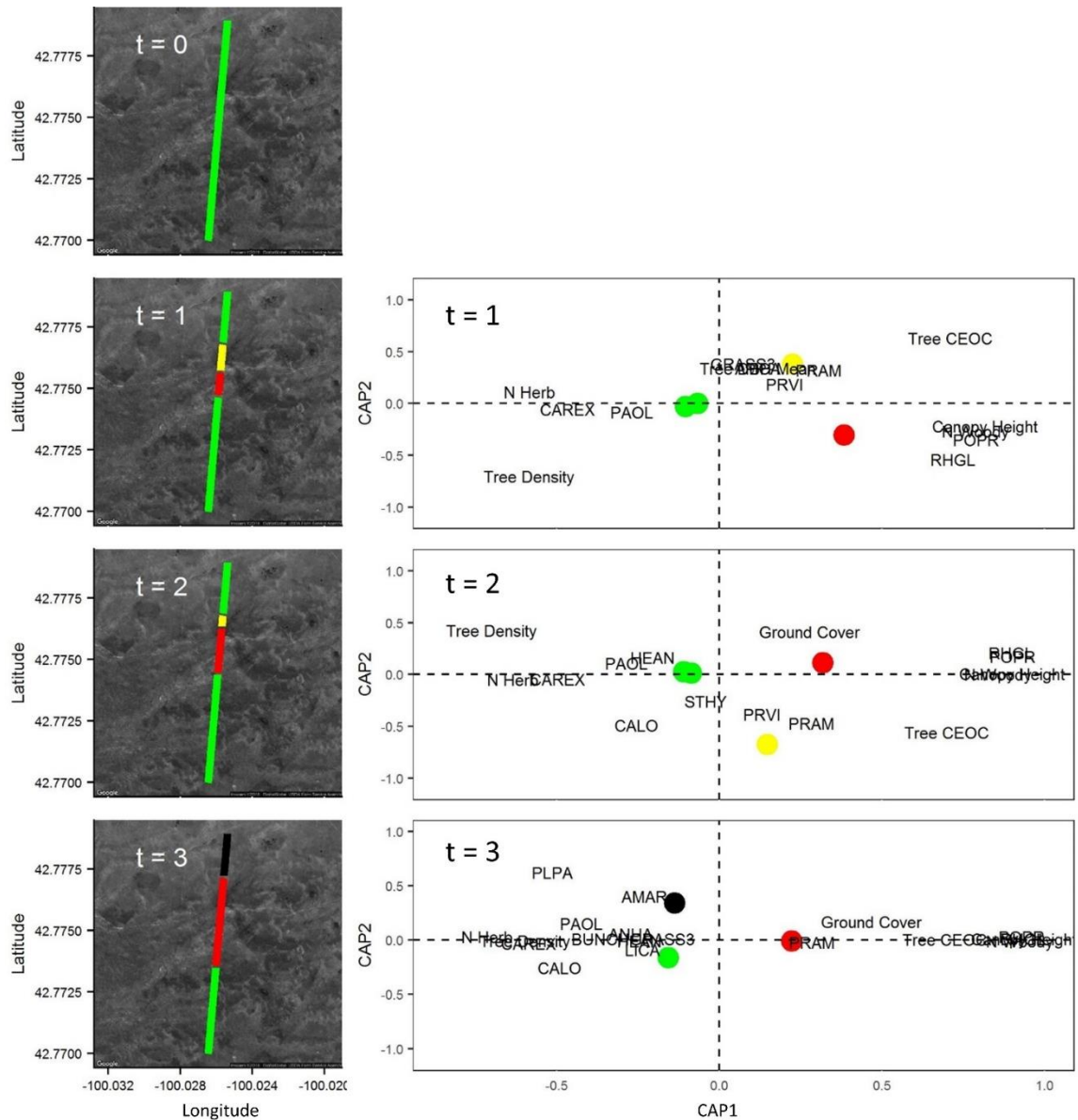


Figure 4. 3: Spatial regimes identified in observed and simulated vegetative structure and composition along the southernmost “Sandhills” portion of the 4 km transect at the Niobrara Valley Preserve, Nebraska, USA. In the left panel, the initial time step (t = 0) used only observed data. A smooth sumac (*Rhus glabra*) shrub “island” was then

simulated (red) and expanded spatially in three consecutive time steps. Spatial regimes are colorized by significant breaks in self-similarity identified by the broken stick model. Numbers in top-left corners of each panel indicates the time step of the simulation (i.e., $t = 0$ is the initial time step [observed data], $t = 1$ is the first simulated time step, etc.). In the right panel, biplots of distance-based redundancy analyses from three consecutive simulations of significant ($P \leq 0.05$) vegetative structure and composition along the southernmost “Sandhills” portion of the 4 km north-south transect at the Niobrara Valley Preserve, Nebraska, USA. Constrained hierarchical clustering outputs from simulations were used as constraints. Colored dots indicate the centroids of the site scores of each spatial regime (constraint), and text indicates the strength of association of “species” scores of the vegetative structural and compositional variables with the first two ordination axes. See Table S1 for text interpretation.

CHAPTER 5: PREDICTING REGIMES SHIFTS IN OPEN, COMPLEX SYSTEMS⁴

ABSTRACT

Predicting where regime shifts are likely to manifest is a major challenge for ecologists this century, but detection has proven elusive in systems with open boundaries and strong spatial order of regime change. Wombling, a method developed to provide probabilistic estimates of the likelihood of two-dimensional spatial ecological boundaries without requiring *a priori* system knowledge, has potential to overcome these challenges in open systems. Here, we test the ability for wombling to (i) identify boundaries between ecological regimes, and (ii) provide spatially-explicit prediction of the vulnerability of one regime to be displaced by another, corresponding to a change in spatial regime boundaries. To accomplish this, we use 26 years of bird community to test strength and scales at which wombling relates to well-known and previously established boundaries of tree-grass vegetative regimes and then use advances in spatial informatics to visualize and interpret how wombling tracks shifting spatial regime boundaries over time. Wombling detected spatial regime boundaries that matched theoretical expectations

⁴ CPR contributed to conceptualization, programming, data validation, formal analysis, data curation, all writing aspects, visualization, and project administration. DRU contributed to programming and formal analysis. DT, CRA, DGA, MOJ, BWA, and DEN contributed to conceptualization and writing selected sections.

for a suite of alternative ecological regimes and predicted changes in boundaries of these regimes over time with no *a priori* system knowledge. Wombling predicted vulnerability to regime shifts in a spatially explicit manner: wombling predicted spatial regime boundaries at up to 1 km from vegetative regime boundaries. If some *a priori* knowledge is available for a given landscape (e.g., knowledge of regimes that are desirable vs. undesirable), wombling can both detect emergence and expansion of an undesirable regime or the maintenance and restoration of a desirable regime in a landscape. As a novel operationalization of the spatial regimes concept, our results demonstrate how wombling can move regime shift theory and prediction beyond mechanistic assumptions and lagged temporal early warnings and towards embracing complexity theory.

INTRODUCTION

Predicting where regime shifts are likely to manifest is one of the grand challenges for ecologists this century (Biggs, Carpenter, & Brock, 2009; Clements & Ozgul, 2018; Scheffer, Carpenter, Foley, Folke, & Walker, 2001). A central premise of ecological theory is that ecological communities will warn of a pending regime shift, but detection has proven elusive in systems with open boundaries and strong spatial order of regime change (Burthe et al., 2016; Hastings & Wysham, 2010). In such systems, multiple alternative regimes can exist alongside each other within a given spatial extent (Hoffmann et al., 2012; Roques, O’connor, & Watkinson, 2001; Scheffer & Carpenter, 2003). For instance, within areas historically dominated by grassland regimes, isolated shrub island regimes and tree-dominated regimes can appear, disappear, expand, or contract according to fire regimes (Ratajczak, Nippert, & Ocheltree, 2014). But because

traditional regime shift prediction methods do not explicitly consider spatial order (e.g., boundaries between alternative regimes existing simultaneously on a landscape) and do assume fixed boundaries, these methods require a sufficient proportion of the system to shift to an alternative regime and exhibit a particular temporal pattern before they register a regime shift signal (Kefi et al., 2014; Wang et al., 2012). Not only will this lead to lags in regime prediction, it does not account for spatial order of alternative regimes in open systems (C. R. Allen et al., 2016). Timely prediction of regime shifts in open, complex systems will require concepts and methods that explicitly incorporate spatial dimensions (Clements & Ozgul, 2018; C. P. Roberts et al., 2018).

The concept of spatial regimes has attempted to resolve these issues for open, complex systems (C. R. Allen et al., 2016; C. P. Roberts et al., 2018; Sundstrom et al., 2017). Spatial regime posit alternative regimes can exist within a given spatial extent, alternative regimes manifest strong spatial order including self-similarity near the spatial center of regimes and measurable boundaries (at a given scale), regime boundaries can shift, expand, and contract to displace other regimes, and the vulnerability to regime shifts increases near the boundaries of alternative regimes (C. R. Allen et al., 2016; C. P. Roberts et al., 2018). To date, spatial regimes have been operationalized by identifying sharp, spatially-explicit transitions in biotic communities or structure (Sundstrom et al., 2017). However, current methods for operationalizing the spatial regimes concept have met challenges (Clements & Ozgul, 2018). For example, multivariate clustering methods rely on discrete, non-statistical (i.e., lacking a hypothesis test) boundary cutoffs, meaning uncertainty in regime identification and the gradual or discrete natures of boundaries

cannot be easily obtained (C. Roberts, Allen, Angeler, & Twidwell, 2019). Additionally, like related boundary detection and gradient analysis concepts, spatial regimes methods have also largely been restricted to one-dimensional space, for example identification along transects (Fagan, Fortin, & Soykan, 2003; C. Roberts et al., 2019; Sundstrom et al., 2017).

Wombling, a method proposed by and named after Womble (1951), has potential to overcome these issues in operationalizing spatial regimes. Wombling was developed to avoid subjective, discrete classification schemes of ecological systems (Barbujani, Oden, & Sokal, 1989; Diniz-Filho, Soares, & Campos Telles, 2016; Womble, 1951). It is designed to provide probabilistic estimates of the likelihood of boundaries between ecological entities without requiring *a priori* system knowledge (Barbujani et al., 1989), and it incorporates two spatial dimensions, granting it the ability to detect spatial boundaries in open, complex systems such as terrestrial landscapes (Kent, Levanoni, Banker, Pe'er, & Kark, 2013). Wombling can detect boundaries using univariate or multivariate data. Wombling has been used in landscape genetics studies for identifying landscape barriers of gene flow and spatially-distinct genotypes (Barbujani & Sokal, 1990; Diniz-Filho et al., 2016), mapping disease spread boundaries in order to identify sources of disease (Ma, Carlin, & others, 2007), and providing spatially explicit estimates of vulnerability and barriers to spread of invasive species (Fitzpatrick et al., 2010).

Wombling could potentially be translated into a regime shift prediction method by inputting spatially-explicit biotic community composition data and tracking changes in wombling-identified boundaries across space, over time (Diniz-Filho et al., 2016; C. P.

Roberts et al., 2018). For instance, in an open, complex system hosting multiple alternative regimes, wombling could be used to identify and track spatial regime boundaries in situations where 1) one regime expands, displacing its neighboring regime, 2) boundaries between two or more regimes remain stationary over time due to negative feedbacks that maintain regime boundaries, 3) one regime becomes dominant and manifests self-similarity in its wake, or 4) landscapes, and the regimes they contain, are highly fragmented (C. R. Allen et al., 2016; C. P. Roberts et al., 2018). In all of these situations, the predicted vulnerability of a given location to a regime shift (i.e., one spatial regime being displaced by another) would be the spatial distance of a wombling-identified boundary to the given location and the pattern of change in boundary location over time; that is, if the boundary is moving toward the location, it would have greater vulnerability to a regime shift (C. R. Allen et al., 2016; C. P. Roberts et al., 2018; C. Roberts et al., 2019).

Here, we test the ability for wombling to (i) identify boundaries between ecological regimes, and (ii) provide spatially-explicit prediction of the vulnerability of one regime to be displaced by another, corresponding to a change in spatial regime boundaries. To accomplish this, we use 26 years of bird community to test strength and scales at which wombling relates to well-known and previously established boundaries of vegetative regimes. We then employ advances in spatial informatics to visualize and interpret how wombling tracks shifting spatial regime boundaries over time.

METHODS

Study site

We conducted this study at Fort Riley Army Base, Kansas, USA (39.09999 N 96.81666 W). Fort Riley is a US military reservation encompassing approximately 41,170 ha. It is located in the Flint Hills ecoregion of the North American Great Plains. The Flint Hills are characterized by strong topographic relief, with sharp inclines from lowland ravines with gallery forests and shrublands to relatively flat uplands (Omernik & Griffith, 2014).

Fort Riley is an ideal study site at which to test regime shift applications of wombling due to its ecological history and suite of alternative regimes (Briggs, Hoch, & Johnson, 2002). Like the rest of the Flint Hills, Fort Riley can support two major alternative regimes: a grass-dominated regime and a tree-dominated regime (Ratajczak et al., 2014). Historically, tallgrass prairie covered most of the Flint Hills, including big bluestem (*Andropogon gerardi*), switchgrass (*Panicum virgatum*), and Indian grass (*Sorghastrum nutans*) (Briggs, Knapp, & Brock, 2002; Limb, Engle, Alford, & Hellgren, 2010). Woody plants, historically rare and limited to areas where they could escape fire (e.g., ravines, rocky outcroppings), include eastern redcedar (*Juniperus virginiana*), sumac (*Rhus* sp.), and roughleaf dogwood (*Cornus drummondii*) (Briggs et al., 2005). These vegetative regimes also correspond with specific avian communities—a suite a grassland bird species that respond negatively to tree cover and require large tracts of grassland, and a suite of forest bird species that are tied to tree cover but can occur in fragmented landscapes (Fuhlendorf, Woodward, Leslie, & Shackford, 2002; Grant, Madden, & Berkey, 2004; Thompson, Arnold, & Amundson, 2014).

Due to fire suppression implemented by European colonists, woody plants have expanded out from their former local boundaries and are invading grasslands (Twidwell et al., 2016). However, within Fort Riley, fire disturbances (both random ignitions from military training and planned, prescribed fires) occur much more frequently and during weather conditions of lower humidity and higher wind speed than the surrounding Flint Hills, meaning Fort Riley's fire regimes are more similar to historic fire regimes that maintained tallgrass prairie regimes (Ratajczak et al., 2016; Ratajczak, Nippert, Briggs, & Blair, 2014). But due to regional pressures and uneven fire regimes across the installation, Fort Riley has also experienced displacement of grassland regimes by tree regimes. Altogether, these competing pressures and regimes make it likely that the situations in which wombling could identify spatial regimes and predict vulnerability will occur at Fort Riley, enabling a test of wombling's regime shift prediction applications (Diniz-Filho et al., 2016; Womble, 1951).

Data

We tested wombling as a predictor of regime shifts by applied wombling to georeferenced bird community composition data and comparing boundaries identified by wombling to boundaries of the two major alternative regimes that occur at Fort Riley—tree regimes and grass regimes. Thus, we collected 26 years of bird community composition data and vegetation data from across Fort Riley. Because bird communities are known to strongly differ between grassland and tree regimes, wombling should relate to tree-grass boundaries at some set of scales.

Vegetation data

We used a novel raster dataset that provides annual percent cover of plant functional groups at a 30 x 30 m resolution (M. O. Jones et al., 2018). This dataset masks urbanized areas (roads, buildings) and water (lakes, ponds, streams, rivers). We extracted percent perennial herbaceous plant cover and percent tree cover by cell. We used these two functional groups to identify spatial boundaries between the two major alternative regimes occurring at Ft. Riley—a tree-dominated regime and a grass-dominated regime (Briggs et al., 2002; Ratajczak et al., 2016).

Bird community data

Using a stratified random design, 59 bird community sampling locations were established in 1991. Stratified classes originated from soil-land cover type combinations and distributed a number of sampling locations within each class proportional to its land area at Ft. Riley. Sampling locations were surveyed from 1991 - 2017 during the breeding season (May - June). Most locations were surveyed annually, but some gaps in survey years occurred for 3 sampling locations. At each sampling location, surveyors quantified bird community composition along a 100 m transect. Transects originated at the sampling location and extended 100 m along a randomly chosen azimuth. The same azimuth was used for all years. Surveyors walked the length of the transect in 6 minutes, stopped for 8 minutes at the end of the transect, and then walked back to the beginning of the transect for 6 minutes. Surveyors recorded the number and species of all birds seen or heard during these surveys. ### Boundary identification

Vegetative boundaries: spatial covariance

We quantified spatial boundaries between tree and grass regimes by calculating spatial covariance between percent tree and percent grass cover for each raster cell via moving windows (D. Uden et al., 2019; Wagner, 2003). To test the strength and scales at which wombling related to known regime boundaries, we calculated spatial covariance at moving window sizes of 9 (3 x 3), 64 (8 x 8), 169 (13 x 13), 529 (23 x 23), and 1089 (33 x 33) pixel neighborhoods.

Spatial covariance ranges continuously from positive to negative values. Positive values indicate spatial synchrony in tree/grass cover (i.e., as tree cover increases, grass cover increases), values near zero indicate spatial similarity (i.e., a given raster cell is surrounded by either all trees or all grass), and negative values indicate spatial asynchrony in tree/grass cover (i.e., as woody cover increases, grass cover decreases). Because tree and grass are alternative regimes, spatial covariance values across Ft. Riley mainly ranged from near zero to strongly negative. To make spatial covariance values comparable across years, we divided the spatial covariance value for each raster cell at each moving window extent by the standard deviation of spatial covariance for each year.

Bird community boundaries: wombling

We used wombling to identify boundaries in bird communities. Specifically, we used a geographically weighted regression (GWR) as a generalized wombling method for point-based data. GWR takes geographic coordinates and an environmental variable, such as ordination values, and produces linear regression statistics (e.g., R^2 values) for each sampling location (Diniz-Filho et al., 2016). Higher R^2 values indicate locations of

abrupt change; that is, boundaries. We first used a Hellinger transformation to correct for rare species and then performed principal components analysis (PCA) on the full transformed dataset (all years, all sampling locations) (Dray, Legendre, & Peres-Neto, 2006). We used the first axis of the PCA as the environmental values for each point, and we used the latitude and longitude of each point as the geographic coordinates (Diniz-Filho et al., 2016). We ran the GWR for each year of our data (1991 - 2017). Overdispersion can cause GWR to fail to converge, so we removed any years in which overdispersion occurred.

Testing wombling

Can wombling identify boundaries between ecological regimes?

We quantified the relationship between boundaries detected by wombling (high R^2 values derived from GWR) and known spatial regime boundaries (negative spatial covariance in tree/grass cover) by developing separate a set of candidate generalized additive mixed models (GAMMs) with different combinations of spatial covariance window sizes (Zuur, Ieno, Walker, Saveliev, & Smith, 2009). In each model, we set R^2 as the response variable and spatial covariances (the value of the raster cell nearest each bird sampling location) as the smoothed predictor variable. We allowed intercept to vary by year. We used Akaike Information Criterion corrected for small sample sizes for model selection.

We tested the spatial relationship between wombling boundaries and known spatial regime boundaries by with the same set of candidate GAMMs as above. In this case, we set R^2 as the response variable, but we used distance (m) to nearest spatial

regime boundary for each window size as smoothed predictor variables. We considered the nearest spatial regime boundary to be the closest raster cell to each bird sampling location with a scaled spatial covariance value of ≤ -1 . This cutoff ensured near zero covariance values were excluded. Because spatial covariance raster pixel size was 30 x 30 m, distances ≤ 30 m would indicate the nearest boundary was the cell the bird survey location fell within. Thus, we replaced any distance ≤ 30 m with 30 m. We allowed intercept to vary by year.

Can wombling predict changes in spatial regime boundaries?

We used spatial informatics to visually determine if wombling predicted and tracked changes in spatial regime boundaries. We mapped spatial covariance rasters for each year of bird community data that we analyzed (i.e., years that GWR did not fail). We used the spatial covariance window size (scale) that most strongly associated with wombling boundaries. We then mapped locations of bird sampling locations as points on top of spatial covariance rasters by year. We set these points to vary in size according to their wombling R^2 value for each year, with larger R^2 values corresponding to larger point sizes.

Finally, we assessed the ability of wombling to predict changes in spatial regime boundaries at two spatial extents. First, we visually inspected selected portions of the study area that 1) were likely to exhibit shifts in spatial regime boundaries (regime shifts) due to encroaching tree regimes into grassland regimes, 2) were likely to have maintained stable tree-grass spatial regime boundaries due to receiving consistent application of fire and being near the center of a grassland regime, 3) were initially boundaries between

tree-grass regimes and became centers of tree regimes as tree regimes displaced grasslands, and 4) were highly fragmented by tree-grass boundaries. Specifically, we chose an area that is less disturbed and is near a ravine from which woody plants could spread, an area that was consistently and heavily disturbed by random and prescribed fires and military training, an area near a major river that would have historically hosted a tree regime and would have provided a source for tree encroachment of grasslands, and an area known to be highly fragmented by tree-grass boundaries. If wombling is able to predict and track changes in spatial regime boundaries, wombling values should increase in areas where spatial regimes boundaries are shifting (e.g., where woody plant regimes encroach on grasslands), remain relatively stable where regime boundaries do not change or near the center of spatial regimes (e.g., in the middle of a grassland, the boundary between upland forests and riparian forests), and decrease as spatial regime boundaries expand away from them (e.g., locations initially at the boundary of tree-grass regimes that become centers of tree regimes due to tree encroachment of grasslands).

Second, we visually inspected wombling patterns at the extent of the entire study area.

RESULTS

Wombling identifies boundaries between ecological regimes

Vegetative boundaries and wombling boundaries

Model selection revealed considerable model uncertainty, with the first four models having similar AICc weights ranging from 27% (top model) to 20% (fourth model; Table

5.1). However, the four top models produced similar patterns across spatial covariance window sizes. We only interpret the top model here.

In the top model, wombling boundaries corresponded to known spatial regime boundaries at window sizes of 90 x 90 m, 390 x 390 m, 690 x 690 m, and 990 x 990 m (Table 5.1). At the smallest window size (90 x 90 m), wombling values (R^2) had a linearly negative relationship with spatial covariance (Figure 5.1). However, at the next largest window size (390 x 390 m), wombling values exhibited a nonlinear relationship with spatial covariance, with a relatively flat—but highly uncertain—pattern at positive spatial covariance values; and this transitioned to a positive relationship between wombling values - spatial covariance at negative spatial covariance values (Figure 5.1). And at the largest window size (990 x 990 m), wombling values were strongly negatively associated with positive spatial covariance, and then the relationship flattened out until another shift to negative association at very low spatial covariance values (Figure 5.1).

Distance to boundary

The top model relating wombling boundaries to distance to known regime boundaries contained the smallest (90 x 90 m), middle (390 x 390 m), and largest (990 x 990 m) spatial covariance window sizes (Table 5.1). Model certainty was greater in this case, with the top model accounting for 62% of AICc weight and second model accounting for 30% of AICc weight (Table 5.1).

In the top model, at the smallest window size (90 x 90 m), wombling values (R^2) had a roughly quadratic relationship with spatial covariance: wombling values peaked at

approximately 300 m from a boundary (Figure 5.2). At the 390 x 390 m window size, wombling values peaked at 90 m from a boundary, and wombling values remained consistent at distances > 400 m (Figure 5.2). Wombling values exhibited a complex relationship with distance to boundaries at the largest window size (990 x 990 m). Wombling values were very low for very far distances (e.g., > 3000 m), then sharply increased to a local peak at 1000 m, then fell, then increased steadily to another peak at 90 m before beginning to decrease at < 90 m from a boundary (Figure 5.2).

Wombling predicts changes in spatial regime boundaries

Selected extents

Wombling predicted changing spatial regimes boundaries at selected spatial extents. Where tree regimes were predicted to displace grassland regimes, wombling R^2 values displayed a clear boundary between tree-grassland regimes at the southwest corner of the extent in 1991–prior to encroachment (Figure 5.3). As tree regimes displaced grassland regimes over time, wombling values near the shifting spatial regime boundaries responded, increasing and displaying heightened stochasticity (Figure 5.3). Within the grassland regime that was being displaced, wombling R^2 values were initially low—as expected for values far from a boundary—but began increasing and displaying heightened stochasticity similar to the points nearer the former spatial regime boundary (Figure 5.3). Interestingly, wombling values within the former “center” of the grassland regime began responding to shifting spatial regime boundaries at > 2 km from encroaching tree spatial regime boundaries (Figure 5.3).

Where tree-grass regime boundaries were predicted to remain stable due to consistent, heavy fire and military training disturbances, wombling R^2 indeed remained stable over the entire study period (Figure 5.4). Near the tree-grass boundary, wombling values stayed high, and near the center of the grassland (highly disturbed) regime, wombling values stayed low (Figure 5.4).

In locations that were initially boundaries between tree-grass regimes and became centers of tree regimes as tree regimes displaced grasslands, in 1991, wombling R^2 values started high at the boundaries, with one point (near the center of the tree regime—that is, in a riparian forest) being markedly low (Figure 5.5). As tree regimes displaced grassland regimes and boundaries became central, wombling values correspondingly decreased, with all tree-regime points becoming more similar to each other (Figure 5.5).

Within an area highly fragmented by tree-grass regime boundaries, wombling R^2 values reflected that all sampling locations were on or near known vegetative boundaries (Figure 5.6). Overall, wombling values were high across all sampling locations in the extent. However, as tree regimes further displaced grass regimes and fragmented boundaries drew closer together, wombling values of sampling locations near the center of the extent decreased (Figure 5.6).

Study area extent

At the extent of the entire study area, wombling values displayed complex patterns that tracked patterns in changing vegetative spatial regime boundaries (Figure 5.7). Overall, wombling R^2 values for sampling locations near the boundaries of the study area (the boundaries of the military installation) tended to be greater than locations nearer the

center of the study area. At sampling locations where spatial covariance indicated changing vegetative spatial regime boundaries over time, wombling R^2 values either increased strongly or evidenced stochastic increases and decreases over time. Wombling R^2 values of sampling locations in areas with low spatial covariance (i.e., locations near the center of grassland regimes) tended to be lower and remain lower than locations near tree-grass regime boundaries (Figure 5.7). Likewise, locations nearer the center of major forested areas (locations near the center of woody plant-dominated regimes) tended to be and remain lower than locations near boundaries. Locations near the more urbanized southern portion of the study area maintained relatively high wombling R^2 values over time.

DISCUSSION

Wombling detected spatial regime boundaries that matched theoretical expectations for a suite of alternative ecological regimes and predicted changes in boundaries of these regimes over time. Wombling predicted regime shifts in space up to 1 km away from known vegetative regime boundaries. These results indicate that wombling represents a major advancement in the detection and prediction of regime shifts. Wombling successfully provided a quantitative, probabilistic method for identifying alternative regimes co-occurring in an open, complex spatial extent (i.e., landscape). Indeed, wombling detected boundaries across a range of spatial regime shift scenarios, including situations in which one regime was clearly being displaced by another as well as situations in which boundaries were less clear and more complex such as highly fragmented areas. Wombling also successfully predicted vulnerability to regime shifts:

locations spatially nearer regime boundaries were more likely to experience (i.e., more vulnerable to) regime shifts than areas farther from boundaries (i.e., near the spatial centers of regimes).

We demonstrate a method for moving regime shift theory and methods beyond mechanistic assumptions and towards embracing complexity theory (C. R. Allen et al., 2016; C. P. Roberts et al., 2018; C. Roberts et al., 2019). Wombling successfully predicted regime shifts with no *a priori* system knowledge and with only the assumption that multiple alternative regimes can coexist in a system (Diniz-Filho et al., 2016). This contrasts with traditional regime shift prediction methods, such as “generic” early warning signals of regime shifts, that make additional mechanistic assumptions, requiring phenomena such as critical slowing down and attendant signals (e.g., rising variance, skewness, kurtosis) to manifest (Burthe et al., 2016; Dakos et al., 2012; Kefi et al., 2014). If fulfilled, these assumptions can provide useful diagnoses of systems undergoing change: for instance, theory predicts that a system exhibiting critical slowing down is reaching a bifurcation point (i.e., not a gradual regime shift or a simple nonlinear transition) (Scheffer & Carpenter, 2003; Van Nes & Scheffer, 2007). But this requires sufficiently long time series data and the manifestation of critical slowing down; and such data and signals are often not obtainable (Clements, Drake, Griffiths, & Ozgul, 2015; Hastings & Wysham, 2010). For example, in our study, we detected a rapid regime shift from a grassland- to tree-regime (Figure that occurred within 5 years. Given our data’s annual time steps and the fact that regime shifts occurred near the beginning of the time steps, early warning and regime shift detection methods would likely have failed to

predict a regime shift until after it occurred (Clements et al., 2015; Hastings & Wysham, 2010). In contrast, wombling detected the beginning of the regime shift after a single time step.

Our results align with both resilience theory, which has long acknowledged the scale-dependence of tipping points and scale specificity when considering coexistence of alternative states, and the closely allied Textural Discontinuity Hypothesis, which posits discontinuous breaks in system resource distributions, spatial structures, and organism resource requirements. Bird regimes (wombling-derived boundaries) corresponded with vegetative boundaries at discontinuous scales. Grassland bird species are known to exhibit a variety of responses to tree cover, with some species exhibiting strong aversion to tree cover occurring up to a kilometer away and other species not responding until rather closer, denser tree cover occurs. That discontinuous relationships between bird regime boundaries and vegetative boundaries manifested in spite of idiosyncratic species responses to tree cover further connects our results to and provides support for the Textural Discontinuity Hypothesis and resilience theory.

Wombling also detected areas of self-similarity within regimes, another hallmark of complexity theory and spatial regimes, and wombling showed these areas were near the centers of regimes (C. R. Allen et al., 2016; Sundstrom et al., 2017). We demonstrate this in two situations—when a tree regime is invading a grass regime and a when a tree regime switches from coexisting with grass regimes to being dominant. In both cases, wombling values in the center of regimes were low (i.e., were more self-similar to their neighbors). Additionally, wombling values fell when sampling locations switched from

being near boundaries to being closer to the center of a regime, meaning self-similarity can expand alongside regime expansion.

Finally, we show wombling is a promising candidate for applied ecological tasks and research. Without any system knowledge, wombling can provide spatially explicit estimates of vulnerability to regime shifts; that is, locations closer to regime boundaries (high wombling values) would have increased vulnerability (Diniz-Filho et al., 2016; Womble, 1951). In this sense, wombling is applied as a “screening” for regime shift vulnerability—similar to early warning methods but with fewer assumptions—and local knowledge and post-hoc analyses can be used to further “diagnose” the vulnerability (D. Uden et al., 2019). But if some system knowledge is available for a given landscape (e.g., knowledge of regimes that are desirable vs. undesirable), wombling can both detect emergence and expansion of an undesirable regime or the maintenance and restoration of a desirable regime in a landscape. For instance, we show that wombling detected the emergence and expansion of undesirable tree regimes in a grassland, and we also show that wombling detected the maintenance of a desirable grassland regime when tree-grass boundaries remained stable. It is also important to note that wombling successfully identified boundaries and predicted regime shift vulnerability using a stratified-random sampling design. Future studies should investigate the performance of wombling in simple random or systematic sampling designs.

LITERATURE CITED

- Allen, C. R., Angeler, D. G., Cumming, G. S., Folke, C., Twidwell, D., & Uden, D. R. (2016). Quantifying spatial resilience. *Journal of Applied Ecology*, 53(3), 625–635.
- Barbujani, G., & Sokal, R. R. (1990). Zones of sharp genetic change in Europe are also linguistic boundaries. *Proceedings of the National Academy of Sciences*, 87(5), 1816–1819.
- Barbujani, G., Oden, N. L., & Sokal, R. R. (1989). Detecting regions of abrupt change in maps of biological variables. *Systematic Zoology*, 38(4), 376–389.
- Biggs, R., Carpenter, S. R., & Brock, W. A. (2009). Turning back from the brink: Detecting an impending regime shift in time to avert it. *Proceedings of the National Academy of Sciences*, 106(3), 826–831.
- Briggs, J. M., Hoch, G. A., & Johnson, L. C. (2002). Assessing the rate, mechanisms, and consequences of the conversion of tallgrass prairie to *Juniperus virginiana* forest. *Ecosystems*, 5(6), 578–586.
- Briggs, J. M., Knapp, A. K., & Brock, B. L. (2002). Expansion of woody plants in tallgrass prairie: A fifteen-year study of fire and fire-grazing interactions. *The American Midland Naturalist*, 147(2), 287–294.
- Briggs, J. M., Knapp, A. K., Blair, J. M., Heisler, J. L., Hoch, G. A., Lett, M. S., & McCARRON, J. K. (2005). An ecosystem in transition: Causes and consequences of the conversion of mesic grassland to shrubland. *AIBS Bulletin*, 55(3), 243–254.

- Burthe, S. J., Henrys, P. A., Mackay, E. B., Spears, B. M., Campbell, R., Carvalho, L., ... others. (2016). Do early warning indicators consistently predict nonlinear change in long-term ecological data? *Journal of Applied Ecology*, 53(3), 666–676.
- Clements, C. F., & Ozgul, A. (2018). Indicators of transitions in biological systems. *Ecology Letters*, 21(6), 905–919.
- Clements, C. F., Drake, J. M., Griffiths, J. I., & Ozgul, A. (2015). Factors influencing the detectability of early warning signals of population collapse. *The American Naturalist*, 186(1), 50–58.
- Dakos, V., Carpenter, S. R., Brock, W. A., Ellison, A. M., Guttal, V., Ives, A. R., ... others. (2012). Methods for detecting early warnings of critical transitions in time series illustrated using simulated ecological data. *PloS One*, 7(7), e41010.
- Diniz-Filho, J. A. F., Soares, T. N., & Campos Telles, M. P. de. (2016). Geographically weighted regression as a generalized wombling to detect barriers to gene flow. *Genetica*, 144(4), 425–433.
- Dray, S., Legendre, P., & Peres-Neto, P. R. (2006). Spatial modelling: A comprehensive framework for principal coordinate analysis of neighbour matrices (pcnm). *Ecological Modelling*, 196(3-4), 483–493.
- Fagan, W. F., Fortin, M.-J., & Soykan, C. (2003). Integrating edge detection and dynamic modeling in quantitative analyses of ecological boundaries. *AIBS Bulletin*, 53(8), 730–738.

- Fitzpatrick, M. C., Preisser, E. L., Porter, A., Elkinton, J., Waller, L. A., Carlin, B. P., & Ellison, A. M. (2010). Ecological boundary detection using bayesian areal wombling. *Ecology*, *91*(12), 3448–3455.
- Fuhlendorf, S. D., Woodward, A. J., Leslie, D. M., & Shackford, J. S. (2002). Multi-scale effects of habitat loss and fragmentation on lesser prairie-chicken populations of the us southern Great Plains. *Landscape Ecology*, *17*(7), 617–628.
- Grant, T. A., Madden, E., & Berkey, G. B. (2004). Tree and shrub invasion in northern mixed-grass prairie: Implications for breeding grassland birds. *Wildlife Society Bulletin*, *32*(3), 807–818.
- Hastings, A., & Wysham, D. B. (2010). Regime shifts in ecological systems can occur with no warning. *Ecology Letters*, *13*(4), 464–472.
- Hoffmann, W. A., JACONIS, S. Y., Mckinley, K. L., Geiger, E. L., Gotsch, S. G., & Franco, A. C. (2012). Fuels or microclimate? Understanding the drivers of fire feedbacks at savanna–forest boundaries. *Austral Ecology*, *37*(6), 634–643.
- Jones, M. O., Allred, B. W., Naugle, D. E., Maestas, J. D., Donnelly, P., Metz, L. J., ... others. (2018). Innovation in rangeland monitoring: Annual, 30 m, plant functional type percent cover maps for us rangelands, 1984–2017. *Ecosphere*, *9*(9), e02430.

- Kefi, S., Guttal, V., Brock, W. A., Carpenter, S. R., Ellison, A. M., Livina, V. N., ...
Dakos, V. (2014). Early warning signals of ecological transitions: Methods for
spatial patterns. *PloS One*, 9(3), e92097.
- Kent, R., Levanoni, O., Banker, E., Pe'er, G., & Kark, S. (2013). Comparing the response
of birds and butterflies to vegetation-based mountain ecotones using boundary
detection approaches. *PloS One*, 8(3), e58229.
- Limb, R. F., Engle, D. M., Alford, A. L., & Hellgren, E. C. (2010). Tallgrass prairie plant
community dynamics along a canopy cover gradient of eastern redcedar
(*Juniperus virginiana* L.). *Rangeland Ecology & Management*, 63(6), 638–644.
- Ma, H., Carlin, B. P., & others. (2007). Bayesian multivariate areal wombling for
multiple disease boundary analysis. *Bayesian Analysis*, 2(2), 281–302.
- Omernik, J. M., & Griffith, G. E. (2014). Ecoregions of the conterminous united states:
Evolution of a hierarchical spatial framework. *Environmental Management*,
54(6), 1249–1266.
- Ratajczak, Z., Briggs, J. M., Goodin, D. G., Luo, L., Mohler, R. L., Nippert, J. B., &
Obermeyer, B. (2016). Assessing the potential for transitions from tallgrass
prairie to woodlands: Are we operating beyond critical fire thresholds? *Rangeland
Ecology & Management*, 69(4), 280–287.

- Ratajczak, Z., Nippert, J. B., & Ocheltree, T. W. (2014). Abrupt transition of mesic grassland to shrubland: Evidence for thresholds, alternative attractors, and regime shifts. *Ecology*, 95(9), 2633–2645.
- Ratajczak, Z., Nippert, J. B., Briggs, J. M., & Blair, J. M. (2014). Fire dynamics distinguish grasslands, shrublands and woodlands as alternative attractors in the central great plains of North America. *Journal of Ecology*, 102(6), 1374–1385.
- Roberts, C. P., Twidwell, D., Burnett, J. L., Donovan, V. M., Wonkka, C. L., Bielski, C. L., ... others. (2018). Early warnings for state transitions. *Rangeland Ecology & Management*, 71(6).
- Roberts, C., Allen, C., Angeler, D., & Twidwell, D. (2019). Shifting spatial regimes in a changing climate. *In Review: Nature Climate Change*.
- Roques, K., O’connor, T., & Watkinson, A. (2001). Dynamics of shrub encroachment in an African savanna: Relative influences of fire, herbivory, rainfall and density dependence. *Journal of Applied Ecology*, 38(2), 268–280.
- Scheffer, M., & Carpenter, S. R. (2003). Catastrophic regime shifts in ecosystems: Linking theory to observation. *Trends in Ecology & Evolution*, 18(12), 648–656.
- Scheffer, M., Carpenter, S., Foley, J. A., Folke, C., & Walker, B. (2001). Catastrophic shifts in ecosystems. *Nature*, 413(6856), 591.

- Sundstrom, S. M., Eason, T., Nelson, R. J., Angeler, D. G., Barichiev, C., Garmestani, A. S., ... others. (2017). Detecting spatial regimes in ecosystems. *Ecology Letters*, 20(1), 19–32.
- Thompson, S. J., Arnold, T. W., & Amundson, C. L. (2014). A multiscale assessment of tree avoidance by prairie birds. *The Condor*, 116(3), 303–315.
- Twidwell, D., West, A. S., Hiatt, W. B., Ramirez, A. L., Winter, J. T., Engle, D. M., ... Carlson, J. (2016). Plant invasions or fire policy: Which has altered fire behavior more in tallgrass prairie? *Ecosystems*, 19(2), 356–368.
- Uden, D., Twidwell, D., Allen, C., Jones, M., Naugle, D., Maestas, J., & Allred, B. (2019). Spatial imaging and screening for regime shifts. *Frontiers in Ecology and Evolution*, *In preparation*.
- Van Nes, E. H., & Scheffer, M. (2007). Slow recovery from perturbations as a generic indicator of a nearby catastrophic shift. *The American Naturalist*, 169(6), 738–747.
- Wagner, H. H. (2003). Spatial covariance in plant communities: Integrating ordination, geostatistics, and variance testing. *Ecology*, 84(4), 1045–1057.
- Wang, R., Dearing, J. A., Langdon, P. G., Zhang, E., Yang, X., Dakos, V., & Scheffer, M. (2012). Flickering gives early warning signals of a critical transition to a eutrophic lake state. *Nature*, 492(7429), 419.
- Womble, W. H. (1951). Differential systematics. *Science*, 114(2961), 315–322.

Zuur, A., Ieno, E., Walker, N., Saveliev, A., & Smith, G. (2009). *Mixed effects models and extensions in ecology with R*. New York, NY: Springer Science; Business Media.

TABLES

Table 5. 1: Model selection using AICc for two questions: 1) assessing relationships between vegetation (tree/grass) and bird community boundaries and 2) determining how bird boundaries responded to distance to vegetation boundaries. Columns indicate the question, the model covariates/smooth terms, the total number of covariates, the estimated AICc value, the delta AICc, and model weight.

Question	Model Covariates	K	AICc	Delta AICc	AICc Weight
Relationship	13, 33	7	247.97	0.00	0.27
Relationship	3, 13, 33	9	248.11	0.15	0.25
Relationship	13, 23, 33	9	248.22	0.25	0.24
Relationship	3, 13, 23, 33	11	248.56	0.59	0.20
Relationship	global	13	252.29	4.32	0.03
Relationship	23, 33	7	296.40	48.43	0.00
Relationship	3, 33	7	317.84	69.88	0.00
Relationship	3, 8	7	353.51	105.54	0.00
Distance to Boundary	3, 13, 33	9	243.49	0.00	0.62
Distance to Boundary	3, 13, 23, 33	11	244.97	1.49	0.30
Distance to Boundary	global	13	248.62	5.14	0.05
Distance to Boundary	13, 33	7	249.89	6.40	0.03
Distance to Boundary	13, 23, 33	9	251.97	8.49	0.01
Distance to Boundary	3, 33	7	255.84	12.35	0.00
Distance to Boundary	23, 33	7	281.45	37.97	0.00
Distance to Boundary	3, 8	7	296.80	53.32	0.00

FIGURES

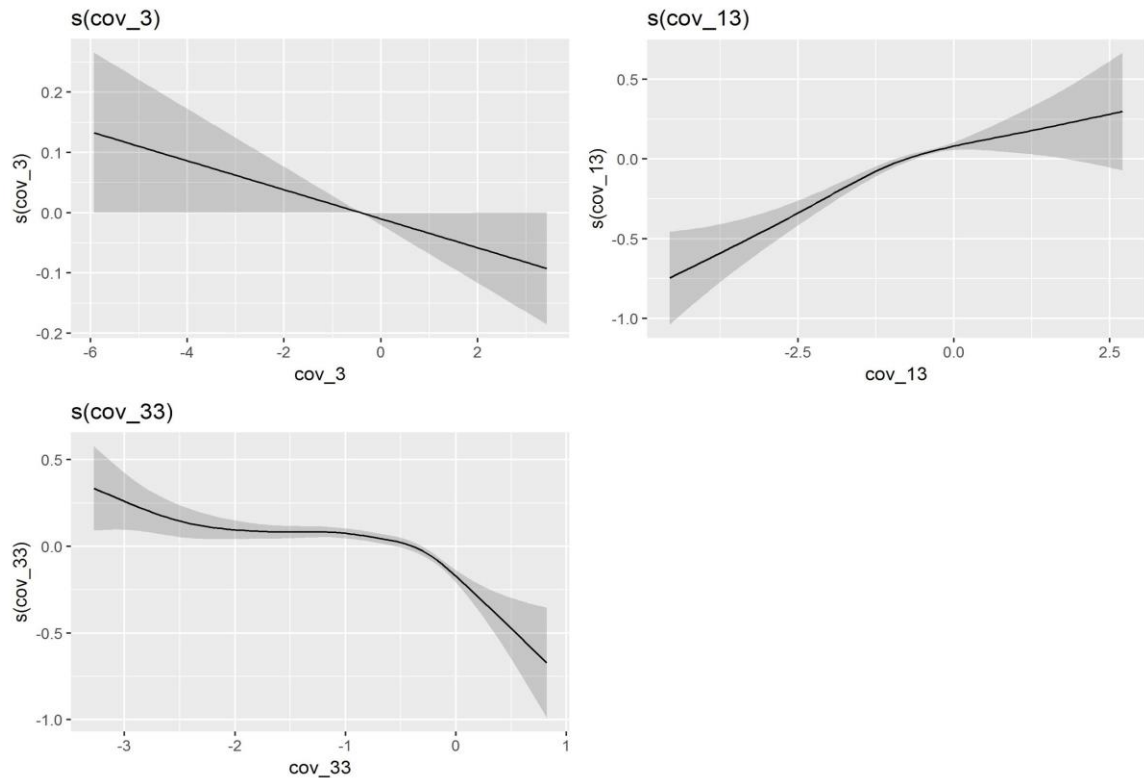


Figure 5. 1: Generalized additive mixed models demonstrate the relationship between spatial regime boundaries derived from a “wombling” method applied to bird community data with known vegetative tree-grassland spatial regime boundaries derived from remotely-sensed spatial covariance. The y-axis depicts the smoothed, predicted relationship between wombling values (R^2) and spatial covariance values (i.e., not the predicted wombling values). The x-axis shows a scaled range of spatial covariance values. Higher wombling values indicate greater likelihood and strength of a boundary. Spatial covariance values at or near zero indicate no tree-grass boundary, and negative spatial covariance values indicate increasingly stark tree-grass regime boundaries.

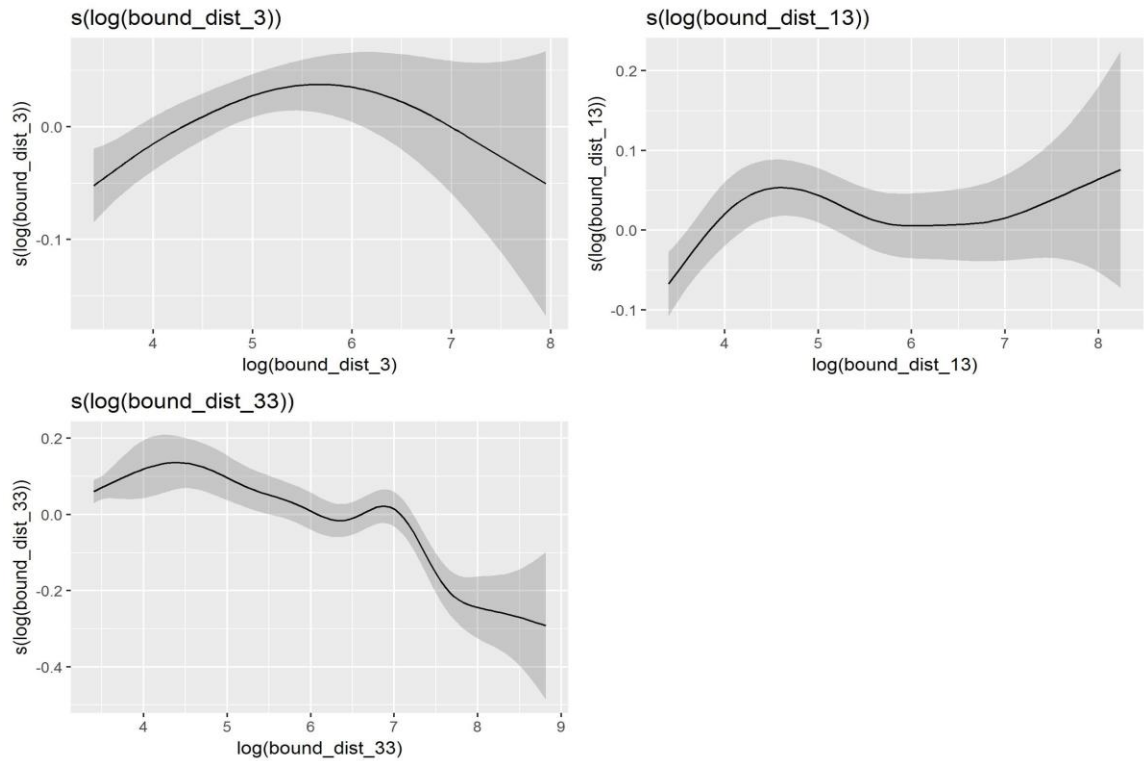


Figure 5. 2: Generalized additive mixed models demonstrate the relationship between spatial regime boundaries derived from a “wombling” method applied to bird community data with distance to known vegetative tree-grassland spatial regime boundaries derived from remotely-sensed spatial covariance. The y-axis depicts the smoothed, predicted relationship between wombling values (R^2) and distance (log-transformed meters) to the nearest spatial regime boundary. Higher wombling values indicate greater likelihood and strength of a boundary.

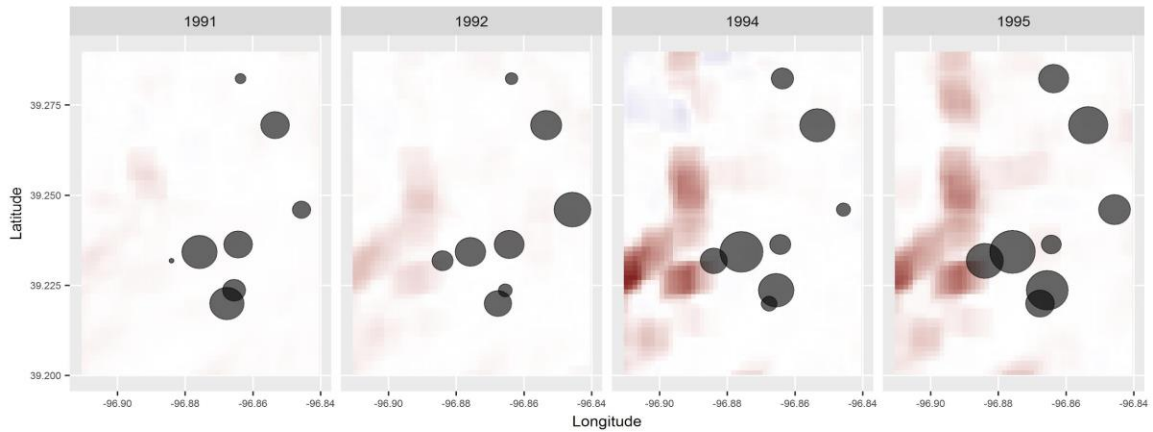


Figure 5. 3: A selected portion of the study area that was likely to exhibit early warnings of changing spatial regime boundaries (regime shifts) due to encroaching tree regimes into grassland regimes. This portion was less disturbed and is near a ravine in which a few trees could have escaped fire and from which tree regimes could expand without fire disturbance. Panels correspond with 4 years in which tree regime boundaries (red shading) rapidly expanded and displaced grassland regimes. Dots indicate bird community sampling locations. Dot size corresponds with wombling (R^2) values, with larger dots indicating greater likelihood of a spatial regime boundary and smaller dots indicating greater similarity lower likelihood of a boundary.

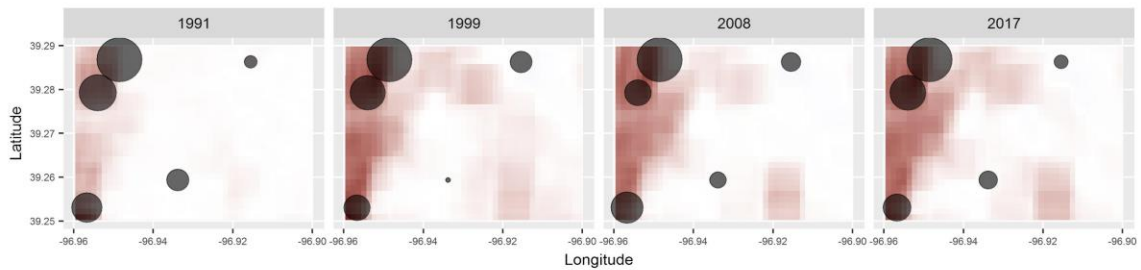


Figure 5. 4: A selected portion of the study area that was likely to have maintained stable tree-grass spatial regime boundaries due to receiving consistent application of fire and being near the center of a grassland regime. This portion was consistently and heavily disturbed by random and prescribed fires and military training. Panels correspond with 4 years of the 27-year-long study period. Dots indicate bird community sampling locations. Dot size corresponds with wombling (R^2) values, with larger dots indicating greater likelihood of a spatial regime boundary and smaller dots indicating greater similarity lower likelihood of a boundary.

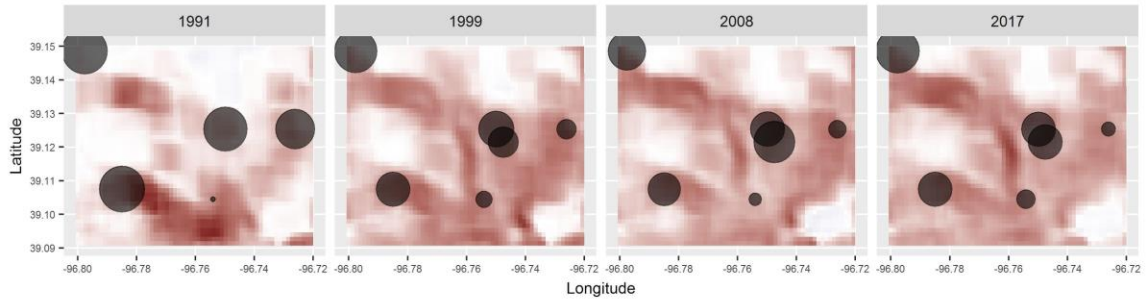


Figure 5. 5: A selected portion of the study area that initially contained a boundary between tree-grass regimes and became centers of tree regimes as tree regimes displaced grasslands. This portion was near a major river that would have historically hosted a tree regime and would have provided a source for tree encroachment of grasslands. Panels correspond with 4 years of the 27-year-long study period. Dots indicate bird community sampling locations. Dot size corresponds with wobble (R^2) values, with larger dots indicating greater likelihood of a spatial regime boundary and smaller dots indicating greater similarity lower likelihood of a boundary.

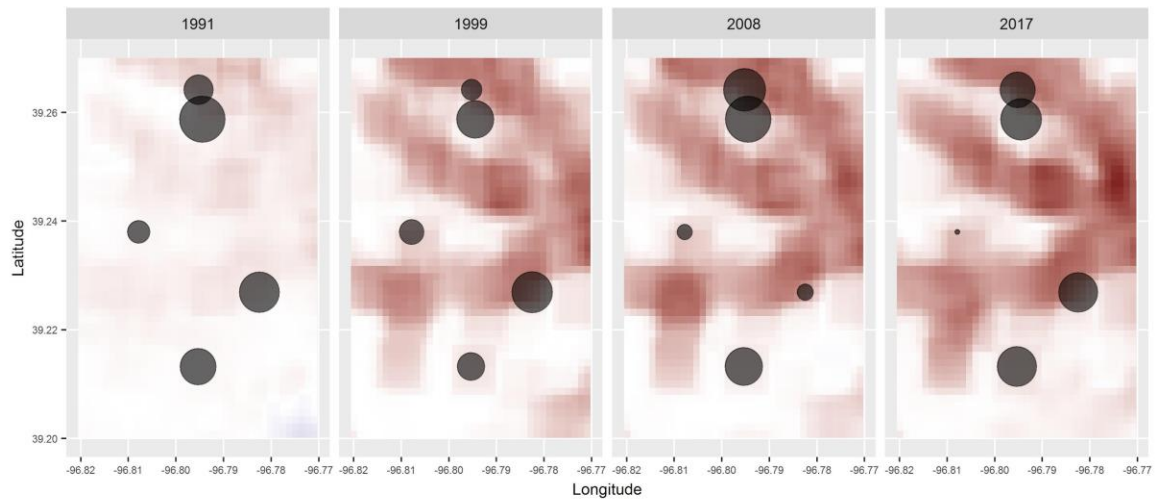


Figure 5. 6: A selected portion of the study area increasingly fragmented by tree-grass regimes. Panels correspond with 4 years of the 27-year-long study period. Dots indicate bird community sampling locations. Dot size corresponds with wobbling (R^2) values, with larger dots indicating greater likelihood of a spatial regime boundary and smaller dots indicating greater similarity lower likelihood of a boundary.

Figure 5. 7: Animation depicting changes in spatial regime boundaries from 1991 - 2017 across the entire study area of Fort Riley Army Base, KS, USA. Dots represent wobbling R^2 values at sampling locations indicating boundaries (large dots) and areas of self-similarity (small dots) and annual shifts. Background coloration indicates spatial

covariance of tree-grass regimes, where deeper reds indicate tree-grass boundaries, white indicates no boundary, and blues indicate positive spatial covariance.

**CHAPTER 6: CONSERVATION IN THE ERA OF NON-STATIONARITY:
RARE SPECIES DIVERSITY TRACKS CONTINENTAL REGIME
MOVEMENT⁵**

ABSTRACT

In an era when global change is leading to ecosystem collapse and regimes are mobilizing across continents, understanding how species distributions respond to ecological non-stationarity is crucial to choosing conservation targets. Currently, predictions of idiosyncratic or species-specific species responses to global change put rare species and species of conservation concern at particular risk: if global change alters or eliminates rare species' habitats, idiosyncratic responses by at-risk species would greatly impede predicting future occurrence and suitable habitat for rare species. Because landscape units with spatially explicit boundaries (i.e. spatial regimes) can shift predictably and directionally, rare species distributions may also shift non-randomly as a function of their proximity to a spatial regime boundary. Here, we test the prediction that the diversity and richness of rare species is highest where vulnerability is lowest. Specifically, we predict rare species richness and diversity will increase as distance to regime boundaries

⁵ CPR contributed to conceptualization, programming, data validation, formal analysis, data curation, all writing aspects, visualization, and project administration. DGA contributed conceptualization, visualization, and to writing all aspects. DT, CRA contributed to conceptualization and writing selected sections.

increases (i.e., far from regime boundaries) and decrease as regime boundaries approach. Using 46 years of avian community data across a spatial transect ranging from the Gulf of Mexico to the southern boreal forest in North America, we identify spatial regime boundaries and compare the richness and diversity of rare species (i.e., defined as species with modelled spatially stochastic abundance patterns) to the distance to spatial regime boundaries. Distance from spatial regime boundary was the strongest predictor of stochastic species richness and diversity. Additionally, stochastic species richness declined nonlinearly over the 46-years period while number of spatial regime boundaries increased linearly over time. Rare species richness and diversity were highest nearest the spatial “centers” of regimes. We show that rare species distributions are non-stationary in space and time, and distributions change with shifting spatial regimes. Our results support a conservation paradigm that prioritizes conservation efforts according to movement trajectories of spatial regime boundaries, actively searches for early warnings of ecological change, and promotes exchanges and cooperation between a network of protected areas across a broad geography.

INTRODUCTION

In an era when global change is leading to ecosystem collapse (Scheffer & Carpenter, 2003) and regimes mobilizing across continents (C. Roberts, Allen, Angeler, & Twidwell, 2018), understanding how species distributions respond to ecological non-stationarity is crucial to choosing conservation targets (Craig, 2010; Spears et al., 2015). Global change drivers such as climate change, agricultural land conversion, and urbanization have led to novel environmental conditions which affect species

distributions in unknown ways (Barnosky et al., 2012; Pacifici et al., 2015; Valladares, Bastias, Godoy, Granda, & Escudero, 2015). This has given rise to idiosyncratic hypotheses of species responses and distribution changes-which would present daunting problems to predicting where and when conservation should be prioritized (Gilman, Urban, Tewksbury, Gilchrist, & Holt, 2010; Twomey et al., 2012; Valladares et al., 2015). Rare species and species of conservation concern are particularly at risk in this scenario: if global change alters or eliminates rare species' habitats, idiosyncratic responses by at-risk species would make predicting future occurrence and suitable habitat for conservation extremely difficult (Ledig, Rehfeldt, Sáenz-Romero, & Flores-López, 2010; Ohlemüller et al., 2008).

Recent advances in quantifying spatial resilience via spatial regimes holds potential for predicting species distributions and prioritizing at-risk species conservation in an era of non-stationarity. Resilience theory predicts landscapes are comprised of multiple regimes with discrete spatiotemporal boundaries within which structures and processes produce positive feedbacks maintaining regime identity, at a given scale (Allen et al., 2016; Groffman et al., 2006; Scheffer & Carpenter, 2003). Recent studies have demonstrated these so-called spatial regimes form discrete boundaries between biotic communities (Sundstrom et al., 2017) and spatial regimes are non-stationary yet follow orderly, directional trajectories (C. Roberts et al., 2019). Because rare species' abundances tend to be highest near the geographic center of their distributions due to their typically narrow environmental requirements (Brown, 1984; Gaston, 1994) and spatial regimes encompass the structures and functions in which biotic communities

reside (Allen et al., 2016), it follows that rare species' distributions might reflect non-stationary-but also non-random-patterns as spatial regimes move in time and space (Twomey et al., 2012). That is, the number of rare species and abundances of individual rare species may track with mobilizing spatial regimes, with rare species richness and diversity being highest near the center of spatial regimes. In an era of non-stationarity, such tractable changes in species distributions would facilitate conservation efforts by enabling prediction of where prioritization and proactive management for rare species would be most effective.

Here, we test the prediction that distributions of rare species are non-stationary but also non-idiosyncratic, our hypothesis being rare species richness and diversity will track the mobilization of ecological regimes in space and time. Our specific predictions are rare species richness and diversity will increase as distance to regime boundaries increases (i.e., far from regime boundaries) and decrease as regime boundaries approach. We use 46 years of avian community data across a spatial transect ranging from the Gulf of Mexico to the southern boreal forest in North America.

METHODS

Data Collection

We collected 45 years (1970 - 2015) of the U.S. Geological Survey's North American Breeding Bird Survey data (BBS), which consists of avian community composition collected by trained observers along permanent, georeferenced roadside routes across the North American continent (Sauer et al., n.d.). Because routes were still being established in the initial years of the BBS, we consider route data starting in 1970, when

approximately 50% of current BBS routes had been established. Along each 39.5 km route, observers make 50 stops (every 0.8 km) and conduct point-count surveys at each stop, recording all the number of individuals of any avian species detected aurally or visually within a 0.402 km radius of the stop. Because the BBS is known to detect water bird families poorly and because spatial regime identification did not include these water bird families in its analysis, we removed these avian families from this analysis as well: Anseriformes, Gaviiformes, Gruiformes, Pelecaniformes, Phaethontiformes, Phoenicopteriformes, Podicipediformes, Procellariiformes, and Suliformes. For more detailed protocols, see C. Roberts et al. (2018) and Sauer et al. (n.d.).

Statistical Analysis

Identifying spatial regimes

To assess distributions of rare species in relation to shifting spatial regimes, we chose a study transect that had already demonstrated mobile spatial regimes (C. Roberts et al., 2019). Specifically, we analyzed all BBS routes that fell within a belt transect on the ecotone of the Great Plains and Eastern Temperate Forests extending from the Gulf of Mexico to the edge of the boreal forest in Canada. The belt transect extended south-north from 28 - 49 degrees latitude (approximately 2300 km) and east-west from 93 - 97 degrees longitude (approximately 440 km).

We identified spatial regimes along the belt transect each year from 1970 - 2015. We identified spatial regime boundaries via discontinuity analysis of body masses of all species detected in BBS routes (Barichievy et al., 2018; C. Roberts et al., 2018). In this context, discontinuity analysis defines boundaries as significant shifts in rank-ordered,

log-transformed body mass patterns (C. P. Roberts et al., 2018; Spanbauer et al., 2016). For taxa with determinant growth, mean body mass has been shown to reliably differentiate size aggregations and is strongly allometric to the scales at which functions are carried out by organisms (Nash et al., 2014). To quantify significant shifts in discontinuity patterns, we conducted constrained hierarchical clustering on discontinuity patterns (e.g., size of body mass aggregations, size of gaps between body mass aggregations, locations of body mass aggregations) via the “chclust” function using the “CONISS” method from the “rioja” package in R on each year’s dissimilarity matrix (C. Roberts et al., 2018; Spanbauer et al., 2016). We used a broken stick model (“bstick.chclust” from the “rioja” package in R) to determine the number of significant clusters (Bennett, 1996). Finally, we defined the latitudes of significant cluster breaks as spatial regime boundaries (C. Roberts et al., 2018).

Identifying rare species

Rarity has been defined differently in the ecological literature and is often based on arbitrary determination approaches (Gaston, 1994; Rabinowitz, 1981). For this study, we define rare species as species with stochastic abundance patterns in space determined objectively by modeling (Angeler, Allen, Uden, & Johnson, 2015; Baho, Drakare, Johnson, Allen, & Angeler, 2014). To identify species with stochastic abundance patterns along the belt transect for each year from 1970 - 2015, we used a spatial modeling technique commonly used to identify spatial structure and scaling (Borcard, Legendre, Avois-Jacquet, & Tuomisto, 2004). Based on Redundancy Analysis (RDA), this method uses distance-based Moran Eigenvector Maps (dbMEM) to model space (Dray et al.,

2012). The dbMEM analysis produced a set of orthogonal spatial variables derived from the latitude and longitude coordinates of each BBS route for each year. We ran dbMEM analyses for each year because over time, more BBS routes were established (adding locations) and not every established route was sampled every year. Because dbMEM is inefficient at handling linear trends, detrending of raw data is required prior to analysis (Dray, Legendre, & Peres-Neto, 2006). We used detrended, orthogonal dbMEM spatial variables, which corresponded with a gradient of broad- to fine-scale patterns in avian community data, as explanatory variables and used forward model selection on these variables to develop a parsimonious spatial model for each year (Dray et al., 2012).

Selected, significant dbMEM variables were retained in the RDA model, linearly combined, and then spatial patterns of bird communities were extracted from Hellinger-transformed species \times space matrices (Legendre & Gallagher, 2001). Essentially, bird species with similar spatial patterns are identified and collapsed onto orthogonal (i.e. statistically independent) RDA axes. We tested significance of the RDA models via 200 permutations. The resulting patterns reflect hierarchical structures (i.e., broad-scale vs fine-scale variation) and other subtle differences in community structure at any spatial scale, bounded by the extent and grain of the data. The number of significant spatial patterns of species groups corresponds with the number of significant RDA axes (Dray et al., 2012). We inspected the adjusted R^2 values of the RDA axes to assess the ecological relevance of each RDA-identified spatial pattern.

Finally, we used Spearman rank correlations to relate the raw abundances of individual avian taxa with the modeled spatial patterns (i.e., to identify stochastic

species). We defined rare species as those with stochastic patterns that were not associated with any significant RDA axis (Angeler et al., 2015; Baho et al., 2014).

Comparing rare species richness, diversity to spatial regime boundaries

We determined how rare species distributions (richness and diversity) related to distance to spatial regime boundaries via model selection techniques. For response variables, we calculated the richness and diversity (inverse Simpson's index) of stochastic species for each BBS route for each year. For predictor variables, we calculated the distance in degrees latitude from each BBS route to the nearest spatial regime boundary for each year. We also included the latitude and longitudes of routes as variables to account for differences in species patterns across the wide geographic range of the belt transect. Because spatial regime boundaries shifted over time, distances from a given BBS route to the nearest spatial regime boundary also changed over time (C. Roberts et al., 2018).

We modeled richness and diversity separately: we used negative binomial generalized mixed models to analyze richness, and we used linear mixed modeling to analyze diversity. We allowed intercepts to vary by year. Models were ranked according to Akaike's Information Criterion adjusted for small sample sizes. We estimated 80% confidence limits with 999 simulations.

Finally, we also compared the mean richness of stochastic species to the number of spatial regime boundaries over time. To do this, we separately modeled 1) mean stochastic species richness change over time and 2) number of spatial regime boundaries over time. We first used generalized additive models (GAMs) to detect nonlinear patterns. If patterns were clearly linear (i.e., estimated degrees of freedom [edf] = 1), we

used linear regression. We conducted all analyses in R 3.5.0 (R Development Core Team 2018) with the packages *adespatial* (dbMEM variables, forward selection), *vegan* (Hellinger transformations, RDA), *merTools* (confidence limit simulations), and *lme4* (mixed modeling).

RESULTS

We detected significant spatial structure across the spatial transect across all years in which spatial regimes were detected (Table 6.1). Across all years, number of significant RDA axes ranged from 4 - 10, with 6.97 ± 0.44 significant axes (95% confidence) on average (Table 6.1). Adjusted R-squared of models ranged from 0.167 - 0.288, with a mean of 0.25 ± 0.01 R-squared (Table 6.1).

We also detected rare species along the transect every year. Number of rare species per BBS route ranged from 0 - 11, and average number of rare species per route was 0.77 ± 0.03 (95% confidence). Inverse Simpson's diversity per route ranged from 0 - 6.4, with a mean of 0.67 ± 0.02 .

Distance from spatial regime boundary was a significant, and the strongest, positive predictor of rare species richness (0.176 ± 0.021) and diversity (0.087 ± 0.014 ; Figure 6.1; Tables 6.2, 6.3). Rare species richness and diversity also significantly increased at higher latitudes (northern latitudes; richness = 0.102 ± 0.020 ; diversity = 0.063 ± 0.013) and lower longitudes (westward longitudes; richness = -0.063 ± 0.018 ; diversity = -0.034 ± 0.012 ; Figure 6.1; Table 6.3). Additionally, rare species richness declined nonlinearly over time ($\text{edf} = 1.72$, $F = 12.25$, $P < 0.001$) while number of spatial

regime boundaries increased linearly over time (0.017 ± 0.013 , $F = 2.82$, $P = 0.10$; Figure 6.2).

DISCUSSION

Rare species richness and abundance followed non-stationary, yet predictable, patterns and tracked with spatial regime movement across a continent. Our results stand in sharp contrast with predictions of species-specific or idiosyncratic responses to global change (Gilman et al., 2010; Valladares et al., 2015). Rare species richness and diversity increased as distance to spatial regime boundaries increased; that is, rare species richness and diversity were highest nearest the spatial “centers” of regimes. These peaks of rare species richness and diversity moved in tandem with spatial regimes, and as the distance between spatial regimes shrank over time (a consequence of the increasing number of regimes), rare species richness and diversity also shrank. Although our conclusions are not causal, we demonstrate a clear predictive relationship linking nonstationary spatial regime boundaries and rare species.

The advent of long-term, continent-spanning data has fueled progress past reliance on stationary snapshots of species assemblages and rare species dynamics within fixed spatiotemporal boundaries. Early studies and syntheses on rare species provided crucial insights on general, stationary abundance patterns—for instance, showing that both rare and common species abundances tend to be greatest near the centers of their spatial distributions (Brown, 1984), that rare species’ spatial distributions differ from common species’ (Condit et al., 2000; Gering, Crist, & Veech, 2003), and the need for methods to deal with the strength of stochasticity when analyzing rare species (Bray & Curtis, 1957;

Nichols, 1977). Advances in multivariate analyses and metacommunity theory then led to studies investigating spatial and environmental drivers of rare species' distribution and abundance patterns (Alahuhta, Johnson, Olker, & Heino, 2014; Siqueira et al., 2012), and some studies hinted at spatiotemporal non-stationarity in rare species' patterns (Baho et al., 2014; De Juan & Hewitt, 2014). We build on this body of literature by explicitly testing for non-stationary patterns of rare species over a long and wide spatiotemporal window. This enabled us to set aside previously requisite assumptions of spatially dimensionless metacommunities and fixed ecosystem boundaries (e.g., (Alahuhta et al., 2014; Siqueira et al., 2012) and show that rare species, while exhibiting stochastic spatial abundance, do not follow idiosyncratic distribution patterns.

Our results provide a path for adapting methods for identifying areas of conservation priority in a non-stationary world. Rare species richness and diversity tracked moving spatial regime boundaries, and spatial regime movement tracked the direction of multiple global change drivers (C. Roberts et al., 2019). Traditionally, areas of conservation concern are identified using current or historical species distributions, protected areas, or environmental characteristics (Ledig et al., 2010; Y. Liu et al., 2017; H. Xu et al., 2015). In particular, rare species, which are often listed as species of conservation concern, can serve as strong reasoning for selecting conservation lands (Gauthier, Debussche, & Thompson, 2010; Marchese, 2015; Myers, Mittermeier, Mittermeier, Da Fonseca, & Kent, 2000). However, our results indicate that, in an era of non-stationarity, successful conservation efforts cannot assume geographically fixed protected areas will continue providing critical habitat, that species distributions will

remain inviolate, or that environmental characteristics will always reliably correspond with particular species or assemblages (Benson & Craig, 2014; Craig, 2010). Instead, our results support a conservation paradigm that prioritizes conservation efforts according to movement trajectories of spatial regime boundaries (C. Roberts et al., 2019), actively searches for early warnings of ecological change (Biggs, Carpenter, & Brock, 2009), and promotes exchanges and cooperation between a network of protected areas across a broad geography (Gauthier et al., 2010; C. N. Johnson et al., 2017).

We also show that rare species (i.e., species with spatially stochastic abundance patterns) richness and diversity were “indicators” of impending ecological change. Declines in species richness and diversity signaled impending regime shifts as spatial regime boundaries approached. Similarly, as number of spatial regime boundaries increased (i.e., as spatial regime shifts became more frequent), rare species richness declined. The promised benefits of indicator species for ecological management and policymaking is that limited resources could be made more cost-effective by monitoring a select group of species that would “indicate” the condition or vulnerability of an ecological system of interest (Landres, Verner, & Thomas, 1988). Our findings provide a pathway for progress beyond system-specificity and best-practice guidelines for selecting indicator species (Carignan & Villard, 2002; Landres et al., 1988; Siddig, Ellison, Ochs, Villar-Leeman, & Lau, 2016). We demonstrate generalizable, theory-based rules to both identify rare species (i.e., species with stochastic abundance patterns) (Angeler et al., 2015; Baho et al., 2014) and identify patterns in rare species at a subcontinental scale

over 46 years that corresponded with trajectories of global change drivers (C. Roberts et al., 2018).

As global change drivers continue pushing spatial regime boundaries poleward over time, our results predict latitudinal shifts in rare species over time. This prediction has been supported many times in the literature: many studies demonstrate latitudinal pressures on biota due to global change drivers such as climate change (Gilman et al., 2010; Ledig et al., 2010; Pacifici et al., 2015). Although distance to spatial regime boundaries was a stronger predictor than latitude, both rare species richness and diversity positively associated with latitude. Because distance to spatial regime boundaries shrank over time at higher latitudes (as spatial regimes moved north), northern latitudes lost rare species richness and diversity. If the patterns we detected are conservative, the southernmost spatial regime, which has increased in size over time, will gain rare species. However, it is unclear if this will happen immediately or with a temporal lag. Our results provide predictive power to the vulnerability of rare species and conservation prioritization in an era of rapid global change.

LITERATURE CITED

Alahuhta, J., Johnson, L. B., Olker, J., & Heino, J. (2014). Species sorting determines variation in the community composition of common and rare macrophytes at various spatial extents. *Ecological Complexity*, 20, 61–68.

Allen, C. R., Angeler, D. G., Cumming, G. S., Folke, C., Twidwell, D., & Uden, D. R. (2016). Quantifying spatial resilience. *Journal of Applied Ecology*, 53(3), 625–635.

- Angeler, D. G., Allen, C. R., Uden, D. R., & Johnson, R. K. (2015). Spatial patterns and functional redundancies in a changing boreal lake landscape. *Ecosystems*, 18(5), 889–902.
- Baho, D. L., Drakare, S., Johnson, R. K., Allen, C. R., & Angeler, D. G. (2014). Similar resilience attributes in lakes with different management practices. *PLoS One*, 9(3), e91881.
- Barichiev, C., Angeler, D. G., Eason, T., Garmestani, A. S., Nash, K. J., Stow, C. A., ... Allen, C. R. (2018). A method to detect discontinuities in census data. *Methods in Ecology and Evolution*.
- Barnosky, A. D., Hadly, E. A., Bascompte, J., Berlow, E. L., Brown, J. H., Fortelius, M., ... others. (2012). Approaching a state shift in earth's biosphere. *Nature*, 486(7401), 52.
- Bennett, K. D. (1996). Determination of the number of zones in a biostratigraphical sequence. *New Phytologist*, 132(1), 155–170.
- Benson, M. H., & Craig, R. K. (2014). The end of sustainability. *Society & Natural Resources*, 27(7), 777–782.
- Biggs, R., Carpenter, S. R., & Brock, W. A. (2009). Turning back from the brink: Detecting an impending regime shift in time to avert it. *Proceedings of the National Academy of Sciences*, 106(3), 826–831.

- Borcard, D., Legendre, P., Avois-Jacquet, C., & Tuomisto, H. (2004). Dissecting the spatial structure of ecological data at multiple scales. *Ecology*, 85(7), 1826–1832.
- Bray, J. R., & Curtis, J. T. (1957). An ordination of the upland forest communities of southern wisconsin. *Ecological Monographs*, 27(4), 325–349.
- Brown, J. H. (1984). On the relationship between abundance and distribution of species. *The American Naturalist*, 124(2), 255–279.
- Carignan, V., & Villard, M.-A. (2002). Selecting indicator species to monitor ecological integrity: A review. *Environmental Monitoring and Assessment*, 78(1), 45–61.
- Condit, R., Ashton, P. S., Baker, P., Bunyavejchewin, S., Gunatilleke, S., Gunatilleke, N., ... others. (2000). Spatial patterns in the distribution of tropical tree species. *Science*, 288(5470), 1414–1418.
- Craig, R. K. (2010). Stationarity is dead-long live transformation: Five principles for climate change adaptation law. *Harv. Envtl. L. Rev.*, 34, 9.
- De Juan, S., & Hewitt, J. (2014). Spatial and temporal variability in species richness in a temperate intertidal community. *Ecography*, 37(2), 183–190.
- Dray, S., Legendre, P., & Peres-Neto, P. R. (2006). Spatial modelling: A comprehensive framework for principal coordinate analysis of neighbour matrices (pcnm). *Ecological Modelling*, 196(3-4), 483–493.

- Dray, S., Péliissier, R., Couteron, P., Fortin, M.-J., Legendre, P., Peres-Neto, P. R., ... others. (2012). Community ecology in the age of multivariate multiscale spatial analysis. *Ecological Monographs*, 82(3), 257–275.
- Gaston, K. J. (1994). What is rarity? In *Rarity* (pp. 1–21). Springer.
- Gauthier, P., Debussche, M., & Thompson, J. D. (2010). Regional priority setting for rare species based on a method combining three criteria. *Biological Conservation*, 143(6), 1501–1509.
- Gering, J. C., Crist, T. O., & Veech, J. A. (2003). Additive partitioning of species diversity across multiple spatial scales: Implications for regional conservation of biodiversity. *Conservation Biology*, 17(2), 488–499.
- Gilman, S. E., Urban, M. C., Tewksbury, J., Gilchrist, G. W., & Holt, R. D. (2010). A framework for community interactions under climate change. *Trends in Ecology & Evolution*, 25(6), 325–331.
- Groffman, P. M., Baron, J. S., Blett, T., Gold, A. J., Goodman, I., Gunderson, L. H., ... others. (2006). Ecological thresholds: The key to successful environmental management or an important concept with no practical application? *Ecosystems*, 9(1), 1–13.
- Johnson, C. N., Balmford, A., Brook, B. W., Buettel, J. C., Galetti, M., Guangchun, L., & Wilmschurst, J. M. (2017). Biodiversity losses and conservation responses in the anthropocene. *Science*, 356(6335), 270–275.

- Landres, P. B., Verner, J., & Thomas, J. W. (1988). Ecological uses of vertebrate indicator species: A critique. *Conservation Biology*, 2(4), 316–328.
- Ledig, F. T., Rehfeldt, G. E., Sáenz-Romero, C., & Flores-López, C. (2010). Projections of suitable habitat for rare species under global warming scenarios. *American Journal of Botany*, 97(6), 970–987.
- Legendre, P., & Gallagher, E. D. (2001). Ecologically meaningful transformations for ordination of species data. *Oecologia*, 129(2), 271–280.
- Liu, Y., Shen, Z., Wang, Q., Su, X., Zhang, W., Shrestha, N., ... Wang, Z. (2017). Determinants of richness patterns differ between rare and common species: Implications for gesneriaceae conservation in china. *Diversity and Distributions*, 23(3), 235–246.
- Marchese, C. (2015). Biodiversity hotspots: A shortcut for a more complicated concept. *Global Ecology and Conservation*, 3, 297–309.
- Myers, N., Mittermeier, R. A., Mittermeier, C. G., Da Fonseca, G. A., & Kent, J. (2000). Biodiversity hotspots for conservation priorities. *Nature*, 403(6772), 853.
- Nash, K. L., Allen, C. R., Angeler, D. G., Barichievy, C., Eason, T., Garmestani, A. S., ... others. (2014). Discontinuities, cross-scale patterns, and the organization of ecosystems. *Ecology*, 95(3), 654–667.
- Nichols, S. (1977). On the interpretation of principal components analysis in ecological contexts. *Vegetatio*, 34(3), 191–197.

- Ohlemüller, R., Anderson, B. J., Araújo, M. B., Butchart, S. H., Kudrna, O., Ridgely, R. S., & Thomas, C. D. (2008). The coincidence of climatic and species rarity: High risk to small-range species from climate change. *Biology Letters*, 4(5), 568–572.
- Pacifici, M., Foden, W. B., Visconti, P., Watson, J. E., Butchart, S. H., Kovacs, K. M., ... others. (2015). Assessing species vulnerability to climate change. *Nature Climate Change*, 5(3), 215.
- Rabinowitz, D. (1981). Seven forms of rarity. *Biological Aspects of Rare Plant Conservation*.
- Roberts, C. P., Twidwell, D., Burnett, J. L., Donovan, V. M., Wonkka, C. L., Bielski, C. L., ... others. (2018). Early warnings for state transitions. *Rangeland Ecology & Management*.
- Roberts, C. P., Allen, C. R., Angeler, D. G., & Twidwell, D. (2019). Shifting spatial regimes in a changing climate. *In Review: Nature Climate Change*.
- Sauer, J. R., Niven, D. K., Hines, J. E., Ziolkowski, D. J., Pardieck, K. L., Fallon, J. E., & Link, W. A. (n.d.). “The North American Breeding Bird Survey, Results and Analysis 1966 - 2015” (Version 2.07.2017 USGS Patuxent Wildlife Research Center, Laurel, MD, 2017. Retrieved from <https://www.pwrc.usgs.gov/bbs/>
- Scheffer, M., & Carpenter, S. R. (2003). Catastrophic regime shifts in ecosystems: Linking theory to observation. *Trends in Ecology & Evolution*, 18(12), 648–656.

- Siddig, A. A., Ellison, A. M., Ochs, A., Villar-Leeman, C., & Lau, M. K. (2016). How do ecologists select and use indicator species to monitor ecological change? Insights from 14 years of publication in ecological indicators. *Ecological Indicators*, 60, 223–230.
- Siqueira, T., Bini, L. M., Roque, F. O., Marques Couceiro, S. R., Trivinho-Strixino, S., & Cottenie, K. (2012). Common and rare species respond to similar niche processes in macroinvertebrate metacommunities. *Ecography*, 35(2), 183–192.
- Spanbauer, T. L., Allen, C. R., Angeler, D. G., Eason, T., Fritz, S. C., Garmestani, A. S., ... Sundstrom, S. M. (2016). Body size distributions signal a regime shift in a lake ecosystem. *Proc. R. Soc. B*, 283(1833), 20160249.
- Spears, B. M., Ives, S. C., Angeler, D. G., Allen, C. R., Birk, S., Carvalho, L., ... others. (2015). Effective management of ecological resilience—are we there yet? *Journal of Applied Ecology*, 52(5), 1311–1315.
- Sundstrom, S. M., Eason, T., Nelson, R. J., Angeler, D. G., Barichievy, C., Garmestani, A. S., ... others. (2017). Detecting spatial regimes in ecosystems. *Ecology Letters*, 20(1), 19–32.
- Twomey, M., Brodte, E., Jacob, U., Brose, U., Crowe, T. P., & Emmerson, M. C. (2012). Idiosyncratic species effects confound size-based predictions of responses to climate change. *Philosophical Transactions of the Royal Society of London B: Biological Sciences*, 367(1605), 2971–2978.

Valladares, F., Bastias, C. C., Godoy, O., Granda, E., & Escudero, A. (2015). Species coexistence in a changing world. *Frontiers in Plant Science*, 6, 866.

Xu, H., Detto, M., Fang, S., Li, Y., Zang, R., & Liu, S. (2015). Habitat hotspots of common and rare tropical species along climatic and edaphic gradients. *Journal of Ecology*, 103(5), 1325–1333.

TABLES

Table 6. 1: Results from spatial modeling of North American breeding bird communities across a south-north belt transect from 1970 - 2015 using Redundancy Analysis (RDA) and distance-based Moran's eigenvector mapping (dbMEM). From left to right, columns indicate year, number of dbMEM axes detected per year, number of significant dbMEM axes per year, number of significant RDA axes per year, and adjusted R^2 of the minimum (final) RDA model.

Year	dbMEMs	Sig. dbMEMs	Sig. RDA axes	adjusted R^2
1970	41	24	7	0.27
1971	36	20	4	0.222
1972	34	21	6	0.275
1973	44	25	6	0.282
1974	35	22	6	0.259
1975	43	25	6	0.274
1976	36	21	6	0.248
1977	39	18	6	0.235
1978	47	23	7	0.241

1979	54	16	6	0.208
1981	52	22	8	0.249
1982	45	22	6	0.253
1983	45	10	5	0.167
1986	45	28	7	0.276
1987	54	27	6	0.265
1988	51	27	7	0.284
1989	48	26	7	0.288
1992	52	27	8	0.259
1993	56	32	8	0.263
1994	59	24	9	0.259
1995	62	28	8	0.243
1996	58	24	7	0.242
1999	60	25	8	0.23
2000	60	25	6	0.245

2002	55	30	9	0.258
2003	63	33	6	0.26
2004	73	30	8	0.264
2005	72	35	7	0.253
2006	67	32	5	0.237
2007	72	31	6	0.225
2008	62	30	6	0.219
2009	72	27	7	0.221
2010	63	27	9	0.253
2011	62	23	8	0.238
2012	75	39	7	0.262
2013	72	27	10	0.254
2014	66	28	10	0.256
2015	62	35	7	0.262

Table 6. 2: Model selection results for analyzing the relationship between richness/diversity of rare bird species (i.e., species with spatially stochastic abundance patterns) to the distance to spatial regime boundaries from 1970 - 2015 North American Breeding Bird Survey. From left to right, columns indicate the response variable, the model, the Akaikie Information Criterion adjusted for small sample sizes (AICc), the delta AICc, and the AICc weight.

Response Variable	Models	K	AICc	Delta AICc
Richness	Distance + Latitude + Longitude	6	13685.4	0
	Distance + Latitude	5	13701.5	16.1
	Distance + Longitude	5	13724.2	38.9
	Distance	4	13739.6	54.3
	Latitude + Longitude	5	13782.5	97.1
	Latitude	4	13796.7	111.3
	Longitude	4	13886.3	201
	Null	3	13898.5	213.2
Diversity	Distance + Latitude + Longitude	6	13962.5	0
	Distance + Latitude	5	13973.8	11.3

	Distance + Longitude	5	14002.9	40.4
	Distance	4	14014.3	51.8
	Latitude + Longitude	5	14020.4	57.9
	Latitude	4	14030.5	68
	Longitude	4	14104.2	141.7
	Null	3	14114	151.5

Table 6. 3: Coefficients from top models resulting from model selection analyzing the relationship between richness/diversity of rare bird species (i.e., species with spatially stochastic abundance patterns) to the distance to spatial regime boundaries from 1970 - 2015 North American Breeding Bird Survey. From left to right, columns indicate the response variable, the predictor variables, the coefficient estimate, the coefficients' standard errors, and the coefficients' test statistics (z-value for richness models, t-value for diversity models).

Response Variable	Predictor Variable	Estimate	SE	Test Statistic
Richness	Intercept	-0.4	0.106	-3.79
	Distance	0.18	0.017	10.11
	Latitude	0.1	0.016	6.42
	Longitude	-0.06	0.015	-4.25
Diversity	Intercept	0.71	0.063	11.35
	Distance	0.09	0.011	7.76
	Latitude	0.06	0.01	6.52
	Longitude	-0.03	0.009	-3.65

FIGURES

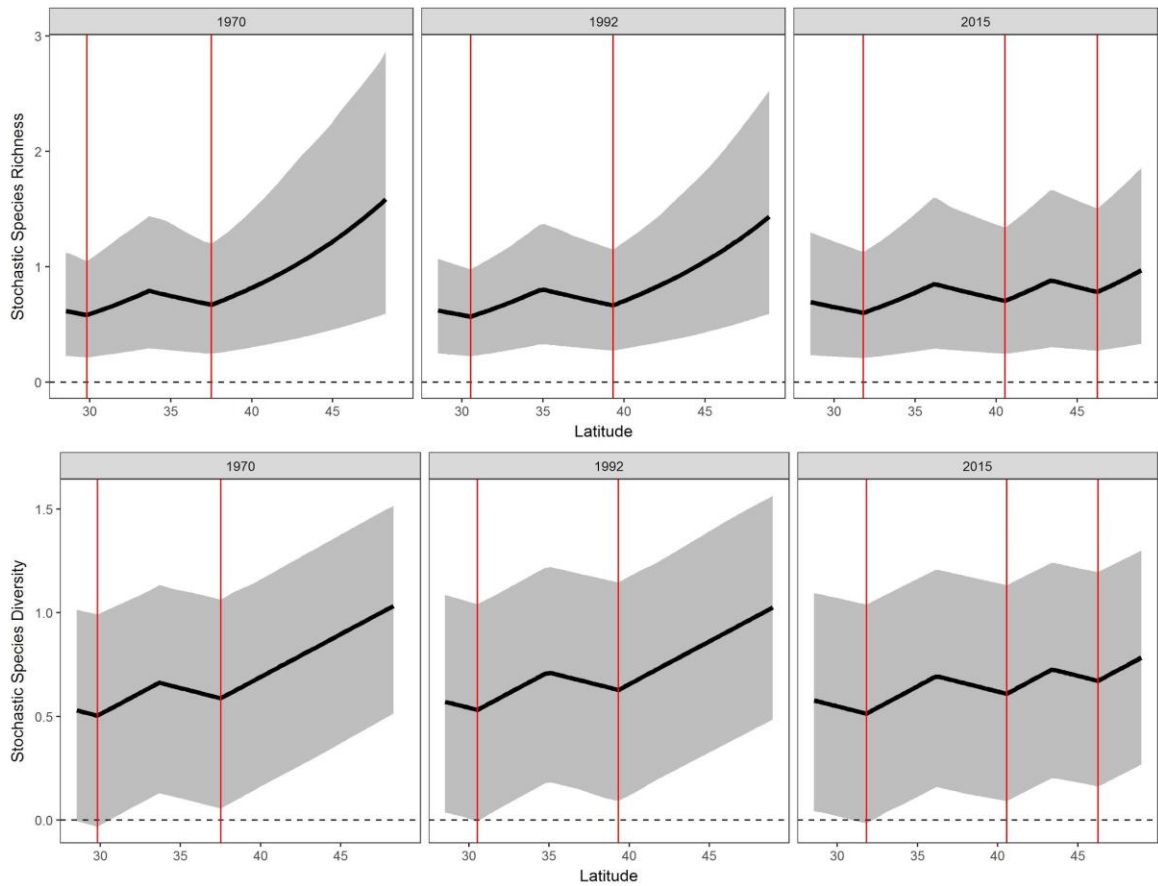


Figure 6. 1: Subcontinental predicted richness (A) and diversity (B) of rare bird species (species with spatially stochastic abundance patterns) over a 46-year period along a south-to-north latitudinal gradient in central North America. The x-axis indicates degrees latitude. Black lines are predicted richness and diversity values, gray-shaded ribbons are 80% bootstrapped confidence limits, and vertical red lines indicate spatial regime boundaries for each year.

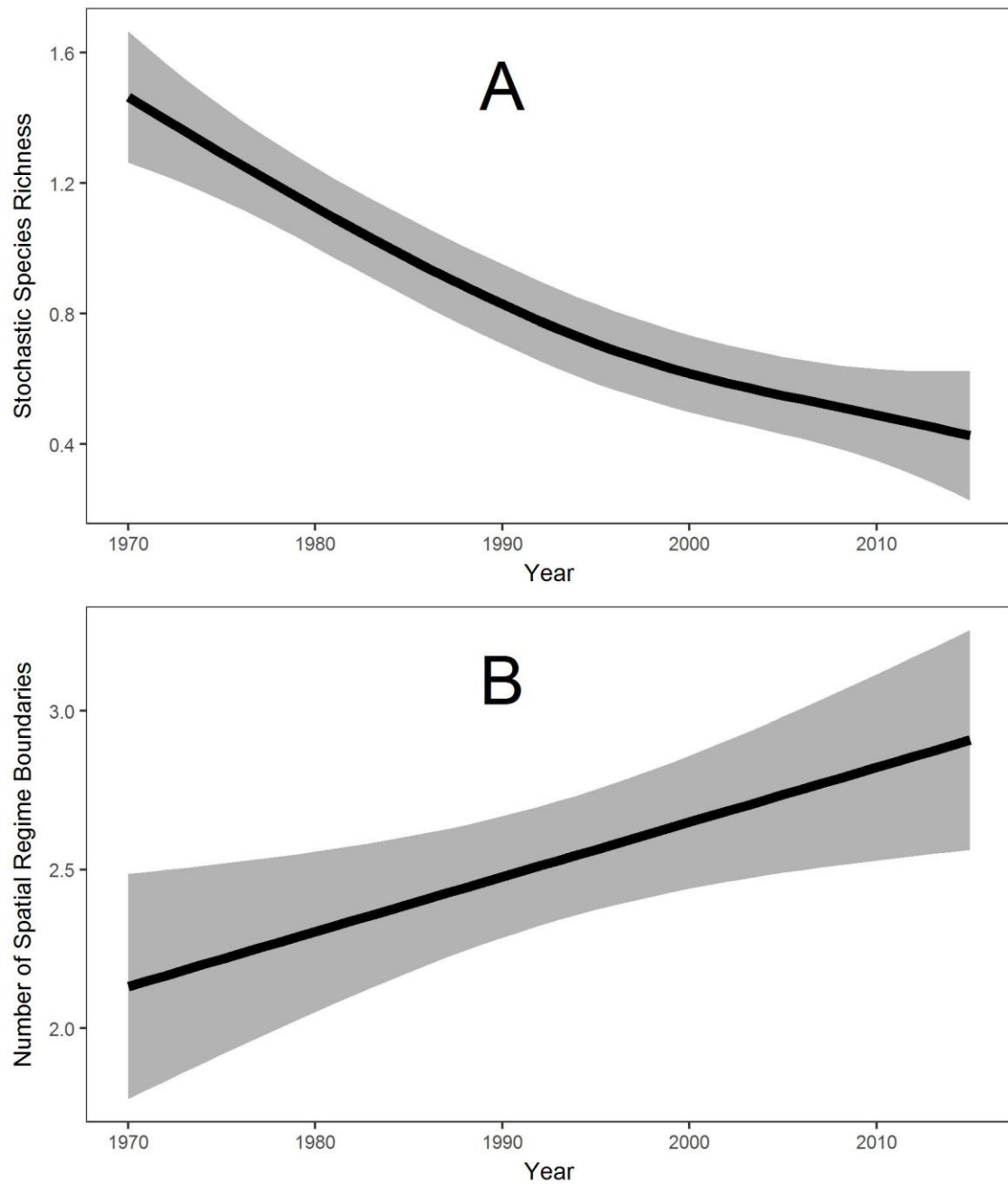


Figure 6.2: Panel A depicts mean species richness of rare bird species (species with spatially stochastic abundance patterns) per North American Breeding Bird Survey route

over a 46-year period along a south-to-north latitudinal gradient in central North America. Panel B depicts number of spatial regime boundaries detected using the breeding bird body mass discontinuities along the same transect over the same time. X-axes show years, black lines are predicted richness values, and gray-shaded ribbons are 80% bootstrapped confidence limits.

CHAPTER 7: CROSS-SCALE RESILIENCE AND COMMUNITY ECOLOGY⁶

ABSTRACT

The related, yet distinct, concepts of ecological stability (e.g., the ability of a system to return to an equilibrium state after a disturbance) and ecological resilience (the capacity of a system to absorb disturbance and reorganize while undergoing change so as to retain essentially the same function and functions) hold potential for predicting community change and collapse-global issues in the Anthropocene. But while key stability metrics such as species richness, turnover, etc. have been well-tested and predictions of stability have received decades of attention, neither the predictions nor metrics of resilience have received the same rigorous testing as stability. For instance, the cross-scale resilience model, a leading operationalization of resilience, provides explicit predictions of how resilience is generated in ecosystems and proposes resilience derives from a combination of diversity of functions within scales and redundancy of functions by species operating at different scales. We use a half-century of sub-continental avian community data aggregated at multiple spatial scales to calculate resilience metrics derived from the cross-scale resilience model and test core assumptions and predictions inherent to

⁶ CPR contributed to conceptualization, programming, data validation, formal analysis, data curation, all writing aspects, visualization, and project administration. DT, DGA, and CRA contributed to conceptualization and writing selected sections.

community persistence and change. Specifically, we ask how cross-scale resilience metrics relate to 1) species richness, 2) species turnover, and 3) community similarity and change. Our results corroborate core resilience theory predictions. We found resilience is related to but distinct from stability: we found low mean cross-correlation between species richness and cross-scale resilience metrics, ranging from $r = 0.16 \pm 0.01$ (cross-scale redundancy; 85% confidence) to $r = 0.63 \pm 0.02$ (cross-scale diversity). Likewise, resilience metrics negatively influenced mean species turnover, but resilience metrics showed little or no association with standard deviation of species turnover. We also demonstrate resilience is weakly related to maintenance of a particular species assemblage: resilience metrics were weak predictors of community similarity over time. Finally, we show shifts in resilience are tied to abrupt shifts in community structure: resilience metrics strongly predicted community change, with shifts in cross-scale redundancy preceding community shifts and shifts in cross-scale diversity synchronizing with community change. Our results begin to distinguish roles of functional redundancy and diversity in community resilience and reemphasize the importance of considering resilience metrics from a multivariate perspective. For resilience theory to progress, it must continue to show itself quantitatively distinct from competing theories, have measurable and interpretable characteristics, and test its assumptions and predictions.

INTRODUCTION

“If there is a worthwhile distinction between resilience and stability it is important that both be measurable.” –Holling 1973

As the Anthropocene progresses, community change and collapse are becoming increasingly common (Folke et al., 2004). The related, yet distinct, concepts of ecological stability (the ability of a system to return to an equilibrium state after a disturbance-also termed “engineering resilience”) and ecological resilience (the capacity of a system to absorb disturbance and reorganize while maintaining essentially similar functions and structures) hold potential for predicting community change and collapse (Angeler & Allen, 2016; Hillebrand et al., 2018; C. S. Holling, 1973). Many stability metrics such as richness, diversity, etc. have been proposed and well-tested, and predictions of stability have received decades of attention, for instance in the decades-long diversity-stability debate (Cardinale et al., 2013; McCann, 2000; Mougi & Kondoh, 2012; Tilman & Downing, 1994; Wagg, Dudenhöffer, Widmer, & Heijden, 2018). But although the pursuit of quantifying resilience has been a long-term pursuit in ecology and multiple metrics have been proposed, neither the predictions nor metrics of resilience have received the same rigorous testing as stability (Baho et al., 2017).

Resilience theory makes key predictions concerning complex, nonlinear, and abruptly shifting system behavior, making it uniquely applicable to Anthropocene issues (L. H. Gunderson, 2000). Resilience theory predicts that a system may fluctuate greatly (have low stability and exhibit non-equilibrium behavior) and have high resilience or conversely fluctuate little and have low resilience (L. H. Gunderson, Allen, & Holling, 2012; C. S. Holling, 1973). And by definition, loss of resilience increases the likelihood of system collapse and regime shifts due to loss of structures, functions, and feedbacks that maintain the current regime (Allen, Gunderson, & Johnson, 2005; Angeler & Allen,

2016). Thus, resilience should be both quantifiably distinct from stability and clearly correspond with community change and collapse (C. S. Holling, 1973; Pimm, 1984; Standish et al., 2014).

In this study, we use a half-century of sub-continental avian community data to calculate resilience metrics derived from the cross-scale resilience model and test these core predictions of resilience theory. Specifically, we ask how cross-scale resilience metrics relate to 1) species richness, 2) species turnover, and 3) community similarity and abrupt shifts. Resilience theory predicts metrics of resilience will weakly correlate with species richness and species turnover (G. Peterson, Allen, & Holling, 1998). It also predicts resilience metrics will weakly correspond with maintenance of a specific species assemblage over time but strongly correspond with measures of community-level change (L. H. Gunderson, 2000).

METHODS

Background on the cross-scale resilience model

The cross-scale resilience model is a leading model for operationalizing and quantifying resilience (G. Peterson et al., 1998; S. M. Sundstrom et al., 2018). It establishes that redundancy and diversity of organism functions across discontinuous scales of resource use in a system confer resilience (G. Peterson et al., 1998). According to this model and the Textural Discontinuity Hypothesis it derives from (C. S. Holling, 1992), redundancy in functions will reduce likelihood of regime shifts, and diversity of functions will increase adaptive capacity. Here, we operationalize the cross-scale resilience model by following the methods of Allen et al. (2005) to calculate resilience metrics. Proposed to

estimate relative resilience of systems, these metrics are calculated by first identifying a biotic community within a system (e.g., an avian forest community, a herpetofauna desert community), determining the discontinuous scale domains at which functions are performed by each species in the biotic community, and finally using functional traits of species across scale domains to estimate functional redundancy and diversity within and across scale domains (Nash et al., 2014). These metrics require census presence/absence data from the community of interest (Allen et al., 2005).

Identifying biotic communities

For biotic community data, we used the North American Breeding Bird Survey (BBS) which estimates bird community composition via yearly roadside avian point-count surveys (Sauer et al., n.d.). Begun in 1966, the BBS is conducted along a series of > 2500 permanent, randomly-distributed routes during the breeding season (Sauer et al., n.d.). We analyzed BBS route data from 1967 - 2014.

We defined avian communities by spatially binning BBS routes according to US Environmental Protection Agency (EPA) ecoregion (Omernik & Griffith, 2014). These ecoregions are spatially hierarchical, meaning that finer-scaled ecoregions are bounded by and nested within larger-scaled ecoregions. Because finer-scale EPA ecoregion boundaries are bounded by USA political boundaries, we only consider BBS routes within the continental United States. To assess differences across scales, we consider avian communities at the three finest scales (Levels II, III, IV).

Calculating cross-scale resilience metrics

We use a discontinuity analysis based on the Gap Rarity Index to identify scale domains by detecting discontinuities in log-ranked organism body masses (Barichievy et al., 2018). For taxa with determinant growth, mean body mass has been shown to reliably differentiate size aggregations and is strongly allometric to the scales at which functions are carried out by organisms (Allen et al., 2006; C. S. Holling, 1992). Because of known negative observation biases for waterfowl and allied families and because water-dwelling avian families' follow different body masses patterns than terrestrial avian families, we removed all species from the Anseriformes, Gaviiformes, Gruiformes, Pelecaniformes, Phaethontiformes, Phoenicopteriformes, Podicipediformes, Procellariiformes, and Suliformes families from the analysis (C. S. Holling, 1992; S. M. Sundstrom, Allen, & Barichievy, 2012). Because Gap Rarity Index tends to overestimate discontinuities in species-poor samples, we removed any route with < 40 species observed (Barichievy et al., 2018; Stow, Allen, & Garmestani, 2007).

We obtained mean body mass estimates for all remaining species from the CRC Handbook of Avian Body Masses (Dunning Jr, 2007). We assigned functional types to each species according to diet and foraging strategies (Ehrlich, Dobkin, & Wheye, 1988). We broke diets into carnivore, herbivore, and omnivore groups, where omnivores are defined as species with approximately even proportions of plant and animal intake (Bouska, 2018). We divided foraging strategies into five groups: water, ground, foliage, bark, and air (S. M. Sundstrom et al., 2012).

We then used body mass aggregations to calculate a number of proposed resilience metrics such as number of body mass aggregations, cross-scale redundancy (the mean number of aggregations containing each functional type), within-scale redundancy (the mean number of species within each functional type in an aggregation), and cross-scale diversity (the mean number of functional types across aggregations) (Allen et al., 2005).

Test 1: Relationship between cross-scale resilience and richness

We assessed degree of correlation between resilience metrics and species richness, a stability metric central to the diversity-stability debate (McCann, 2000). We used cross-correlation to compare species richness with each cross-scale resilience metric (number of body mass aggregations, cross-scale redundancy, within-scale redundancy, cross-scale diversity) for each ecoregion across -5 to 5 lags. That is, we used cross-correlation to determine quantify temporal covariance of richness and resilience metrics, asking if patterns of resilience metrics preceded (back to 5 time steps before) or followed (forward to 5 time steps after) patterns of richness. For each lag, we averaged the absolute values of correlation coefficients across ecoregions.

Test 2: Relationship between cross-scale resilience and turnover

Second, we determined the relationship between cross-scale resilience metrics and species turnover. We calculated relative species turnover (the proportion of the species pool that turns over annually) using the following equation (Diamond, 1969; Wonkka, West, Twidwell, & Rogers, 2017):

$$\text{Turnover}_{t+1} = (U_t + U_{t+1}) / (S_t + S_{t+1})$$

where U_t is the number of species present in the ecoregion at year t that were not present in year $t + 1$; U_{t+1} is the number of species present in the ecoregion at year $t+1$ that were not present in year t ; S_t is the total number of species present in the ecoregion at year t ; and S_{t+1} is the total number of species present in the ecoregion at year $t + 1$. We then developed two linear mixed models: to determine if resilience metrics influenced the magnitude of species turnover, we used the mean of the absolute value of species turnover over time as the response variable, and to determine if resilience metrics influenced the variability of species turnover, we used the standard deviation of species turnover over time as the response variable. For both models, we set mean resilience metrics over time as the predictor variables. We allowed intercepts to vary by hierarchically nested EPA ecoregions (e.g., for level III ecoregions, random effect in R package “lme4” syntax was “(1 | Level I / Level II)”). To minimize collinearity, we calculated variance inflation factors (VIF) and sequentially removed predictor variables (resilience metrics) with the highest VIF until VIF for all variables was ≤ 3 .

Test 3: Relationship between cross-scale resilience and community similarity and abrupt shifts

We first determined the relationship between cross-scale resilience metrics and patterns of community similarity over time. We estimated community similarity over time via the Jaccard index (*sensu* Dornelas et al., 2014); that is, we calculated Jaccard similarity between each year of BBS data for each ecoregion and then used linear regression to

estimate change in community identity over time (i.e., slope). Because the Jaccard index ranges from 0 (complete dissimilarity in species) to 1 (complete similarity in species), a slope of zero indicates no change in community composition over time, and a slope of -1 indicates a complete change in species pool. We then developed linear mixed models, setting the slope of the Jaccard index as the response variable. For predictor variables, we used initial resilience metric values (the chronologically first value for each resilience metric for each ecoregion) and mean resilience metric values (the average of each resilience metric value across the time series for each ecoregion). To account for variance in certainty of Jaccard slope fits, we used $1 / \text{standard error of each Jaccard slope fit}$ as prior weights for linear mixed models. We used the same methods for minimizing collinearity as above.

Second, we determined whether significant temporal shifts in cross-scale resilience metrics synchronized with significant temporal shifts in community structure. We 1) performed detrended correspondence analysis (DCA; “decorana” function from the vegan package in R) on relative abundances of species in each ecoregion over time, 2) extracted the first DCA axis (DCA1) for each year, 3) extracted predicted response values from generalized additive models (GAM) on DCA1 with time (year) as a smoothed predictor for each ecoregion, and 4) determined where community structure significantly changed by first calculating derivatives and 85% confidence limits around the derivatives from the GAM predictions and then locating ranges in the time series where derivative confidence limits did not encompass zero (Simpson, 2018). We located shifts in cross-scale resilience metrics in a similar fashion—by extracting GAM predictions, calculating

derivatives and confidence intervals, and locating ranges where confidence limits did not encompass zero. To test for synchrony between cross-scale resilience metrics and structural community change, we encoded DCA1 and resilience metric time series as binary variables, where either a significant shift (85% confidence limit of derivative did not encompass zero) occurred or did not for each time step (i.e., each year of BBS data). We aggregated significant increases and decreases into an absolute value because both significant increases and decreases in ordinated values (e.g., DCA) could signal regime shifts and higher values, regardless of directionality, are generally hypothesized to confer greater resilience. We set the binary DCA1 variable as the response and binary resilience metrics predictors in a binomial generalized linear mixed model. We checked for collinearity with VIFs.

RESULTS

Relationship between cross-scale resilience and richness

Mean cross-correlation between richness and resilience metrics was low across scales and individual metrics, ranging from $r = 0.16 \pm 0.01$ (cross-scale redundancy at lag -5 at the finest scale) to $r = 0.63 \pm 0.02$ (cross-scale diversity at lag 0 at the finest scale; Figure 7.1). Patterns were consistent across scales: the strongest correlation between richness and all metrics at all scales occurred at lag zero (annually) after which correlation decreased sharply. At the broadest scale (level II), confidence limits show little difference between individual metrics' correlations with richness. At the finer scales (levels III, IV), cross-scale diversity correlated most strongly with richness. Within-scale redundancy showed the second greatest correlation with richness (max $r = 0.50 \pm 0.02$ at level IV, lag

0). Cross-scale redundancy ($r = 0.34 \pm 0.02$ at lag 0) and number of aggregations (0.29 ± 0.02 at lag 0) displayed the weakest correlation with richness at finer scales.

Relationship between cross-scale resilience and turnover

Resilience metrics had significantly negative relationships with mean annual species turnover at all scales, but resilience metrics showed little or no association with standard deviation of annual species turnover (Figure 7.2; Table 7.1). Cross-scale diversity was significant predictor of mean species turnover at the broadest scale and the strongest predictor at the finest scale (-0.027 ± 0.001 and -0.034 ± 0.002 at levels II and IV respectively), and cross-scale diversity was a significant negative predictor of standard deviation in species turnover at the finest scale (-0.004 ± 0.002). Cross-scale redundancy was a significant predictor at all scales, although its strength decreased at finer scales until it was the weakest predictor at the finest scale (-0.018 ± 0.011 , -0.015 ± 0.001 , and -0.0059 ± 0.004 at ecoregion levels II, III, and IV respectively). Cross-scale redundancy also significantly negatively predicted standard deviation in species turnover at the finest scale (-0.005 ± 0.003). Within-scale redundancy was a significant predictor at the middle scale (-0.017 ± 0.006), and number of aggregations was a significant predictor of middling strength at the finest scale (-0.018 ± 0.004).

Relationship between cross-scale resilience and community similarity and abrupt shifts

At the broadest and middle scales (levels II, III), neither initial nor mean resilience metric values significantly predicted changes in community similarity over time (Table 7.2). But at the finest scale (level IV), initial values of cross-scale diversity (0.0002 ± 0.0001) and number of aggregations (0.0002 ± 0.0001) significantly, albeit weakly, predicted reduced

community change (i.e., pushed Jaccard slopes closer to zero—no net community change; Table 7.2).

At all scales, resilience metrics synchronized significantly with abrupt community shifts (Figures 3, 4; Table 7.3). At the broadest scale (level II), cross-scale diversity (1.0 ± 0.53) and cross-scale redundancy (0.67 ± 0.55) synchronized with community change (Figure 7.4). At the middle scale (level III), number of aggregations (0.21 ± 0.20) and within-scale redundancy (0.62 ± 0.20) exhibited synchrony with community change (Figure 7.3). However, cross-scale redundancy exhibited asynchrony (i.e., a negative model coefficient; -0.3 ± 0.19) with community change (Figure 7.3, 4). And at the finest scale (level IV), all resilience metrics synchronized with abrupt community shifts: cross-scale diversity showed the strongest synchrony (0.58 ± 0.08 ; Figure 7.3), and number of aggregations showed the weakest synchrony (0.11 ± 0.09).

DISCUSSION

Using a half-century of subcontinental community data, we provide quantitative support for core predictions of resilience theory. We also provide interpretability for cross-scale resilience metrics in a community ecology context: we distinguish the roles of functional redundancy and diversity in maintaining community similarity and change (G. Peterson et al., 1998; Walker, Kinzig, & Langridge, 1999). Per Holling's original call in his seminal manuscript on resilience theory (C. S. Holling, 1973), we found resilience is related to but distinct from stability. Importantly, our results also distinguish ecological resilience from allied concepts such as engineering resilience, “bounce-back” time to equilibrium, resistance, and elasticity (L. H. Gunderson, 2000; Pimm, 1984; Standish et

al., 2014). Specifically, we found resilience is weakly related to maintenance of a particular species assemblage. But at the same time, shifts in resilience are strongly related to abrupt community shifts.

Our results reaffirm the importance of avoiding the conflation of ecological resilience and ecological stability. At its core, stability theory predicts a particular community composition (e.g., higher species richness) will reduce variance in system functionality but makes no assertions concerning alternative states (Allan et al., 2011; Cardinale et al., 2013; Tilman, 1996; Wagg et al., 2018). Additionally, stability typically does not consider ecological complexity features, such as spatial and temporal scaling structures, thresholds and alternative regimes, in resilience metrics while those features are not accounted for in stability measures (Baho et al., 2017). In contrast, resilience theory predicts resilient systems may exhibit wide ranges of variance, community composition will be dynamic and adaptive, and scaling patterns of functional redundancy and diversity within communities (instead of particular community compositions) will determine the ability of a system to remain within one of multiple alternative regimes (Allen, Angeler, Garmestani, Gunderson, & Holling, 2014; Chillo, Anand, & Ojeda, 2011; G. Peterson et al., 1998; S. M. Sundstrom et al., 2018). Our results support these core differences between stability versus resilience: resilience metrics had low degrees of correlation with species richness. That is, greater richness did not necessarily beget greater resilience-which contrasts with a pervasive conflation of richness (a key metric in diversity-stability relationships) and resilience (Bellwood & Hughes, 2001; J. Fischer et al., 2007; Oliver et al., 2015; Standish et al., 2014). As expected, cross-scale diversity

exhibited the highest correlation with richness, although its correlation was much less than typical cutoffs for collinearity. Cross-scale resilience metrics also did not predict variability in community composition (standard deviation in species turnover) except weakly at the finest scale.

Similarly, resilience theory predicts systems with higher resilience will be more likely to retain similar structures and functions over time, but unlike stability, resilience theory makes few predictions on the maintenance of a particular species assemblage (Allen & Holling, 2010; Bellwood & Hughes, 2001; L. H. Gunderson, 2000). We support this premise. Cross-scale resilience metrics did not strongly associate with maintenance of a particular group of species. Instead, resilience metrics predicted maintenance of overall community structure per their synchrony with abrupt community shifts across scales. That is, resilience metrics predicted significant abrupt community shifts but not community similarity over time. However, higher resilience metrics did weakly predict maintenance of community composition over time as well as predicting reduced mean species turnover which still supports a connection between species composition and resilience.

The cross-scale resilience model differentiates the roles of functional redundancy and functional diversity, and we corroborate this (Bellwood & Hughes, 2001; Elmqvist et al., 2003; Nash, Graham, Jennings, Wilson, & Bellwood, 2016; G. Peterson et al., 1998). For instance, the model predicts losses in critical functions across scaling domains will increase the propensity for ecological regime shifts; but more specifically, redundancy is expected to confer resilience via response diversity (Elmqvist et al., 2003; Walker et al.,

1999), while diversity confers resilience via ability to produce and adapt to novelty (Allen & Holling, 2010; L. H. Gunderson & Holling, 2002). And indeed, we show shifts in functional redundancy across scales (cross-scale redundancy) were asynchronous with community-level change, whereas shifts in functional diversity across scales (cross-scale diversity) were synchronous with abrupt community shifts. Thus, tracking changes in functional redundancy could determine system propensity for regime shifts, whereas tracking functional diversity could identify periods of reorganization during a disturbance that could result in a regime shift.

Because resilience is an emergent property of complex systems, no single metric can encapsulate it (Angeler & Allen, 2016). The peril of developing resilience metrics is reliance on one or a few to measure a given property of interest. For example, within the stability literature, the diversity-stability debate has long been buffeted by waves of interest in one metric (e.g., species richness) or another (functional diversity, phylogenetic diversity, evenness, etc.) as well as conflicting results from the same metric (Hillebrand et al., 2018; Ives & Carpenter, 2007; McCann, 2000). Likewise, within resilience literature, this has played out in the search for univariate generic early warning signals of regime shifts (Burthe et al., 2016; Clements, Drake, Griffiths, & Ozgul, 2015; Van Nes & Scheffer, 2007), specific distance-to-thresholds for a specified context (i.e. the resilience of what to what) (Carpenter, Walker, Anderies, & Abel, 2001; Groffman et al., 2006). In contrast, the cross-scale resilience model and its metrics require and assume simultaneous consideration of multiple metrics to quantify resilience (Allen et al., 2005; Angeler & Allen, 2016; S. M. Sundstrom & Allen, 2014; S. M.

Sundstrom et al., 2018). We show that individual resilience metrics varied in their relationships with tested stability and abrupt community shifts metrics, meaning each metric reflects unique aspects of system resilience. Thus, our results support considering metrics of resilience from a multivariate perspective.

For resilience theory to progress, it must have measurable and interpretable characteristics. For instance, although we demonstrate the ability of resilience metrics to compare changes in a system's resilience over time, how to compare relative resilience between systems remains unclear. Also, it is not obvious that a system with more body mass aggregations is more resilient than a system with fewer (Allen et al., 2005) or what increases versus decreases in resilience metrics mean for propensity toward regime shifts. This may be a result of the present "relative" nature of resilience metric units. However, the clarity of signal in resilience metrics that we demonstrate (with noisy data spanning half a century and much of a continent) suggest comparable patterns exist, and comparisons can improve if measurements over time provide refined pictures of system resilience (Angeler & Allen, 2016; Baho et al., 2017). This bodes well for the usefulness of resilience metrics in the Anthropocene, where the need for understanding system resilience to change and collapse is only increasing.

LITERATURE CITED

Allan, E., Weisser, W., Weigelt, A., Roscher, C., Fischer, M., & Hillebrand, H. (2011).

More diverse plant communities have higher functioning over time due to turnover in complementary dominant species. *Proceedings of the National Academy of Sciences*, 108(41), 17034–17039.

Allen, C. R., & Holling, C. (2010). Novelty, adaptive capacity, and resilience. *Ecology and Society*, 15(3).

Allen, C. R., Angeler, D. G., Garmestani, A. S., Gunderson, L. H., & Holling, C. S. (2014). Panarchy: Theory and application. *Ecosystems*, 17(4), 578–589.

Allen, C. R., Garmestani, A., Havlicek, T., Marquet, P. A., Peterson, G., Restrepo, C., ... Weeks, B. (2006). Patterns in body mass distributions: Sifting among alternative hypotheses. *Ecology Letters*, 9(5), 630–643.

Allen, C. R., Gunderson, L., & Johnson, A. (2005). The use of discontinuities and functional groups to assess relative resilience in complex systems. *Ecosystems*, 8(8), 958.

Angeler, D. G., & Allen, C. R. (2016). Quantifying resilience. *Journal of Applied Ecology*, 53(3), 617–624.

Baho, D. L., Allen, C. R., Garmestani, A., Fried-Petersen, H., Renes, S. E., Gunderson, L., & Angeler, D. G. (2017). A quantitative framework for assessing ecological resilience. *Ecology and Society*, 22(3).

- Barichievsky, C., Angeler, D. G., Eason, T., Garmestani, A. S., Nash, K. L., Stow, C. A., ... Allen, C. R. (2018). A method to detect discontinuities in census data. *Ecology and Evolution*, 8(19), 9614–9623.
- Bellwood, D. R., & Hughes, T. P. (2001). Regional-scale assembly rules and biodiversity of coral reefs. *Science*, 292(5521), 1532–1535.
- Bouska, K. L. (2018). Discontinuities and functional resilience of large river fish assemblages. *Ecosphere*, 9(7), e02351.
- Burthe, S. J., Henrys, P. A., Mackay, E. B., Spears, B. M., Campbell, R., Carvalho, L., ... others. (2016). Do early warning indicators consistently predict nonlinear change in long-term ecological data? *Journal of Applied Ecology*, 53(3), 666–676.
- Cardinale, B. J., Gross, K., Fritschie, K., Flombaum, P., Fox, J. W., Rixen, C., ... Wilsey, B. J. (2013). Biodiversity simultaneously enhances the production and stability of community biomass, but the effects are independent. *Ecology*, 94(8), 1697–1707.
- Carpenter, S., Walker, B., Anderies, J. M., & Abel, N. (2001). From metaphor to measurement: Resilience of what to what? *Ecosystems*, 4(8), 765–781.
- Chillo, V., Anand, M., & Ojeda, R. A. (2011). Assessing the use of functional diversity as a measure of ecological resilience in arid rangelands. *Ecosystems*, 14(7), 1168–1177.

- Clements, C. F., Drake, J. M., Griffiths, J. I., & Ozgul, A. (2015). Factors influencing the detectability of early warning signals of population collapse. *The American Naturalist*, 186(1), 50–58.
- Diamond, J. M. (1969). Avifaunal equilibria and species turnover rates on the Channel Islands of California. *Proceedings of the National Academy of Sciences*, 64(1), 57–63.
- Dornelas, M., Gotelli, N. J., McGill, B., Shimadzu, H., Moyes, F., Sievers, C., & Magurran, A. E. (2014). Assemblage time series reveal biodiversity change but not systematic loss. *Science*, 344(6181), 296–299.
- Dunning Jr, J. B. (2007). *CRC handbook of avian body masses*. CRC press.
- Ehrlich, P., Dobkin, D. S., & Wheye, D. (1988). *Birder's handbook*. Simon; Schuster.
- Elmqvist, T., Folke, C., Nyström, M., Peterson, G., Bengtsson, J., Walker, B., & Norberg, J. (2003). Response diversity, ecosystem change, and resilience. *Frontiers in Ecology and the Environment*, 1(9), 488–494.
- Fischer, J., Lindenmayer, D., Blomberg, S. P., Montague-Drake, R., Felton, A., & Stein, J. (2007). Functional richness and relative resilience of bird communities in regions with different land use intensities. *Ecosystems*, 10(6), 964–974.
- Folke, C., Carpenter, S., Walker, B., Scheffer, M., Elmqvist, T., Gunderson, L., & Holling, C. S. (2004). Regime shifts, resilience, and biodiversity in ecosystem management. *Annu. Rev. Ecol. Evol. Syst.*, 35, 557–581.

- Groffman, P. M., Baron, J. S., Blett, T., Gold, A. J., Goodman, I., Gunderson, L. H., ... others. (2006). Ecological thresholds: The key to successful environmental management or an important concept with no practical application? *Ecosystems*, 9(1), 1–13.
- Gunderson, L. H. (2000). Ecological resilience—in theory and application. *Annual Review of Ecology and Systematics*, 31(1), 425–439.
- Gunderson, L. H., & Holling, C. S. (2002). *Panarchy: Understanding transformations in systems of humans and nature*. Island Press, Washington, DC.
- Gunderson, L. H., Allen, C. R., & Holling, C. S. (2012). *Foundations of ecological resilience*. Island Press.
- Hillebrand, H., Langenheder, S., Lebet, K., Lindström, E., Östman, Ö., & Striebel, M. (2018). Decomposing multiple dimensions of stability in global change experiments. *Ecology Letters*, 21(1), 21–30.
- Holling, C. S. (1973). Resilience and stability of ecological systems. *Annual Review of Ecology and Systematics*, 4(1), 1–23.
- Holling, C. S. (1992). Cross-scale morphology, geometry, and dynamics of ecosystems. *Ecological Monographs*, 62(4), 447–502.
- Ives, A. R., & Carpenter, S. R. (2007). Stability and diversity of ecosystems. *Science*, 317(5834), 58–62.
- McCann, K. S. (2000). The diversity–stability debate. *Nature*, 405(6783), 228.

- Mougi, A., & Kondoh, M. (2012). Diversity of interaction types and ecological community stability. *Science*, 337(6092), 349–351.
- Nash, K. L., Allen, C. R., Angeler, D. G., Barichievy, C., Eason, T., Garmestani, A. S., ... others. (2014). Discontinuities, cross-scale patterns, and the organization of ecosystems. *Ecology*, 95(3), 654–667.
- Nash, K. L., Graham, N. A., Jennings, S., Wilson, S. K., & Bellwood, D. R. (2016). Herbivore cross-scale redundancy supports response diversity and promotes coral reef resilience. *Journal of Applied Ecology*, 53(3), 646–655.
- Oliver, T. H., Heard, M. S., Isaac, N. J., Roy, D. B., Procter, D., Eigenbrod, F., ... others. (2015). Biodiversity and resilience of ecosystem functions. *Trends in Ecology & Evolution*, 30(11), 673–684.
- Omernik, J. M., & Griffith, G. E. (2014). Ecoregions of the conterminous united states: Evolution of a hierarchical spatial framework. *Environmental Management*, 54(6), 1249–1266.
- Peterson, G., Allen, C. R., & Holling, C. S. (1998). Ecological resilience, biodiversity, and scale. *Ecosystems*, 1(1), 6–18.
- Pimm, S. L. (1984). The complexity and stability of ecosystems. *Nature*, 307(5949), 321.
- Sauer, J. R., Niven, D. K., Hines, J. E., Ziolkowski, D. J., Pardieck, K. L., Fallon, J. E., & Link, W. A. (n.d.). “The North American Breeding Bird Survey, Results and

- Analysis 1966 - 2015” (Version 2.07.2017 USGS Patuxent Wildlife Research Center, Laurel, MD, 2017. Retrieved from <https://www.pwrc.usgs.gov/bbs/>
- Simpson, G. L. (2018). Modeling palaeoecological time series using generalized additive models. *bioRxiv*, 322248.
- Standish, R. J., Hobbs, R. J., Mayfield, M. M., Bestelmeyer, B. T., Suding, K. N., Battaglia, L. L., ... others. (2014). Resilience in ecology: Abstraction, distraction, or where the action is? *Biological Conservation*, 177, 43–51.
- Stow, C., Allen, C. R., & Garmestani, A. S. (2007). Evaluating discontinuities in complex systems: Toward quantitative measures of resilience. *Ecology and Society*, 12(1).
- Sundstrom, S. M., & Allen, C. R. (2014). Complexity versus certainty in understanding species’ declines. *Diversity and Distributions*, 20(3), 344–355.
- Sundstrom, S. M., Allen, C. R., & Barichievy, C. (2012). Species, functional groups, and thresholds in ecological resilience. *Conservation Biology*, 26(2), 305–314.
- Sundstrom, S. M., Angeler, D. G., Barichievy, C., Eason, T., Garmestani, A., Gunderson, L., ... others. (2018). The distribution and role of functional abundance in cross-scale resilience. *Ecology*, 99(11), 2421–2432.
- Tilman, D. (1996). Biodiversity: Population versus ecosystem stability. *Ecology*, 77(2), 350–363.
- Tilman, D., & Downing, J. A. (1994). Biodiversity and stability in grasslands. *Nature*, 367(6461), 363.

- Van Nes, E. H., & Scheffer, M. (2007). Slow recovery from perturbations as a generic indicator of a nearby catastrophic shift. *The American Naturalist*, 169(6), 738–747.
- Wagg, C., Dudenhöffer, J.-H., Widmer, F., & Heijden, M. G. van der. (2018). Linking diversity, synchrony and stability in soil microbial communities. *Functional Ecology*, 32(5), 1280–1292.
- Walker, B., Kinzig, A., & Langridge, J. (1999). Plant attribute diversity, resilience, and ecosystem function: The nature and significance of dominant and minor species. *Ecosystems*, 2(2), 95–113.
- Wonkka, C. L., West, J. B., Twidwell, D., & Rogers, W. E. (2017). Grass mortality and turnover following core rangeland restoration practices. *Rangeland Ecology & Management*, 70(3), 290–300.

TABLES

Table 7. 1: Results from linear mixed models testing the relationship between mean annual species turnover and mean resilience metrics (Response = Mean) and the standard deviation (Response = SD) of annual species turnover and mean resilience metrics at multiple hierarchical scales. Species turnover and resilience metrics were calculated from avian community data recorded at North American Breeding Bird Survey routes from 1966 - 2014 aggregated by US Environmental Protection Agency ecoregions. Columns indicate ecoregion level, response type, variable name, coefficient estimate, standard error of coefficient estimate, and t-value estimate for coefficient.

Ecoregion Level	Response	Variable	Estimate	SE	t-value
LII	Mean	Intercept	0.079	0.0092	8.5
LII	Mean	Cross-scale Redundancy	-0.018	0.0073	-2.5
LII	Mean	Cross-scale Diversity	-0.027	0.0065	-4.1
LIII	Mean	Intercept	0.11	0.0077	14
LIII	Mean	Within-scale Redundancy	-0.017	0.0042	-4
LIII	Mean	Cross-scale Redundancy	-0.015	0.0037	-4.1
LIV	Mean	Intercept	0.15	0.0056	26
LIV	Mean	Cross-scale Redundancy	-0.0059	0.0026	-2.3
LIV	Mean	Number of Aggregations	-0.018	0.003	-5.9
LIV	Mean	Cross-scale Diversity	-0.034	0.0021	-16
LII	SD	Intercept	0.053	0.015	3.4
LII	SD	Cross-scale Redundancy	0.011	0.0093	1.2
LII	SD	Cross-scale Diversity	-0.0032	0.0088	-0.36
LIII	SD	Intercept	0.046	0.0058	8
LIII	SD	Within-scale Redundancy	-0.0025	0.0047	-0.54

LIII	SD	Cross-scale Redundancy	-4.00E-05	0.0042	-0.0086
LIV	SD	Intercept	0.052	0.0037	14
LIV	SD	Cross-scale Redundancy	-0.0049	0.0017	-2.8
LIV	SD	Number of Aggregations	0.0017	0.002	0.88
LIV	SD	Cross-scale Diversity	-0.0043	0.0014	-3

Table 7. 2: Results from linear mixed models testing the relationship between community compositional change over time (slope of Jaccard index over time) and initial and mean resilience metrics at multiple hierarchical scales. Jaccard index and resilience metrics were calculated from avian community data recorded at North American Breeding Bird Survey routes from 1966 - 2014 aggregated by US Environmental Protection Agency ecoregions. Columns indicate ecoregion level, variable name, coefficient estimate, standard error of coefficient estimate, and t-value estimate for coefficient.

Ecoregion Level	Variable	Estimate	SE	t-value
LII	Intercept	-0.0019	0.00039	-4.8
LII	Within Red Initial	-0.00043	0.00094	-0.46
LII	Cross Red Mean	3.00E-05	0.00038	0.092
LII	Cross Red Initial	-7.00E-05	0.00042	-0.16
LIII	Intercept	-0.0021	0.00015	-14
LIII	Within Red Mean	-0.00014	0.00021	-0.66
LIII	Cross Red Mean	0.00018	0.00021	0.86
LIII	Cross Red Initial	0.00015	0.00016	0.93
LIII	Cross Div Initial	0.00014	0.00012	1.2
LIV	Intercept	-0.0022	0.00015	-14
LIV	Num Aggs Mean	-1.00E-05	0.00015	-0.064
LIV	Num Aggs Initial	0.00016	1.00E-04	1.5
LIV	Cross Red Mean	0	0.00015	0.029
LIV	Cross Red Initial	-4.00E-05	9.80E-05	-0.45
LIV	Cross Div Initial	0.00024	8.60E-05	2.8

Notes: *Within Red Initial* = Within-scale Redundancy initial metric value; *Cross Red Mean* = Cross-scale Redundancy mean metric value; *Cross Red Initial* = Cross-scale Redundancy initial metric value; *Within Red Mean* = Within-scale Redundancy mean metric value; *Cross Div Initial* = Within-scale Diversity

initial metric value; Num Aggs Mean = Number of Body Mass Aggregation mean value; Num Aggs Inital = Number of Body Mass Aggregation initial value.

Table 7. 3: Results from binomial generalized linear mixed models testing synchrony between regime shifts (significant changes in detrended correspondence analysis axis-1 [DCA1]) and resilience metrics at multiple hierarchical scales. DCA1 and resilience metrics were calculated from avian community data recorded at North American Breeding Bird Survey routes from 1966 - 2014 aggregated by US Environmental Protection Agency ecoregions. Columns indicate ecoregion level, variable name, coefficient estimate, standard error of coefficient estimate, z-value estimate for coefficient, and P-value estimate for coefficient.

Ecoregion Level	Variable	Estimate	SE	z-value	P-value
LII	Intercept	2.2	0.8	2.8	0.0052
LII	Number of Aggregations	0.045	0.42	0.11	0.91
LII	Cross-scale Redundancy	0.67	0.38	1.8	0.075
LII	Cross-scale Diversity	1	0.37	2.8	0.0048
LII	Within-scale Redundancy	0.3	0.35	0.84	0.4
LIII	Intercept	1.6	0.26	6.1	1.20E-09
LIII	Number of Aggregations	0.21	0.14	1.5	0.14
LIII	Cross-scale Redundancy	-0.3	0.13	-2.3	0.023
LIII	Cross-scale Diversity	0.14	0.13	1	0.3
LIII	Within-scale Redundancy	0.62	0.14	4.6	5.00E-06
LIV	Intercept	0.66	0.15	4.4	1.10E-05
LIV	Number of Aggregations	0.11	0.061	1.8	0.08
LIV	Cross-scale Redundancy	0.35	0.057	6.2	6.70E-10
LIV	Cross-scale Diversity	0.58	0.051	11	1.10E-29
LIV	Within-scale Redundancy	0.23	0.054	4.3	1.90E-05

FIGURES

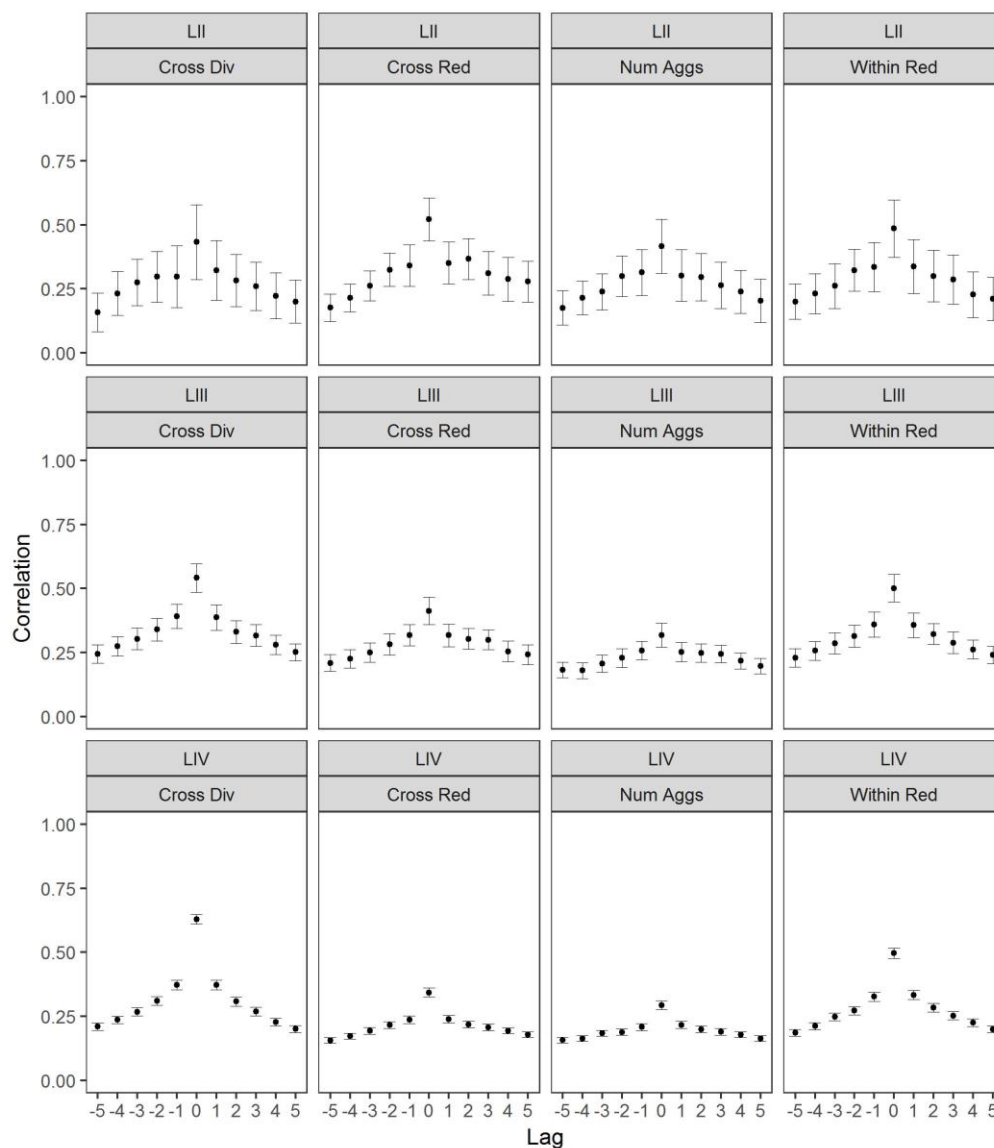


Figure 7. 1: Mean cross-correlation estimates and 85% confidence limits between species richness and cross-scale resilience metrics at multiple hierarchical scales. Y-axis indicates degree of correlation (r), and x-axis indicates lags ranging from -5 to 5, where lag 0 indicates annual correlation. Richness and resilience metrics were calculated from avian community data recorded at North American Breeding Bird Survey routes from

1966 - 2014 aggregated by US Environmental Protection Agency ecoregions. Ecoregions range from broad (Level II) to fine (Level IV). *Note: Cross Div = cross-scale diversity; Cross Red = cross-scale redundancy; Num Aggs = number of body mass aggregations; Within Red = within-scale redundancy.*

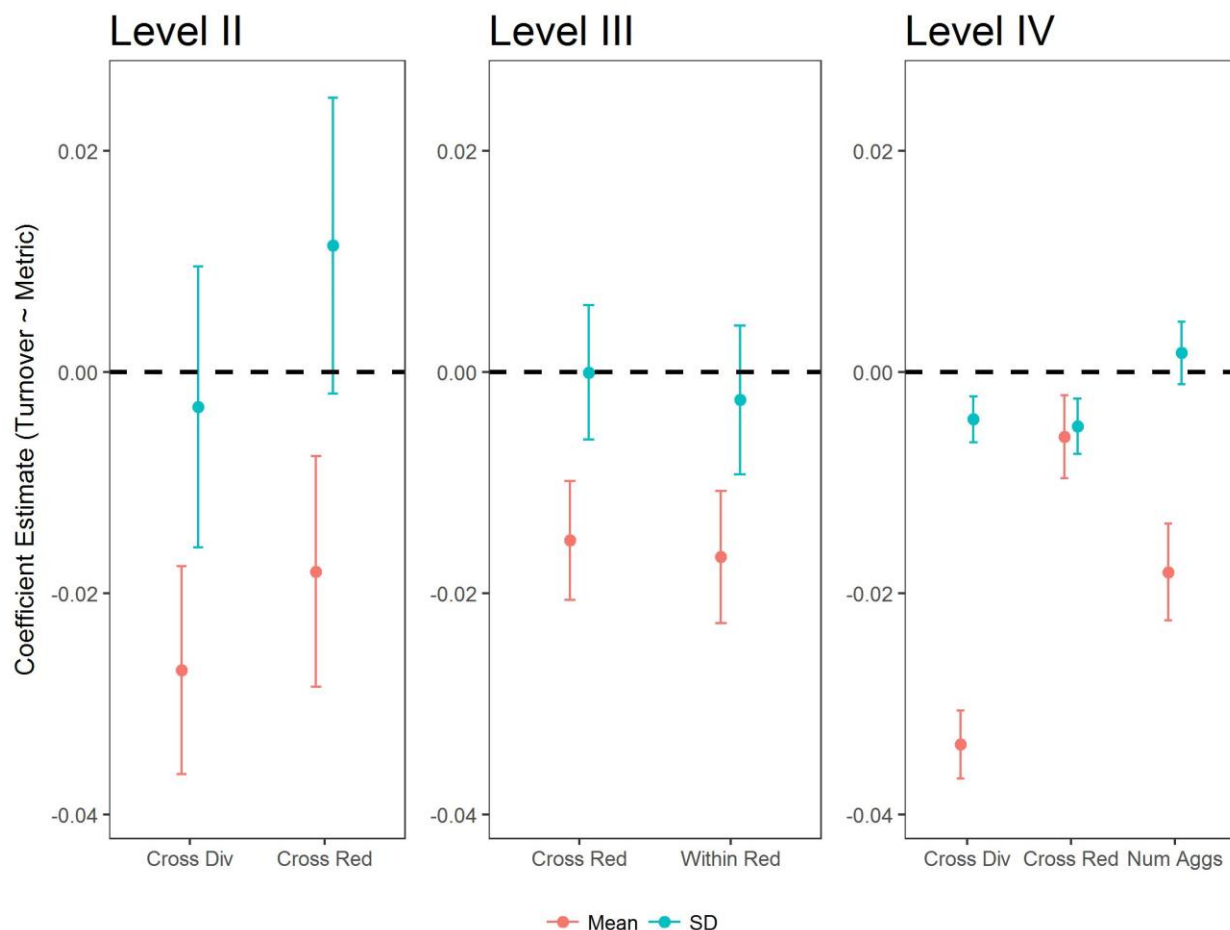


Figure 7. 2: Coefficient estimates and 85% confidence limits from linear mixed models testing the relationship between mean annual species turnover and mean resilience metrics (red dots) and the standard deviation (SD) of annual species turnover and mean resilience metrics (blue dots) at multiple hierarchical scales. Species turnover and resilience metrics were calculated from avian community data recorded at North American Breeding Bird Survey routes from 1966 - 2014 aggregated by US Environmental Protection Agency ecoregions. Ecoregions range from broad (Level II) to fine (Level IV). *Note: Cross Div = cross-scale diversity; Cross Red = cross-scale*

redundancy; Num Aggs = number of body mass aggregations; Within Red = within-scale redundancy.

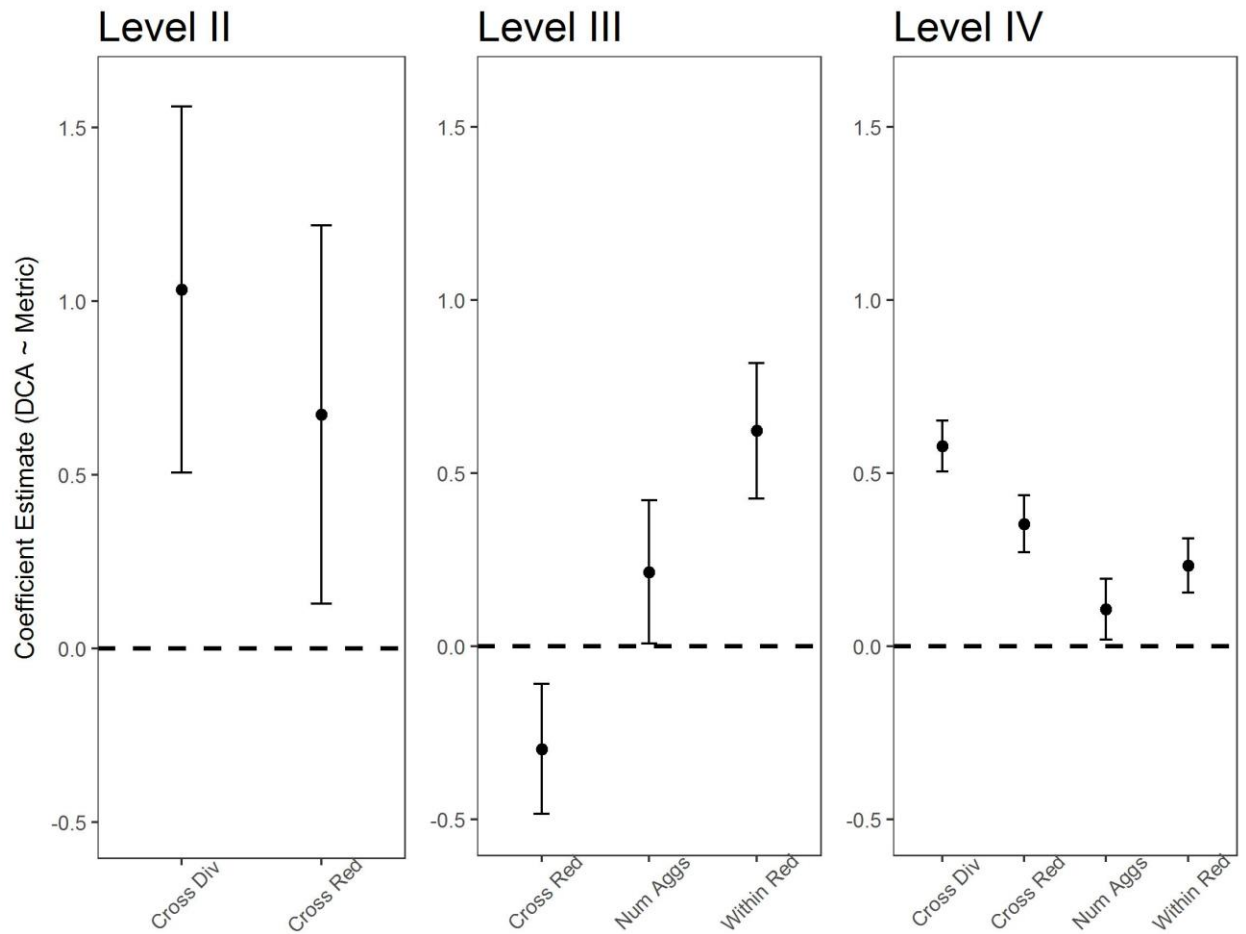


Figure 7. 3: Coefficient estimates and 85% confidence limits from binomial generalized linear mixed models testing synchrony between abrupt community shifts and resilience metrics at multiple hierarchical scales. Synchrony is defined as simultaneous occurrence of regime shifts (i.e., significant change in first axis of Detrended Correspondence Analysis) and significant shifts in resilience metrics. Abrupt community shifts and resilience metrics were derived from avian community data recorded at North American Breeding Bird Survey routes from 1966 - 2014 aggregated by US Environmental Protection Agency ecoregions. Ecoregions range from broad (Level II) to fine (Level IV).

Note: DCA = first axis of detrended correspondence analysis; Cross Div = cross-scale diversity; Cross Red = cross-scale redundancy; Num Aggs = number of body mass aggregations; Within Red = within-scale redundancy.

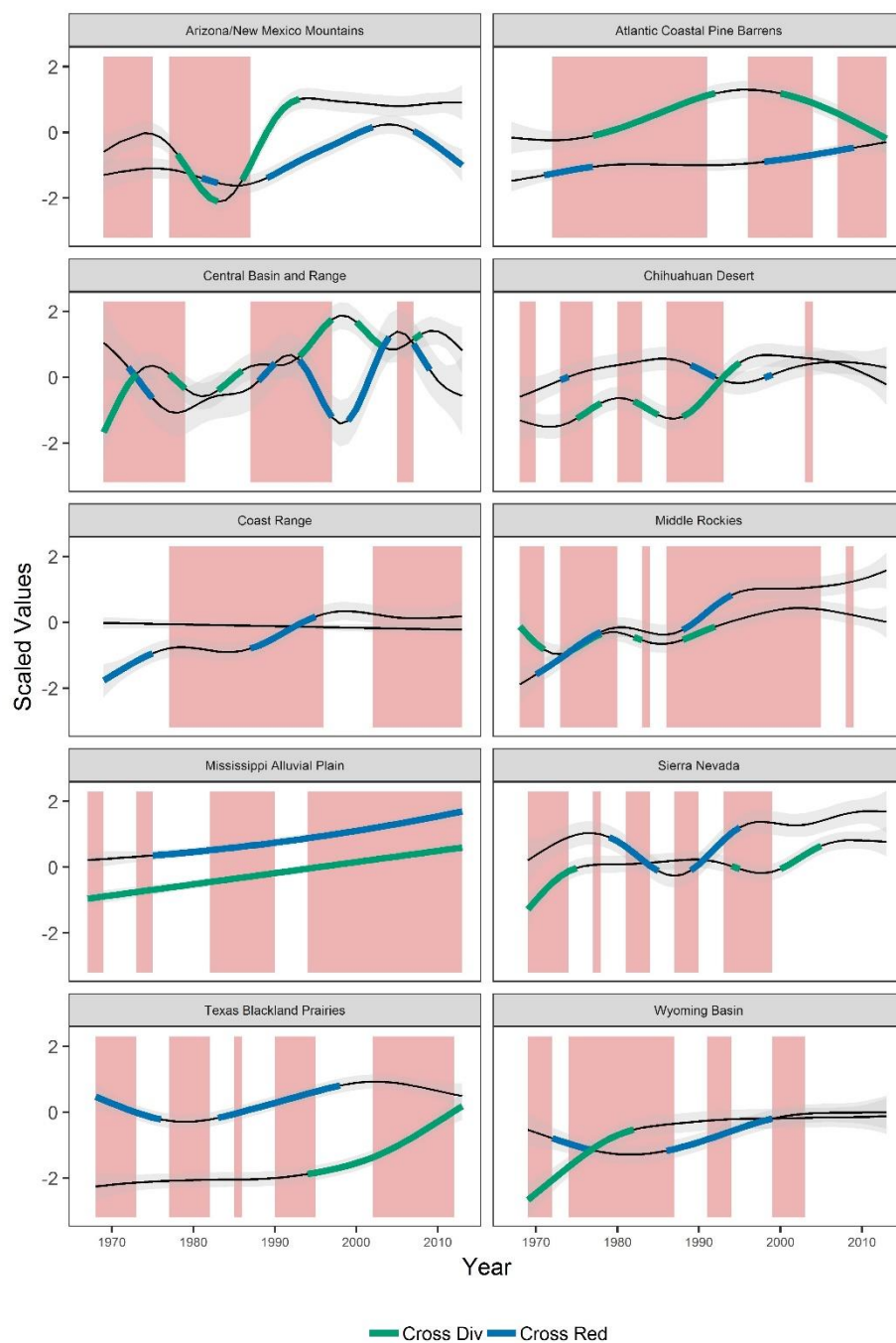


Figure 7. 4: Comparison of synchrony between periods of significant avian abrupt community shifts (red blocks) and periods of significant changes in cross-scale resilience metrics across a sample of Level III Environmental Protection Agency ecoregions from

1966 - 2014. Black lines indicate predicted values from GAMs, grey shading indicates pointwise 85% confidence limits around predictions, and colored sections indicate regions of significant change in time series (where simulated confidence limits of derivatives from GAMs did not encompass zero). *Note: Cross Div = cross-scale diversity; Cross Red = cross-scale redundancy.*

CHAPTER 8: A TEST OF THE SPATIAL PREDICTION OF THE CROSS-SCALE RESILIENCE MODEL⁷

ABSTRACT

The cross-scale resilience model predicts that loss of resource aggregations at particular scale domains will result in loss of functional redundancy across scales and functional diversity within scales; that is, a loss of resilience. We test this prediction in a spatial context by comparing abundance of avian taxa within scale domains to level of resource aggregation loss resulting from oil and gas development in rangeland-dominated ecoregions of central North America. We used discontinuity analysis to identify scale domains via avian body mass and then used generalized additive mixed models to determine if responses of scale domain abundances were non-random according to scale domain and scale of disturbance (i.e., spatial resource loss by oil and gas development). We identified as many 28 scale domains in a single ecoregion, but scale domain responses fell non-randomly into four broad groups of scale domains. The smallest scale domains (3 - 30 g) responded negatively at intermediate spatial scales of disturbance, the second smallest group of scale domains (33 - 90 g) responded positively to disturbance at

⁷ CPR contributed to conceptualization, programming, data validation, formal analysis, data curation, all writing aspects, visualization, and project administration. DT and CRA contributed to conceptualization. BWA contributed to data curation and formal analysis.

small spatial scales, the third largest group (247 - 1191 g) responded negatively to disturbance at small spatial scales, and we detected no response to disturbance by abundances of the largest scale domains. We also found clear evidence that oil and gas development led to loss of ecological resilience in rangeland systems: declining scale domains contained 33% of all carnivore species at meso-scale domains and 77% of all omnivore species at the smallest scale domains. Theory indicates that a directional trend in total abundance within a scale domain means changes to the scales at which resources are aggregated in the system and thus potentially a regime shift. And indeed, we detected directional trends in total abundance within multiple scale domains resulting from resource loss at specific spatial scales due to oil and gas development. Our results support the spatial prediction of the cross-scale resilience model and provide a foundation for harnessing the predictive power of the model for contextualizing the “of what, to what” concept of resilience in hierarchical spatial scale domains.

INTRODUCTION

Ecological resilience theory predicts that loss of functional redundancy and diversity within and across scales reduces resilience and increases system vulnerability to regime shifts (Bellwood, Hoey, & Choat, 2003; C. S. Holling, 1973; B. Walker, Kinzig, & Langridge, 1999). The cross-scale resilience model operationalizes these predictions by positing ecological systems are hierarchically organized into discontinuous scale domains, and resilience is maintained by functional redundancy across scales and functional diversity within scales (C. R. Allen, Gunderson, & Johnson, 2005; G. Peterson, Allen, & Holling, 1998). For instance, a forest system may contain multiple

granivorous taxa that perform seed dispersal functions (Nash et al., 2014a). The smallest of these taxa likely operate at small, rapid scales, taking advantage of local resources, and thus dispersing seeds at local scales. Larger taxa will then operate at progressively larger scales, use larger resource aggregations, and perform seed dispersal functions at broader spatiotemporal scales. The repetition of the seed dispersal function across scales is then a factor that confers resilience (Nash, Graham, Jennings, Wilson, & Bellwood, 2016; Shana M Sundstrom et al., 2018). Diversity of function within scales provides response diversity to disturbance as well the ability to adapt to novel disturbances (Allen & Holling, 2010; Elmqvist et al., 2003).

Embedded in these predictions is critical assumption: taxa operating at a given scale domain require resources to be available, or aggregated, at that scale (Nash et al., 2014b; G. Peterson et al., 1998). It follows that loss of resource aggregations at that particular scale domain will cause declines in abundances or, in the most drastic case, extinctions of species that take advantage of resources at that scale domain (G. Peterson et al., 1998; Shana M Sundstrom et al., 2018). For instance, loss of resource aggregations at large scales may adversely affect species that operate at large scales (Szabo & Meszéna, 2006). Therefore, the cross-scale resilience model predicts that loss of resource aggregations at particular scale domains will result in loss of functional redundancy across scales and functional diversity within scales; that is, a loss of resilience (Angeler & Allen, 2016; G. Peterson et al., 1998). Further, directional shifts in species abundances within scale domains (and thus the resource aggregations that rely on) are predicted to lead to or signal regime shifts (Shana M Sundstrom et al., 2018).

Testing this spatial prediction of the cross-scale resilience model could help realize the hypothesized predictive power of the model. If taxa respond non-randomly to loss of resources according to their scale domains, system resilience to disturbances at specific scales can be empirically understood (Allen & Holling, 2008; Bouska, 2018; Wardwell, Allen, Peterson, & Tyre, 2008). For instance, the “of what, to what” concept for quantifying resilience could be contextualized by spatiotemporal scale domain (Angeler et al., 2016; Carpenter, Walker, Anderies, & Abel, 2001). This would enable managers to monitor for changes in taxa abundance across scales, pinpoint the scales that a given disturbance affects, and understand how cross-scale functional redundancy and diversity (i.e., system resilience) will respond (Angeler et al., 2016; Nash et al., 2016; B. Walker, 1992).

Here, we test this prediction by comparing pooled abundance of avian taxa within scale domains to level of resource aggregation loss resulting from oil and gas development in rangeland systems. The spatial pattern of oil and gas development and its effects on resource availability and the scales of resource aggregations make it an ideal disturbance for testing the spatial prediction of the cross-scale resilience model. Oil and gas well pads translate into direct resource loss in rangelands via loss of productivity (Allred et al., 2015), and wells fragment rangelands via the pads themselves and interconnecting roads (Bernath-Plaisted & Koper, 2016; Thompson, Johnson, Niemuth, & Ribic, 2015). Thus, according to the cross-scale resilience model, we expect scale domain abundances to respond non-randomly to differing scales of oil and gas development (Shana M Sundstrom et al., 2018). Specifically, we expect loss of resource

aggregations at large spatial scales (well development at large spatial extents) will reduce abundances in larger scale domains, whereas abundances within smaller scale domains would not respond until resource loss “filled in” at meso-scales (development becomes dense at meso- spatial extents. However, we expect abundances of meso-scale domains to decline when resource aggregations at small scales are lost (development at small spatial extents) due to meso-fauna not being able to take advantage of fragmented resources or move between isolated patches.

METHODS

Study area

We set our study in these central North American ecoregions created by the U.S. Environmental Protection Agency: the Flint Hills, Cross Timbers, High Plains, Central Great Plains, Northwestern Great Plains, Northwestern Glaciated Plains, Aspen Parkland/Northern Glaciated Plains, and Wyoming Basin (Omernik & Griffith, 2014). We chose these ecoregions based on three criteria. First, because they were historically rangeland-dominated, they will have comparable resource aggregations—and thus they will have comparable cross-scale community responses to disturbances to resource aggregations (Omernik & Griffith, 2014; S. M. Sundstrom & Allen, 2014). Second, oil and gas development data was only available in central North America (Allred et al., 2015). Third, these ecoregions contained a sufficient range of oil and gas development to perform analyses.

Data collection

Biotic community data

We used the U.S. Geological Survey's North American Breeding Bird Survey data (BBS) (Sauer, Link, Fallon, Pardieck, & Ziolkowski, 2013). This is a publicly-available dataset of avian community composition collected by trained observers along permanent, georeferenced roadside routes distributed throughout North America. Along each approximately 39.5 km route, observers make 50 stops (once every 0.8 km) and conduct point-count surveys at each stop. For each point-count survey, observers record the abundance of any bird species they detect visually or aurally within a 0.402 km radius for three minutes. Surveys begin 30 minutes before local sunrise and last until the whole route is completed. Surveys are only conducted on days with low wind speeds, high visibility, and minimal or no precipitation. Routes are distributed relatively evenly throughout North America. Start dates for route surveys vary due to latitudinal differences in breeding season timing, ranging from early May to late July.

To account for known negative observation biases for waterfowl and allied families and because terrestrial and water-dwelling avian families exhibit distinct body mass patterns, we removed all species from the Anseriformes, Gaviiformes, Gruiformes, Pelecaniformes, Phaethontiformes, Phoenicopteriformes, Podicipediformes, Procellariiformes, and Suliformes families from the analysis (Crawford S Holling, 1992; Sauer et al., 2013; S. M. Sundstrom, Allen, & Barichievy, 2012). We also removed hybrids and unknowns. We condensed subspecies to their respective species.

Spatial disturbance data

For spatial disturbance data, we used exhaustive oil and gas well data which included all wells drilled in central North America from 1900 - 2012 (Allred et al., 2015). Data was comprised of well spatial location (latitude, longitude), fluid type, license date, and drill date. These data were both proprietary (purchased from state oil and gas commissions, IHS Inc.) and freely-available. We removed wells with no dates (mostly within the states of Kansas and Texas, comprising approximately 86,000 and 194,000 wells, respectively) from analyses. We all analyzed wells that produced fluid types of oil, gas, coalbed methane, and 'not available' fluid types in analyses. To calculate resource loss via oil and gas development, we conservatively estimated each well pad to cover 33000 m² of land, per Allred et al. (2015). Additionally, because data on roads connecting pads were not available, this estimate of resource loss is even more conservative.

To align disturbance data with biotic community data (BBS surveys), we aggregated well data by year of drill date (Allred et al., 2015). If drill date was not available, we substituted license date. Because BBS routes are surveyed during the breeding season, we used a median breeding season date (June 15th) as the cutoff for assigning "year" to each well, with drill dates after June 16th being assigned to the following year.

Identifying scale domains in bird communities

We identified scale domains in bird communities by locating discontinuities in rank-ordered species body masses in ecoregion in each year (C. R. Allen et al., 2005). In taxa with determinant growth, body mass is strongly allometric to the scales at which

resources are aggregated in a system and can thus be used to identify scale domains (Crawford S Holling, 1992; Nash et al., 2014a). Thus, we performed “discontinuity analysis” on the rank-ordered log-transformed species body mass data using the so-called “discontinuity detector” method, which is based on the Gap Rarity Index for detecting discontinuities in continuous data (Barichievy et al., 2018). For each ecoregion and each year, we included any species observed in at least one BBS route in the discontinuity analysis. We obtained mean body mass estimates from the CRC Handbook of Avian Body Masses (Dunning Jr., 2002). We used a power table to account for sample size (the number of species observed in each ecoregion in each year) and average variance in body masses to adjust the critical threshold (the value based on Monte Carlo simulations that identifies significant discontinuities) where number of species varied (Lipsey, 1990).

Statistical analysis

Data preparation

We analyzed bird community data from 2001 - 2012. These dates aligned with the sharpest increases in well drilling in our study area as well as more consistent surveying of BBS routes.

To assess the level of resource loss for each BBS route, we buffered BBS routes by an array of radii and counted all wells that had been drilled within the buffer cumulative to each year. We chose buffer sizes to capture the range of average home range sizes of bird species occurring within the study area. Thus, our buffer sizes were 100 m, 250 m, 500 m, 1000 m, 2500 m, 5000 m, 10000 m, 250000 m, and 50000 m

(Rodewald, 2015). The range of resource loss via well pad coverage ranged from 0 - 50% at the 100 m buffer, 0 - 56% at the 500 m buffer, and 0 - 65% at the 50000 m buffer.

Scale domain abundance responses to oil and gas

We determined the response of scale domain abundances to oil and gas development via negative binomial generalized linear models, setting pooled abundance of each body mass aggregation as the response variable and log-transformed number of drilled oil and gas wells per buffer size as the predictor variables. To account for resource aggregation differences across ecoregions and for stochastic interannual differences in scaling domains (body mass aggregations) resulting from the single visit nature of the BBS, we developed separate models for each ecoregion-year combination.

We controlled for collinearity in covariates (number of wells per X buffer size) via backwards selection of covariates using a variance inflation factor (VIF) threshold (Mouillot, Villéger, Scherer-Lorenzen, & Mason, 2011). That is, we set a threshold of $VIF \leq 10$, and starting with the global model (all buffer size covariates), we removed the covariate with the highest VIF, reran models, and continued until all covariate VIFs were below the threshold. We used this backwards selection procedure because in some ecoregion/year combinations, there were fewer BBS routes than variables, meaning there were not sufficient degrees of freedom to allow for all buffer covariates to be used. Because of this, traditional information criterion model selection (e.g., AIC, AICc, BIC) could have led to problematic model fits.

Testing spatial prediction of cross-scale resilience model

Using these reduced models, we extracted all significant coefficient values ($P \leq 0.1$). These coefficient estimates indicated significant pooled abundance responses to oil and gas development at particular buffer sizes. With the significant coefficient estimates, we developed a model to test if scale domain abundances responded differentially and non-randomly to oil and gas development. Specifically, we used a generalized additive mixed model (GAMM) (Zuur, Ieno, Walker, Saveliev, & Smith, 2009). We set significant coefficient estimates as the response variable. To make the body mass aggregations comparable across ecoregions and years, we used the median log-transformed body mass for each body mass aggregation as the predictor variable; that is, if a body mass aggregation had three species with log-transformed body masses of 3.0, 3.5, and 4.0, the aggregation was represented by 3.5. We fit separate smooth terms by buffer size, and we set the random effect to allow slope to vary by ecoregion and intercept to vary by year.

We evaluated GAMM outputs to determine if and how body mass aggregations responded to loss of resource aggregations. If the GAMM smooth term for a given buffer size was non-random (i.e., significant at 95% confidence), we considered body mass aggregation responses to vary by resource aggregation. If the GAMM smooth term for a given buffer size had no discernable pattern (i.e., non-significant).

Assessing changes in cross-scale functional redundancy, diversity

Finally, we assessed changes in functional redundancy and diversity using the results of the GAMM. We obtained functional group data for all bird species detected in the study area from Ehrlich, Dobkin, & Wheye (1988), dividing functional traits broadly by

carnivore, omnivore, and herbivore. We defined omnivores as species with approximately even intakes of animal and plant matter (Bouska, 2018). Using the GAMM output, we noted which scale domains were increasing versus decreasing in abundance, and we counted the number of species per functional group in each affected scale domain.

RESULTS

Scale domain responses to disturbance

GAMM smooth term coefficients were significant at the 100 m (edf = 4.025; $F = 3.517$; $P = 0.008$) and 500 m (edf = 2.175; $F = 5.226$; $P = 0.004$) buffer sizes (Table 8.1; Figure 8.1). This indicated that responses of abundances were both non-random and nonlinear across scale domains.

At the 100 m buffer size, species in scale domains with medians between approximately 33 - 90 g (e.g., from Townsend's Solitaires to Blue Jays) had slightly positive responses to increasing number of wells, whereas species in scale domains with a median between approximately 247 - 1191 g (e.g., from Willets to Great Horned Owls) responded negatively to increasing number of wells (Figure 8.1; Table 8.2). For instance, model coefficients predict that with a 50% increase in number of wells, pooled species abundance in scale domains with medians of 55 g would increase up to 11% on average and 4 - 18% at extremes (95% confidence; Figure 8.1; Table 8.1). In contrast, abundances in scale domains with a median of 665 g would decrease on average 23% and between 8 - 38% at extremes (95% confidence; Figure 8.1; Table 8.1).

At the 500 m buffer size, species in scale domains with medians between 3 - 30 g (e.g., from Calliope Hummingbirds to Mountain Bluebirds) responded negatively to increasing number of wells. In this range, smaller scale domains fared worst, with negative responses fading at larger scale domains. For the smallest scale domains (median = 3 g), a 50% increase in number of wells would decrease pooled species abundance by 28% on average and between 4 - 56% at extremes (95% confidence; Figure 8.1; Table 8.1). For the larger scale domains (median = 30 g), a 50% increase in number of wells would decrease pooled species abundance by 6% on average and between 2 - 11% at extremes (95% confidence; Figure 8.1; Table 8.1).

Changes in cross-scale functional redundancy, diversity

Trends from GAMMs revealed changes in functional redundancy and diversity across scale domains (Figure 8.2). For instance, in the declining scale domains with median between 247 - 1191 g are comprised of 43 unique species across all ecoregions, and 33 of these species were carnivores, 4 were herbivores, and 3 were omnivores (Figure 8.2, Table 8.2). And across all scale domains, only 101 species are carnivores (Table 8.2). This means declines in 247 - 1191 g scale domains translates to declines in 33% of carnivore species across all scale domains (Figure 8.2, Table 8.2).

Similarly, the declines we detected in 3 - 30 g scale domains translate to declines in 106 omnivore species, 1 herbivore, and 36 carnivores (Figure 8.2, Table 8.2). And across scale domains, only 137 species are omnivores (Table 8.2). Thus, declines in 3 - 30 g scale domains reflect declines in 77% of omnivore species across all scale domains (Figure 8.2, Table 8.2).

And though we detected increases in 33 - 90 g scale domains, these scale domains altogether only consist of 19 species of carnivores, 5 herbivores, and 29 omnivores (Figure 8.2, Table 8.2). Thus, increases in functional groups within these scale domains do not appear to offset the losses in functional redundancy and diversity in the smaller and larger scale domains (Figure 8.2).

DISCUSSION

Our results support a key spatial prediction of the cross-scale model: we found non-random abundance responses to changes in resource aggregations at specific scale domains (Peterson et al., 1998; Sundstrom et al., 2018). Discontinuity analysis revealed as many as 28 scale domains in an ecoregion, but we found scale domain responses fell non-randomly into four broader groups of scale domains. First, the smallest scale domains responded negatively at intermediate spatial scales of disturbance, the second smallest group of scale domains responded positively to disturbance at small spatial scales, the third largest group (hereafter dubbed the “meso-scale domains”) responded negatively to disturbance at small spatial scales, and we detected no response to disturbance by abundances of the largest scale domains. Interestingly, models show that these scale domain response groups do not overlap. Although our study cannot provide mechanistic interpretation of this phenomenon, it underscores the validity of differential responses by discrete scale domains.

That we detected negative responses of meso-scale domains at the smallest spatial scale aligns with the cross-scale model’s predictions: species of meso-scale domains require relatively large resource aggregations but will likely be unable to travel far to take

advantage of highly fragmented patches (Szabo & Meszéna, 2006). Forest fragmentation studies support this finding: for example, mid-sized mammal abundance tended to decline in disconnected forest fragments (Pardini, Souza, Braga-Neto, & Metzger, 2005). But the cross-scale model also predicts species within the smallest scale domains would be able to carry out their life histories in small, fragmented patches, hence no response at the smallest buffer size. This is echoed in other studies: for instance, carrion and dung beetles in the Amazon had differential responses to forest fragmentation, with smaller body mass species able to take advantage of even the small fragments (Klein, 1989). However, when resource loss occurs more completely at scales matching smaller species home range sizes, even species in the smallest scale domains will respond negatively.

That we did not detect responses at the largest scale may be because species in the largest scale domains are likely able to transverse long distances to take advantage of disconnected resource aggregations—such as fragmented patches between or within oil and gas development (Pardini et al., 2005). This means large scale domains may not respond until the resource loss is near complete. And indeed, we found the greatest resource loss (i.e., percent of land within a given buffer covered by oil and gas development) never exceeded 65% at any buffer size and was typically much lower. Studies of mammal species assemblages in Atlantic rainforests support this: select larger mammals were able to persist by traveling between isolated forest patches (Da Silva & Pontes, 2008; Pardini et al., 2005). Because birds are volant, their ability to opportunistically use isolated patches may also be increased compared to other taxa (Cornelius, Cofré, & Marquet, 2000).

We also found clear evidence that oil and gas development led to loss of ecological resilience in rangeland systems. This is a result of loss of functional diversity and redundancy within and across scales via declines in abundance in multiple scale domains (G. Peterson et al., 1998). Theory indicates that a directional trend in total abundance within a scale domain means changes to the scales at which resources are aggregated in the system and thus potentially a regime shift (Dossena et al., 2012; O’Gorman et al., 2012; Shana M Sundstrom et al., 2018). Although we did not search for regime shifts in our study, we did detect directional trends in total abundance within multiple scale domains resulting from resource loss at specific spatial scales due to oil and gas development. T. L. Spanbauer et al. (2016) supports this by showing that shifts in diatom scale domains over time coincided with a regime shift. Likewise, Roberts, Allen, Angeler, & Twidwell (2019) documented regime shifts in avian communities via strong, directional shifts in body mass patterns across the North American continent—across some ecoregions included in the present study. These shifts corresponded with known global change drivers which included energy development (e.g., oil and gas development) (Allred et al., 2015). At best, our results indicate oil and gas development increases system vulnerability to regime shifts, and at worst, our results demonstrate a regime shift in progress across multiple ecoregions in central North America.

Our results show that species’ responses to disturbance and resource loss are not idiosyncratic but are instead predictable via the cross-scale model. Investigating taxa responses to disturbance without regard to scales of resource use will produce disparate findings (e.g., Thompson et al., 2015; Betts et al., 2014). For example, S. M. Sundstrom

& Allen (2014) found that accounting for scale domain when modeling avian extinctions in North American grasslands outperformed traditional predictors of extinction vulnerability such as functional group. Likewise, focusing on presence-absence metrics such as species richness and other diversity measures may mask taxa responses to disturbance (T. F. Allen & Starr, 2017; Shana M Sundstrom et al., 2018). Presence-absence metrics represent coarse measurements in regards to scale, whereas metrics such as abundance and biomass are finer-scale measurements (T. F. Allen & Starr, 2017). The result is that presence-absence metrics will likely produce lagged signals of change that abundance metrics would detect sooner (i.e., at local, more rapid scales). However, even within a given body mass aggregation, species will likely display differential responses to resource aggregation loss (Nash et al., 2014a). For instance, species on the “edges” of body mass aggregations exhibit greater variance in abundance and are more likely to go extinct than species near the “centers” of body mass aggregations (Allen & Holling, 2008). This is hypothesized to result from species nearer centers of body mass aggregations to match best with typical resource aggregations in a system (Crawford S Holling, 1992).

LITERATURE CITED

- Allen, C. R., & Holling, C. S. (2008). *Discontinuities in ecosystems and other complex systems*. Columbia University Press.
- Allen, C. R., & Holling, C. S. (2010). Novelty, adaptive capacity, and resilience. *Ecology and Society*, 15(3), 24.
- Allen, C. R., Gunderson, L., & Johnson, A. (2005). The use of discontinuities and functional groups to assess relative resilience in complex systems. *Ecosystems*, 8(8), 958.
- Allen, T. F., & Starr, T. B. (2017). *Hierarchy: Perspectives for ecological complexity*. University of Chicago Press.
- Allred, B., Smith, W., Twidwell, D., Haggerty, J., Running, S., Naugle, D., & Fuhlendorf, S. (2015). Ecosystem services lost to oil and gas in North America. *Science*, 2, 3.
- Angeler, D. G., & Allen, C. R. (2016). Quantifying resilience. *Journal of Applied Ecology*, 53(3), 617–624.
- Angeler, D. G., Allen, C. R., Barichievy, C., Eason, T., Garmestani, A. S., Graham, N. A., ... others. (2016). Management applications of discontinuity theory. *Journal of Applied Ecology*, 53(3), 688–698.
- Barichievy, C., Angeler, D. G., Eason, T., Garmestani, A. S., Nash, K. L., Stow, C. A., ... Allen, C. R. (2018). A method to detect discontinuities in census data. *Ecology and Evolution*, 8(19), 9614–9623.

- Bellwood, D. R., Hoey, A. S., & Choat, J. H. (2003). Limited functional redundancy in high diversity systems: Resilience and ecosystem function on coral reefs. *Ecology Letters*, 6(4), 281–285.
- Bernath-Plaisted, J., & Koper, N. (2016). Physical footprint of oil and gas infrastructure, not anthropogenic noise, reduces nesting success of some grassland songbirds. *Biological Conservation*, 204, 434–441.
- Betts, M. G., Fahrig, L., Hadley, A. S., Halstead, K. E., Bowman, J., Robinson, W. D., ... Lindenmayer, D. B. (2014). A species-centered approach for uncovering generalities in organism responses to habitat loss and fragmentation. *Ecography*, 37(6), 517–527.
- Bouska, K. L. (2018). Discontinuities and functional resilience of large river fish assemblages. *Ecosphere*, 9(7), e02351.
- Carpenter, S., Walker, B., Anderies, J., & Abel, N. (2001). From metaphor to measurement: Resilience of what to what? *Ecosystems*, 4(8), 765–781.
- Cornelius, C., Cofré, H., & Marquet, P. A. (2000). Effects of habitat fragmentation on bird species in a relict temperate forest in semiarid chile. *Conservation Biology*, 14(2), 534–543.
- Da Silva, A. P., & Pontes, A. R. M. (2008). The effect of a mega-fragmentation process on large mammal assemblages in the highly-threatened pernambuco endemism centre, north-eastern brazil. *Biodiversity and Conservation*, 17(6), 1455–1464.
- Dossena, M., Yvon-Durocher, G., Grey, J., Montoya, J. M., Perkins, D. M., Trimmer, M., & Woodward, G. (2012). Warming alters community size structure and

- ecosystem functioning. *Proceedings of the Royal Society of London B: Biological Sciences*, 279(1740), 3011–3019.
- Dunning Jr., J. (2002). *CRC Handbook of Avian Body Masses*. CRC press.
- Ehrlich, P., Dobkin, D. S., & Wheye, D. (1988). *Birder's Handbook*. Simon; Schuster.
- Elmqvist, T., Folke, C., Nystrom, M., Peterson, G., Bengtsson, J., Walker, B., & Norberg, J. (2003). Response diversity, ecosystem change, and resilience. *Frontiers in Ecology and the Environment*, 1(9), 488–494.
- Holling, C. S. (1973). Resilience and stability of ecological systems. *Annual Review of Ecology and Systematics*, 1–23.
- Holling, C. S. (1992). Cross-scale morphology, geometry, and dynamics of ecosystems. *Ecological Monographs*, 62(4), 447–502.
- Klein, B. C. (1989). Effects of forest fragmentation on dung and carrion beetle communities in central amazonia. *Ecology*, 70(6), 1715–1725.
- Lipsey, M. W. (1990). *Design sensitivity: Statistical power for experimental research* (Vol. 19). Sage.
- Mouillot, D., Villéger, S., Scherer-Lorenzen, M., & Mason, N. W. (2011). Functional structure of biological communities predicts ecosystem multifunctionality. *PloS One*, 6(3), e17476.
- Nash, K. L., Allen, C. R., Angeler, D. G., Barichievy, C., Eason, T., Garmestani, A. S., ... others. (2014a). Discontinuities, cross-scale patterns, and the organization of ecosystems. *Ecology*, 95(3), 654–667.

- Nash, K. L., Allen, C. R., Barichievy, C., Nyström, M., Sundstrom, S., & Graham, N. A. (2014b). Habitat structure and body size distributions: Cross-ecosystem comparison for taxa with determinate and indeterminate growth. *Oikos*, *123*(8), 971–983.
- Nash, K. L., Graham, N. A., Jennings, S., Wilson, S. K., & Bellwood, D. R. (2016). Herbivore cross-scale redundancy supports response diversity and promotes coral reef resilience. *Journal of Applied Ecology*, *53*(3), 646–655.
- Omernik, J. M., & Griffith, G. E. (2014). Ecoregions of the conterminous united states: Evolution of a hierarchical spatial framework. *Environmental Management*, *54*(6), 1249–1266.
- O’Gorman, E. J., Pichler, D. E., Adams, G., Benstead, J. P., Cohen, H., Craig, N., ... others. (2012). Impacts of warming on the structure and functioning of aquatic communities: Individual-to ecosystem-level responses. In *Advances in ecological research* (Vol. 47, pp. 81–176). Elsevier.
- Pardini, R., Souza, S. M. de, Braga-Neto, R., & Metzger, J. P. (2005). The role of forest structure, fragment size and corridors in maintaining small mammal abundance and diversity in an atlantic forest landscape. *Biological Conservation*, *124*(2), 253–266.
- Peterson, G., Allen, C. R., & Holling, C. S. (1998). Ecological resilience, biodiversity, and scale. *Ecosystems*, *1*(1), 6–18.
- Roberts, C., Allen, C., Angeler, D., & Twidwell, D. (2019). Shifting spatial regimes in a changing climate. In *Review: Nature Climate Change*.

- Rodewald, P. (2015). *The Birds of North America*: <https://birdsna.org>. Cornell Laboratory of Ornithology, Ithaca, NY.
- Sauer, J. R., Link, W. A., Fallon, J. E., Pardieck, K. L., & Ziolkowski, D. J. J. (2013). The North American Breeding Bird Survey 1966-2011: Summary Analysis and Species Accounts. *North American Fauna*, 79(doi:10.3996/nafa.79.0001), 1–32.
- Spanbauer, T. L., Allen, C. R., Angeler, D. G., Eason, T., Fritz, S. C., Garmestani, A. S., ... Sundstrom, S. M. (2016). Body size distributions signal a regime shift in a lake ecosystem. *Proc. R. Soc. B*, 283(1833), 20160249.
- Sundstrom, S. M., & Allen, C. R. (2014). Complexity versus certainty in understanding species' declines. *Diversity and Distributions*, 20(3), 344–355.
- Sundstrom, S. M., Allen, C. R., & Barichievy, C. (2012). Species, functional groups, and thresholds in ecological resilience. *Conservation Biology*, 26(2), 305–314.
- Sundstrom, S. M., Angeler, D. G., Barichievy, C., Eason, T., Garmestani, A., Gunderson, L., ... others. (2018). The distribution and role of functional abundance in cross-scale resilience. *Ecology*, 99(11), 2421–2432.
- Szabo, P., & Meszéna, G. (2006). Spatial ecological hierarchies: Coexistence on heterogeneous landscapes via scale niche diversification. *Ecosystems*, 9(6), 1009–1016.
- Thompson, S. J., Johnson, D. H., Niemuth, N. D., & Ribic, C. A. (2015). Avoidance of unconventional oil wells and roads exacerbates habitat loss for grassland birds in the north american great plains. *Biological Conservation*, 192, 82–90.

- Walker, B. (1992). Biodiversity and ecological redundancy. *Conservation Biology*, 6(1), 18–23.
- Walker, B., Kinzig, A., & Langridge, J. (1999). Plant attribute diversity, resilience, and ecosystem function: the nature and significance of dominant and minor species. *Ecosystems*, 2(2), 95–113.
- Wardwell, D. A., Allen, C. R., Peterson, G. D., & Tyre, A. J. (2008). A test of the cross-scale resilience model: Functional richness in mediterranean-climate ecosystems. *Ecological Complexity*, 5(2), 165–182.
- Zuur, A., Ieno, E., Walker, N., Saveliev, A., & Smith, G. (2009). *Mixed effects models and extensions in ecology with R*. New York, NY: Springer Science and Business Media.

TABLES

Table 8. 1: Smooth term coefficient output for the generalized additive mixed model comparing response of breeding bird abundances across scale domains to oil and gas development at different spatial extents. From left to right, columns indicate the smoothed predictor term (numbers indicate meters), estimated degrees of freedom of smooth term, the pseudo F statistic, and the estimated p-value.

Variable	edf	F	p-value
s(100)	4.025	3.517	0.008
s(250)	2.175	1.338	0.214
s(500)	2.125	5.226	0.004
s(1000)	1.665	0.901	0.254
s(2500)	1.000	0.585	0.444
s(5000)	1.462	0.319	0.728
s(10000)	1.858	1.137	0.228
s(25000)	1.000	0.103	0.748
s(50000)	2.230	1.894	0.211

Table 8. 2: Species recorded across rangeland-dominated ecoregions in central North America, their functional groups, their mean log-transformed and untransformed body masses in grams.

Species	Functional Group	Body Mass (log(g))	Body Mass (g)
Calliope Hummingbird	omnivore	0.975	2.6
Ruby-throated Hummingbird	omnivore	1.131	3.1
Black-chinned Hummingbird	omnivore	1.224	3.4
Broad-tailed Hummingbird	omnivore	1.267	3.6
Black-tailed Gnatcatcher	omnivore	1.649	5.2
Bushtit	omnivore	1.668	5.3
Blue-gray Gnatcatcher	carnivore	1.758	5.8
Ruby-crowned Kinglet	omnivore	1.825	6.2
Golden-crowned Kinglet	omnivore	1.825	6.2
Verdin	omnivore	1.917	6.8

Wilson's Warbler	omnivore	1.974	7.2
Prairie Warbler	carnivore	2.035	7.7
Northern Parula	carnivore	2.063	7.9
Brown Creeper	omnivore	2.092	8.1
Virginia's Warbler	carnivore	2.104	8.2
American Redstart	omnivore	2.11	8.2
Bell's Vireo	omnivore	2.14	8.5
Black-throated Gray Warbler	carnivore	2.163	8.7
Black-capped Vireo	omnivore	2.197	9
Orange-crowned Warbler	omnivore	2.197	9
Sedge Wren	carnivore	2.216	9.2
Chestnut-sided Warbler	omnivore	2.23	9.3
Yellow Warbler	omnivore	2.241	9.4
Lesser Goldfinch	omnivore	2.251	9.5
Common Yellowthroat	omnivore	2.257	9.5
Yellow-throated Warbler	carnivore	2.272	9.7
Red-breasted Nuthatch	omnivore	2.282	9.8
Bewick's Wren	carnivore	2.293	9.9
Golden-cheeked Warbler	carnivore	2.293	9.9
Least Flycatcher	omnivore	2.303	10
Carolina Chickadee	omnivore	2.303	10
Brown-headed Nuthatch	omnivore	2.322	10.2
Dusky Flycatcher	carnivore	2.342	10.4
MacGillivray's Warbler	carnivore	2.342	10.4
Hammond's Flycatcher	carnivore	2.347	10.5
Hooded Warbler	carnivore	2.356	10.6
Pygmy Nuthatch	omnivore	2.361	10.6
Black-capped Chickadee	omnivore	2.38	10.8
Marsh Wren	carnivore	2.383	10.8
House Wren	carnivore	2.385	10.9
Black-and-white Warbler	carnivore	2.389	10.9
Brewer's Sparrow	omnivore	2.389	10.9
Clay-colored Sparrow	omnivore	2.416	11.2
Mountain Chickadee	omnivore	2.416	11.2
White-eyed Vireo	omnivore	2.434	11.4
Philadelphia Vireo	omnivore	2.442	11.5
Mourning Warbler	carnivore	2.464	11.7
Canyon Wren	carnivore	2.485	12
Chipping Sparrow	omnivore	2.501	12.2
Gray Flycatcher	carnivore	2.51	12.3
Field Sparrow	omnivore	2.526	12.5

Acadian Flycatcher	omnivore	2.534	12.6
Alder Flycatcher	omnivore	2.542	12.7
Warbling Vireo	omnivore	2.542	12.7
Pine Siskin	omnivore	2.542	12.7
Bank Swallow	carnivore	2.544	12.7
American Goldfinch	omnivore	2.549	12.8
Henslow's Sparrow	omnivore	2.549	12.8
Le Conte's Sparrow	omnivore	2.565	13
Willow Flycatcher	omnivore	2.595	13.4
Black-throated Sparrow	omnivore	2.603	13.5
Kentucky Warbler	omnivore	2.639	14
Violet-green Swallow	carnivore	2.65	14.2
Prothonotary Warbler	carnivore	2.66	14.3
Vermilion Flycatcher	carnivore	2.667	14.4
Indigo Bunting	omnivore	2.688	14.7
Lazuli Bunting	omnivore	2.741	15.5
Painted Bunting	omnivore	2.744	15.6
Northern Rough-winged Swallow	carnivore	2.754	15.7
Swamp Sparrow	omnivore	2.779	16.1
Red-eyed Vireo	omnivore	2.783	16.2
Northern Waterthrush	carnivore	2.791	16.3
Lincoln's Sparrow	omnivore	2.809	16.6
Sage Sparrow	omnivore	2.837	17.1
Grasshopper Sparrow	omnivore	2.869	17.6
Barn Swallow	omnivore	2.889	18
Yellow-throated Vireo	omnivore	2.89	18
Baird's Sparrow	omnivore	2.894	18.1
Black Phoebe	carnivore	2.926	18.6
Rufous-crowned Sparrow	omnivore	2.929	18.7
Ovenbird	carnivore	2.934	18.8
Cassin's Sparrow	omnivore	2.939	18.9
Carolina Wren	carnivore	2.946	19
Cave Swallow	carnivore	2.958	19.3
Orchard Oriole	omnivore	2.968	19.4
Eastern Phoebe	carnivore	2.981	19.7
Louisiana Waterthrush	carnivore	2.991	19.9
Savannah Sparrow	omnivore	3.004	20.2
Chestnut-collared Longspur	omnivore	3.011	20.3
Bachman's Sparrow	omnivore	3.035	20.8
Say's Phoebe	omnivore	3.04	20.9
White-breasted Nuthatch	omnivore	3.045	21

Tree Swallow	omnivore	3.054	21.2
House Finch	herbivore	3.063	21.4
Cliff Swallow	omnivore	3.073	21.6
Tufted Titmouse	omnivore	3.073	21.6
Song Sparrow	omnivore	3.126	22.8
Purple Finch	omnivore	3.148	23.3
Chimney Swift	carnivore	3.161	23.6
White-throated Sparrow	omnivore	3.195	24.4
Yellow-breasted Chat	omnivore	3.215	24.9
Sprague's Pipit	omnivore	3.239	25.5
Downy Woodpecker	omnivore	3.246	25.7
Vesper Sparrow	omnivore	3.246	25.7
Dickcissel	omnivore	3.269	26.3
Western Bluebird	omnivore	3.275	26.4
Cassin's Finch	omnivore	3.277	26.5
House Sparrow	omnivore	3.28	26.6
McCown's Longspur	omnivore	3.285	26.7
Blue Grosbeak	omnivore	3.311	27.4
Eastern Bluebird	omnivore	3.314	27.5
Western Tanager	omnivore	3.336	28.1
White-crowned Sparrow	omnivore	3.336	28.1
Ash-throated Flycatcher	omnivore	3.339	28.2
Scarlet Tanager	omnivore	3.339	28.2
Lark Sparrow	omnivore	3.367	29
Summer Tanager	omnivore	3.372	29.2
Green-tailed Towhee	omnivore	3.381	29.4
Mountain Bluebird	omnivore	3.388	29.6
Hermit Thrush	omnivore	3.405	30.1
Swainson's Thrush	omnivore	3.411	30.3
Bobolink	omnivore	3.452	31.6
Cedar Waxwing	omnivore	3.453	31.6
Ladder-backed Woodpecker	omnivore	3.454	31.6
Veery	omnivore	3.463	31.9
White-throated Swift	carnivore	3.469	32.1
Olive-sided Flycatcher	carnivore	3.469	32.1
Townsend's Solitaire	omnivore	3.503	33.2
Fox Sparrow	omnivore	3.506	33.3
Horned Lark	omnivore	3.513	33.5
Green Kingfisher	carnivore	3.522	33.9
Pyrrhuloxia	omnivore	3.561	35.2
Gray Catbird	omnivore	3.564	35.3

Red Crossbill	herbivore	3.57	35.5
Scott's Oriole	omnivore	3.597	36.5
Lark Bunting	omnivore	3.627	37.6
Cactus Wren	carnivore	3.661	38.9
Scissor-tailed Flycatcher	omnivore	3.671	39.3
Western Kingbird	omnivore	3.679	39.6
Eastern Kingbird	omnivore	3.687	39.9
Spotted Sandpiper	carnivore	3.699	40.4
Brown-headed Cowbird	omnivore	3.706	40.7
Rose-breasted Grosbeak	omnivore	3.738	42
Snowy Plover	carnivore	3.745	42.3
Northern Cardinal	omnivore	3.753	42.6
Sage Thrasher	omnivore	3.789	44.2
Cassin's Kingbird	omnivore	3.82	45.6
Least Tern	carnivore	3.827	45.9
Black-headed Grosbeak	omnivore	3.853	47.1
Inca Dove	herbivore	3.861	47.5
Williamson's Sapsucker	omnivore	3.863	47.6
Lesser Nighthawk	carnivore	3.881	48.4
Northern Mockingbird	omnivore	3.882	48.5
Red-naped Sapsucker	omnivore	3.882	48.5
Wood Thrush	omnivore	3.915	50.2
Yellow-bellied Sapsucker	omnivore	3.918	50.3
Black-billed Cuckoo	carnivore	3.93	50.9
Loggerhead Shrike	carnivore	3.946	51.7
Red-winged Blackbird	omnivore	3.959	52.4
Purple Martin	carnivore	3.985	53.8
Piping Plover	carnivore	3.996	54.4
Pine Grosbeak	herbivore	4.032	56.4
American Dipper	carnivore	4.039	56.8
Evening Grosbeak	herbivore	4.049	57.4
Wilson's Phalarope	omnivore	4.094	60
Bendire's Thrasher	omnivore	4.13	62.2
Brewer's Blackbird	omnivore	4.138	62.7
Crissal Thrasher	omnivore	4.138	62.7
Bronzed Cowbird	omnivore	4.142	62.9
Hairy Woodpecker	carnivore	4.148	63.3
Yellow-billed Cuckoo	carnivore	4.159	64
Yellow-headed Blackbird	omnivore	4.167	64.5
Black Tern	carnivore	4.179	65.3
Long-billed Thrasher	carnivore	4.214	67.6

Brown Thrasher	carnivore	4.231	68.8
Red-bellied Woodpecker	omnivore	4.243	69.6
Red-headed Woodpecker	omnivore	4.271	71.6
Gray Jay	omnivore	4.272	71.7
European Starling	omnivore	4.357	78
American Robin	carnivore	4.363	78.5
Common Nighthawk	carnivore	4.373	79.3
Curve-billed Thrasher	omnivore	4.39	80.6
Golden-fronted Woodpecker	omnivore	4.393	80.9
Blue Jay	omnivore	4.477	88
Eastern Meadowlark	omnivore	4.529	92.7
Mountain Plover	carnivore	4.562	95.8
Killdeer	carnivore	4.57	96.5
Western Meadowlark	omnivore	4.612	100.7
Northern Saw-whet Owl	carnivore	4.646	104.2
Pinyon Jay	herbivore	4.654	105
Common Grackle	carnivore	4.664	106.1
Chuck-will's-widow	carnivore	4.691	109
American Kestrel	carnivore	4.755	116.2
Mourning Dove	herbivore	4.779	119
Steller's Jay	herbivore	4.852	128
Common Tern	carnivore	4.864	129.5
Clark's Nutcracker	herbivore	4.868	130
Sharp-shinned Hawk	carnivore	4.911	135.7
Belted Kingfisher	carnivore	4.997	148
Forster's Tern	carnivore	5.004	149
Burrowing Owl	carnivore	5.015	150.7
White-winged Dove	herbivore	5.03	153
Upland Sandpiper	omnivore	5.069	159
Great-tailed Grackle	carnivore	5.13	169
Northern Bobwhite	herbivore	5.147	172
Black-billed Magpie	carnivore	5.179	177.5
Scaled Quail	herbivore	5.215	184
Black-necked Stilt	carnivore	5.226	186
Merlin	carnivore	5.25	190.5
Willet	carnivore	5.51	247.3
Mississippi Kite	carnivore	5.628	278
Franklin's Gull	carnivore	5.635	280
Fish Crow	carnivore	5.652	285
Pileated Woodpecker	omnivore	5.66	287.3
Long-eared Owl	carnivore	5.7	299

American Avocet	carnivore	5.719	304.5
Laughing Gull	carnivore	5.73	308
Short-eared Owl	carnivore	5.784	325
Marbled Godwit	carnivore	5.882	358.5
Band-tailed Pigeon	herbivore	5.906	367.3
Greater Roadrunner	carnivore	5.93	376
Northern Harrier	carnivore	5.994	401
Gray Partridge	omnivore	6.005	405.5
Cooper's Hawk	carnivore	6.084	439
American Crow	omnivore	6.115	452.7
Broad-winged Hawk	carnivore	6.12	455
Chukar	omnivore	6.222	503.5
Ring-billed Gull	carnivore	6.251	518.5
Ruffed Grouse	herbivore	6.277	532
Chihuahuan Raven	carnivore	6.28	534
Long-billed Curlew	carnivore	6.374	586.5
Red-shouldered Hawk	carnivore	6.409	607
Caspian Tern	carnivore	6.485	655
California Gull	carnivore	6.538	691
Barred Owl	carnivore	6.574	716.5
Prairie Falcon	carnivore	6.599	734
Peregrine Falcon	carnivore	6.664	783.3
Sharp-tailed Grouse	herbivore	6.786	885
Northern Goshawk	carnivore	6.804	901.7
Common Raven	carnivore	6.847	941
Swainson's Hawk	carnivore	6.865	958.5
Crested Caracara	carnivore	6.938	1031
Herring Gull	omnivore	6.998	1094
Red-tailed Hawk	carnivore	7.012	1110.2
Ring-necked Pheasant	omnivore	7.034	1135
Great Horned Owl	carnivore	7.083	1191.2
Ferruginous Hawk	carnivore	7.293	1469.5
Osprey	carnivore	7.304	1485.5
Turkey Vulture	carnivore	7.347	1552
Black Vulture	carnivore	7.549	1899.5
Golden Eagle	carnivore	8.358	4263.5
Bald Eagle	carnivore	8.464	4740
Wild Turkey	omnivore	8.708	6050

FIGURES

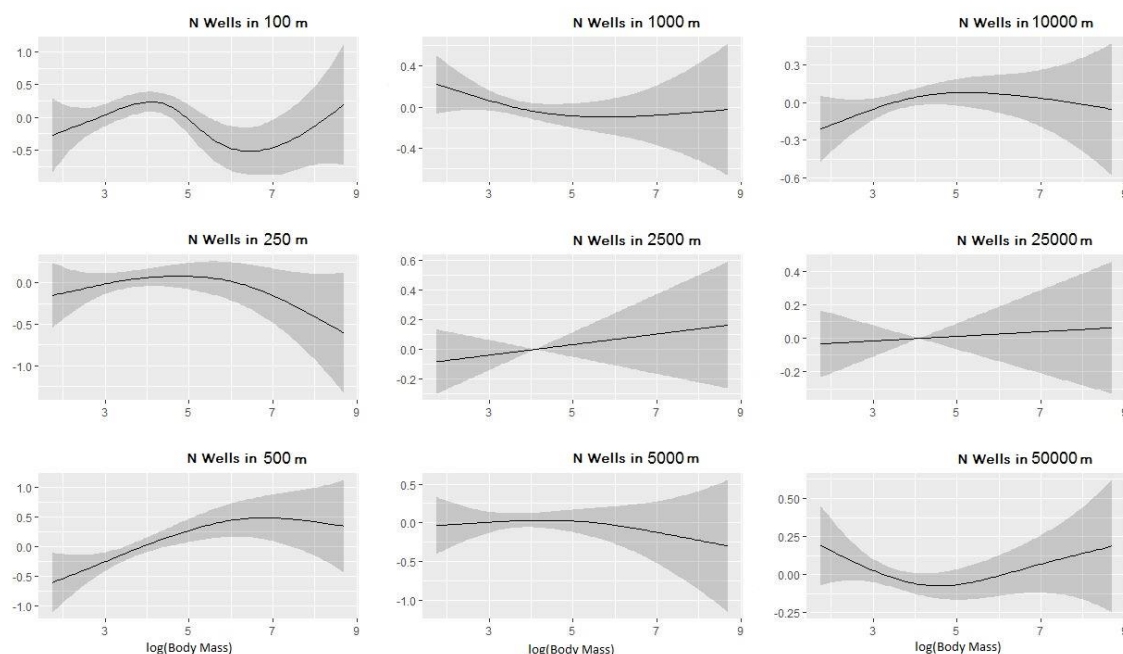


Figure 8. 1: Outputs from generalized additive mixed models testing the spatial prediction of the cross-scale resilience model, namely that response to loss of resource aggregations across scales will cause non-random declines in biota according to their scale domains. Y-axes indicate modeled responses of scale domains to oil and gas development (resource loss), and x-axes indicate the range of scale domains (median log-transformed body masses) detected in breeding bird communities in rangeland ecoregions in central North America. Panels reflect scales of resource loss (buffer size around bird survey transects).

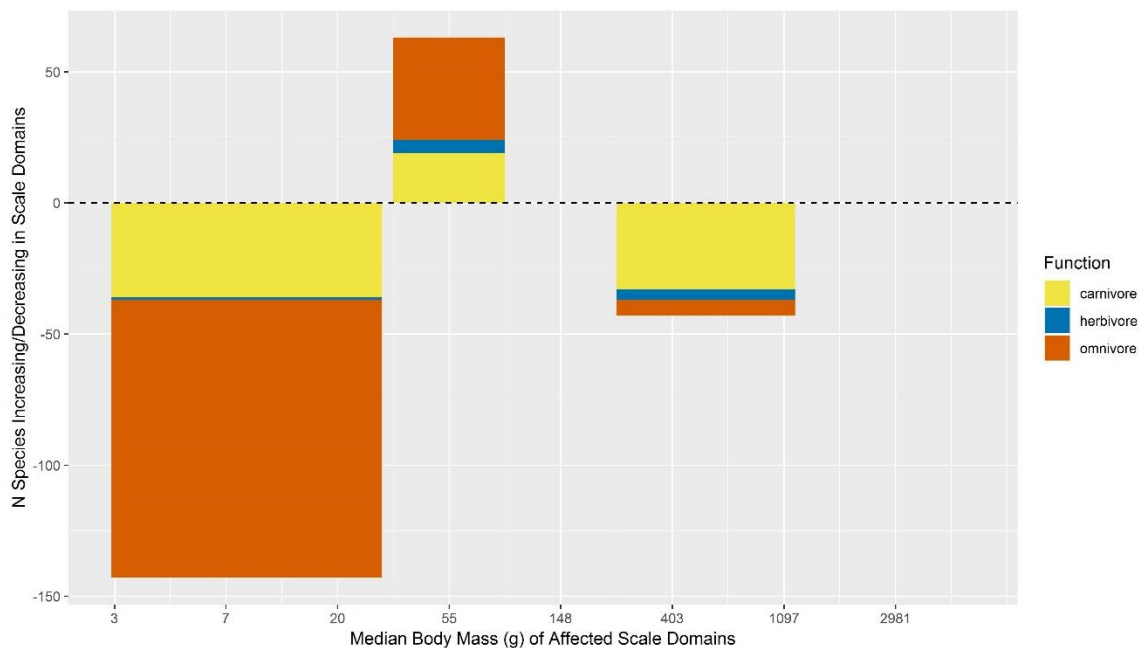


Figure 8. 2: Changes in cross-scale resilience of breeding birds resulting from oil and gas development. Y-axis indicates number of species in scale domains determined to be affected by oil and gas development, colored by functional group. X-axis indicates the range of scale domains (median body masses) detected in breeding bird communities across rangeland ecoregions in central North America. The x-axis is on a natural log scale.

CHAPTER 9: DOUBLETHINK AND SCALE MISMATCH POLARIZE POLICIES FOR AN INVASIVE TREE⁸

ABSTRACT

Mismatches between invasive species management policies and ecological knowledge can lead to profound societal consequences. For this reason, natural resource agencies have adopted the scientifically-based density-impact invasive species curve to guide invasive species management. We use the density-impact model to evaluate how well management policies for a native invader (*Juniperus virginiana*) match scientific guidelines. *Juniperus virginiana* invasion is causing a sub-continental regime shift from grasslands to woodlands in central North America, and its impacts span collapses in endemic diversity, heightened wildfire risk, and crashes in grazing land profitability. We (1) use land cover data to identify the stage of *Juniperus virginiana* invasion for three ecoregions within Nebraska, USA, (2) determine the range of invasion stages at individual land parcel extents within each ecoregion based on the density-impact model, and (3) determine policy alignment and mismatches relative to the density-impact model

⁸ Roberts, C. P., Uden, D. R., Allen, C. R., & Twidwell, D. (2018). Doublethink and scale mismatch polarize policies for an invasive tree. PloS one, 13(3), e0189733.

CPR contributed to conceptualization, programming, data validation, formal analysis, data curation, all writing aspects, visualization, and project administration. DT and DRU contributed to conceptualization and all writing aspects. CRA contributed to conceptualization.

in order to assess their potential to meet sustainability targets and avoid societal impacts as *Juniperus virginiana* abundance increases. We found that nearly all policies evidenced doublethink and policy-ecology mismatches, for instance, promoting spread of *Juniperus virginiana* regardless of invasion stage while simultaneously managing it as a native invader in the same ecoregion. Like other invasive species, theory and literature for this native invader indicate that the consequences of invasion are unlikely to be prevented if policies fail to prioritize management at incipient invasion stages. Theory suggests a more realistic approach would be to align policy with the stage of invasion at local and ecoregion management scales. There is a need for scientists, policy makers, and ecosystem managers to move past ideologies governing native versus non-native invader classification and toward a framework that accounts for the uniqueness of native species invasions, their anthropogenic drivers, and their impacts on ecosystem services.

INTRODUCTION

To avoid ecological and economic consequences from invasive species (Pimentel, Zuniga, & Morrison, 2005; Vilà et al., 2011), natural resources agencies must make and follow proactive, scientifically-supported invasive species management policies (Chaffin et al., 2016; Stewart-Koster, Olden, & Johnson, 2015). Mismatches between policy and ecology can lead natural resource agencies toward a “doublethink” mentality (where contradictory thoughts exist without acknowledged cognitive dissonance) that produces policies that simultaneously promote and control invasive species (Carey, Sanderson, Barnas, & Olden, 2012; Vítková, Müllerová, Sádlo, Pergl, & Pyšek, 2017). This doublethink mentality manifests from the need to respond to opposite demands of diverse

citizenry, misunderstanding scales of invasion, and “nebulous” concepts such as native invaders (Ganguli, Engle, Mayer, & Fuhlendorf, 2008; Nackley, West, Skowno, & Bond, 2017; Simberloff, Souza, Nuñez, Barrios-Garcia, & Bunn, 2012; Twidwell et al., 2013c; Wilgen et al., 2012). The actions and behaviors resulting from doublethink misalign invasive species management policies with basic ecological invasion theory. This mismatch eliminates the potential for management tactics to meet goals meant to prevent (Epanchin-Niell & Liebhold, 2015), eradicate (Epanchin-Niell, Haight, Berec, Kean, & Liebhold, 2012), or simply control (Epanchin-Niell & Hastings, 2010) invasions, thereby increasing the likelihood for sharp declines in ecosystem services and regime shifts to hysteretic, undesirable alternative states.

Natural resource agencies have adopted the scientifically-derived “density-impact invasive species curve” model to guide management actions, prioritize investments, and prevent policy-ecology mismatches (Yokomizo, Possingham, Thomas, & Buckley, 2009). The density-impact invasive species curve (hereafter the “density-impact model”) provides theoretical insight into the economic impacts of invasive species as they increase in abundance and density over time (Figure 9.10.1). The model has been used as the basis for understanding the feasibility and effectiveness of management strategies at different stages of the invasion process, and it can help identify mismatches in policy where doublethink poses large risks to economic assets. Misunderstanding the density-impact model results in doublethink management that under-invests (lags behind) at the early stages of invasion and then over-invests (tries to catch up) at later stages (Epanchin-

Niell & Hastings, 2010; Epanchin-Niell & Liebhold, 2015; Epanchin-Niell et al., 2012; Simberloff, 2003; Yokomizo et al., 2009).

Invasive species policy has been slow to adapt to a non-stationary and rapidly changing world (Head et al., 2015). Species that did not pose risks in the past but which are now invading and responsible for major socio-economic losses due to their impacts to other resources are particularly likely to escape policies built around assumptions of equilibrium (Chaffin et al., 2016; Vítková et al., 2017). A key uncertainty surrounds native invaders, which are now known to have impacts that rival non-native invaders but which also have traits that make them valuable in specific contexts (Ganguli et al., 2008; Nackley et al., 2017). It is unclear how disparate existing policies are for native invaders that are known to have strong density-related impacts.

We use the density-impact model to identify the degree of mismatch between science and policy for a native invader in central North America, eastern redcedar (*Juniperus virginiana*). Scientists and natural resource professionals have reached consensus on the invasive potential and sharp social, economic, and ecological impacts of this native tree as its density increases (Fuhlendorf, Archer, Smeins, Engle, & Taylor Jr, 2008; Institute of Agriculture and Natural Resources, University of Nebraska-Lincoln, n.d.; Nebraska Invasive Species Council, n.d.). Our policy assessment stems from collaborations with USA federal and state agencies seeking to better conserve temperate grasslands at the front-line of juniper invasions in the Great Plains. In this paper, we (1) use land cover data to identify the stage of eastern redcedar invasion for three ecoregions within the State of Nebraska, USA, (2) determine the range of invasion stages at

individual land parcel extents within each ecoregion based on the density-impact model, and (3) determine policy alignment and mismatches relative to the density-impact model in order to assess their potential to meet sustainability targets and avoid societal impacts as eastern redcedar abundance increases.

METHODS

Focal species

Eastern redcedar is a dioecious, non-resprouting conifer that has the broadest range of any conifer in North America (Engle, Coppedge, & Fuhlendorf, 2008). Due to human fire suppression and intentional planting, eastern redcedar has become a native invader in the Great Plains of the USA-expanding its geographic range at an exponential rate (Meneguzzo & Liknes, 2015) -and has initiated biome-level regime shifts from grasslands to woodlands (Briggs et al., 2005; Engle et al., 2008; Twidwell et al., 2016). Historically, frequent human burning of Great Plains landscapes constrained eastern redcedar's geographic distribution to isolated locations (e.g., lowlands and rough topographies) (Bessey, 1900; Streit Krug, Uden, Allen, & Twidwell, 2017; Twidwell et al., 2013c). In the absence of fire, eastern redcedar has no known environmental filter except open water and wetland sites (Engle et al., 2008; Lawson, 1990), meaning only dispersal time (lag) and abiotic factors that influence rate of invasion (e.g., soil type, precipitation) mediate a given site's vulnerability to invasion (Ratajczak et al., 2016; Streit Krug et al., 2017).

Eastern redcedar invasion incurs sharp social and economic losses due to reduction in profitability of grazing lands (Bidwell, Engle, Moseley, & Master, 1990;

Briggs, Hoch, & Johnson, 2002; Briggs et al., 2005), loss of public school funding (Institute of Agriculture and Natural Resources, University of Nebraska-Lincoln, n.d.; Simonsen, Fleischmann, Whisenhunt, Volesky, & Twidwell, 2015), heightened wildfire risk (Institute of Agriculture and Natural Resources, University of Nebraska-Lincoln, n.d.), and reductions in the diversity and abundance of endemic taxa, in some cases causing local extinctions (Coppedge, Engle, Masters, & Gregory, 2001; Horncastle et al., 2005; Limb, Engle, Alford, & Hellgren, 2010). More than 50 years of study on *Juniperus* species in the Great Plains have provided detailed knowledge of invasion pattern, spread rates, and sensitivity to management tactics (Briggs et al., 2002; Limb et al., 2010; Twidwell, Fuhlendorf, Taylor, & Rogers, 2013b), but the high cost of mechanical removal and policy-driven fire suppression inhibit management at spatial extents greater than individual land parcels (Simonsen et al., 2015).

Eastern redcedar shares basic mechanisms of spread with non-native invaders (e.g., removal of environmental constraints induces spread, temporal lags in invasion, density-impact relationship) (Briggs et al., 2002, 2005; Meneguzzo & Liknes, 2015; Ratajczak et al., 2016; Twidwell et al., 2016) and incurs costs that rival other non-native invaders in North America (Fuhlendorf et al., 2008; Simonsen et al., 2015). Despite these similarities with non-native invaders, the uniqueness of native invaders such as eastern redcedar can lead to doublethink in management actions (Carey et al., 2012; Ganguli et al., 2008; Nackley et al., 2017). For instance, because prevention and eradication must be scale-dependent strategies for native invaders (i.e., eradicating a native invader from many adjacent land parcels may be desirable, but not from its entire historic range),

doublethink can occur if policies prohibit or fail to incentivize prevention or eradication at any scale (Cumming, Olsson, Chapin, & Holling, 2013). This can lead to waiting to initialize management until the exponential growth phase (the control stage), or in some instances, density-impacts may have already passed acceptable thresholds, making only long-term mitigation and resource protection feasible (Epanchin-Niell & Hastings, 2010; Pimentel et al., 2005; Uden, Allen, Angeler, Corral, & Fricke, 2015; Vilà et al., 2011; Yokomizo et al., 2009). Additionally, native invaders, such as eastern redcedar, can be profitable in certain circumstances (e.g., selling seedlings grown in government-funded nurseries) (Ganguli et al., 2008), but also incur steep social, economic, and ecological costs that natural resources agencies must manage (Fuhlendorf et al., 2008).

In this paper, we evaluated if policy for managing eastern redcedar invasion matches the density-impact model in Nebraska. Although many regions within the USA's southern plains have already reached the carrying capacity/local control stage of invasion, northern plains states such as Nebraska are on the "front line" of eastern redcedar invasion and have not yet experienced regime shifts at broader spatial extents (Bidwell et al., 1990; Twidwell et al., 2013c). Natural resource agencies in front line states have the opportunity to halt ecological regime shifts and economic losses by developing and implementing policy that matches ecological knowledge (Twidwell et al., 2016). In 2014, the Nebraska state Conservation Roundtable identified eastern redcedar as one of the greatest threats to conservation in the state (Nebraska Conservation Roundtable. 2014., n.d.). Since then, momentum for matching policy and ecology for eastern redcedar management has grown, with the Nebraska Invasive Species Council affirming eastern

redcedar as a native invader and multiple local stakeholders and working groups calling for more proactive and ecologically-supported policy and management actions (Loess Canyons Rangeland Alliance, n.d.; Nebraska Invasive Species Council, n.d.; Sandhills Task Force, n.d.).

Study site

In Nebraska, the Nebraska Natural Legacy Project (Schneider et al., 2011) serves as the State Wildlife Action Plan. The overarching objectives of the Nebraska Natural Legacy Project are to conserve the flora, fauna, and natural habitats of the state. To achieve these objectives, management actions are focused in 39 ecoregions termed “biologically unique landscapes” (hereafter referred to simply as “ecoregions”) across the state, which collectively offer opportunities for conserving the full array of the state’s biodiversity. We chose three ecoregions within Nebraska that were historically grass-dominated systems and that have been invaded by eastern redcedar to varying degrees: the Cherry County Wetlands, the Central Loess Hills, and the Loess Canyons (Figure 9.2) (Johnsgard, 2005). We also selected these ecoregions because the Nebraska Invasive Species Council (Nebraska Invasive Species Council, n.d.) and stakeholders have identified eastern redcedar as a potential “resource concern” (i.e., threatening economic, ecological, and social resources) to federal and state agencies in these ecoregions. We obtained elevation data for our study sites from 30 meter resolution digital elevation model imagery downloaded from the website of the Nebraska Department of Natural Resources (“Nebraska Department of Natural Resources,” n.d.). We obtained precipitation data for our study sites by summing mean monthly precipitation values from

one kilometer resolution mean monthly precipitation raster data over a 50-year time period (1950-2000) in each ecoregion (“U.S. Geological Survey,” n.d.).

Cherry County Wetlands

The Cherry County Wetlands ecoregion is located in the northern portion of the Sandhills in Cherry County, Nebraska (Schneider et al., 2011). Numerous lakes, wet meadows, marshes, and fens are situated in valleys between sand dunes covered in relatively unbroken Sandhills mixed-grass prairie. Agricultural land use consists primarily of haying and cattle grazing, although some row crop production is supported by center-pivot irrigation in river valleys. Elevation ranges from 778 to 1,227 meters above sea level. Mean average annual precipitation between the years 1950 and 2000 ranged from 461 to 570 millimeters (mm).

Central Loess Hills

The Central Loess Hills ecoregion is located in central Nebraska and consists of rolling to steep hills dissected by the Middle Loup and North Loup River Valleys (Schneider et al., 2011). Hilly upland areas were traditionally reserved for grazing, but rowcrop production is now moving beyond the flat river valleys and into farmable upland areas. Playa wetlands can be found in relatively high densities in the northwestern portion of the landscape. Although grassland and cropland are the dominant land cover classes, the spread of eastern redcedar is increasing the proportion of the landscape in woodland/forest (Schneider et al., 2011). Elevation ranges from 612 to 951 meters above sea level. Mean average annual precipitation ranged from 555 to 647 mm between the years 1950 and 2000.

Loess Canyons

The Loess Canyons ecoregion is situated south of the Platte River in portions of Lincoln, Dawson, and Frontier Counties of Nebraska (Schneider et al., 2011). Steep loess hills and canyons are characteristic landscape elements, with row crop fields being interspersed amidst blocks of mixed-grass prairie. Several historical accounts indicate the presence of dense stands of eastern redcedar in local canyons along the Platte River in the mid-nineteenth century, but not in upland areas beyond the river (Frémont, 1845; Ware, 1960). In recent decades, the spread of eastern redcedar trees into upland prairies has become an economic and ecological concern, and removal projects by private landowners and conservation organizations are underway (Schneider et al., 2011). Elevation ranges from 781 to 989 meters above sea level. Mean average annual precipitation ranged from 510 to 563 millimeters between the years 1950 and 2000.

Data collection

Policy identification

Financial incentive programs and technical guidance are derived from a hierarchical set of policies used to prioritize the identification and management of invasive species in the USA (Figure 9.3). This general process was identified as part of our involvement in conservation partnerships with diverse representations spanning public, private, and academic sectors. A key difference between policies for native and non-native invaders is that native invaders are not included in policy directives that establish federal mandates for invasive species management (e.g. Executive orders, Figure 9.3). Native invaders can only be captured within regional-to-local policy directives.

For the purposes of this assessment, we worked with natural resource agencies to identify specific policies that have become institutionalized in the behaviors and practices of federal and state natural resource agencies. We focused on those policies that most affected decision-making and conservation investments on private lands. Nebraska, like other states throughout the Great Plains, is almost entirely owned and managed by private landowners (97% private land ownership), so we focused less on internal agency policies that were more relevant to public land management. For purposes of transparency, we include our involvement and interactions for each relevant level of the hierarchical policy process.

The Nebraska Invasive Species Council and Nebraska Conservation Roundtable are regional legislative councils that serve as government agency platforms for discussions on eastern redcedar policies. In 2014, the Nebraska Conservation Roundtable crafted a white paper listing eastern redcedar as one of the greatest conservation threats in Nebraska (Nebraska Conservation Roundtable. 2014., n.d.). In 2017, the Nebraska Invasive Species Advisory Council listed eastern redcedar as a ‘problematic’ invader because of scientifically-established information on economic and environmental declines associated with eastern redcedar invasions (Nebraska Invasive Species Council, n.d.). This designation overcame traditional tendencies to equate invasive with non-native and to critique the potential efficacy of programs at lower levels of the hierarchy (Figure 9.3).

With this in mind, we conducted an in-depth search of publicly-available policy documents to go alongside previous assessments of internal agency management

frameworks that govern program implementation and technical guidance across millions of acres of private land in the USA (Twidwell, Allred, & Fuhlendorf, 2013a). Our in-depth review can be thought of as a *Program by Program* compilation of policy-relevant documents. We reviewed cost-share/financial incentive programs, management plans, official memos, official protocols, or published technical guides for private landowners that related to eastern redcedar management in grasslands, forestry, or agriculture. This resulted in diverse policy representation spanning examples from multiple state and federal groups. We also engaged representatives from private citizen-led organizations in the region, such as the Sandhills Task Force, Loess Canyon Rangeland Alliance, and Nebraska Prescribed Fire Council, to identify landowner perceptions about relevant policies most affecting them. Specific policies are referenced in our policy assessment.

Land cover

We used 30 m resolution land cover data for the Nebraska which was provided by the Rainwater Basin Joint Venture (RWBJV) (Bishop, Barenberg, Volpe, & Grosse, 2011). This land cover dataset was created in 2010 by integrating 12 existing land cover datasets (e.g., the Landsat-derived National Land Cover Dataset, the Natural Agriculture Statistics Service land cover data, and the National Wetlands Inventory), in which classifications of layers higher in the stack superseded those of lower layers (Bishop et al., 2011). We chose the RWBJV dataset because it represents the most current Nebraska land cover dataset containing eastern redcedar as an explicit cover class. The resulting land cover was classified and hierarchically organized into divisions (i.e., level 1), types (i.e., level

2), associations (i.e., level 3), and conditions (i.e., level 4). Full details about the RWBJV dataset can be found in the RWBJV's report (Bishop et al., 2011).

The RWBJV dataset includes a specific eastern redcedar cover class, which we used to estimate percent cover of eastern redcedar in each ecoregion and the range of cover across individual land parcels. Within the hierarchical classification of the RWBJV dataset, the Eastern Redcedar cover class is nested within the Upland Forest/Woodland Association, which is nested within the Forests/Woodlands type, which is nested within the Terrestrial Division. In an informal evaluation, Bishop et al. (2011) found classification accuracy in the dataset to be ~95% for broad landscape categories (e.g., cropland, grassland, and woodland). Because the 30 m resolution of the RWBJV dataset may not detect low densities of eastern redcedar (incipient invasions) and a large proportion of the higher level classification of upland forest/woodland is likely eastern redcedar (but was not classified as eastern redcedar due to lower certainty), we expect eastern redcedar's cover across ecoregions to be somewhat under-represented (Bishop et al., 2011). Because eastern redcedar is actively removed from agricultural croplands and cannot invade extremely mesic sites (e.g., open water, riverine systems, and wetlands), we excluded these classes from the analysis.

We estimated eastern redcedar invasion stage by calculating percent coverage of eastern redcedar from RWBJV land cover data at the extent of each ecoregion. We selected ecoregions because many management strategies and priorities in Nebraska are directly or indirectly associated with the Natural Legacy Plan, which focuses on ecoregion-level planning and action across the entire state (Schneider et al., 2011). We

classified invasion stages according to the density-impact model, which establishes four invasive species management strategy stages based on sections of the sigmoidal curve and the range of invasive species percent cover/densities over which each strategy is most cost-effective. We derived specific percent cover cutoffs for each invasion stage classification from literature that quantified eastern redcedar's sigmoidal density/cover-economic impacts (e.g., the livestock industry) (Fuhlendorf et al., 2008) and grassland taxa biodiversity (Limb et al., 2010) relationship. The relationship between density-impact and population growth pattern has been established as sigmoidal for *Juniperus virginiana*, although there is uncertainty in exact locations of density-impact curve inflection points due to site differences (soils, precipitation) and the case-study nature of past published studies (Briggs et al., 2002; Fuhlendorf et al., 2008; Limb et al., 2010). Management and policy are tied to stages of invasive species' sigmoidal population growth and impacts patterns, with prevention being the strategy when an invasive species is absent or rare, eradication being the strategy during incipient invasion up until the beginning of rapid increase in impact/population just before peak growth rate on the sigmoidal curve, control being the strategy during the peak impact/population growth rate, and long-term management being the strategy just before the impact/population growth rate declines and becomes asymptotic (Yokomizo et al., 2009). The point at which impact approaches its maximum in the eastern redcedar density-impact relationship ranges between 60 and 90% cover due to site-dependent uncertainty (e.g., differences in soil type, precipitation) (Engle et al., 2008; Fuhlendorf et al., 2008), but because invasion ecology theory establishes the benefits of early and quick management

actions, we established our invasion stage cutoff based on the lowest (60% cover) estimate (Simberloff, 2003; Yokomizo et al., 2009). Accordingly, we classified 0 - <1% cover as the prevention stage, 1 - 10% cover as the eradication stage, 11 - 59% cover as the control stage, and >60% cover as the long-term management stage.

We then quantified the range of eastern redcedar cover in individual land parcels within each ecoregion. We received agency data to define the scale at which financial incentives programs are being operationalized on private lands and, thus, the appropriate scale to use as the basis for our policy assessment. Assessment of agency data showed eastern redcedar management policies are on average operationalized at 50-acre (approximately 20.2 ha) land parcels in Nebraska (Simonsen et al., 2015). For each ecoregion, we searched for the presence or absence of 20.2 ha cells (approximately 450 m x 450 m, or 225 pixels at 30 m resolution) that fell within each of the four invasion stages we established; that is, we searched for at least one 20.2 ha cell in which percent eastern redcedar percent cover corresponded to the prevention stage (0 - <1% cover), one cell for the eradication stage (1 - 10% cover), etc.

Evaluating policy-ecology agreement

We used policy and land cover data to assess the level of agreement between the specific eastern redcedar management policies of agencies and the general management recommendations derived from the density-impact model (Yokomizo et al., 2009). Our policy assessment focused on two functional scales: (1) the extent of individual ecoregions, and (2) the average spatial extent used for policy delivery. Both spatial scales

are currently used to make policy decisions and to provide technical guidance, even though related policies are not spatially-explicit.

RESULTS

Ecoregion-level abundance

Land cover data identified the stage of eastern redcedar invasion for three historically grass-dominated ecoregions within Nebraska (Table 9.1). Estimates of juniper woodland ranged from 19.66% in the Loess Canyons to 0.02% in the Cherry County Wetlands (Figure 9.4). Juniper woodland occurred on 9.54% of the Central Loess Hills (Figure 9.4).

Individual land parcels (20-ha)

Data on individual land parcels within each ecoregion showed that the minimum and maximum percent cover of eastern redcedar invasion in the Cherry County Wetlands was 0% - 22.67% cover, whereas invasion spanned the full range of cover (0 - 100% cover) in the Central Loess Hills and Loess Canyons ecoregions (Figure 9.5). According to the density-impact model adapted to the known density-impact relationship of eastern redcedar (Fuhlendorf et al., 2008), individual land parcels in the Cherry County Wetlands spanned the prevention, eradication, and control invasion stages, and land parcels in the Central Loess Hills and Loess Canyons ranged from prevention to long-term management stages (Figures 9.5, 9.6).

Policy assessment

Our policy assessment revealed that existing policies fail to align with theoretical expectations of the density-impact model for eastern redcedar. At the extent of an ecoregion, there is no evidence for prevention, eradication, or long-term management in policy (Table 9.2). Instead, policy promotes invasion (Table 9.2). Planting occurs in all ecoregions studied here. Statewide, natural resource agencies distributed on average 850,000 eastern redcedar seedlings per year from 1925 - 2001 (Ganguli et al., 2008), shifting to approximately 310,000 seedlings per year from 2001 to the present (Twidwell, D: (University of Nebraska-Lincoln, Lincoln, NE). Conversation with: Rich Gilbert (U.S. Forest Service, Nursery Manager, Bessey Nursery, Nebraska National Forest and Grassland). 2017., n.d.). Moreover, our study confirms that current practices and programs align primarily with levels of invasion that require controls to be implemented (Table 9.2). The controls are put into practice on a *Program by Program* basis following the identification of eastern redcedar as a resource concern (Figure 9.2). Controls are then authorized via policy to attempt to freeze the system in the desired range of percent cover. If these controls are not effective, or if they are not implemented prior to reaching a more advanced stage of invasion, then few directives are in place currently to implement long-term management at the extent of an entire ecoregion (Table 9.2).

We found no evidence that the density-impact model was being used to guide practices and behaviors at the ecoregion extent. All ecoregions are managed as if they are in the control stage of the invasion process. However, Cherry County Wetlands falls within the prevention stage at the ecoregion extent (Table 9.1). The Central Loess Hills

are at the eradication stage (Table 9.1), and the Loess Canyons were at levels of abundance consistent with the control stage (Tables 1 and 2). In summary, policies were implemented the same statewide, irrespective of the stage of invasion within each ecoregion (Table 9.2).

For individual land parcels, the average spatial extent at which financial incentives programs are typically delivered (20-ha), policies failed to match the density-impact invasion curve, except at the control stage (Table 9.2; Figure 9.6). Policy-guided prevention of incipient invasions were not prioritized on individual parcels of land in any ecoregion (Figure 9.6). Advocating planting of eastern redcedar was more evident, followed by control on the same given 20.2 ha parcel (e.g., establishing a windbreak and then removing invasions resulting from the windbreak) (Donovan et al., 2018). For the eradication stage, text within one policy (Natural Resources Conservation Service) (Natural Resources Conservation Service, n.d.-a) that encouraged treatment at relatively low density levels, but conservation expenditures for preventative treatments received little to no actual financial support/enrollment and incentives for acting at the control stage were the majority (Simonsen et al., 2015). At the control stage, policy was relatively consistent with the density-impact model (Table 9.2; Figure 9.6). However, we also found a control stage policy (from the Nebraska Forest Service) that states financial incentives or cost-share “CANNOT [emphasis theirs] be used to remove all tree vegetation from a site. A forest stand with [eastern red]cedar crop trees must remain after management” (Nebraska Forest Service, n.d.-a). In areas where the stage of invasion varies greatly, such as the Loess Canyons and Central Loess Hills, the invasion model

indicates that resources are typically best prioritized when invasive species are absent or in low abundance, and yet financial incentive programs prioritized funds in areas with greatest abundance (Figure 9.7; Table 9.2). Prevention in areas without eastern redcedar were given the least incentives (Figure 9.7). As an example, the Natural Resources Conservation Service's Environmental Quality Incentives Program in 2018 will provide \$196.48 per acre to help accomplish eastern redcedar removal in areas with high cover, \$95.48 per acre for moderate cover, \$37.50 per acre for low cover, and \$0 for when eastern redcedar is absent (Twidwell, D: (University of Nebraska-Lincoln, Lincoln, NE). Conversation with: Ritch Nelson (Natural Resources Conservation Service, Lincoln, Nebraska). 2017., n.d.). Policy delineating control from long-term management was not obvious, in general, but one policy did indicate that management actions beyond a 70% cover threshold may be economically infeasible (Natural Resources Conservation Service) (Natural Resources Conservation Service, n.d.-a).

DISCUSSION

We demonstrate that eastern redcedar management policy is mired in a doublethink mentality between historical management strategies that assume eastern redcedar is in equilibrium with its environment, and therefore, facilitate its spread, while simultaneously managing eastern redcedar as a native invader outside of equilibrium during late invasion stages (Engle et al., 2008; Fuhlendorf, Smeins, & Grant, 1996; Limb et al., 2010). Stalling management until later invasion stages means that policy effectively tries to halt eastern redcedar spread at its most rapid rate. Unless the mismatch between science and policy is resolved, there is no evidence that the current management

approach in Nebraska can stop grasslands from transitioning to eastern redcedar woodlands. Instead, both theory in invasion ecology and studies from other regions in the Great Plains on this native invader provide clear evidence for large-scale grass-to-woody transitions with profound impacts to ecosystem services (e.g., loss of education funding, livestock forage, and grassland ecosystems, increased pollen allergies, etc.) (Briggs et al., 2002; Mack et al., 2000; Twidwell et al., 2013c; Yokomizo et al., 2009).

Species invasions threaten ecosystem services at a range of scales from individual stakeholder land parcels to entire ecoregions, but policy and management actions often focus only on a single spatiotemporal scale or operate without consideration of the problems of scale in ecology (Simberloff, 2003; Wilgen et al., 2012). For instance, in Nebraska, although inter-agency management strategies (but not policies) are crafted at the extent of individual ecoregions (Schneider et al., 2011), the Natural Resources Conservation Service typically administers management piecemeal on an individual landowner basis-50 acre (20.2 ha) parcels on average (Simonsen et al., 2015; Twidwell et al., 2013a). This has led to local success in control and asset protection but has not affected the larger ecoregion or biome-scale transformation caused by eastern redcedar's spread (Engle et al., 2008; Twidwell et al., 2013c). Similarly, eastern redcedar management policies are not consistent among natural resource agencies and instead reflect a localized decision-making process and value-oriented disparities (e.g., wildlife habitat and windbreak plantings versus grassland restoration-motivated removal) that inhibit consistent, effective policy implementation.

Scale mismatches also reduce the potential for policy to meet sustainability targets. Information from one spatial extent can prevent policy change or necessary investments when information at another spatial scale warns of impending change within the socio-ecological system. This often results from misconceptions about the temporal scaling of invasion relative to the social constraints that limit the spatial extent of management interventions (Twidwell et al., 2016). As a result, invasions can temporarily go undetected or be ignored, despite clear scientific knowledge showing temporal lags between introduction and rapid population growth (Carey et al., 2012; Crooks, 2005; Crooks, Soulé, & Sandlund, 1999; Epanchin-Niell & Liebhold, 2015; Simberloff, 2009; Simberloff et al., 2012; Wittmann, Metzler, Gabriel, & Jeschke, 2014). This study provides a key example of scale mismatches in policy. For example, in the Cherry County Wetlands, the apparent lack of eastern redcedar spread at the ecoregion extent (percentage of ecoregion with juniper woodland = 0.02%) has been cited as an indication that eastern redcedar will never pose a threat in that ecoregion and can therefore be planted indiscriminately (Yokomizo et al., 2009). Counter to this logic, we demonstrate incipient invasions in the Cherry County Wetlands at the level of individual land parcels. This indicates that using a finer spatial resolution should be used to guide changes in program implementation would be more effective and science-supported, particularly given the economic costs of failing to act at the early stages of the invasion process. Understanding the scale to operationalize information and justify policy decisions that would therefore avoid tendencies to misidentify risks within an ecoregion. This is particularly important to the livelihoods for citizens within the Cherry County Wetlands,

which is located in the Sandhills ecoregion-one of the largest intact grassland remaining in the USA, where the economy relies heavily on grasslands for livestock production.

To succeed at preventing or mitigating damage from invasive species, theory and literature emphasize the importance of matching management actions with the scale of invasion (Chaffin et al., 2016; Nel et al., 2004; B. W. Van Wilgen et al., 2011). Policies and management actions that prevent or eradicate invasions in their early stages clearly match theory on the spatiotemporal scale of invasions, and consequently, are orders of magnitude more cost-effective than waiting for studies to find the most refined methods for combatting invasions (Mack et al., 2000; Simberloff, 2003; @ Yokomizo et al., 2009). For example, conducting a prescribed burn to eradicate eastern redcedar from grasslands capable of carrying fire can potentially have negligible costs, whereas the Nebraska Natural Resources Conservation Service's policy indicates that lands with >70% eastern redcedar cover are economically infeasible to manage (Natural Resources Conservation Service, n.d.-a; Simonsen et al., 2015). Despite this, one example of doublethink is that policy from one agency provides tax-supported payment programs for eastern redcedar control that increase reimbursements with increasing eastern redcedar cover (Twidwell, D: (University of Nebraska-Lincoln, Lincoln, NE). Conversation with: Ritch Nelson (Natural Resources Conservation Service, Lincoln, Nebraska). 2017., n.d.), while policy from another agency insists that some mature, seed-bearing eastern redcedar remain after control treatments to continue to facilitate their spread (Nebraska Forest Service, n.d.-a). Because eastern redcedar does not resprout after cutting and high intensity burn treatments have been shown to cause 100% mortality even in mature trees

(Twidwell et al., 2013b), management at any invasion stage could potentially lead to eradication from locations where eastern redcedar is unlikely to have been present historically. However, fire ban policies, strict liability for fire damage, and lack of private citizen knowledge of safe prescribed burning techniques precludes high intensity fires for late-stage management in many cases (Twidwell et al., 2013c, 2016).

Policy implications

Our results highlight the need for scientists, policy makers, and ecosystem managers to move past ideologies governing the classification of native versus non-native invaders and toward a new framework that takes into account the scale of invasions, the uniqueness of native species invasions in policy creation, and their impacts on ecosystem services. Doublethink policy approaches that simultaneously acknowledge the spread of native invaders as problematic while facilitating that spread, as in the case of eastern redcedar in the Great Plains, can result in just as deleterious consequences as those associated with the spread of non-native invaders (Carey et al., 2012; Twidwell et al., 2016). Scientists could further advance the scientific basis of management for the native invader eastern redcedar, and others, by adapting additional existing models originally designed for non-native species which include their transport, distribution, scale issues, and colonization of new areas. By continuing to match and extend policy with current scientifically-based models, natural resource agencies can dispel doublethink in their policies and increase chances of success in invasive species management.

Federal policy directives governing invasive species management can be used as a path forward for local-to-regional policy revisions. Federal policies for invasive species

have built-in controls meant to avoid doublethink (Figure 9.2). Agencies are not authorized to fund or conduct actions that cause or promote the introduction or spread of invasive species, unless public declarations have been made that the benefits of such actions clearly outweigh potential social and environmental damages (U.S. Presidential Executive Order 13112 Invasive Species, n.d.). Waiting to initiate management and/or to cease intentional introductions until it becomes a discernable socio-ecological problem represents a classical challenge in invasive species management that the executive mandate was meant to resolve (Figure 9.3). Federal policy also fosters transparency by requiring agencies to publicly declare that the benefits of promoting an invasive species clearly outweigh the potential for socioeconomic and environmental damages. For eastern redcedar invasions, policies make the equilibrium-based assumption that management can freeze eastern redcedar abundance within a desirable range that allows the benefits of planting while also minimizing or avoiding damages. However, literature and past invasive species management failures warn that these doublethink policies lack empirical support and are not science-based. The evidence instead indicates that such narratives over-promise benefits to society while also underplaying risks to the sustainability of ecosystem services into the future. In the case of eastern redcedar invasions, the risks to ecosystem services have been well-documented, but the local benefits (e.g., individual windbreak plantings) have not been shown to outweigh the economic losses associated with biome-level regime shifts across the Great Plains.

Understanding the risks of these equilibrial policy assumptions will allow policy-makers and natural resource agencies to craft ecologically-informed policies that question

deeply-rooted practices known to erode resilience in socio-ecological systems. In reflexive law, the principle of information disclosure has been useful for providing the ability to shift away from past governance ideologies and toward more resilience-based governance structures when attempting to justify current recommendations and technical guidance (Garmestani & Benson, 2013). This is the basis for federal disclosure of non-native invasions, and our study highlights the need to disclose such information for native invaders like eastern redcedar. We demonstrate an example of invasive species management policy that essentially communicates that the benefits of establishing eastern redcedar trees clearly outweighs the potential consequences (i.e., by promoting eastern redcedar regardless of invasion stage). This clear example of doublethink counters the current scientific consensus and prevents the adaptation of existing policy to include preventative actions under the authority of natural resource professionals.

LITERATURE CITED

- Bessey, C. E. (1900). *The forests and forest trees of Nebraska. Reprinted from the Annual Report of the Nebraska State Board of Agriculture, 1899*. State journal Company Printers, Lincoln, NE, USA.
- Bidwell, T. G., Engle, D. M., Moseley, M. E., & Master, R. E. (1990). Invasion of Oklahoma rangelands and forests by eastern redcedar and Ashe juniper. *Oklahoma State University Extension*.
- Bishop, A. A., Barenberg, A., Volpe, N., & Grosse, R. (2011). Nebraska land cover development, Rainwater Basin Joint Venture report. Available from:

<http://rwbjv.org/wp-content/uploads/2013/06/Nebraska-Landcover-Version-101.pdf>.

- Briggs, J. M., Hoch, G. A., & Johnson, L. C. (2002). Assessing the rate, mechanisms, and consequences of the conversion of tallgrass prairie to *Juniperus virginiana* forest. *Ecosystems*, 5(6), 578–586.
- Briggs, J. M., Knapp, A. K., Blair, J. M., Heisler, J. L., Hoch, G. A., Lett, M. S., & McCARRON, J. K. (2005). An ecosystem in transition: Causes and consequences of the conversion of mesic grassland to shrubland. *BioScience*, 55(3), 243–254.
- Carey, M. P., Sanderson, B. L., Barnas, K. A., & Olden, J. D. (2012). Native invaders—challenges for science, management, policy, and society. *Frontiers in Ecology and the Environment*, 10(7), 373–381.
- Chaffin, B. C., Garmestani, A. S., Angeler, D. G., Herrmann, D. L., Stow, C. A., Nyström, M., ... Allen, C. R. (2016). Biological invasions, ecological resilience and adaptive governance. *Journal of Environmental Management*, 183, 399–407.
- Coppedge, B. R., Engle, D. M., Masters, R. E., & Gregory, M. S. (2001). Avian response to landscape change in fragmented southern Great Plains grasslands. *Ecological Applications*, 11(1), 47–59.
- Crooks, J. A. (2005). Lag times and exotic species: The ecology and management of biological invasions in slow-motion. *Ecoscience*, 12(3), 316–329.

- Crooks, J. A., Soulé, M. E., & Sandlund, O. (1999). Lag times in population explosions of invasive species: Causes and implications. In *Invasive species and biodiversity management* (pp. 103–125). Springer Science & Business Media.
- Cumming, G. S., Olsson, P., Chapin, F., & Holling, C. (2013). Resilience, experimentation, and scale mismatches in social-ecological landscapes. *Landscape Ecology*, 28(6), 1139–1150.
- Donovan, V. M., Burnett, J. L., Bielski, C. H., Birgé, H. E., Bevans, R., Twidwell, D., & Allen, C. R. (2018). Social–ecological landscape patterns predict woody encroachment from native tree plantings in a temperate grassland. *Ecology and Evolution*, 8(19), 9624–9632.
- Engle, D. M., Coppedge, B. R., & Fuhlendorf, S. D. (2008). From the dust bowl to the green glacier: Human activity and environmental change in Great Plains grasslands. *Western North American Juniperus Communities*, 253–271.
- Epanchin-Niell, R. S., & Hastings, A. (2010). Controlling established invaders: Integrating economics and spread dynamics to determine optimal management. *Ecology Letters*, 13(4), 528–541.
- Epanchin-Niell, R. S., & Liebhold, A. M. (2015). Benefits of invasion prevention: Effect of time lags, spread rates, and damage persistence. *Ecological Economics*, 116, 146–153.

Epanchin-Niell, R. S., Haight, R. G., Berec, L., Kean, J. M., & Liebhold, A. M. (2012).

Optimal surveillance and eradication of invasive species in heterogeneous landscapes. *Ecology Letters*, 15(8), 803–812.

Frémont, J. C. (1845). *Report of the exploring expedition to the Rocky Mountains in the year 1842 and to Oregon and North California in the years 1843-44: Printed by order of the Senate of the United States* (Vol. 174). Gales & Seaton.

Fuhlendorf, S. D., Archer, S. A., Smeins, F., Engle, D. M., & Taylor Jr, C. A. (2008). The combined influence of grazing, fire, and herbaceous productivity on tree–grass interactions. In *Western North American Juniperus communities* (pp. 219–238). Springer.

Fuhlendorf, S. D., Smeins, F. E., & Grant, W. E. (1996). Simulation of a fire-sensitive ecological threshold: A case study of Ashe juniper on the Edwards Plateau of Texas, USA. *Ecological Modelling*, 90(3), 245–255.

Ganguli, A. C., Engle, D. M., Mayer, P. M., & Fuhlendorf, S. D. (2008). When are native species inappropriate for conservation plantings? *Rangelands*, 30(6), 27–32.

Garmestani, A. S., & Benson, M. H. (2013). A framework for resilience-based governance of social-ecological systems. *Ecology and Society*, 18(1).

Head, L., Larson, B. M., Hobbs, R., Atchison, J., Gill, N., Kull, C., ... others. (2015).

Living with invasive plants in the anthropocene: The importance of understanding practice and experience. *Conservation and Society*, 13(3), 311.

Horncastle, V. J., Hellgren, E. C., Mayer, P. M., Ganguli, A. C., Engle, D. M., & Leslie Jr, D. M. (2005). Implications of invasion by *Juniperus virginiana* on small mammals in the southern Great Plains. *Journal of Mammalogy*, 86(6), 1144–1155.

Institute of Agriculture and Natural Resources, University of Nebraska-Lincoln. (n.d.). Eastern Redcedar Science Literacy Project. Available from:
<https://agronomy.unl.edu/eastern-redcedar-science-literacy-project/impacts>.
 Accessed 2017-11-15.

Johnsgard, P. A. (2005). *The nature of Nebraska: Ecology and biodiversity*. U of Nebraska Press.

Lawson, E. R. (1990). *Juniperus virginiana* L. eastern redcedar. *Silvics of North America*, 1, 131–140.

Limb, R. F., Engle, D. M., Alford, A. L., & Hellgren, E. C. (2010). Tallgrass prairie plant community dynamics along a canopy cover gradient of eastern redcedar (*Juniperus virginiana* L.). *Rangeland Ecology & Management*, 63(6), 638–644.

Loess Canyons Rangeland Alliance. (n.d.). Available from:
<http://www.loesscanyonsburngroup.com/>. Accessed 2017-11-16.

Mack, R. N., Simberloff, D., Mark Lonsdale, W., Evans, H., Clout, M., & Bazzaz, F. A. (2000). Biotic invasions: Causes, epidemiology, global consequences, and control. *Ecological Applications*, 10(3), 689–710.

- Meneguzzo, D. M., & Liknes, G. C. (2015). Status and trends of eastern redcedar (*Juniperus virginiana*) in the central United States: Analyses and observations based on forest inventory and analysis data. *Journal of Forestry*, 113(3), 325–334.
- Nackley, L. L., West, A. G., Skowno, A. L., & Bond, W. J. (2017). The nebulous ecology of native invasions. *Trends in Ecology & Evolution*, 32(11), 814–824.
- Natural Resources Conservation Service. (n.d.-a). Brush Management Design Procedure 314DP. Available from:
<https://efotg.sc.egov.usda.gov/references/public/NE/NE314DP.pdf>. Accessed 2017-05-13.
- Natural Resources Conservation Service. (n.d.-b). Conservation Practice Standard: Brush Management 314. Available from:
<https://efotg.sc.egov.usda.gov/references/public/NE/NE314.pdf>. Accessed 2017-05-13.
- Natural Resources Conservation Service. (n.d.-c). Conservation Practice Standard: Tree/Shrub Establishment 612. Available from:
<https://efotg.nrcs.usda.gov/references/public/NE/NE612.pdf>. Accessed 2017-05-13.
- Natural Resources Conservation Service. (n.d.-d). Conservation Practice Standard: Windbreak/Shelterbelt Establishment 380. Available from:
https://efotg.sc.egov.usda.gov/references/public/NE/NE380_SOW.pdf. Accessed 2017-05-13.

Natural Resources Conservation Service. (n.d.-e). Environmental Quality Incentives

Program. Available from:

<https://www.nrcs.usda.gov/wps/portal/nrcs/main/ne/programs/financial/equip/>.

Accessed 2017-06-18.

Natural Resources Conservation Service. (n.d.-f). Tree/Shrub Establishment Design

Procedure 612DP. Available from:

<https://efotg.sc.egov.usda.gov/references/public/NE/NE612DP.pdf>. Accessed

2017-05-13.

Nebraska Conservation Roundtable. 2014. (n.d.). Available from: . Accessed 2017-11-17.

Nebraska Department of Natural Resources. (n.d.).

<https://dnr.nebraska.gov/data/elevation-data>.

Nebraska Forest Service. (n.d.-a). Fuels Reduction/Forest Restoration. Available from:

<http://nfs.unl.edu/fuels-assistance>. Accessed 2017-06-13.

Nebraska Forest Service. (n.d.-b). { Windbreak Management. Available from:

https://www.google.com/url?sa=t&rct=j&q=&esrc=s&source=web&cd=1&cad=rja&uact=8&ved=0ahUKEwjJxuqi7-3TAhVhw4MKHShAA34QFggnMAA&url=http%3A%2F%2Fdigitalcommons.unl.edu%2Fextensionhist%2F838%2F&usg=AFQjCNFVxp8bWLCBBACLZ1SjfLGBRzJa6w&sig2=SjdAwDTsrh_5CkHqQySTTw.

Accessed 2017-05-13.

Nebraska Forest Service. (n.d.-c). Windbreak Design. Available from:

https://www.google.com/url?sa=t&rct=j&q=&esrc=s&source=web&cd=1&cad=rja&uact=8&ved=0ahUKEwjAop-_7u3TAhVh34MKHRD9AAsQFggnMAA&url=http%3A%2F%2Fnfs.unl.edu%2Fdocuments%2Fwindbreakdesign.pdf&usg=AFQjCNG1XwR8FYIHWeJbz1GfCGrz3CVQxQ&sig2=C5JX4To6clY0gFactD4X8g. Accessed 2017-05-13.

Nebraska Invasive Species Council. (n.d.). Nebraska Invasive Species Program.

Available from: <https://neinvasives.com/species/plants/eastern-redcedar/>.
Accessed 2017-11-15.

Nebraska Natural Resource Districts. (n.d.-a). Conservation Trees for Nebraska: Eastern Red Cedar. Available from:

http://www.nrdtrees.org/species.php?image=e_red_cedar_full.jpg. Accessed 2017-05-13.

Nebraska Natural Resource Districts. (n.d.-b). Conservation Trees for Nebraska:

Services. Available from: <http://www.nrdtrees.org/services.html>. Accessed 2017-05-13.

Nel, J., Richardson, D., Rouget, M., Mgidi, T., Mdzeke, N., Le Maitre, D., ... Naser, S.

(2004). A proposed classification of invasive alien plant species in South Africa: Towards prioritizing species and areas for management action: Working for water. *South African Journal of Science*, 100(1-2), 53–64.

- Pimentel, D., Zuniga, R., & Morrison, D. (2005). Update on the environmental and economic costs associated with alien-invasive species in the United States. *Ecological Economics*, 52(3), 273–288.
- Ratajczak, Z., Briggs, J. M., Goodin, D. G., Luo, L., Mohler, R. L., Nippert, J. B., & Obermeyer, B. (2016). Assessing the potential for transitions from tallgrass prairie to woodlands: Are we operating beyond critical fire thresholds? *Rangeland Ecology & Management*, 69(4), 280–287.
- Sandhills Task Force. (n.d.). Available from: <http://sandhillstaskforce.org/>. Accessed 2017-11-16.
- Schneider, R., Stoner, K., Steinauer, G., Panella, M. J., Humpert, M., Game, N., ... others. (2011). *The Nebraska natural legacy project: State wildlife action plan*.
- Simberloff, D. (2003). How much information on population biology is needed to manage introduced species? *Conservation Biology*, 17(1), 83–92.
- Simberloff, D. (2009). The role of propagule pressure in biological invasions. *Annual Review of Ecology, Evolution, and Systematics*, 40, 81–102.
- Simberloff, D., Souza, L., Nuñez, M. A., Barrios-Garcia, M. N., & Bunn, W. (2012). The natives are restless, but not often and mostly when disturbed. *Ecology*, 93(3), 598–607.

- Simonsen, V. L., Fleischmann, J. E., Whisenhunt, D. E., Volesky, J. D., & Twidwell, D. (2015). Act now or pay later: Evaluating the cost of reactive versus proactive eastern redcedar management. *Nebraska Extension Publications*.
- Stewart-Koster, B., Olden, J. D., & Johnson, P. T. (2015). Integrating landscape connectivity and habitat suitability to guide offensive and defensive invasive species management. *Journal of Applied Ecology*, 52(2), 366–378.
- Streit Krug, A., Uden, D. R., Allen, C. R., & Twidwell, D. (2017). Culturally induced range infilling of eastern redcedar: A problem in ecology, an ecological problem, or both? *Ecology and Society*, in press.
- Twidwell, D., Allred, B. W., & Fuhlendorf, S. D. (2013a). National-scale assessment of ecological content in the world's largest land management framework. *Ecosphere*, 4(8), 1–27.
- Twidwell, D., Fuhlendorf, S. D., Taylor, C. A., & Rogers, W. E. (2013b). Refining thresholds in coupled fire–vegetation models to improve management of encroaching woody plants in grasslands. *Journal of Applied Ecology*, 50(3), 603–613.
- Twidwell, D., Rogers, W. E., Fuhlendorf, S. D., Wonkka, C. L., Engle, D. M., Weir, J. R., ... Taylor, C. A. (2013c). The rising great plains fire campaign: Citizens' response to woody plant encroachment. *Frontiers in Ecology and the Environment*, 11(s1).

Twidwell, D., West, A. S., Hiatt, W. B., Ramirez, A. L., Winter, J. T., Engle, D. M., ...

Carlson, J. (2016). Plant invasions or fire policy: Which has altered fire behavior more in tallgrass prairie? *Ecosystems*, 19(2), 356–368.

Twidwell, D: (University of Nebraska-Lincoln, Lincoln, NE). Conversation with: Rich Gilbert (U.S. Forest Service, Nursery Manager, Bessey Nursery, Nebraska National Forest and Grassland). 2017. (n.d.).

Twidwell, D: (University of Nebraska-Lincoln, Lincoln, NE). Conversation with: Ritch Nelson (Natural Resources Conservation Service, Lincoln, Nebraska). 2017. (n.d.).

U.S. Geological Survey. (n.d.).

<https://www.sciencebase.gov/catalog/item/4fb55169e4b04cb937751d9b>.

U.S. Presidential Executive Order 13112 Invasive Species. (n.d.). Executive Order 13112 Invasive Species. Available from:
<https://www.invasivespeciesinfo.gov/laws/execorder.shtml>. Accessed 2017-11-16.

Uden, D. R., Allen, C. R., Angeler, D. G., Corral, L., & Fricke, K. A. (2015). Adaptive invasive species distribution models: A framework for modeling incipient invasions. *Biological Invasions*, 17(10), 2831–2850.

United States Forest Service. (n.d.-a). Bessey Woody Encroachment Project. Available from: <https://www.fs.usda.gov/project/?project=49547>. Accessed 2017-05-13.

United States Forest Service. (n.d.-b). Charles E. Bessey Tree Nursery. Available from:

<https://www.fs.usda.gov/detail/nebraska/about-forest/districts/?cid=stelprdb5343059>. Accessed 2017-05-13.

United States Forest Service. (n.d.-c). Decision Memo: McKelvie Woody Encroachment

Project. Available from: <https://www.fs.usda.gov/project/?project=43769>. Accessed 2017-05-13.

United States Forest Service. (n.d.-d). Decision Memo: Bessey Woody Encroachment

Project. Available from:

https://www.google.com/url?sa=t&rct=j&q=&esrc=s&source=web&cd=2&cad=rja&uact=8&ved=0ahUKEwiAtvr97-3TAhVkxYMKHfoSC8MQFggrMAE&url=http%3A%2F%2Fa123.g.akamai.net%2F7%2F123%2F11558%2Fabc123%2Fforestservic.download.akamai.com%2F11558%2Fwww%2Fnepa%2F98093_FSPLT3_1664434.pdf&usg=AFQjCNFUWXJSyW7IIDdwdeXE9cIRpZk6BA&sig2=hbDlDEhu6nxEWi2_0CNxhw. Accessed 2017-05-13.

Van Wilgen, B. W., Dyer, C., Hoffmann, J. H., Ivey, P., Le Maitre, D. C., Moore, J. L.,

... Wilson, J. R. (2011). National-scale strategic approaches for managing introduced plants: Insights from Australian acacias in South Africa. *Diversity and Distributions*, 17(5), 1060–1075.

- Vilà, M., Espinar, J. L., Hejda, M., Hulme, P. E., Jarošík, V., Maron, J. L., ... Pyšek, P. (2011). Ecological impacts of invasive alien plants: A meta-analysis of their effects on species, communities and ecosystems. *Ecology Letters*, *14*(7), 702–708.
- Vítková, M., Müllerová, J., Sádlo, J., Pergl, J., & Pyšek, P. (2017). Black locust (*Robinia pseudoacacia*) beloved and despised: A story of an invasive tree in central Europe. *Forest Ecology and Management*, *384*, 287–302.
- Ware, E. F. (1960). *The Indian War of 1864*. St. Martin's Press.
- Wilgen, B. W. van, Forsyth, G. G., Le Maitre, D. C., Wannenburgh, A., Kotzé, J. D., Berg, E. van den, & Henderson, L. (2012). An assessment of the effectiveness of a large, national-scale invasive alien plant control strategy in south africa. *Biological Conservation*, *148*(1), 28–38.
- Wittmann, M. J., Metzler, D., Gabriel, W., & Jeschke, J. M. (2014). Decomposing propagule pressure: The effects of propagule size and propagule frequency on invasion success. *Oikos*, *123*(4), 441–450.
- Yokomizo, H., Possingham, H. P., Thomas, M. B., & Buckley, Y. M. (2009). Managing the impact of invasive species: The value of knowing the density–impact curve. *Ecological Applications*, *19*(2), 376–386.

TABLES

Table 9. 1: Percent land cover estimates for three ecoregions in Nebraska, USA. Columns indicate ecoregion name, the total land area within each ecoregion, the subset of land within ecoregions susceptible to eastern redcedar (ERC) invasion, the total land area classified as eastern redcedar, and the percent of susceptible land (i.e., cropland, riverine systems, wetland, and open water classes were not susceptible and were therefore removed from the analysis) covered by eastern redcedar. Land cover was estimated in 2010 and is derived from the Rainwater Basin Joint Venture 30 m remotely-sensed land cover dataset.

Ecoregion	Total Area (ha)	Area Susceptible to ERC (ha)	ERC Cover Area (ha)	Percent ERC Cover
Cherry County Wetlands	709,202.07	627,533.73	140.49	0.02%
Central Loess Hills	567,620.19	389,500.02	37,168.29	9.54%
Loess Canyons	136,765.53	112,993.74	22,214.79	19.66%

Table 9. 2: Examples of agency policies and programs used to manage eastern redcedar and how they align with the scientific basis for invasive species management based on the density-impact invasion curve. Asterisks denote agency programs with scientific support.

Invasion stage	Degree of policy alignment with scientific recommendations	Policy description	Examples of agency programs
Prevention	Strongly misaligned	Spread is encouraged and facilitated. Preventative actions are not evident.	<ul style="list-style-type: none"> Nurseries grow and distribute seedlings¹. Planting for windbreaks/shelterbelts, wildlife habitat, soil erosion control facilitated².
Eradication	Misaligned	Spread is encouraged and facilitated. Eradication only occurs at small scales within heavily-invaded landscapes.	<ul style="list-style-type: none"> Planting for windbreaks/shelterbelts, wildlife habitat, soil erosion control facilitated³. Management is not implemented until cover reaches 5-20%⁴. Eradication implemented for small patches within eastern redcedar woodlands⁵. Landowners encouraged to remove eastern redcedar by themselves at less than 5% cover⁶.
Control	Mostly aligned	Removal encouraged and facilitated, but control actions are typically implemented at local-scales. Planting is still facilitated.	<ul style="list-style-type: none"> Planting for windbreaks/shelterbelts, wildlife habitat, soil erosion control facilitated⁷. Cost-share for control available⁸.* Control suggested before 70% cover is reached⁹.* On average, management focuses on 50 acre land parcels¹⁰. Mature crop trees must remain after cost-share removal¹¹.
Long-term Management	Misaligned	Removal facilitated at local-scales to protect resources of importance, but more	<ul style="list-style-type: none"> Planting for windbreaks/shelterbelts, wildlife habitat, soil erosion control facilitated¹².

resources are allocated
than theory supports.
Planting is still
facilitated.

- Large-scale management is considered economically infeasible^{13,*}
- Eastern redcedar removed to protect isolated grassland and livestock forage resources^{14,*}
- Financial incentive programs for eastern redcedar removal provide the greatest payments for the most heavily-invaded parcels¹⁵.

NOTES: Asterisks indicate policies that align with ecology. Superscript numbers indicate the following citations:

¹ (Nebraska Natural Resource Districts, n.d.-a, -b; Twidwell, D: (University of Nebraska-Lincoln, Lincoln, NE). Conversation with: Rich Gilbert (U.S. Forest Service, Nursery Manager, Bessey Nursery, Nebraska National Forest and Grassland). 2017., n.d.; United States Forest Service, n.d.-b)

² (Natural Resources Conservation Service, n.d.-c, -f, -d; Nebraska Forest Service, n.d.-b, -c)

³ (Natural Resources Conservation Service, n.d.-c, -f, -d; Nebraska Forest Service, n.d.-b, -c; Nebraska Natural Resource Districts, n.d.-a, -b; Twidwell, D: (University of Nebraska-Lincoln, Lincoln, NE). Conversation with: Rich Gilbert (U.S. Forest Service, Nursery Manager, Bessey Nursery, Nebraska National Forest and Grassland). 2017., n.d.; United States Forest Service, n.d.-b)

⁴ (Natural Resources Conservation Service, n.d.-a, -b; Twidwell, D: (University of Nebraska-Lincoln, Lincoln, NE). Conversation with: Ritch Nelson (Natural Resources Conservation Service, Lincoln, Nebraska). 2017., n.d.)

⁵ (United States Forest Service, n.d.-d, -a, -c)

⁶ (Natural Resources Conservation Service, n.d.-f)

⁷ (Natural Resources Conservation Service, n.d.-c, -f, -d; Nebraska Forest Service, n.d.-b, -c; Nebraska Natural Resource Districts, n.d.-a, -b; Twidwell, D: (University of Nebraska-Lincoln, Lincoln, NE). Conversation with: Rich Gilbert (U.S. Forest Service, Nursery Manager, Bessey Nursery, Nebraska National Forest and Grassland). 2017., n.d.; United States Forest Service, n.d.-b)

⁸ (Natural Resources Conservation Service, n.d.-e; Nebraska Forest Service, n.d.-a)

⁹ (Natural Resources Conservation Service, n.d.-b, -a)

¹⁰ (Simonsen et al., 2015)

¹¹ (Nebraska Forest Service, n.d.-a)

¹² (Natural Resources Conservation Service, n.d.-c, -f, -d; Nebraska Forest Service, n.d.-b, -c; Nebraska Natural Resource Districts, n.d.-a, -b; Twidwell, D: (University of Nebraska-Lincoln, Lincoln, NE). Conversation with: Rich Gilbert (U.S. Forest Service, Nursery Manager, Bessey Nursery, Nebraska National Forest and Grassland). 2017., n.d.; United States Forest Service, n.d.-b)

¹³ (Natural Resources Conservation Service, n.d.-b, -a)

¹⁴ (Natural Resources Conservation Service, n.d.-e; Nebraska Forest Service, n.d.-a; United States Forest Service, n.d.-d, -a, -c) (Natural Resources Conservation Service, n.d.-e; Nebraska Forest Service, n.d.-a; Twidwell, D: (University of Nebraska-Lincoln, Lincoln, NE). Conversation with: Ritch Nelson (Natural Resources Conservation Service, Lincoln, Nebraska). 2017., n.d.)

¹⁵ (Natural Resources Conservation Service, n.d.-e; Nebraska Forest Service, n.d.-a; Twidwell, D: (University of Nebraska-Lincoln, Lincoln, NE). Conversation with: Ritch Nelson (Natural Resources Conservation Service, Lincoln, Nebraska). 2017., n.d.)

FIGURES

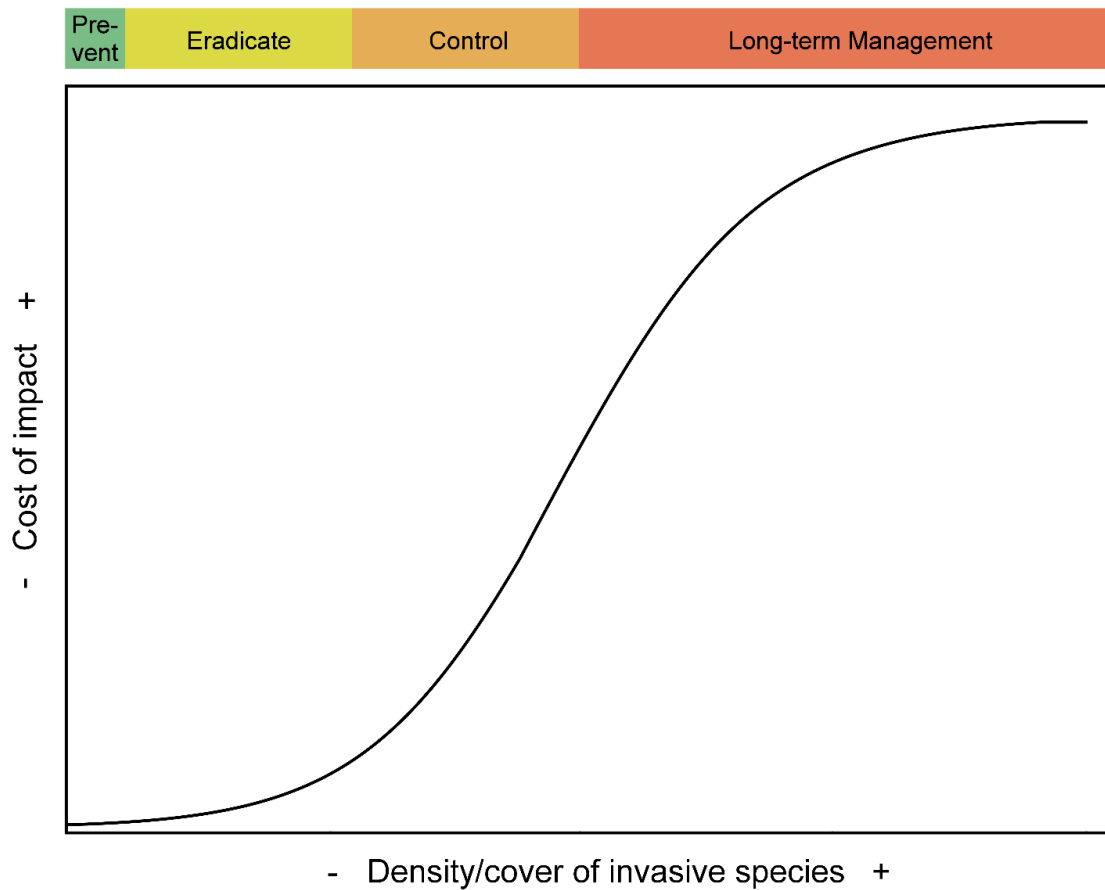


Figure 9. 1: Type II density-impact invasion curve adapted from Yokomizo et al. (2009).

Depicts the sigmoidal relationship between an invasive species' density or area covered and the cost or impact to socio-ecological systems. The colored bar above the curve shows preferable management strategies for the four stages of invasion based on feasibility, likelihood of success, and cost-effectiveness.

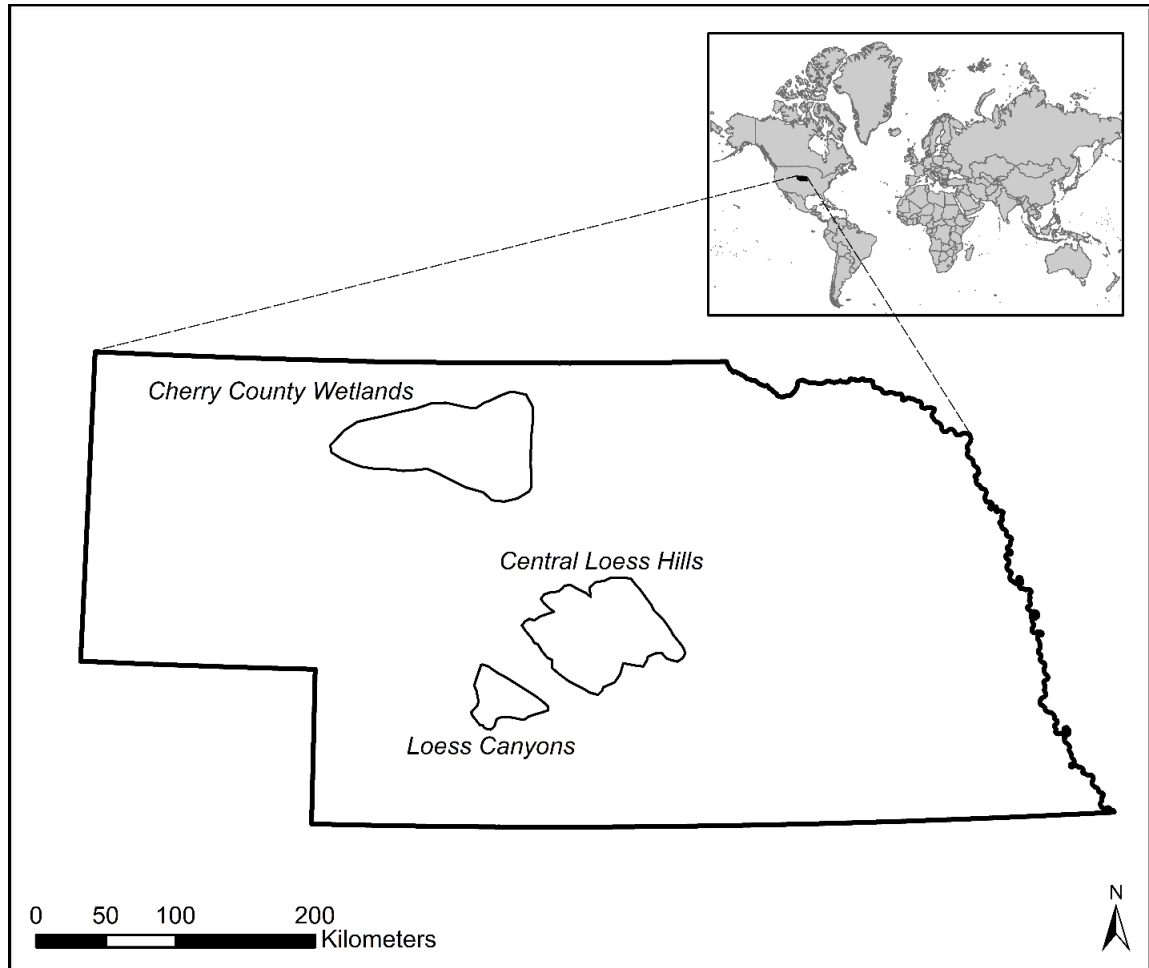


Figure 9. 2: Study site. Locations of three ecoregions that are a priority for grassland conservation, according to the Nebraska Legacy Project, and which form the basis for assessing the degree of concordance between policy and science in the management of the native invader eastern redcedar (*Juniperus virginiana*) in Nebraska, USA.




Invasive species policy process	Policy directives	Duty and authority
Federal legal mandates 	Executive order 1332, 13751	<ul style="list-style-type: none"> Prevent the introduction of exotic invasive species, respond rapidly to control exotic invasions in a cost-effective and environmentally sound manner, monitor exotic invasives accurately and reliably, restore native species and habitat conditions in ecosystems that have been invaded, conduct research and develop technologies to prevent introduction and provide for sound control, and promote public education on invasive species and the means to address them. Do not authorize, fund, or carry out actions that cause or promote the introduction or spread of exotic invasive species unless the agency has determined and made public that the benefits of such actions clearly outweigh the potential harm and that all feasible and prudent measures to minimize risk of harm will be taken in conjunction with the actions.
Regional legislative councils 	Nebraska Invasive Species Council	<ul style="list-style-type: none"> Recommend actions to minimize the effects of harmful invasive species on Nebraska's citizens in order to promote the economic and environmental well-being of the state. Develop and periodically update a statewide adaptive management plan for invasive species as described in section 15 of the (state) legislation. Serve as a forum for discussion, identification, and understanding of invasive species issues. Facilitate communication, cooperation, and coordination of local, state, federal, private, and nongovernmental entities for prevention, control, and management of invasive species. Assist with public outreach and awareness of invasive species issues. Provide information to the legislature for decision-making, planning, and coordination of invasive species management and prevention.
Internal agency frameworks/policies 	State-and-transition models in USDA NRCS Ecological Site Description Database	<ul style="list-style-type: none"> Recommend, develop and support policy and procedures to review, approve, and provide quality controls and assurance and manage data. Identify and define sites and transitions for use in inventory, monitoring, evaluation and management of rangelands.
Program by program (contextual) basis	National or state EQIP Initiatives; Landscape Conservation Initiatives; Local working groups; Multi-stakeholder district meetings	<ul style="list-style-type: none"> Enhance the locally driven process to better address nationally and regionally important conservation goals that transcend localities. Implement contracts and easement agreements through existing programs authorities. Connect partners with producers and private landowners to design and implement voluntary conservation solutions. Demonstrate solutions, contributions, innovation and participation so that benefits extend beyond the Federal investments.

Figure 9. 3: Outline of the hierarchical invasive species management policy creation process for USA natural resources agencies. Arrows indicate the direction of hierarchical control, with federal legal mandates being the highest level. Columns represent the policy creation process (first column), examples of groups that create, enforce, and implement the policies (second column), and the policy-directed duties of the groups at each level (third column).

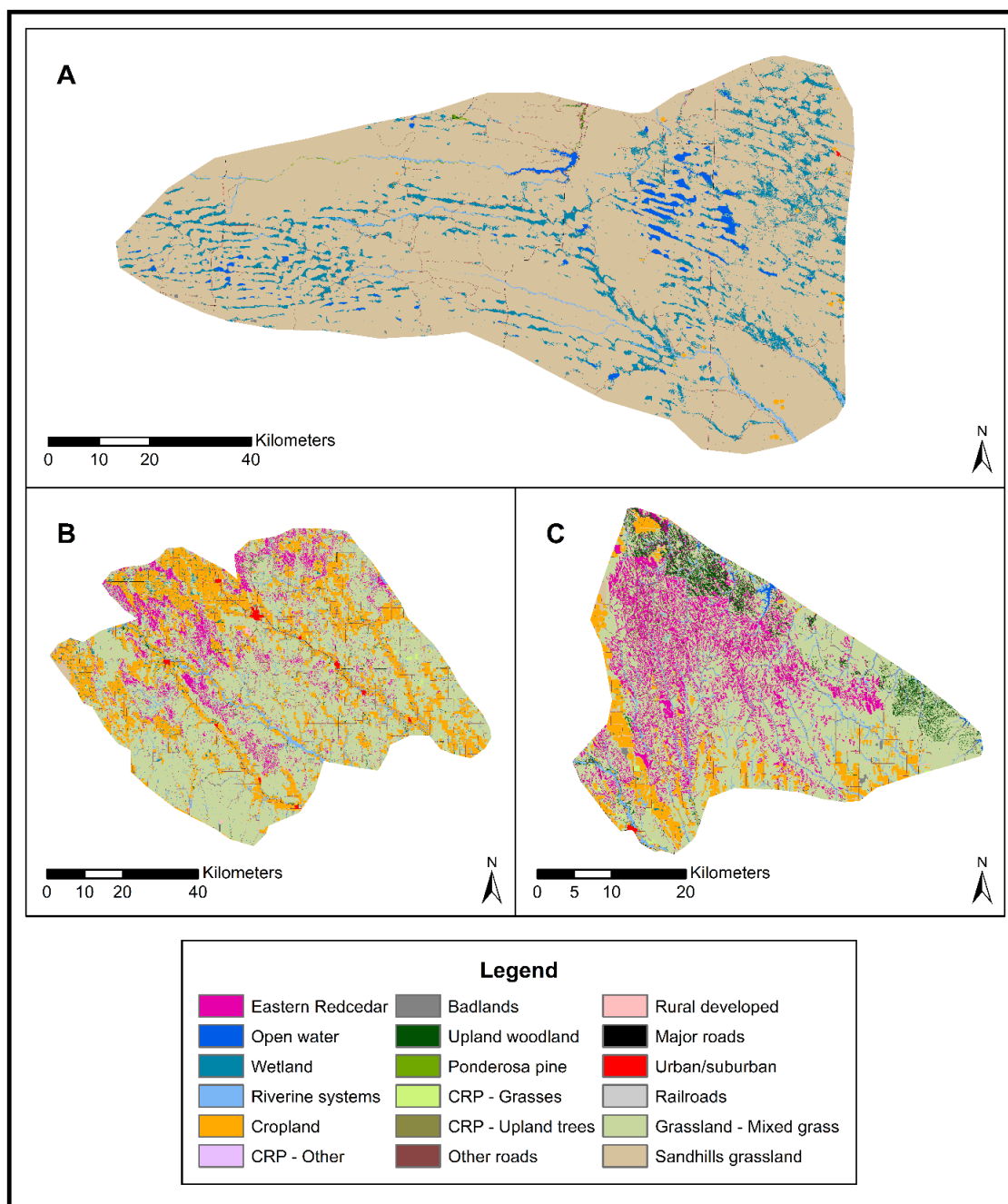


Figure 9. 4: Land cover classifications for the three ecoregions used in our assessment. A: Cherry County Wetlands, B: Central Loess Hills, C: Loess Canyons. Dataset used with permission from the Rainwater Basin Joint Venture.

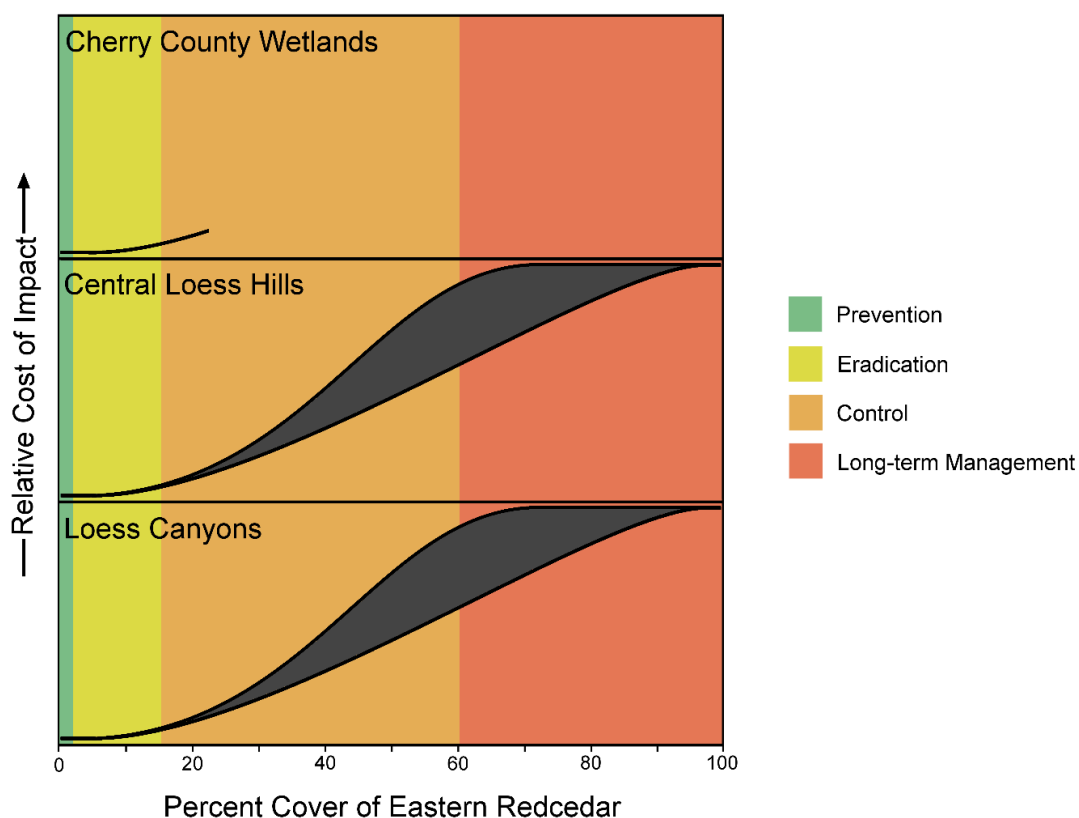


Figure 9. 5: The relative impact costs of eastern redcedar on individual land parcels in each ecoregion. Shown here is the range of impacts related to abundance (not the relative distribution of land with eastern redcedar cover within each ecoregion). Sigmoidal line lengths depict the range of eastern redcedar density/cover located in at least one 50 acre (20.2 ha; 450 m x 450 meter) cell in each ecoregion in 2010, relative to eastern redcedar's known sigmoidal density-impact relationship.

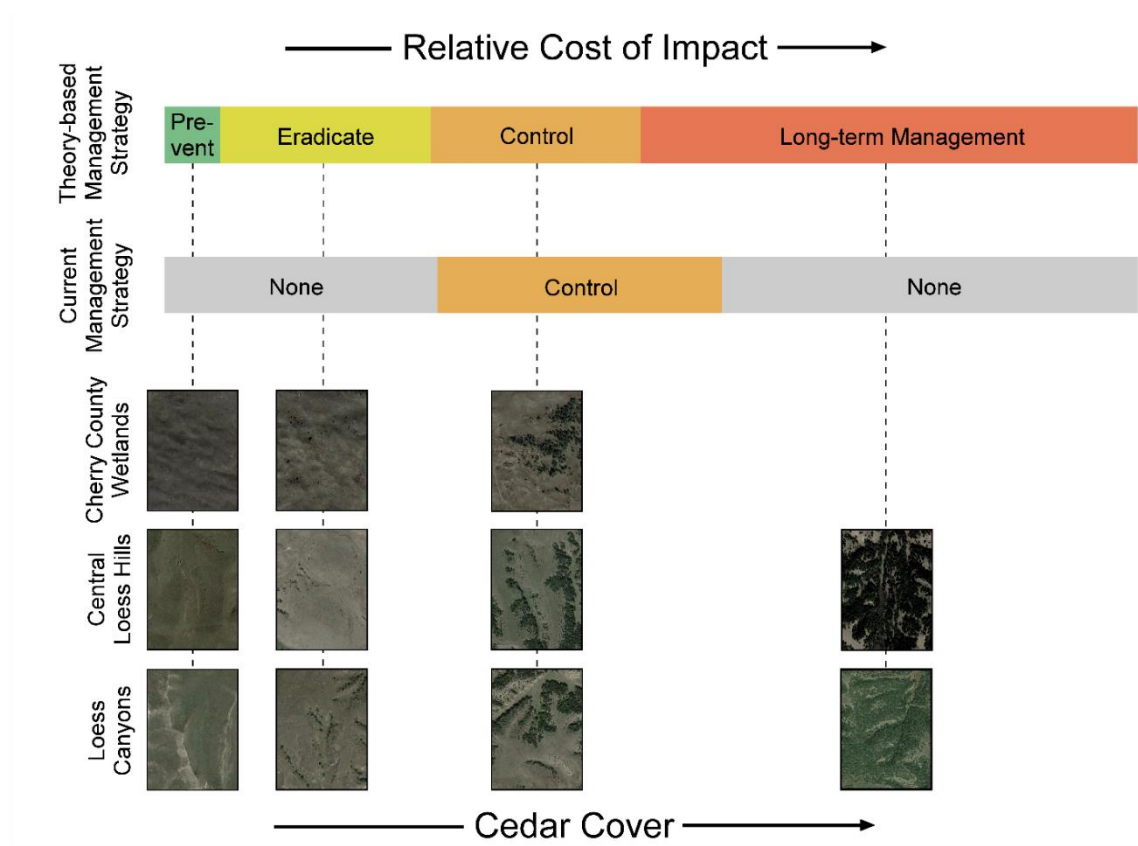


Figure 9. 6: Mismatch between the science and policy of managing eastern redcedar invasions in Nebraska, USA. Aerial photographs show examples of each eastern redcedar invasion stage found in 20.2 ha parcels of land from each ecoregion. Photographs are arranged under the “theory-based management strategy” that would maximize the returns based on the density-impact model as well as under the “current management strategy” implemented in natural resources agency policies. As shown here, control of eastern redcedar only occurs during periods of exponential growth. Policies promote spread during incipient invasions and ignore opportunities for restoration following a regime shift.

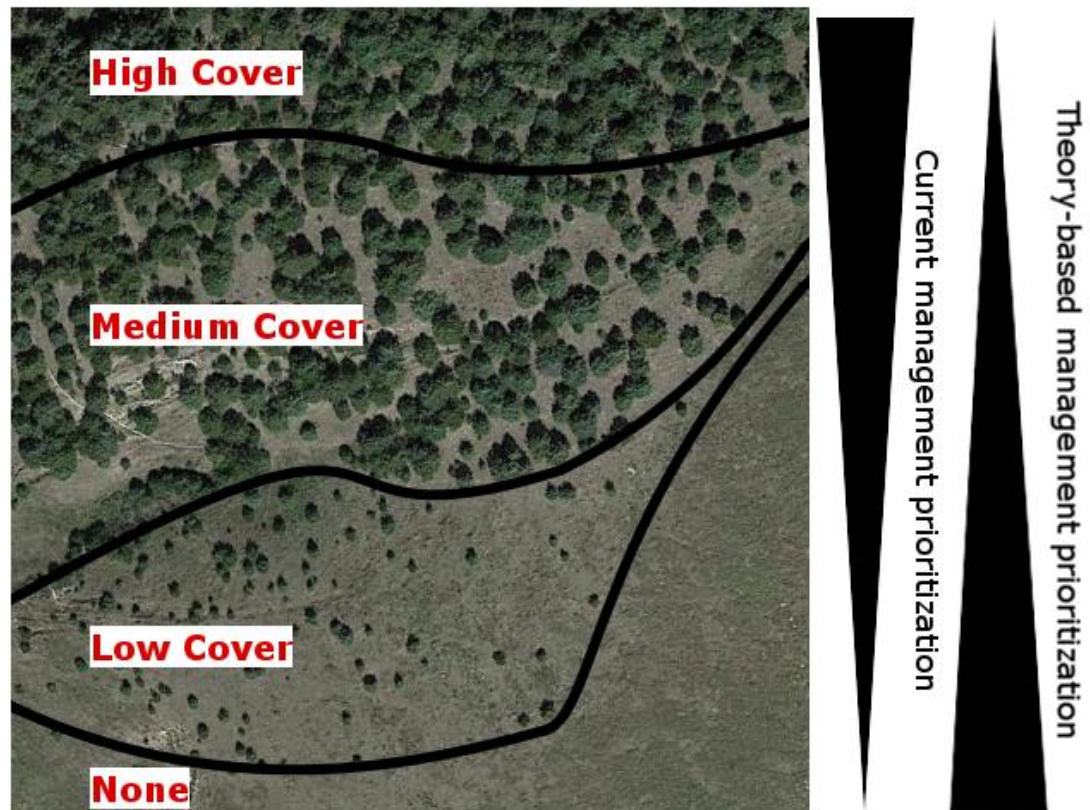


Figure 9. 7: Agency policy prioritization for managing eastern redcedar invasions. Current natural resources agency prioritization (shown as downward-pointing triangle, where greater width indicates greater prioritization) is based on eastern redcedar density and spatial pattern of abundance, but this directly counters theoretical foundations that guide non-native species invasions (shown as upward-pointing triangle, where greater width indicates greater prioritization). The aerial image is from Google Earth.

CHAPTER 10: FIRE LEGACIES IN EASTERN PONDEROSA PINE FORESTS⁹

ABSTRACT

1. Disturbance legacies structure communities and ecological memory, but due to increasing changes in disturbance regimes, it is becoming more difficult to characterize disturbance legacies or determine how long they persist.
2. We sought to quantify the characteristics and persistence of material legacies (e.g., biotic residuals of disturbance) that arise from variation in fire severity in an eastern ponderosa pine forest in North America. We compared forest stand structure and understory woody plant and bird community composition and species richness across unburned, low-, moderate-, and high-severity burn patches in a 27-year-old mixed-severity wildfire that had received minimal post-fire management.
3. We identified distinct tree densities (high: 14.3 ± 7.4 trees per ha, moderate: 22.3 ± 12.6 , low: 135.3 ± 57.1 , unburned: 907.9 ± 246.2) and coarse woody debris

⁹ Roberts, C. P., Donovan, V. M., Wonkka, C. L., Powell, L. A., Allen, C. R., Angeler, D. G., ... & Twidwell, D. (2019). Fire legacies in eastern ponderosa pine forests. *Ecology and Evolution*. doi.org/10.1002/ece3.4879

CPR contributed to conceptualization, programming, data validation, formal analysis, data curation, all writing aspects, visualization, and project administration. VMD contributed to conceptualization, data curation, formal analysis, visualization, all writing aspects, and project administration. CLW, DT, CRA, DGA, LAP, and DAW contributed to conceptualization and writing selected sections.

cover (high: 8.5 ± 1.6 % cover per 30 m transect, moderate: 4.3 ± 0.7 , low: 2.3 ± 0.6 , unburned: 1.0 ± 0.4) among burn severities.

4. Understory woody plant communities differed between high severity patches, moderate- and low- severity patches, and unburned patches (all $P < 0.05$). Bird communities differed between high- and moderate- severity patches, low-severity patches, and unburned patches (all $P < 0.05$). Bird species richness varied across burn severities: low-severity patches had the highest (5.29 ± 1.44) and high-severity patches had the lowest (2.87 ± 0.72). Understory woody plant richness was highest in unburned (5.93 ± 1.10) and high severity (5.07 ± 1.17) patches, and it was lower in moderate (3.43 ± 1.17) and low severity (3.43 ± 1.06) patches.
5. We show material fire legacies persisted decades after the mixed-severity wildfire in eastern ponderosa forest, fostering distinct structures, communities, and species in burned versus unburned patches and across fire severities. At a patch scale, eastern and western ponderosa system responses to mixed-severity fires were consistent.

INTRODUCTION

Globally, changes are propagating in the timing, frequency, intensity, and attendant legacies of disturbances that lead to unique assortments of plant and animal species in many ecosystems (Vitousek et al 1997; Turner 2010). Disturbance legacies are defined as “biologically derived legacies that persist in an ecosystem or landscape following disturbance” (Johnstone et al 2016). There are two types of disturbance legacies: information legacies, which are adaptations to a disturbance regime represented by the distribution of species traits in a community, and material legacies, which are the “biotic and abiotic residuals” (e.g., post-disturbance structures and community compositions) that remain in an ecosystem following a disturbance event (Johnstone et al 2016). Material legacies influence the trajectory of post-disturbance systems because they provide individuals that subsequently make up the community and the physical materials that influence the establishment of individuals in an area (Franklin 2000; Peterson 2002). Material legacies thereby provide ecological memory of the pre-disturbance system to recovering systems, making them instrumental in keeping systems within “safe operating spaces” (Peterson 2002; Johnstone et al 2016). Because material legacies are determined by the particular characteristics of a disturbance, alteration of disturbance regimes often involves alteration of material legacies (e.g., Tinker et al 2000; Collins et al 2010). Over time, altering material legacies can lead to an erosion of ecological memory as material legacies are lost or altered (Johnstone et al 2016). However, in many cases, it is unclear how long material legacies persist and remain important influences of biotic structures and communities post-disturbance.

Fire is one of the most altered disturbance regimes on the planet (Bowman et al 2009; Twidwell et al 2016). Human actions that reduce fire severity, frequency, and distribution can unintentionally eliminate material legacies that keep systems within “safe operating spaces” (Dale et al 2001; Carpenter et al 2015). For instance, current forest management policies often attempt to constrain fire regimes to low severity, suppress fire altogether, or mitigate effects of severe and mixed-severity fires via thinning treatments or post-fire salvage logging (Covington et al 1997, Reynolds et al 2013). Efforts are growing to disentangle past fire legacies from contemporary trajectories in order to determine their role in shaping historical ecosystem structure and composition and maintaining safe operating spaces (Odion et al 2014; Swetnam et al. 2016; Metlen et al. 2018). But as fire regime alteration becomes more prevalent in forested systems, opportunities to study material legacies of fire over longer time scales has become increasingly rare (Hutto et al 2016), limiting our understanding of how long material legacies persist following disturbance (Odion and Hanson 2013).

Ponderosa pine (*Pinus ponderosa*) forests of North America are fire-dependent systems thought to require only frequent, low-intensity fire to retain safe operating space and biodiversity (Brown et al. 2004). Recent studies have questioned these assumptions: they suggest that historically, ponderosa systems also experienced mixed-severity fires, defined by variability in intensities (including some areas of high intensity), every several decades or centuries (Williams and Baker 2012; Odion et al. 2014). These mixed-severity fires are thought to have led to diversity in forest succession and stand structure across the burned area (Williams and Baker 2012; Figure 10.1). Further studies have debated the

importance of mixed-severity fire in maintaining ponderosa systems (Fulé et al. 2014; Levine et al. 2017), particularly its historic frequency (Merschel et al. 2018) and geographic ubiquity (Stevens et al. 2016). Because ponderosa systems vary across their geographic range, it is unclear that either view of the role of mixed-severity fire regimes holds across the entire North American continent (Fulé et al. 2014; Odion et al. 2014). For instance, the relatively contiguous (at a landscape scale) western ponderosa forests embedded in mixed-conifer systems may respond differently to mixed-severity fire than eastern ponderosa pine systems (i.e., within the Great Plains of North America) that are typified by an ecotonal, patchy spatial distribution of ponderosa monocultures within grassland matrices at landscape scales (Brown and Sieg 1999).

Despite the debate on its historic prevalence, examples exist of mixed-severity fire and resultant legacies promoting diversity in ponderosa pine systems (DellaSala et al. 2017; Figure 10.1). For example, the diversity of biotic structures (e.g., varying snag, live tree, and coarse woody debris) resulting from mixed-severity fire in ponderosa pine systems fosters diversity in biotic communities (Huffman et al. 2017; Malone et al. 2018). Numerous species require the open habitats created by high-severity fire (e.g., Hutto 2008; Fornwalt and Kaufmann 2014), others prefer low tree densities that low-severity fire fosters (Kotliar et al. 2007; Abella and Fornwalt 2015), and still other species require high tree densities retained in areas that escape fire (Fontaine and Kennedy 2012). Additionally, there is evidence that mixed-severity fire legacies can provide ponderosa systems with adaptations to future environmental changes such as

climate change and the resultant disturbance regimes (e.g., more frequent droughts and fires; Baker 2018).

Determining how mixed-severity fire material legacies affect and maintain diversity in ponderosa pine systems will require studying systems in which disturbance legacies remain unaltered, an increasingly difficult task due to pervasive human-alterations of legacies (Donato et al 2006; Hutto and Patterson 2016). Additionally, quantifying the role of mixed-severity fire in structuring ponderosa systems where their prevalence is unknown but are nevertheless considered “catastrophic threats”, such as in eastern ponderosa pine systems (Schneider et al. 2005), provides data-driven assessment of the impacts of mixed-severity fire on shaping ecosystems. Here, we aim to quantify the characteristics and persistence of material legacies that arise from variation in fire severity in an eastern ponderosa pine forest. We quantified biotic residuals of disturbance (one aspect of material legacies) by measuring forest stand structure (tree density and coarse woody debris) and biotic communities (understory woody plant and bird communities) within a 27-year-old mixed-severity wildfire perimeter that experienced minimal pre- or post- fire management treatment. This provides a rare example of relatively unaltered material legacies three decades after disturbance.

METHODS

Study Site

We conducted this study in the Pine Ridge region of Nebraska, USA in 2016. The Pine Ridge Escarpment is a semi-arid region in the northwestern corner of Nebraska marking the northern border of the Northern High Plains and the southern border of the

unglaciated Missouri Plateau (Urbatsch and Eddy, 1973). The escarpment sits hundreds of meters above the surrounding plains and is characterized by rocky ridges, vertical slopes, and deep canyons with a mean elevation of approximately 1,219 m. The escarpment is an ecotonal region characterized by ponderosa pine interspersed with mixed grass prairie (Schneider et al, 2005). Being ecotonal, the Pine Ridge hosts both forest (e.g., *Mahonia repens*, *Prunus virginiana*) and grassland species (e.g., *Artemesia tridentata*, *Ericameria* sp.; Johnsgard 2005). Likewise, both eastern (e.g., Eastern Kingbird, Eastern Bluebird) and western (e.g., Western Kingbird, Mountain Bluebird) North American species inhabit the escarpment (Johnsgard 2005).

Although the Pine Ridge is largely thought to have experienced a low-severity wildfire regime (Brown and Sieg 1999; Savage and Mast 2005), the region has experienced multiple large mixed-severity fires over at least the last three decades (MTBS 2016). In 1989, the Fort Robinson mixed-severity wildfire burned 18, 975 hectares across the Pine Ridge escarpment, much of which occurred within Fort Robinson State Park and the Peterson Wildlife Management Area (42.6693° N, 103.4689° W; Figure 10.2). We define mixed-severity fire following Agee's (1990, 1993) definition, where 20% to 70% of the fire that occurred in forested areas was stand replacing. Approximately 1330 hectares were classified as high-severity, 3604 hectares as moderate severity, and 5971 hectares as low-severity within the fire perimeter. Areas that were designated as moderate and high severity were limited to forested regions, while low severity areas burned through both forest and grasslands. Prior to the 1989 fire, land management suppressed all fire. However, for the past 27 years post-fire, the burned area

has received no post-fire treatments or manipulations such as salvage logging or tree thinning. Limited cattle (*Bos taurus*) and horse (*Equus caballus*) grazing has occurred across the study area pre- and post-fire.

Site Selection

In summer 2016, we collected data at Fort Robinson State Park and the Peterson Wildlife Management Area, two public lands within the Pine Ridge Escarpment that burned in the Fort Robinson wildfire of 1989. We selected 3598 ha with adequate road access within these public lands that captured a full range of burn severities and unburned forest (Figure 10.2). Unburned and burned forest sites occurred on the same butte system, separated by a ~ 4 km pasture area. Burn severity classes followed the Monitoring Trends in Burn Severity project (MTBS 2016) severity designations (unburned forest, low severity burned forest, moderate severity burned forest, high severity burned forest; Eidenshink et al 2007).

We used a stratified-random design to distribute 14 sampling sites in each of the four burn severity classes for a total of 56 sites. We mapped burn severity classes to the study area with MTBS geospatial raster data for the 1989 Fort Robinson fire. For each burn severity class, we randomly generated 14 points and selected the closest patch of that class to each randomly generated point. We then placed sites in a central location within the patch. Because both grassland and forest are categorized under the same burn severity classes in MTBS data, we used historic USGS satellite imagery from Google

Earth to confirm that forest, rather than grassland, was present at the time of the wildfire for each burn class. We separated all sites by a minimum of 100 m.

To identify legacy effects 27 years after a mixed-severity fire, we collected forest stand structure, understory woody plant community, and bird community data at each sampling site. For stand structure, we surveyed tree density and total coarse woody debris cover. For community data, we estimated understory woody plant and bird community compositions and richness.

Tree density and Coarse Woody Debris

We used the point-center quarter method to estimate tree density, placing a single point at each sample site (Cottam and Curtis 1956). At each site, we estimated live tree and snag densities. We defined live trees as woody plants standing ≥ 1.4 m (diameter at breast height). Similarly, we defined snags as free-standing dead trees ≥ 1.4 m in height. Because of tree scarcity across many of our sites, we only measured trees up to 100 m from the point center. If no trees were within this distance, we entered a value of 101 m.

To sample coarse woody debris (woody debris with a diameter greater than or equal to 10 cm; CWD), we established a 30-m transect in a randomly selected north-south or east-west direction at each site. We measured the length of the transect line that was covered with CWD and then divided this value by the total transect length (30 m), multiplied by 100, to determine the percent CWD cover at each site.

Understory Woody Plant Community Composition

To estimate understory woody plant community composition, we collected species presence-absence data at each sampling site. We defined understory woody plants as

woody plants < 1.4 m in height (i.e., less than diameter at breast height level). We distributed five circular sampling plots with 5-m radii around each sampling site. We placed one at the center of the sampling site, and the four others 15 meters from center of the sampling site in each of the cardinal directions. In each plot, we recorded all understory woody plant species rooted within the plot. If a species was present in any of the five plots, we counted it as present for the sampling site.

Bird Community Composition

From May 25 – June 6, we estimated bird community composition from species presence-absence data. At each sampling site, we recorded bird species presence with visual and acoustic point-count surveys. We conducted surveys within a 5.5 hour sampling window starting 30 minutes prior to sunrise and ending five hours after sunrise. We did not survey if winds exceeded 20 kilometers/hour or during precipitation events (Huff et al 2000, Flanders et al 2006). For each point-count survey, we recorded all bird species we saw or heard during a five-minute period within 50 m of the point to ensure recorded species were using the burn severity at which the point was situated and to maximize detection probability (Buckland et al 2001). We revisited each point once within five days to increase the probability of capturing all present species (Sliwinski et al 2015). For analyses, we pooled the species recorded from both visits.

Analyses

We used general linear models to test for legacy effects of burn severity on tree density and CWD cover. To differentiate legacy effects on patterns in live trees and snags, we developed separate models for live tree and snag density data. Where necessary, data

was log-transformed to meet model assumptions. We conducted multiple comparisons of slopes among burn severities with false discovery rate p-value adjustments (Hothorn et al 2008; 'glht' function; R package multcomp).

To examine differences in understory woody plant and bird community composition across burn severities, we 1) estimated mean species richness by severity class and compared 95% confidence limits across severities, and 2) we compared multivariate community composition by severity class. To compare multivariate community composition, we first assessed community compositions visually via ordination. Because our data was presence-absence and fit unimodal assumptions (i.e., we sampled across the full range of burn severities), we use canonical correspondence analysis (CCA), setting burn severity as the constraining variable (Palmer 1993). We estimated the mean center and 95% confidence limits for the site ordination scores of each burn severity category for the first two CCA axes.

Following ordination, we used a permutational multivariate analysis of variance (PERMANOVA) to confirm any significant community composition differences across burn severities (Anderson 2005). We determined if the overall effect of burn severity significantly predicted community composition. We then compared the community compositions of each burn severity, using false discovery rate p-value adjustments for multiple comparisons. Because PERMANOVA can be sensitive to variability between groups, we tested for homogeneity of variances for all comparisons using the permutational test of multivariate dispersions (PERMDISP; Anderson and Walsh 2013).

All ordination and significance tests were conducted with R software using the “vegan” package (Oksanen et al. 2007; R Core Team 2015).

RESULTS

Tree Density

Burn severity was a significant predictor of live ($F_{3,51} = 26.260$, $P < 0.001$) and dead ($F_{3,33} = 18.250$, $P < 0.001$; Table 10.1; Figure 10.3) tree density 27 years after fire (Figure 10.1). The live tree density generalized linear model ($y = 1.221 + 2.646$ (*low*) + 0.816 (*moderate*) + 5.184 (*unburned*)) indicated that low-severity burn and unburned classes were positively related to tree density ($P \leq 0.001$; Table 10.1). Only the unburned class was positively related to snag density in the dead density model ($y = 2.029 + 0.684$ (*low*) – 0.363 (*moderate*) + 4.357 (*unburned*); $P < 0.001$; Table 10.1; Figure 10.1). Live tree density differed significantly among all burn severity levels, except moderate and high severities ($t = 0.816$, $P = 0.597$; $t = 0.307$, $P = 0.990$, respectively; Table 10.1). Snag density only distinguished unburned patches from burned patches (all $P < 0.001$; Table 10.1).

Coarse Woody Debris

Coarse woody debris varied across the burn severity gradient 27 years after fire, with fire severity being a significant predictor of coarse woody debris cover ($F_{3,56} = 16.74$, $P < 0.001$; Figure 10.3; Table 10.1). Our coarse woody debris model indicated that moderate and high severities had similar coarse woody debris cover and low and unburned severities had similar coarse woody debris cover. Coarse woody debris was significantly

higher in moderate and high severity burned forest than in low severity and unburned forest ($y = [8.476 - 6.149 (low) - 4.138 (moderate) - 7.526 (unburned)]^4$; Table 10.1).

Understory Woody Plant Community Composition

We observed 18 understory woody plant species across all sampling sites (Table 10.2), with 10 species in high severity patches, 12 in moderate severity patches, 9 in low severity patches, and 15 in unburned patches (Table 10.2). Moderate severity, low severity, and unburned patches had two, one and three unique species respectively (Table 10.2). We observed no species unique to high severity patches (Table 10.2). Understory woody plant richness was highest in unburned (5.93 ± 1.10) and high severity (5.07 ± 1.17) patches, and it was lower in moderate (3.43 ± 1.17) and low severity patches (3.43 ± 1.06 ; Figure 10.4).

In the CCA, the constraints explained 11.8% of variance, and the three constrained axes explained 59.6%, 22.9%, and 17.5% of total constrained variance respectively. Because the first two CCA axes explained approximately 83% of the total constrained variance, we only considered these axes in the results. The first CCA axis distinguished burned and unburned communities, and the second CCA axis differentiated high severity communities from moderate and low severity communities (Figure 10.5). The mean and 95% confidence limits of the constrained site scores from the first and second CCA axes and PERMANOVA results confirmed that burn severity was a significant predictor of understory woody plant community composition 27 years after

wildfires (pseudo $F_{3,53} = 4.502$, $P = 0.001$; Figure 10.5; Table 10.3). Multiple PERMANOVA comparisons corroborated the CCA results as well: both unburned and high severity understory woody plant communities were distinct from all others (all $F > 9.099$, all $P = 0.002$; Table 10.3). Low and moderate severity communities were not different ($F = 0.663$, $P = 0.624$; Table 10.3). High severity communities differed from all others (all $F > 5.680$, all $P < 0.005$; Table 10.3). Ordination showed that *Pinus ponderosa* strongly associated with unburned sites; additionally, two *Ribes* species (*Ribes oxycanthoides* and *Ribes aurem*), *Prunus americana*, *Prunus virginiana*, *Ribes odoratum*, and some mesophilic plants such as *Mahonia repens* and *Acer negundo* associated with unburned sites (Figure 10.5). *Prunus virginiana* and *Ribes odoratum* were also associated with high severity sites; *Rosa woodsii*, *Symphoricarpos occidentalis*, and *Ribes americanum* were also common in high severity sites (Figure 10.5). Moderate and low severity communities showed high overlap and shared several species including *Ulmus americana*, *Juniperus communis*, *Ericameria* sp., *Gutierrezia sarothrae*, *Rhus trilobata*, and *Toxicodendron radicans* (Figure 10.5).

Bird Community Composition

We observed 40 bird species throughout the study area (Table 10.4). We observed a total of 14 species in high-severity, 19 in moderate-severity, 24 in low-severity, and 23 in unburned classes (Table 10.4). We also detected unique bird species in each burn severity category that were not found in other areas: 1 in high-severity, 3 in moderate-severity, 2 in low-severity, and 6 in unburned (Table 10.4). Bird species richness patterns differed

from understory woody plant richness patterns (Figure 10.4). Bird species richness varied across burn severities: low-severity patches had the highest (5.29 ± 1.44) and high-severity patches had the lowest (2.87 ± 0.72 ; Figure 10.4).

Like understory woody plant community composition, in the bird CCA, constraints explained 10.1% of the variance, and the three constrained axes explained 59.3%, 24.5%, and 16.3% of the total constrained variance. Again, the first and second CCA axis site scores differentiated three bird communities (explaining approximately 84% of constrained variance), based on means and 95% confidence limits (Figure 10.5). But in this case, the first CCA axis differentiated both burned vs. unburned as well as burn severities; whereas the second axis only slightly distinguished burn severities (Figure 10.5). Regardless, the initial PERMANOVA also confirmed CCA results, demonstrating that burn severity was a significant predictor of bird community composition (pseudo $F_{3,53} = 6.193$, $P = 0.001$; Table 10.3), and the PERMDISP did not find heterogeneity in spread (pseudo $F_{3,53} = 0.840$, $P = 0.479$). Multiple PERMANOVA comparisons reiterated differences shown in the CCA (Table 10.3). Bird communities did not differ between high- and moderate-severities ($F = 1.284$, $P = 0.260$), but bird communities in low-severity and unburned patches differed from all other patch types (Table 10.3). Unburned sites were strongly characterized by several species typical of closed-canopy habitats such as Yellow-rumped Warbler, Black-capped Chickadee, Cedar Waxwing, and Plumbeous Vireo, and unburned sites were also loosely associated with some cavity-nesting species such as American Kestrel, Eastern Bluebird, and House Wren (Figure 10.5). Low severity sites shared species with unburned sites such as House

Wren, Spotted Towhee, American Goldfinch, and Chipping Sparrow (Figure 10.5), and low severity also shared some species with high/moderate severity sites, including several open habitat-associated species such as Western Meadowlark, Cassin's Kingbird, and Rock Wren, as well as some late decay stage cavity nesters such as Red-headed Woodpeckers and Northern Flickers (Figure 10.5). High and moderate severity sites were strongly associated with open habitat associated species such as Lark Sparrow and Western Meadowlark (Figure 10.5).

DISCUSSION

Mixed-severity fire created multi-decadal material legacies in forest stand structure and biotic communities in an eastern ponderosa pine forest. We identified distinct tree densities, coarse woody debris cover, understory woody plant communities, and bird communities across the current landscape which coincide with a burn severity gradient from a fire that occurred 27 years prior to sampling. Stand structure, understory woody plant communities, and bird communities differed between unburned, high severity, and low severity burn patches. Even 27 years post-fire, low severity burn patches hosted many grassland bird species (e.g., Western Meadowlark, Cassin's Kingbird) that were absent in unburned forest patches while also maintaining relatively high tree densities. High severity burn patches still tended strongly toward grassland conditions, with low tree density and understory woody plant and bird species typical of grasslands. Moderate severity burn patches showed the least distinction, overlapping with high severity in tree density and bird communities and with low severity in coarse woody debris and understory woody plant communities. Although we detected the highest

number of unique species and species richness in unburned patches of ponderosa, we also detected unique structures, understory woody plant species, and bird species across a range of burn severities; further, we show that high severity patches supported higher understory woody plant species richness than moderate or low severity patches 27 years post-fire. Thus, our study is among the first to show that mixed-severity fire produces multi-decadal material legacies that support unique species assemblages in eastern ponderosa pine systems. This contrasts with the assumption that mixed-severity fire represents a “catastrophic” stressor for eastern ponderosa systems (Schneider et al. 2005). Our results also build upon shorter-term studies in conifer systems demonstrating how fire legacies influence structure in burned versus unburned forests (Hutto 1995; Fontaine et al 2009) and across fire severities (Fontaine and Kennedy 2012; Stephens et al 2015).

At a patch scale, we found overall eastern ponderosa system responses to mixed-severity fire matched western ponderosa system responses to mixed-severity fire (Keyser et al. 2008; Stevens-Rumann et al. 2012). In the first decade following a mixed-severity fire in western ponderosa systems, live trees are known to experience high mortality (and conversely lead to greater snag densities) in high- and moderate- severity patches, experience attenuated mortality (and thus leave fewer snags) in low-severity patches, and, of course, unburned patches retain high live tree densities and lower snags densities (Allen et al. 2002; Dunn and Bailey 2016; Eskelson and Monleon 2018). But 27 years post-fire, Passovoy and Fule (2006) found ponderosa snag densities decline sharply in the decades following the fire event; our results echo these and add that snag densities were statistically indistinguishable across fire severities (i.e., they only differed between

burned versus unburned patches). Similarly, Passovoy and Fule (2006) found a corresponding increase in coarse woody debris cover 27 years post-fire as snags fell, to which we add significant differences across fire severities.

Biotic community responses were consistent with post-fire legacy patterns observed in western ponderosa pine systems at a patch level (Kotliar et al. 2007; Fornwalt and Kaufmann 2014). Although snag densities only differed between burned versus unburned, the unique bird and woody plant communities among fire severities indicates other material legacies persist across a fire severity gradient and continue to influence biotic communities. For instance, in the same system, Keele et al. (in press) found that, when comparing multiple forest stand structural characteristics, coarse woody debris was the strongest indicator of cavity-nesting bird community composition 27 years post-fire. This difference in structure may explain some disparities between our study and others in bird-fire severity associations: for example, Hairy Woodpeckers and Western Wood Pewees were more strongly associated with higher burn severities in other studies than in ours (Smucker et al. 2005; Fontaine and Kennedy 2012). But conversely, we show that several species exhibited similar fire severity associations both less than a decade and 27 years post fire: for example, Yellow-rumped Warbler and Cedar Waxwing strongly declined with increasing severity, House Wren and Northern Flicker were positively associated with burn severity, and Spotted Towhee and Mourning Dove showed little relationship to burn severity (Smucker et al 2005; Kotliar et al. 2007). And while other studies on understory woody plant community responses to mixed-severity fire also show that higher severities promoted diversity in the first decade post-fire

(Halofsky et al. 2011; Crotteau et al. 2013; Fornwalt and Kaufmann 2014; Abella and Fornwalt 2015), our study is among the first to demonstrate woody plant diversity persisting in high-severity burn patches for nearly three decades.

Moving beyond the assumption of identical starting points on pre-disturbance landscapes (i.e., burned versus unburned) and quantifying the influence of past material legacies on current patterns will allow scientists to more fully disentangle the effects of fire legacies on biodiversity (i.e., information legacies) and forest persistence (Peterson 2002; Johnstone et al 2016). Many studies (including ours) operate under the assumption of an identical starting point for all patches (Carpenter et al 2015; Twidwell et al 2016). This assumption can prevent understanding of the extent to which past material legacies persist to influence structure and function of a system and similarly how these legacies interact with other disturbances and landscape features that function at different scales (Turner 2010). For instance, our study site is fragmented by human development and has experienced frequent grazing by cattle and horses for multiple decades. How the legacies of these disturbances persist and interact with the legacies of mixed severity fire to alter patterns in community and structure is unknown. Studies that invest in long-term investigation of responses to disturbance with an eye for tracking changes in biotic residuals via repeated sampling (e.g., Turner et al. 2016) can provide direct tests of prior conditions and disturbance legacies. In the absence of pre-disturbance data, indirect methods, such as reconstructing pre-fire overstory structure, can be used to partially assess pre-disturbance conditions (e.g., Keyser et al. 2008; Stevens-Rumann et al. 2012; Dunn and Bailey 2016), but where reconstruction is not possible, such as in aging and

disappearing biotic residuals (e.g., falling snags) as in our study, these methods may prove insufficient for assessing disturbance legacies.

Evidence is building in support of adopting an "ecologically-informed view" of mixed-severity fires in forest systems (Hutto et al 2016) instead of the command-and-control view of the past (Holling and Meffe 1996; Lindenmayer and Noss 2006). Management focused on a climax or idealized ponderosa pine system state excludes unique structures, communities, and individual species such as those we detected across a full suite of burn severities (Hutto et al. 2008a, 2008b), and the previous negative view of high- and mixed-severity fires for ponderosa pine systems has come into question in light of recent evidence that these fires did indeed play a role in historical forest structure and function (Parks et al 2014; Hutto and Patterson 2016). Given the persistence of these material legacies in ponderosa pine systems for (at least) 27 years, our study supplements research highlighting how mixed-severity fire in ponderosa pine systems can foster structural and biological diversity via persistence of multi-decadal material legacies (Odion et al. 2014; Hutto et al. 2016; DellaSala et al. 2017).

ACKNOWLEDGEMENTS

This work was supported by the USDA NIFA, McIntire Stennis project 1008861, the Department of Defense Strategic Environmental Research Development Program W912HQ-15-C-0018, and the University of Nebraska-Lincoln's Department of Agronomy & Horticulture. The Nebraska Cooperative Fish and Wildlife Research Unit is

jointly supported by Hatch Act funds through a cooperative agreement between the U.S. Geological Survey, the Nebraska Game and Parks Commission, the University of Nebraska Agricultural Research Division, Lincoln, Nebraska the United States Fish and Wildlife Service and the Wildlife Management Institute. We extend special thanks to the Nebraska Game and Parks Commission, especially to Mike Morava at Fort Robinson State Park and Greg Schenbeck at Peterson Wildlife Management Area, for allowing us to conduct this research on their lands. Finally, we thank Sarah Nodskov and Emma Keele for assistance in data collection. Finally, we thank the associate editor, two anonymous reviewers, and Edward J Raynor for their comments and suggestions. Any use of trade, firm or product names is for descriptive purposes only and does not imply endorsement by the U.S. Government.

LITERATURE CITED

- Abella, S. R., Fornwalt, P. J. (2015). Ten years of vegetation assembly after a North American mega fire. *Global Change Biology*, 21, 789-802.
- Allen, C. D., Savage, M., Falk, D. A., Suckling, K. F., Swetnam, T. W., Schulke, T., ... Klingel, J. T. (2002). Ecological restoration of southwestern ponderosa pine ecosystems: A broad perspective. *Ecological Applications*, 12, 1418–1433.
- Anderson, M. J. (2005). PERMANOVA: a FORTRAN computer program for permutational multivariate analysis of variance. Department of Statistics, University of Auckland, New Zealand, 24.

- Anderson, M. J., Walsh, D. C. (2013). PERMANOVA, ANOSIM, and the mantel test in the face of heterogeneous dispersions: What null hypothesis are you testing? *Ecological Monographs*, 83, 557–574.
- Baker, W. L. (2018). Transitioning western US dry forests to limited committed warming with bet- hedging and natural disturbances. *Ecosphere*, 9, e02288.
- Bowman, D. M., Balch, J. K., Artaxo, P., Bond, W. J., Carlson, J. M., Cochrane, M. A., ... Johnston, F. H. (2009). Fire in the earth system. *Science*, 324, 481–484.
- Brown, P. M., Sieg, C. H. (1999). Historical variability in fire at the ponderosa pine-northern Great Plains prairie ecotone, southeastern Black Hills, South Dakota. *Ecoscience*, 6, 539–547.
- Brown, R. T., Agee, J. K., Franklin, J. F. (2004). Forest restoration and fire: Principles in the context of place. *Conservation Biology*, 18, 903–912.
- Buckland, S. T., Anderson, D. R., Burnham, K. P., Laake, J. L., Borchers, D. L., Thomas, L. (2001). Introduction to distance sampling estimating abundance of biological populations. Oxford University Press.
- Carpenter, S. R., Brocks, W., Folke, C., van der Nees, E., Scheffer, M. (2015). Allowing variance may enlarge the safe operating space for exploited ecosystems. *Proceedings of the National Academy of Sciences*, 112, 14384–14389.
- Collins, B. M., Stephens, S. L., Moghaddas, J. J., Battles, J. (2010). Challenges and approaches in planning fuel treatments across fire-excluded forested landscapes. *Journal of Forestry*, 108, 24–31.

- Cottam, G., Curtis, J. T. (1956). The use of distance measures in phytosociological sampling. *Ecology*, 37, 451–460.
- Covington, W. W., Fule, P. Z., Moore, M. M., Hart, S. C., Kolb, T. E., Mast, J. N., ... Wagner, M. R. (1997). Restoring ecosystem health in ponderosa pine forests of the southwest. *Journal of Forestry*, 95, 23.
- Crotteau, J. S., Varner, III J. M., Ritchie, M. W. (2013). Post-fire regeneration across a fire severity gradient in the southern Cascades. *Forest Ecology and Management*, 287, 103-112.
- Dale, V. H., Joyce, L. A., McNulty, S., Neilson, R. P., Ayres, M. P., Flannigan, M. D., Simberloff, D. (2001). Climate change and forest disturbances: climate change can affect forests by altering the frequency, intensity, duration, and timing of fire, drought, introduced species, insect and pathogen outbreaks, hurricanes, windstorms, ice storms, or landslides. *BioScience*, 51, 723–734.
- DellaSala, D. A., Hutto, R. L., Hanson, C. T., Bond, M. L., Ingalsbee, T., Odion, D., Baker, W. L. (2017). Accommodating mixed-severity fire to restore and maintain ecosystem integrity with a focus on the Sierra Nevada of California, USA. *Fire Ecology*, 13, 148-171.
- Donato, D., Fontaine, J., Campbell, J., Robinson, W. D., Kauffman, J. B., Law, B. E. (2006). Post-wildfire logging hinders regeneration and increases fire risk. *Science*, 311, 352–352.

- Dunn, C. J., Bailey, J. D. (2016). Tree mortality and structural change following mixed-severity fire in *Pseudotsuga* forests of Oregon's western Cascades, USA. *Forest Ecology and Management*, 365, 107-118.
- Eidenshink, J. C., Schwind, B., Brewer, K., Zhu, Z. L., Quayle, B., Howard, S. (2007). A project for monitoring trends in burn severity. *Fire Ecology*, 3, 3-21.
- Eskelson, B. N., Monleon, V. J. (2018). Post-fire surface fuel dynamics in California forests across three burn severity classes. *International Journal of Wildland Fire*, 27, 114-124.
- Flanders, A. A., Kuvlesky, Jr W. P., Ruthven, III D. C., Zaiglin, R. E., Bingham, R. L., Fulbright, T. E., ... Brennan, L. A. (2006). Effects of invasive exotic grasses on south Texas rangeland breeding birds. *The Auk*, 123, 171-182.
- Fontaine, J. B., Donato, D. C., Robinson, W. D., Law, B. E., Kauffman, J. B. (2009). Bird communities following high-severity fire: Response to single and repeat fires in a mixed-evergreen forest, Oregon, USA. *Forest Ecology and Management*, 257, 1496-1504.
- Fontaine, J. B., Kennedy, P. L. (2012). Meta-analysis of avian and small-mammal response to fire severity and fire surrogate treatments in US fire-prone forests. *Ecological Applications*, 22, 1547-1561.

- Fornwalt, P. J., Kaufmann, M. R. (2014). Understorey plant community dynamics following a large, mixed severity wildfire in a *Pinus ponderosa*–*Pseudotsuga menziesii* forest, Colorado, USA. *Journal of Vegetation Science*, 25, 805-818.
- Fulé, P. Z., Swetnam, T. W., Brown, P. M., Falk, D. A., Peterson, D. L., Allen, C. D., ... Keane, R. E. (2014). Unsupported inferences of high- severity fire in historical dry forests of the western United States: response to Williams and Baker. *Global Ecology and Biogeography*, 23, 825-830.
- Halofsky, J. E., Donato, D. C., Hibbs, D. E., Campbell, J. L., Cannon, M. D., Fontaine, J. ... Law, B. E. (2011). Mixed- severity fire regimes: lessons and hypotheses from the Klamath- Siskiyou Ecoregion. *Ecosphere*, 2(4), 1-19.
- Holling, C. S., Meffe, G. K. (1996). Command and control and the pathology of natural resource management. *Conservation Biology*, 10, 328–337.
- Hothorn, T., Bretz, F., Westfall, P. (2008). Simultaneous inference in general parametric models. *Biometrical Journal*, 50, 346–363.
- Huff, M. H., Bettinger, K. A., Ferguson, H. L., Brown, M. J., Altman, B. (2000). A habitat-based point-count protocol for terrestrial birds, emphasizing Washington and Oregon. U.S. Department of Agriculture, Forest Service General Technical Report PNW-GTR-501.
- Huffman, D. W., Meador, A. J. S., Stoddard, M. T., Crouse, J. E., Roccaforte, J. P. (2017). Efficacy of resource objective wildfires for restoration of ponderosa pine (*Pinus ponderosa*) forests in northern Arizona. *Forest Ecology and Management*, 389, 395-403.

- Hutto, R. L. (1995). Composition of bird communities following stand-replacement fires in northern Rocky Mountain (USA) conifer forests. *Conservation Biology*, 9, 1041–1058.
- Hutto, R. L. (2008b). The ecological importance of severe wildfires: Some like it hot. *Ecological Applications*, 18, 1827–1834.
- Hutto, R. L., Conway, C. J., Saab, V. A., Walters, J. R. (2008a). What constitutes a natural fire regime? Insight from the ecology and distribution of coniferous forest birds in North America. *Fire Ecology*, 4, 115.
- Hutto, R. L., Keane, R. E., Sherriff, R. L., Rota, C. T., Eby, L. A., Saab, V. A. (2016). Toward a more ecologically informed view of severe forest fires. *Ecosphere*, 7, 2.
- Hutto, R. L., Patterson, D. A. (2016). Positive effects of fire on birds may appear only under narrow combinations of fire severity and time-since-fire. *International Journal of Wildland Fire*, 25, 1074–1085.
- Johnsgard, P. A. (2005). The nature of Nebraska: ecology and biodiversity. University of Nebraska Press, Lincoln, Nebraska, USA.
- Johnstone, J. F., Allen, C. D., Franklin, J. F., Frelich, L. E., Harvey, B. J., Higuera, P. E., ... Schoennagel, T. (2016). Changing disturbance regimes, ecological memory, and forest resilience. *Frontiers in Ecology and the Environment*, 14, 369–378.
- Keele, E., Donovan, V. M., Roberts, C. P., Nodskov, S., Wonkka, C. L., Allen, C. R., ... Twidwell, D. (2019). Relationships between a burn severity gradient, cavity-nesting birds and habitat in ponderosa pine forests. *In press: American Midland Naturalist*.

- Keyser, T. L., Lentile, L. B., Smith, F. W., Shepperd, W. D. (2008). Changes in forest structure after a large, mixed-severity wildfire in ponderosa pine forests of the Black Hills, South Dakota, USA. *Forest Science*, 54, 328-338.
- Kotliar, N. B., Kennedy, P. L., Ferree, K. (2007). Avifaunal responses to fire in southwestern montane forests along a burn severity gradient. *Ecological Applications*, 17, 491–507.
- Levine, C. R., Cogbill, C. V., Collins, B. M., Larson, A. J., Lutz, J. A., North, M. P., ... Battles, J. J. (2017). Evaluating a new method for reconstructing forest conditions from General Land Office survey records. *Ecological Applications*, 27, 1498-1513.
- Lindenmayer, D., Noss, R. (2006). Salvage logging, ecosystem processes, and biodiversity conservation. *Conservation Biology*, 20, 949–958.
- Malone, S. L., Fornwalt, P. J., Battaglia, M. A., Chambers, M. E., Iniguez, J. M., Sieg, C. H. (2018). Mixed-severity fire fosters heterogeneous spatial patterns of conifer regeneration in a dry conifer forest. *Forests*, 9, 45.
- Merschel, A. G., Heyerdahl, E. K., Spies, T. A., Loehman, R. A. (2018). Influence of landscape structure, topography, and forest type on spatial variation in historical fire regimes, Central Oregon, USA. *Landscape Ecology*, 33, 1195-1209.
- Metlen, K. L., Skinner, C. N., Olson, D. R., Nichols, C., Borgias, D. (2018). Regional and local controls on historical fire regimes of dry forests and woodlands in the Rogue River Basin, Oregon, USA. *Forest Ecology and Management*, 430, 43-58.

MTBS Project (USDA Forest Service/U.S. Geological Survey) (2016) MTBS Data

Access: Individual Fire-Level Geospatial Data online: Retrieved from

<http://www.mtbs.gov/data/individualfiredata.html>.

Odion, D. C., Hanson, C. T. (2013). Projecting impacts of fire management on a biodiversity indicator in the Sierra Nevada and Cascades, USA: The black-backed woodpecker.

Odion, D. C., Hanson, C. T., Arsenault, A., Baker, W. L., DellaSala, D. A., Hutto, R. L., ... Williams, M. A., (2014). Examining historical and current mixed-severity fire regimes in ponderosa pine and mixed-conifer forests of western North America. *PLoS ONE*, 9, e87852.

Oksanen, J., Kindt, R., Legendre, P., O'Hara, B., Stevens, M. H. H., Oksanen, M. J., & Suggests, M. A. S. S. (2007). The vegan package. *Community ecology package*, 10, 631-637.

Palmer, M. W. (1993). Putting things in even better order: The advantages of canonical correspondence analysis. *Ecology*, 74, 2215–2230.

Parks, S. A., Miller, C., Nelson, C. R., Holden, Z. A. (2014). Previous fires moderate burn severity of subsequent wildland fires in two large western US wilderness areas. *Ecosystems*, 17, 29–42.

Passovoy, M. D., Fulé, P. Z. (2006). Snag and woody debris dynamics following severe wildfires in northern Arizona ponderosa pine forests. *Forest Ecology and Management*, 223, 237–246.

- Peterson, G. D. (2002). Contagious disturbance, ecological memory, and the emergence of landscape pattern. *Ecosystems*, 5, 329-338.
- Reynolds, R. T., Meador, A. J. S., Youtz, J. A., Nicolet, T., Matonis, M. S., Jackson, P. L., ... Graves, A. D. (2013). Restoring composition and structure in southwestern frequent-fire forests: a science-based framework for improving ecosystem resiliency. General Technical Report RMRS-GTR-310. U.S. Department of Agriculture, Forest Service, Rocky Mountain Research Station, Fort Collins, CO. 76 pp.
- Savage, M., Mast, J. N. (2005). How resilient are southwestern ponderosa pine forests after crown fires? *Canadian Journal of Forest Research*, 35, 967-977.
- Schneider, R., Humpert, M., Stoner, K., Steinauer, G. (2005). The Nebraska Natural Legacy Project: A comprehensive wildlife conservation strategy. Nebraska Game and Parks Commission, Lincoln, NE.
- Sliwinski, M., Powell, L., Koper, N., Giovanni, M., Schacht, W. (2015). Research design considerations to ensure detection of all species in an avian community. *Methods in Ecology and Evolution*, 7, 456-462.
- Smucker, K. M., Hutto, R. L., Steele B. M. (2005). Changes in bird abundance after wildfire: Importance of fire severity and time since fire. *Ecological Applications*, 15, 1535-1549.
- Stephens, J. L., Ausprey, I. J., Seavy, N. E., Alexander, J. D. (2015). Fire severity affects mixed broadleaf-conifer forest bird communities: Results for 9 years following fire. *The Condor*, 117, 430-446.

- Stevens, J. T., Safford, H. D., North, M. P., Fried, J. S., Gray, A. N., Brown, P. M., ... Franklin, J. F. (2016). Average stand age from forest inventory plots does not describe historical fire regimes in ponderosa pine and mixed-conifer forests of western North America. *PLoS ONE*, 11, p.e0147688.
- Stevens-Rumann, C. S., Sieg, C. H., Hunter, M. E. (2012). Ten years after wildfires: How does varying tree mortality impact fire hazard and forest resiliency? *Forest Ecology and Management*, 267, 199-208.
- Swetnam, T. W., Farella, J., Roos, C. I., Liebmann, M. J., Falk, D. A., Allen, C. D. (2016). Multiscale perspectives of fire, climate and humans in western North America and the Jemez Mountains, USA. *Phil. Trans. R. Soc. B*, 371, 20150168.
- R Core Team. (2015). R: A language and environment for statistical computing [internet]. Vienna, Austria: R foundation for statistical computing.
- Turner, M. G. (2010). Disturbance and landscape dynamics in a changing world. *Ecology*, 91, 2833–2849.
- Turner, M. G., Whitby, T. G., Tinker, D. B., Romme, W. H. (2016). Twenty- four years after the Yellowstone Fires: Are postfire lodgepole pine stands converging in structure and function? *Ecology*, 97(5), 1260-1273.
- Twidwell, D., West, A. S., Hiatt, W. B., Ramirez, A. L., Winter, J. T., Engle, D. M., ... Carlson, J. D. (2016). Plant invasions or fire policy: Which has altered fire behavior more in tallgrass prairie? *Ecosystems*, 19, 356–368.

- Urbatsch, L. E., Eddy, R. (1973). A floristic study of Dawe's County, Nebraska. Transactions of the Nebraska Academy of Sciences and Affiliated Societies, Paper 392.
- Vitousek, P. M., Mooney, H. A., Lubchenco, J., Melillo, J. M. (1997). Human domination of earth's ecosystems. *Science*, 277, 494–499.
- Williams, M. A., Baker, W. L. (2012). Spatially extensive reconstructions show variable-severity fire and heterogeneous structure in historical western United States dry forests. *Global Ecology and Biogeography*, 21, 1042–1052.

TABLES

Table 10. 1: Multiple comparisons of mean tree density and mean coarse woody debris at Fort Robinson State Park, Nebraska, 2016 by burn severity using linear models and Tukey post hoc tests. The first column indicates which burn severities are being compared. The following columns contain the t-values and adjusted p-values for live and snag densities. The burn severity classes represent high-severity (H), moderate-severity (M), low-severity (L), and unburnt (U).

Comparison	Tree Density				CWD	
	Dead		Live			
	t-value	Adj. P-value	t-value	Adj. P-value	t-value	Adj. P-value
H vs. L	1.351	0.532	2.646	0.001	-4.313	<0.001
H vs. M	-0.788	0.856	0.816	0.597	-1.515	0.436
H vs. U	6.727	0.001	5.184	0.001	-6.494	<0.001
L vs. M	-1.972	0.215	-1.830	0.029	2.798	0.035
L vs. U	5.251	0.001	2.538	0.001	-2.181	0.141
M vs. U	7.076	0.001	4.368	0.001	-4.979	<0.001

Table 10. 2: Understory wood plant species observed across a burn severity gradient at Fort Robinson State Park, Nebraska, 2016. The species column indicates the scientific name of each species. The burn severity classes represent (from left to right): high-severity (H), moderate-severity (M), low-severity (L), and unburnt (U). Burn severity column values show the number of sampling locations for a given burn severity class in which species were detected. The number of asterisks indicate if a species was only observed in a single severity class (*) or a single site within a single severity class (**).

Species	U	L	M	H
<i>Acer negundo</i> **	1	0	0	0
<i>Ericameria</i> sp.**	0	0	1	0
<i>Gutierrezia sarothrae</i>	1	10	8	10
<i>Juniperus communis</i> **	0	0	1	0
<i>Juniperus scopulorum</i>	2	0	0	2
<i>Mahonia repens</i> *	4	0	0	0
<i>Pinus ponderosa</i>	14	4	3	2
<i>Prunus americana</i>	5	0	1	0
<i>Prunus virginiana</i>	10	4	2	7
<i>Rhus trilobata</i>	13	13	11	11
<i>Ribes americanum</i>	2	0	2	6
<i>Ribes aureum</i> **	1	0	0	0
<i>Ribes odoratum</i>	3	1	0	3

337

<i>Ribes oxycanthoides</i>	1	0	1	0
<i>Rosa woodsii</i>	7	3	4	9
<i>Symphoricarpos occidentalis</i>	8	2	5	9
<i>Toxicodendron radicans</i>	12	10	9	12
<i>Ulmus americana</i> **	0	1	0	0

Table 10. 3: Multiple comparisons of understory woody plant and bird community compositions at Fort Robinson State Park, Nebraska, 2016 by burn severity using PERMANOVAs. The first column indicates which burn severities are being compared via PERMANOVA, the second column contains the initial F-values (from which unadjusted p-values derived), and the third column contains resultant p-values using false discovery rates to adjust for multiple comparisons. The burn severity classes represent high-severity (H), moderate-severity (M), low-severity (L), and unburnt (U).

Comparison	Understory Shrub		Bird	
	F-Value	Adjusted P-value	F-value	Adjusted P-value
H vs. L	6.874	0.002	3.055	0.009
H vs. M	5.680	0.005	1.284	0.260
H vs. U	16.061	0.002	13.007	0.002
L vs. M	0.663	0.624	2.898	0.014
L vs. U	10.417	0.002	4.674	0.002
M vs. U	9.099	0.002	11.388	0.002

Table 10. 4: Avian species observed across a burn severity gradient at Fort Robinson State Park, Nebraska, 2016. The burn severity classes represent (from left to right): high-severity (H), moderate-severity (M), low-severity (L), and unburnt (U). Burn severity column values show the number of sampling locations for a given burn severity class in which species were detected. The number of asterisks indicate if a species was only observed in a single severity class (*) or a single site within a single severity class (**).

Species	H	M	L	U
American Goldfinch	0	2	6	8
American Kestrel	0	1	0	1
American Robin	0	1	1	0
Audubon's Warbler	0	0	1	7
Barn Swallow *	0	0	0	2
Black-beaked Magpie **	0	1	0	0
Black-capped Chickadee	0	1	1	5
Blue-gray Gnatcatcher	0	1	4	1
Brown-headed Cowbird	5	5	9	8
Black-headed Grosbeak **	0	0	0	1
Brewer's Blackbird	3	3	2	0
Brown Thrasher **	1	0	0	0
Bullock's Oriole **	0	0	1	0
Cassin's Kingbird	1	5	3	0
Cedar Waxwing *	0	0	0	3

Chipping Sparrow	0	0	3	3
Common Nighthawk **	0	0	1	0
Eastern Bluebird	1	0	0	2
Eastern Kingbird	2	0	1	0
Hairy Woodpecker	0	0	1	1
House Wren	2	3	5	7
Lark Sparrow	2	7	0	0
Mountain Bluebird	1	0	2	1
Mourning Dove	2	3	3	2
Northern Flicker	5	2	3	0
Orchard Oriole **	0	1	0	0
Ovenbird **	0	0	0	1
Pinyon Jay *	0	0	2	0
Plumbeous Vireo *	0	0	0	3
Prairie Falcon **	0	1	0	0
Pygmy Nuthatch **	0	0	0	1
Red-breasted Nuthatch **	0	0	0	1
Red-headed Woodpecker	2	0	2	0
Rock Wren	2	0	5	1
Red-tailed Hawk **	0	1	0	0
Spotted Towhee	0	2	4	5
Turkey Vulture	0	0	1	1

Western Kingbird **	0	0	0	1
Western Meadowlark	14	13	11	0
Western Wood Pewee	0	1	2	0

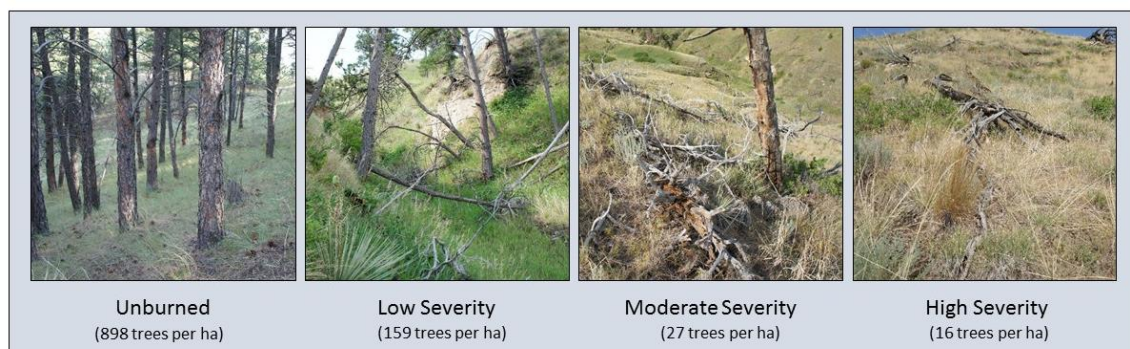
FIGURES

Figure 10. 1: Images of a typical study site sampled in the summer of 2016 for unburned forest and low, moderate and high severity burned forests from the 1989 Fort Robinson wildfire.

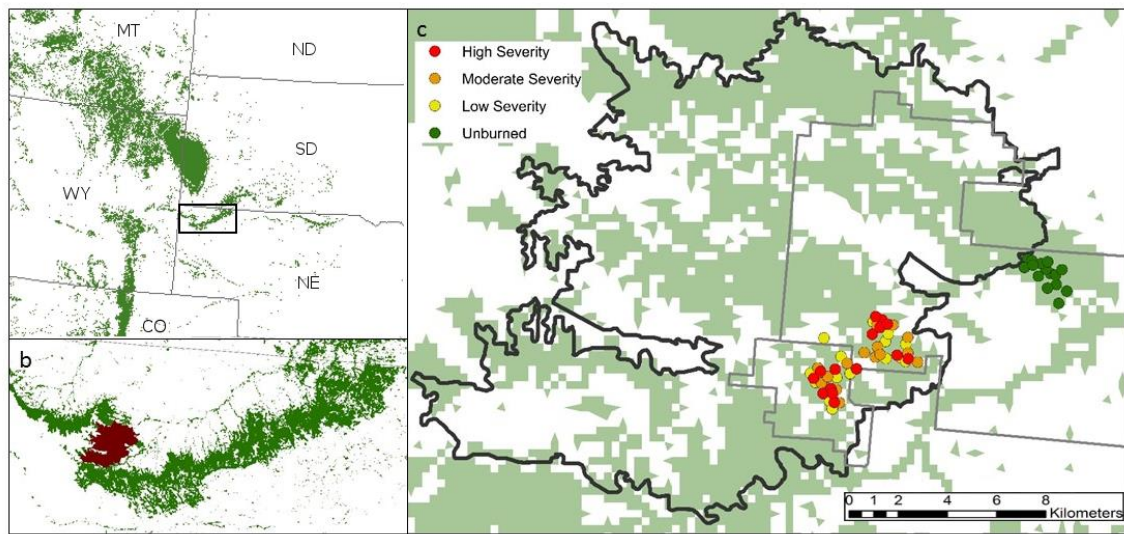


Figure 10. 2: a. The northeastern distribution of ponderosa pine in the United States provided by the US Forest Service indicated in green b. The Pine Ridge region of Nebraska, with the 1989 Fort Robinson wildfire in red and ponderosa pine distribution in green c. The distribution of sampling sites of different fire severity classes, indicated by colored points, within the Fort Robinson (42.6693° N, 103.4689° W) wildfire perimeter (black), ponderosa distribution in green and public land boundaries for Fort Robinson State Park and Peterson Wildlife Management Area (grey).

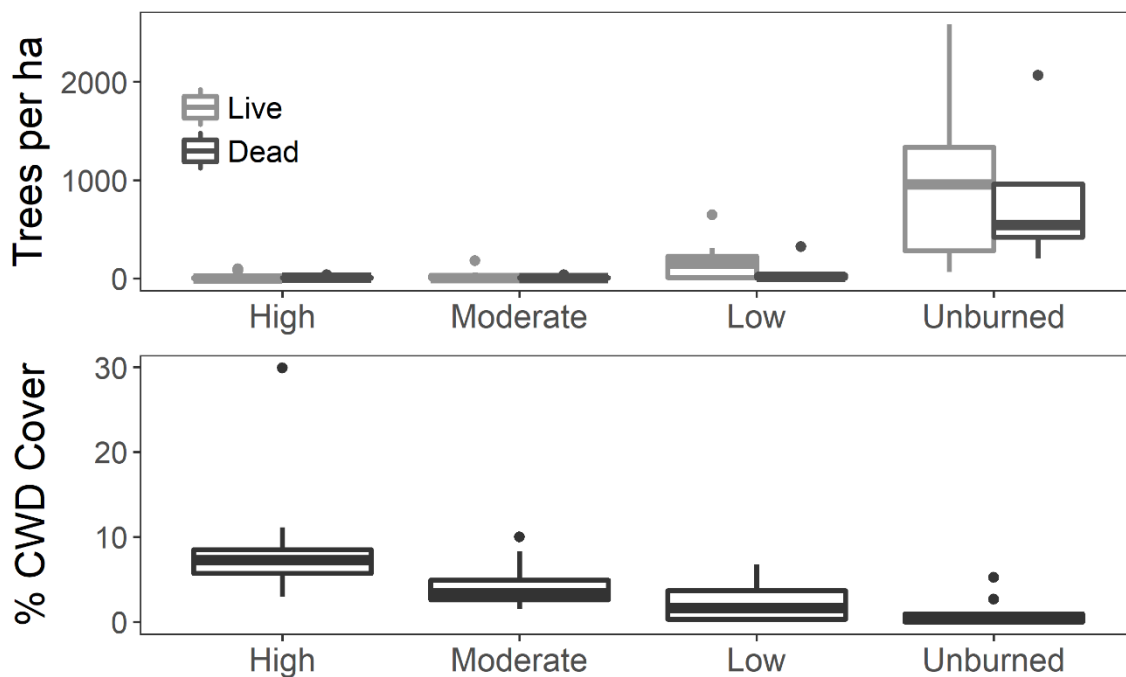


Figure 10. 3: Forest stand structure across a 27-year-old burn severity gradient at Ft. Robinson State Park, Nebraska, 2016. The top panel shows boxplots of tree density per hectare for each burn severity class. The bottom panel shows boxplots of percent cover per 30 m transect of coarse woody debris for each burn severity class. The burn severity classes represent high-severity (High), moderate-severity (Moderate), low-severity (Low), and unburned (Unburned).

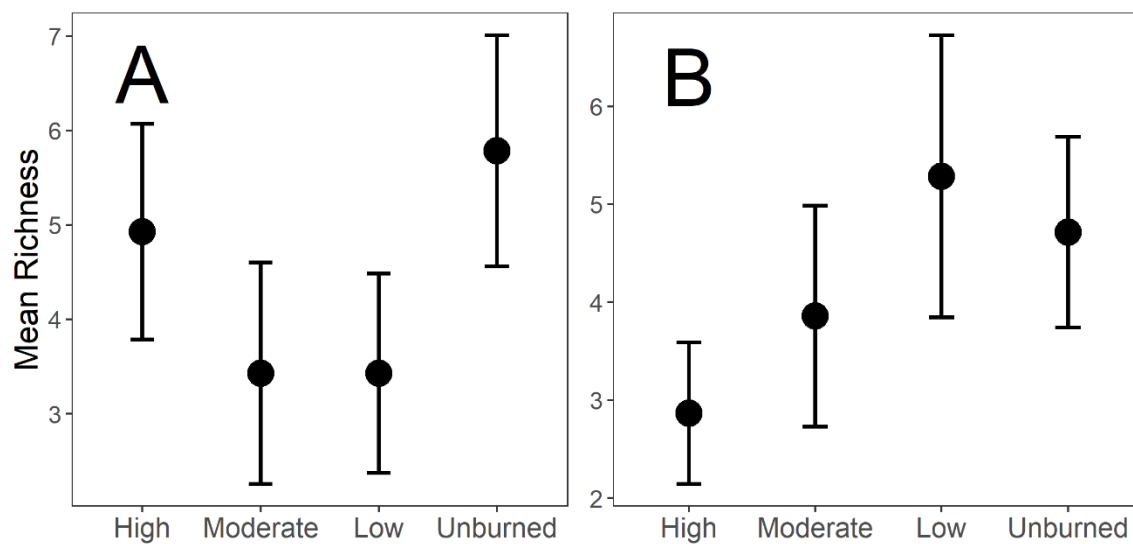


Figure 10. 4: Mean understory woody plant (panel A) and bird (panel B) species richness by burn severity in Fort Robinson State Park, Nebraska, 2016. Bars indicate 95% confidence limits. The burn severity classes represent high-severity (High), moderate-severity (Moderate), and low-severity (Low), and unburned (Unburned).

Figure 10. 5: Mean constrained site scores and species scores for the first two axes of a canonical correspondence analysis for understory woody plant (panel A) and bird (panel B) community composition data across a burn severity gradient in Fort Robinson State Park, Nebraska. Bars indicate 95% confidence limits of the mean site scores. The burn severity classes represent high-severity (H), moderate-severity (M), low-severity (L), and unburned (U). Plant species scores are represented by the first two letters of genus and

the first two letters of species, and bird species scores correspond to American Ornithological Union species abbreviations. See Tables S2, S4 for plant and bird species, respectively.

APPENDIX A: TO HOLD A BEAUTIFUL, BURNING SNAKE¹⁰*I.*

They said the Thompson Ridge wildfire was a good fire. It began on May 31, 2013, at the southern foot of Redondo Peak in the Jemez Mountains of New Mexico. A dead aspen, black and brown sheaves of bark sloughing off in the droughty summer, fell into a power line and ignited. When the United States Forest Service declared the Thompson Ridge fire 100 percent contained on July 1st, it had burned 23,965 acres of the spruce-fir, ponderosa pine, and grasslands covering Redondo Peak. It left a mosaic of blackened matchsticks and green, unburned forest, creating unique and diverse habitats for an array of species. No one died. No private property was damaged. It was a well-behaved, ecologically-beneficial fire.

A few weeks later, lightning snaked down from the sky and ignited another wildfire in the dry hills near the town of Yarnell, Arizona. Within 24 hours, the Forest Service had scrambled an army of helicopters, fire trucks, and hotshot crews, several of which were pulled from the nearly-contained Thompson Ridge fire. Unlike in the Jemez Mountains, there was valuable real estate in Yarnell to protect, so quick suppression was the goal. In

¹⁰ Roberts, C.P. (2018). To Hold a Beautiful, Burning Snake. Terrain.org: A Journal of the Built + Natural Environments. Available from: <https://www.terrain.org/2018/nonfiction/hold-beautiful-burning-snake/>.

the end, the Yarnell Hill fire burned just 8,400 acres of piñon-juniper woodlands, destroyed 127 buildings in Yarnell, and killed 19 hotshots. Three of the dead hotshots had fought the Thompson Ridge fire.



Wildfire, smoke, and helicopter in the Valles Caldera National Preserve, New Mexico.

Photo by Jacob Daly.

Fire is controllable and quantifiable. In a laboratory with metal floors, walls, and ceilings, researchers set up tiny wooden slats like dominoes, light the dominoes from the safety of

a fire-proof viewing window, and then record and analyze the fire's behavior as it leaps and twists and coils from slat to slat, becoming an inferno, turning all but its metal cage to ash. There are equations and diagrams that create looping spider webs of logic to predict fire behavior in carefully-controlled microcosms, and there are Forest Service standard computer algorithms that predict the path and toll fires will take by lighting virtual flames across pixelated landscapes. There are also the not-so-mysterious fireplaces and campfires, encircled by concentric rings of stones and people reclining in canvas chairs holding beers in koozies, wearing fleece jackets, watching the flames leap and dance for them.

Fire is beneficial and necessary. Ecologically, it fosters ecosystem resilience and biodiversity. In ponderosa pine forests, fire burns heterogeneously, creating as much new habitat as it destroys. It opens up the canopy and forest floor for meadows of bunchgrasses, scrub oak, and aspen. It leaves some trees untouched for the chickadees and pygmy nuthatches and Audubon's warblers. It leaves burned-out snags for great-horned owls and pine martens and three-toed woodpeckers to excavate and build dry, safe nests. In prairies, fire cuts out the old, dead grass choking the new, nutrient-rich shoots that cattle seek. It coaxes out leafy forbs like coneflowers and milkweed and prairie phacelia. It halts encroaching woody plants like juniper and mesquite, killing them to make room for dancing prairie chicken leks and the trembling whistles of bobolinks and dickcissels.

But fire is wild too. It's easy to forget that people burn just like the trees and grass.



Caleb Roberts scans for elk in the Valles Caldera.

Photo by Sara Bailey Roberts.

When the Thompson Ridge fire started, I was standing next to my diesel pickup on a gravel road in the [Valles Caldera National Preserve](#). Behind me, the forest-covered Redondo Peak loomed. But I was focused on the expanse of grassland in front of me. I was triangulating radio-collared elk in the Valle Grande, part of a research project

investigating responses of large mammals to forest thinning and fires. Waving my copper-antennaed yagi in the direction I thought the elk were, I pressed my ear against the receiver, trying to hear the strongest signal and find the most accurate azimuth. I knew they liked to settle near the center of the valle, around the East Fork of the Jemez River during midday, sometimes dipping into the waters when the heat or insects became too much.

When the stream of vehicles began speeding past me, I was annoyed by the dust and noise. I lowered the yagi, thinking I would resume after the trucks passed. But then one of the trucks pulled over, and the preserve foreman leaned out of the driver's side window. Long, graying beard neat, cowboy hat askew, he informed me that a wildfire had started on the back side of Redondo. He said I needed to get out of the preserve immediately. Whipping around, I saw the white smoke plume rising from behind Redondo, already as high as the clouds. I jumped into my pickup and revved out onto the washboard road, trying to catch up to the last truck in the caravan. The foreman had not waited.

That evening, the hotshots and fire trucks began rolling into Jemez Springs, the village below the preserve where all the researchers and most of the preserve staff live. My coworkers, our field technicians, and a few of the preserve staff had all congregated at Los Ojos, the only bar in town. We sat quietly around a booth, sipping beer, listening to a band of middle-aged, bandana-wearing men cover Johnny Cash. We weren't sure what the following days would look like, if our research projects, like Redondo, would go up

in smoke. The VCNP had declared the Caldera closed until the Thompson Ridge fire was 100 percent contained. We knew it was for people's safety. I wondered why the fire had to happen now, this year. Why couldn't it happen in the fall, after I had collected all my data for the season?

We asked one of the guys at the booth, the preserve's wildlife biologist, what he thought the fire would be like. How big would it get? How long did it take to contain the last fire? Shrugging, he said he had no idea. He said in 2011, the Las Conchas wildfire burned more than 157,000 acres. He said it got so hot that at one point it was burning an acre per second, trees simply exploding, needles and leaves evaporating. You could see the fire's twisting towers all the way from Santa Fe. It had even begun making its own weather, pushing away rainclouds that would douse it and summoning winds to feed it. He paused, taking a long drink. It was scary, he said, like it had a mind of its own. It wasn't the fire crews that contained it or put it out, either, he said. It was the monsoons in late July. Something bigger than us or the fire.

That same night, we drove up the mountain, hoping to see the fire for ourselves. Halfway up, we came to a roadblock of orange cones and Forest Service SUVs. We lowered our windows as a ranger approached. She told us to turn around, that they feared the fire might jump the highway tonight. Her jacket was rumpled. She looked tired.

But we still wanted to see the fire. So we turned our vehicle around and parked at the closest pullout we could find, about a quarter mile back. Looking northward, toward Redondo, we could see the red and orange glow of the fire above the trees, fading gently

into the black and stars of the sky. No cars passed. A soft wind set the pine boughs swishing. We knew some houses sat back there in the woods, nearer the fiery glow. Was it as calm there?

The next morning the fire crews reopened the highway. People who had cottages tucked into the drought-dried trees near Jemez Springs but worked in Los Alamos needed to get to work. Vehicles were simply cautioned to slow down when smoke crossed the road. I didn't mind the highway reopening. I still needed to collect behavioral data on the elk.

That evening I drove to a pullout overlooking the Valle Grande. I set up my tripod and spotting scope on the asphalt and scanned the valle. Several elk herds congregated in the narrow strip of green around the East Fork, as if they had not moved since the fire began. They sauntered through the grass, necks bent low, carefully choosing their bites, heedless of the same haze causing my nose to crinkle and eyes to water. A cow elk lay in the tall grass, staring, chewing cud. Her head was turned so that she may have been watching the distant smoke and flames. But she also may have been watching the river flow by, gently rocking the rushes on the banks.

I watched them until the sun sank behind Redondo, smoke turning the sky molten red and pink.



Fiery sunset behind Redondo Peak as the Thompson Ridge wildfire burns.

Photo by Jacob Daly.

II.

I have a friend who studies fire. She used to think she wanted to be a hotshot, to go fight fires out west. But one of the first prescribed fires she helped manage changed her mind.

The fire was planned for 650 acres of a ranch in the Sandhills of Nebraska. Out there, from horizon to horizon, hills like ocean waves sprawl, grassy slopes falling fast to narrow valleys. In recent years, the local ranchers had started using fire to burn out the junipers creeping into their cattle's range and improve the nutrient content of their pasturage.

The morning of the fire, my friend stood with the other volunteers, the wind tugging at her hair, listening to the burn boss atop a hill. He wore flannel and a cowboy hat. They watched his fingers draw out the plan across the hills and valleys, tracing where they would set the backfire near the top of a ridge and where they would set the frontfire at the valley floor. When he finished, he clapped his hands and told them to get to it. Everyone broke up. Another cowboy, wrinkled, clean-shaven, and smiling, took her to the frontline in his truck. They waited, watching the first billows of smoke signaling the backfire had been lit. Then they got out of the truck, and the cowboy pointed east and told her to light the grass in a straight line until she reached a barbed wire fence, a mile off. Then he handed her a drip torch, showed her how to ignite it, and left her to set the fire.

She tramped through waist-high grass, holding the drip torch perpendicular to her path. It piddled out globs of burning oil from its curlicue spout. She watched each footfall. She did not want to trip on prickly pear or yucca or twist an ankle in a badger hole. All she could hear was the swish and crackle of her steps and the fire. She only paused once to catch her breath. Inhaling deeply, she glanced back at the fire she had lit. It looked like a striped ribbon flowing from her torch, caught in the breeze. Orange strands faded and tore into the blue sky. Brown and black lines of burned earth and grass stretched into the distance.

After what seemed a long time, she met up with another volunteer and traded her drip torch for his fire swatter and a Gatorade. Realizing just then how dry and chalky her throat was, how hot and taut her skin felt, she guzzled the whole thing. Throwing the

bottle into her pack, she gazed around. The fire now streamed into the canyons. Smoke plumed white and pillowy into the sky. An echoing whoosh caught her ear. A juniper had exploded, flames slaving 20 feet up for a few seconds, then dying down as the naked pale-silver limbs caught and carried the flames.

She lost herself in the hunt for escaped flames. With the fire swatter, she patted out spark-lit fires that were just waiting for the wind to change and fan them up. She sought smoldering shrub islands inside the fire perimeter that would pulse red like a beating heart into the night and flare at the slightest gust. She climbed up hillsides, her pants blackening from the ash, and slid down hillsides, sand and gravel grinding under her boots.

She came to a hilltop with several other fire tenders. A few roamed about, poking at the ground with their fire swatters. But most stood, leaning folded arms on their fire swatter poles, watching smoke and heat haze rising from the valley. It was like a grill, marinating the valley, preparing it for summer grazing. She stopped to watch too. She felt proud that she had helped start it.

But then the smoke began falling. Like a mouth, the valley began sucking it down. The chain of white smoke linked to the sky broke. The smoke in the valley began to turn, but slowly, like a poorly-greased wheel. My friend looked to the others, but no one spoke or moved. They just watched.

The churning in the valley began to speed up, but the smoke had sunk so low, only tufts were visible. It looked like water frothing at a whirlpool's edge. A hollow roar, as if from far off, filled the air. Then my friend noticed figures on opposite hill, silent miniatures. They were running up the ridge, away from the valley.

The roar rose, came closer. Her neighbors were backing up, but she did not move. Hair whipped into her eyes, and she pushed it back. She could not take her eyes from the roiling smoke clouds. Across the valley, another cedar burst into flame with the sound of a shotgun fire. The roar came closer.

A pillar of fire rose from the valley. Churning and writhing, it grew, taller than the hills. It looked like a tornado, but upside down and made of bright writhing scales of red and orange. Like a monstrous serpent, it could have swallowed every person on the hilltop in a sweep of its coils. It looked like a beautiful and terrible snake, undulating to the music of the whistling, cracking fire.

My friend could hear only the roar. She took a step back. At the edges of her vision, she saw some of the others turning, running. But she did not take her eyes from the pillar. She told me she had never seen anything like it before or since. She could not look away.

The serpent thrashed from side to side. Anything it touched erupted into new coils of flame. It slammed into a thick, gnarled cottonwood in the valley. The tree's bark fractured and flaked to the ground. Limbs broke and burned and fell. Whip-cracks of

cedar ignitions, swaying grass fires, and smoke, smoke all around, turning, swirling, filling the great snake's belly and its valley kingdom.

And then the snake died. Its body guttered, exposing its gaseous innards. It swayed. And then it withered and fell, its bright belly and head dissipating to nothing before it met the valley floor.

My friend said it ended just like that. Everyone who had run shuffled back up to the hilltop, laughing loudly, whooping, slapping each other on the back, trying to gloss over the fear that still nestled behind their eyes. The prescribed fire was finished. The fire tornado left nothing but a few embers and glowing stumps. There was nothing else to burn.

After telling me all this, my friend made me promise two things: I was to let anyone who reads this know that the rancher reported huge improvements in his range quality and cattle weight gains. I was also not to name those who ran from the fire they started.



The Thompson Ridge wildfire burns through the night.

Photo by Jacob Daly.

Snakes bite. They hiss and rattle and swell out their necks. If held against their will, they squirm and flail, elusive in the hands, mouths agape, yearning to escape and willing to strike to do so.

But in many cultures, snakes symbolize fertility, renewal, and immortality. Think of a fat scarlet-and-gold striped kingsnake sliding out of its crinkled, white-dead skin, slithering out shiny and sleek, newly glossy eyes peering out at the same old world. Think of the caduceus: two intertwined serpents on a rod, glowing blue or white from hospital signs late at night. The divine staff that could ease people's death throes. Or bring the dead

back to life.



After the fire: the burned mixed-conifer landscape of the Valles Caldera.

Photo by Caleb Roberts.

III.

On July 1, 2013, a month and a day after ignition, the Forest Service fire crew declared the Thompson Ridge fire 100 percent contained, meaning the fire was unlikely to spread

further. In fact, the Thompson Ridge fire continued burning for several weeks after containment. On July 2, the VCNP deemed the fire safe enough to for researcher access.

The following evening, I drove into the caldera to attempt a night-long elk behavioral survey. I needed to track down a herd first, so I had attached an omni-directional antenna to my truck to pick up signals from radio-collared elk. Bumping along the windy dirt road at Redondo's feet, I listened for a strong, consistent beep from the receiver. I passed still-smoking snags, old ponderosas with only their bases charred, and barren hills that had been green with trees a month before. I imagined driving through a war zone. I was hoping to find a herd in an open grassland. That would allow me to stay in the truck all night, use the truck as a blind, and maintain a wide field of view. I would also have maximum light intake for the monocular night-vision goggles I had borrowed from the VCNP.

Thankfully, the radio signals led me to the narrow Valle de Jaramillo. The grasses of the valle met the spruce-fir and ponderosa-covered foothills of Redondo Peak in a patchy, winding boundary to the south and west. I had been noticing that the elk tended to retreat to the forest edge in the middle of the night, so the narrowness of the Jaramillo made me confident that I could accurately record their behaviors, even if they bedded under the trees. So I settled in for the night, ready with my coffee thermos, apple-cinnamon Pop-Tarts, bananas, and audiobooks. I would work until 0800 the following morning.

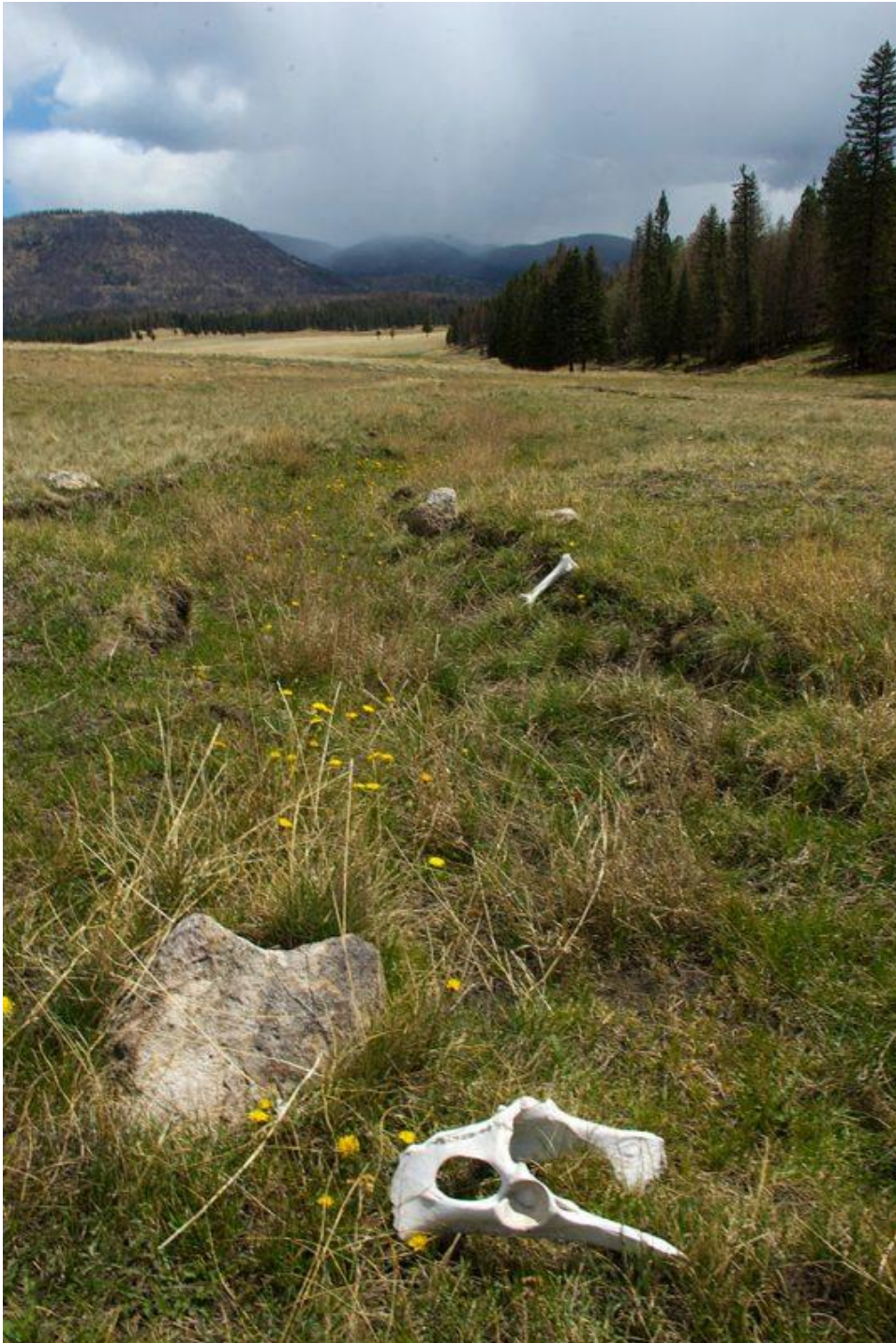
I watched the elk through my binoculars, my pencil scratching letters and numbers on the clipboard in my lap, until the sun set behind the caldera rim. Bright reds and purples

juxtaposed the shadowed mountains, beautiful—though not as beautiful as during the height of the fire. I rolled down the window, donned my night-vision goggles, and continued. My flannel, thick pants, and socks kept me warm, though the night mountain air felt wet and chill on my exposed face and hands. By about midnight, the herd had sauntered out of the grasses, their crepuscular inner-clocks telling them to rest until morning. Through the goggles, the resting elk looked like darker blobs against a dark ground amongst dark tree trunks.

Around 0200, I noticed a pulsing light on the ground near the elk. Through light-amplifying nightvision goggles, anything brighter than moonlight shimmering on the swaying grass looks like a flare gun discharge. And this thing looked like several stars had settled into the valle. But taking off the goggles and squinting, I could only barely see a glow. With my thermos hours-drained, my snacks all eaten, and my eyes drooping no matter how hard I tried to keep them open, it took me a moment to identify that brilliant glow as a remnant of the Thompson Ridge fire, still burning away at remaining duff and felled logs. I estimated less than 50 feet separated the elk from the fire. Unfazed, the elk slept right next to the thing that had until just recently been raging and consuming and changing their mountain refuge. I suppose they just have to accept that they have no control over the where a fire burns and where it doesn't.

I hate when I anthropomorphize animals. Perhaps they do not accept, only react. Perhaps they simply look at the world with their wide, deep, black eyes and see mountains and valleys blackened by fire one year and covered in grass and new aspen shoots the next.

They walk along draws, newly carved by fire and rain. They walk beside boulders, exposed for the first time since the volcanic upheavals formed the mountain. They may tread paths contouring the slopes, never ascending directly, to make their beds on bare ground or spruce needles. Or they may pause here or there to browse, taking the chance to eat the new grass, still wet with dew. But wherever they go, it is with, not against.



The Valles Caldera during the summer monsoon.

Photo by Jacob Daly.

I had managed to get above and upwind of them on a ridge. The fire had thinned the canopy enough for me to estimate that there were 17, all bedded down. Hoping to get a better view, I began sidestepping down the ridge, grasping charred saplings to support my slow, deliberate footfalls. I reached the bottom without jarring a single piece of obsidian or pumice. I stood still for a few seconds, controlling my breathing. I always thought that if the elk heard a twig break or pebbles grinding under my boots, a moment's pause on my part would make them think *Oh, it was nothing* and go back to chewing their cud. They did not stir when I began slowly moving forward at a crouch. But I wasn't lucky.

A dusky grouse exploded from the ground a few yards ahead of me. The beating boom of its wings echoed off the charred trees. I nearly fell over in fright.

The elk appeared to feel the same: they jumped up and disappeared over the next ridge. Holding my chest and breathing heavily, I let out a string of whispered curses. I needn't have bothered whispering. There wouldn't be any chance of catching those elk, unawares or not. So I started back down the mountain.

I took my time, trying to absorb the beauty of my surroundings, hoping to salvage something from the day. I came upon a steep, narrow draw filled with many burned trees. From where I stood, they looked like a blackened pile of pick-up sticks. House-sized pumice boulders, the yellowish color of bones, jutted from the incised walls of the draw. After hard rains, I had seen boulders that size washed down the mountains and across

roads in the valles, blocking my truck's path. Hard to believe anything, let alone fire, could have budged them.

I veered from the draw and headed down a gently sloping ridgeline. Soon, my path pushed past the surrounding ridgelines, revealing a panorama of the valle and all the eastern rim of the caldera.

In a documentary, this might have been a pan-out moment, perhaps with a helicopter circling above me, shooting a video. The video would slowly pull away from me to show more and more of the mountainside. It would show me on the black ridge weaving in and out of burned trees, shrinking to a speck as I navigated the sharp descent of the ridgeline's end. Then I would be lost in the trees, and the view would broaden to the ridges and draws, each tinted a slightly different black or green or brown. This patchwork would melt together as the whole of Redondo filled the camera, a mottled giant encircled by grassy valles made green by the early monsoons that year. And as the video faded into the next scene, Redondo would shrink and blend in with its neighbors, each green mound just one vertebra in the spine of the Jemez Mountains.

But of course all I saw was the valle ahead and the slope at my feet. Slivers of obsidian shifted under my feet, so I gripped the trees again to keep from slipping. When the incline lessened, I paused to scrub sooty hands across my brown canvas pants and looked around. Just a few feet away, I saw a skull, sitting upright, teeth sunk into the black earth.

Excited, I hunched down to identify it. I collect skulls, and I hoped this one would be a new species for my collection. It was a beautiful bobcat skull, scraped clean and white. It had all its teeth, and all the bones looked solid, although some of interstitial connections seemed loose. It only lacked the lower jaw, but that was no problem. The joy of such a find in the wild, by myself, was more than enough.

I rocked off the balls of my feet and sat down. Looking around, I saw no other sign of bones, just black earth, black trunks, some twigs, and some newly-sprouted bunchgrasses. Reaching out, I stroked what would have been the nose of the cat. It was rough, and a bit of bone flaked off at my touch. I could tell it was old.

I tried to imagine how it ended up here, sitting out in the open. Before the fire, six inches of needles, half-rotted branches, orange ponderosa bark, and fir cones might have covered it. It would have been the only thing the pillbugs and millipedes could not chew away, and too deep for passing deer mice or voles to gnaw for calcium. When the fire came, it probably only burned the first inch of duff above the skull, like a face peel. Then the fireline would have marched on, toward the hotshots feverishly digging a firebreak at Redondo's feet while helicopters dropped hundreds of gallons of water to protect one of the few remaining ponderosa groves in the preserve that predated Europeans and their clear-cutting. That night, the remaining litter above the skull would continue smoldering. Smoke would have risen like silent steam from the ground. An occasional gust of wind would have swept near the ground, and in the darkness, the earth would have glowed a deep orange for a long moment, and then would have faded back into the night. Over

days, the litter would have burned, crumbled to ash, burned, and crumbled to ash, like water draining from a tub. The skull would have gradually surfaced, baking in the heat waves spiraling from the earth around it, its sutured bones swelling against their seams. And when the rains finally began sizzling against the earth in early July, loose ash would have trickled around the skull and raced downhill. But its teeth would have held firm.

And now it was in front of me, waiting. I just needed to wrap it in a rag, take it home, and put it right on my shelf next to my opossum, beaver, house cat, fox, and badger skulls. Imagining it made me smile.

So I cupped my hand around it and slowly, softly, pulled it away from the ground.

The skull fell apart in my hands, splitting in two at the crest. The mandible disintegrated, leaving the teeth stuck in the ground. My grip was so loose that it all fell back to the earth, like sand through a sieve. But then I noticed something underneath the shards and bone dust: a mound of black earth shaped exactly like the skull, as if the fire, earth, and rain had purposefully cast the skull in black plaster.

I stood up, regarding the mound and shattered skull, and nudged one of the larger pieces of bone with the toe of my boot. I wondered if I still might be able to salvage it, perhaps scoop the pieces and stitch it back together with super glue. But that seemed hollow.

I looked up and around the gutted forest. The deer mice and voles that couldn't previously reach the skull would appreciate me leaving it. I imagined a little tree or tuft of grass sprouting from the skull-cast mound, a symbol of the mountain's regeneration.

I laughed at myself. It would never be so simple. Those bones—probably the mound, too—would wash away with the next rain. I left the pieces and continued down the mountain.